Origin of Palaeo Proglacial Lake Sediments in Taylor Valley, Antarctica

A thesis
submitted in partial fulfilment
of the requirements for the Degree
of
Master of Science
at the University of Waikato
by

SARAH MILICICH

THE UNIVERSITY OF
WAIKATO
Te Whare Wānanga o Waikato

University of Waikato
2005

ABSTRACT

The origin of carbonates found at three locations in the Taylor Valley and their association with different glacial advances is presented. Samples were collected from three locations through the Taylor Valley, specifically Nussbaum Riegel west of Lake Fryxell, Sollas Bench on the slopes above Lake Bonney, and from Pearse Valley. Carbonates were collected primarily from the surficial glacial sediment, though at one site at Nussbaum Riegel a pit indicated the stratigraphy contained multiple carbonate horizons. The carbonate from Nussbaum Riegel was *in situ*, while at the other two sites the carbonate was incorporated into moraines.

The oxygen isotope values indicate that carbonates were deposited in lakes with two different origins. $\delta^{18}O$ values of approximately -28‰ to -32‰ for the Nussbaum Riegel carbonate samples indicate "Glacial Lake Nussbaum" likely formed during glacial conditions when grounded ice expanded in McMurdo Sound pushing a lobe of ice up the mouth of the Taylor Valley. $\delta^{18}O$ values of approximately -33‰ to 38‰ for carbonate samples from Pearse Valley and Sollas bench indicate that "Glacial Lake Pearse" and the proglacial lake in which the Sollas Bench carbonates were deposited would have formed during interglacial conditions. It is proposed that an expanded Taylor Glacier was advancing though its own proglaical lakes, reworking carbonate sediment deposited in the lakes. The carbon isotopes reflect the nature of the carbon dioxide cycling within the lakes. Strongly positive $\delta^{13}C$ values are interpreted as reflecting low temperature equilibrium with atmospheric carbon dioxide or freezing processes causing precipitation.

The trace element chemistry of the carbonates is inferred to indicate that the origin of their composition is primarily controlled by the composition of the precipitating fluid and the mineralogy of the carbonate. Samples containing higher proportions of aragonite have higher concentrations of the larger ions such as barium and strontium, while those with more calcite in the mineral structure contain more of the smaller ions such as magnesium.

XRD analyses indicate that the Nussbaum Riegel carbonate samples are a mix of dominantly aragonite with some calcite. SEM images of the carbonate crystals show that they are cementing detrital material. Petrographic analysis of the Nussbaum Riegel carbonates indicate that much of the detrital material is volcanic in nature and was likely sourced from the McMurdo Volcanics. The Sollas Bench and Pearse Valley carbonate samples are predominantly aragonite as shown by XRD analyses. SEM images show the crystals in these samples are a mix of radiating needles and randomly oriented needles, pointing to two different processes during precipitation. SEM images also showed the presence of halite within the carbonate samples.

The Nussbaum Riegel carbonates are inferred to have been deposited during periods of lake level fluctuation, where draining of ground water towards a lower lake level resulted in evaporation at the lake margins and cementation of the surficial sediment. The Sollas Bench and Pearse Valley carbonates were likely deposited under a regime of water removal, either via evaporation or freezing, making these carbonates a mix of evaporites and "cryorites". Cryorite is a new term, being defined as deposits precipitated as a result of concentration by removal of water due to freezing. In this case they appear to be primarily "cryorites". Halite was identified within many of the carbonate samples and gypsum was found associated with them. This suggests that there was a strongly concentrated brine present at the time of precipitation.

The source of the salt in the western end in the Taylor Valley is likely to be an evaporate sequence in a subglacial depression indicated on subglacial profiles, currently being overridden by Taylor Glacier. The evaporites could have deposited during a warmer period when the Ferrar Valley was a fjord. Seawater would then have overflowed into Taylor Valley at its convergence with the Ferrar Valley. The resulting lakes then evaporating in the deep depression. Salts are currently being reworked into the valley, a similar situation is proposed for the Sollas Bench carbonates.

ACKNOWLEDGMENTS

First and foremost I would like to thank Chris Hendy for his guidance in the writing and editing of this thesis, it's ok, I'll stop harassing you now!! Thank you to Brenda Hall for your help and advice during field work and teaching me the basics of Antarctic glaciology. There's no better teaching aid than seeing it first hand.

Funding came from Antarctica New Zealand, Office of Polar Programs in National Science Foundation and the University of Waikato. Thank you to Antarctica NZ and NSF for their logistical support during field work.

Penny Cooke and Steve Hood, thanks for being bouncing boards for many of my ideas and answering numerous questions. When it came to editing, Peter Kamp, Penny Cooke and Mum did a great job. I'm sorry Mum, I know most of it went straight over your head, but you read it all anyway. Thanks to Adam Vonk and Kyle Bland for teaching me the basics of GIS and helping solve the many problems I had with both GIS and Freehand. Great thanks go to Annie Barker for her assistance in lab work. Thank you to my fellow Masters students, many of you have answered questions or listened to my complaining.

Thank you to all the staff in the Earth Science department for imparting your knowledge and making my five years at university most enjoyable.

Thank you to the field team for Antarctica 2002/03, Sean Birkel, Jake Croall, Mary-Anne DeMello, Brenda Hall, Amber Hawkins, Chris Hendy, Aaron Schlosser, and Tom Whittaker. You guys are awesome and made for an amazing experience, remember to "rumpus" and you'll never be cold again!!

Finally, thank you to Mum and Dad (Graeme and Judy). Without your support and encouragement over the last five years I would not have achieved what I have. I love you and thank you xoxo.

TABLE OF CONTENTS

FIGURES

TABLES

CHAPTER ONE:

INTRODUCTION

1.0 INTRODUCTION

This chapter will contain an outline of the aim of the research, identifying the key areas of research and the anticipated outcomes. This will be followed by an introduction to the geomorphology and glacial system of the Taylor Valley, along with background information to Taylor Valley and its surrounds.

1.1 RESEARCH OBJECTIVES

The Taylor Valley in the Dry Valleys region of McMurdo Sound, Antarctica provides a rare opportunity to examine the glacial history of Antarctica. As much of Antarctica is under ice, the evidence of its expansions and contractions is not easily found. Only in rare ice-free regions do the deposits resulting from fluctuations of ice cover become available for interpretation. The Dry Valleys of McMurdo Sound provide one of the largest areas for such investigation. Carved by the advances of outlet glaciers from the East Antarctic Ice Sheet (EAIS), these valleys are affected by both the expansion of the EAIS and Ross Sea Ice Shelf, making them ideal for examining the interrelations of the two.

Much work has been done on characterising and dating the glacial deposits of Taylor Valley, particularly those of the Ross Sea Glaciation and Bonney Glaciation, while lacustrine deposits of glacial advances older than these have yet to be examined. The objective of this research is to interpret the glacial history of the Taylor Valley, Antarctica using older proglacial lake sediments. Particular emphasis will be put on their mechanisms of emplacement/deposition. An attempt will also be made to determining when they were emplaced, thereby constraining these glacial events that are known to be beyond the reach of U-Th dating (ie. >350,000 yr. B.P.).

This research involved field work that was undertaken in Taylor Valley over the 2002/2003 season. The field work involved 6 weeks working in the Taylor Valley investigating the lacustrine sedimentation associated with incursions of the Ross Sea ice and Taylor Glacier expansions.

The use of geochemical techniques such as x-ray diffraction and scanning electron microscopy will help with the understanding of the geochemical events that occurred during the glacial events. This can be used to answer questions such as the source of the waters for the lake from which the carbonate was deposited, the depositional environment, the trigger for the deposition of the lake beds and the origin of the salts in the Taylor Valley.

1.2 INTRODUCTION TO THE GLACIAL SYSTEM OF TAYLOR VALLEY

Studies of Antarctica have shown that the majority of the continent has had ice cover throughout the Quaternary, and possibly since the early Miocene (Hughes, 1973; Kennet et al., 1974).

Outlet glaciers drain the inland ice sheets of East Antarctica through the Transantarctic Mountains. It is this outflowing that has resulted in the carving of valleys such as Taylor Valley. The original cutting of the valley could have occurred during the early phases of the rock uplift that has led to the Transantarctic Mountains. The distribution and age of moraines suggests that multiple glaciations have occurred during the last 4 million years, concurrent with gradual uplift of the Transantarctic Mountains. These glaciations have been termed the Taylor Glaciations, and result from increased outflow of East Antarctic Ice during glacial intervals (Denton et al., 1970; Hendy et al., 1979). The EAIS has been demonstrated to be relatively stable undergoing only small-scale fluctuations and subject to change only after prolonged change of climatic conditions (Hollin, 1962).

In contrast to the passage of inland ice towards the Ross Sea as outlet glaciers through the Transantarctic Mountains, there have been Ross Sea Ice Sheet expansions up the valleys. It appears that ice grounded in McMurdo Sound, fed by increased outflow of the south-west outlet glaciers of the Ross Sea region, have pushed westward towards and into the McMurdo Dry Valleys region. This has caused the damming of valley mouths by ice, resulting in the deposition of glacial erratics, moraine ridges, and the formation of large proglacial lakes (Denton et al., 1970;

Whillans, 1976; Stuiver et al., 1981; Hall et al., 2000). The grounded nature of the ice during these times means that these ice sheets rest on topography that is largely below sea level and therefore is inherently unstable. This could have led to rapid changes in the extent of the ice shelf (Whillans, 1976). This most recent of the grounded ice sheets is the Ross Sea Ice Sheet (Denton et al., 1970).

1.3 TAYLOR VALLEY

1.3.1 LOCATION AND TOPOGRAPHY

The Taylor Valley (Fig. 1.1) is part of an extensive ice-free area in the Transantarctic Mountains that fringes the west coast of McMurdo Sound. The valley trends east-west at S77°30' to 77 °45' latitude and E162 ° to E164 ° longitude. The head of the Taylor Valley is located near the Taylor Dome on the EAIS, and extends for approximately 125 km to New Harbour in McMurdo Sound. The walls of the valley are made on the northern side by the Asgard Range, and to the south by the Kukri Hills (Fig. 1) (Haskell et al., 1965; Higgins et al., 2000a).

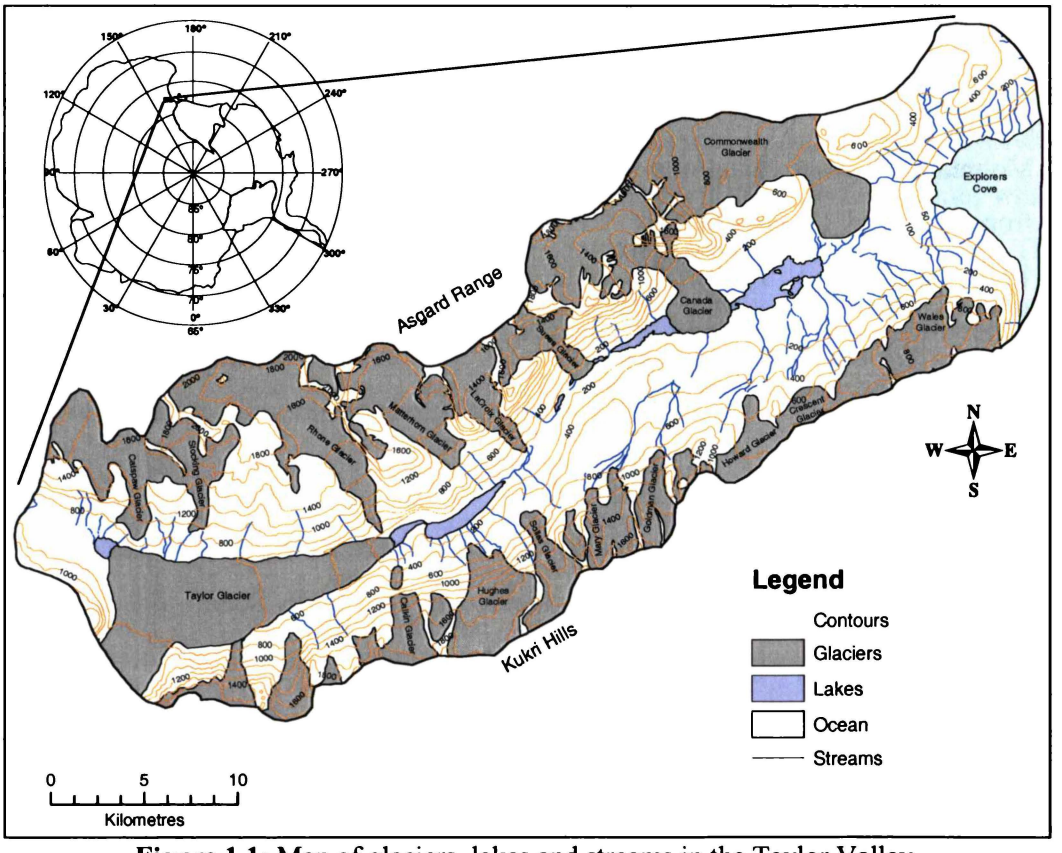

Figure 1.1: Map of glaciers, lakes and streams in the Taylor Valley.

The Taylor Valley drains from the EAIS, and fills upper Taylor Valley between Taylor Dome at 2400 m elevation, and the terminus at the margin of the western lobe of Lake Bonney at 57 m elevation. The eastern half of the valley is currently free of ice, except for small alpine glaciers on the valley walls. Lakes, the largest of which are Lake Bonney, Lake Hoare and Lake Fryxell, occupy parts of the floor of the valley. The valley cross profile is characterised by a narrow, inner U-shaped valley set within an outer valley consisting of broad benches that meet the steep, straight valley walls with an open-U profile. (Armstrong et al., 1968; Denton et al., 1970; Higgins et al., 2000a). Meanders and a v-shaped profile beneath Taylor Glacier (Morse et al., 2003) suggest that the valley may have originated as a river channel subsequently modified by glacial erosion.

The glacial history in the Taylor Valley is dominated by two main systems. The first of these is outlet ice from the EAIS. The Transantarctic Mountains partially dam the ice sheet. The Taylor Glacier is a small tongue of the ice sheet that has spilled over the mountain barrier and occupies the western end of the Taylor Valley (Denton and Armstrong, 1968; Denton et al., 1970). The second system is the Ross Ice Shelf that floats on the surface of the Ross Sea to the east of the Transantarctic Mountains. The ice supplied to the Ross Ice Shelf consists of direct accumulation of snow, discharge from the West Antarctic ice sheet, and discharge from the outlet glaciers draining the EAIS, to the south of McMurdo Sound. The alpine glaciers that flow down the walls of Taylor Valley have played a minor role in the glacial history of the valley (Denton and Armstrong, 1968; Denton et al., 1970).

1.3.2 CLIMATE

The formation of the McMurdo Dry Valleys, of which Taylor Valley is the largest, is the result of several factors. Currently there is a lesser flow of glacier ice being fed into the valleys from the Polar Plateau than has occurred in the past. The occurrence of katabatic winds has a large effect on the climate of the valley. As the winds drop some 3500 to 1800 m in elevation from the top of the polar plateau into the valley due to gravity, the air mass is subjected to increasing atmospheric pressure. The rise

in pressure causes the temperature of the air mass to increase adiabatically. During winter when the strongest winds occur, the winds can increase the local air temperatures by as much as 20 to 30 °C and drop the relative humidity by 20 to 30%. The valleys can also experience strong local glacier drainage winds. The ablation caused by these winds results in negative accumulation of snow in the valley (Clow et al., 1988; Doran and Wharton, 1996; Nylen et al., 2004).

The Dry Valleys are amongst the most extreme deserts in the world, with the annual mean precipitation being about 100 mm/p.a. exclusively received as snow (Bromley, 1985). The temperatures lie between –17 to –20 °C (Thompson et al., 1971; Riordian, 1973; Keys, 1980; Bromley, 1985; Friedman et al., 1987; Clow et al., 1988). The precipitation levels are much lower than the ablation rates, which have been measured at 150 to 500 mm/year (Henderson et al., 1965; Clow et al., 1988). The combination of low precipitation and dry katabatic winds result in extremely arid conditions. During non-winter months, climate is controlled by variation in the solar flux and slightly more moderate winds. Clow et al. (1988) have shown that 73% of sublimation off Lake Hoare occurred during the non-winter months of 1986 and 1987.

Observations of the snowline and accumulation on the alpine glaciers by Keys (1980) and Lyons (2000) show that there is a precipitation gradient in the valley, with more snowfall near the valley outlet at McMurdo Sound and less snowfall at the head of the valley at the Taylor Glacier. In the weeks of field investigation for this study there were several storms and it was noted that the snow line rose steadily away from the McMurdo Sound end of the valley.

1.3.3 BEDROCK GEOLOGY

Bedrock exposures in the Taylor Valley occur primarily on the valley walls. The bedrock in Taylor Valley consists of Precambrian to early Paleozoic Skelton Group (schist, marble, quartzite, and hornfels), Larsen Granodiorite, Theseus Granodiorite, and Irizar Granite (Haskell et al., 1965). Vanda Lamprophyre and Porphyry dikes

intrude this basement complex. Paleozoic to early-Mesozoic age Beacon Supergroup sedimentary rocks unconformably overlie the basement complex. Jurassic-age tholeiitic sills of Ferrar Dolerite Formation intrude both the basement complex and Beacon Supergroup. The youngest rocks are Neogene olivine basinite cones of the McMurdo Volcanic Group on the walls of central Taylor Valley (Wilch et al., 1993). Kenyte, a rare phonolite with only two known occurrences in the world (Ross Island and Mt. Kenya), does not crop out in the Taylor Valley, though there are numerous kenyte erratics in Ross Sea drift in the eastern part of the valley (Stuiver et al., 1981).

1.3.4 SURFICIAL DEPOSITS

The surface of the Taylor Valley is covered by glacial drift as a result of glaciation in the valley (Fig. 1.2).

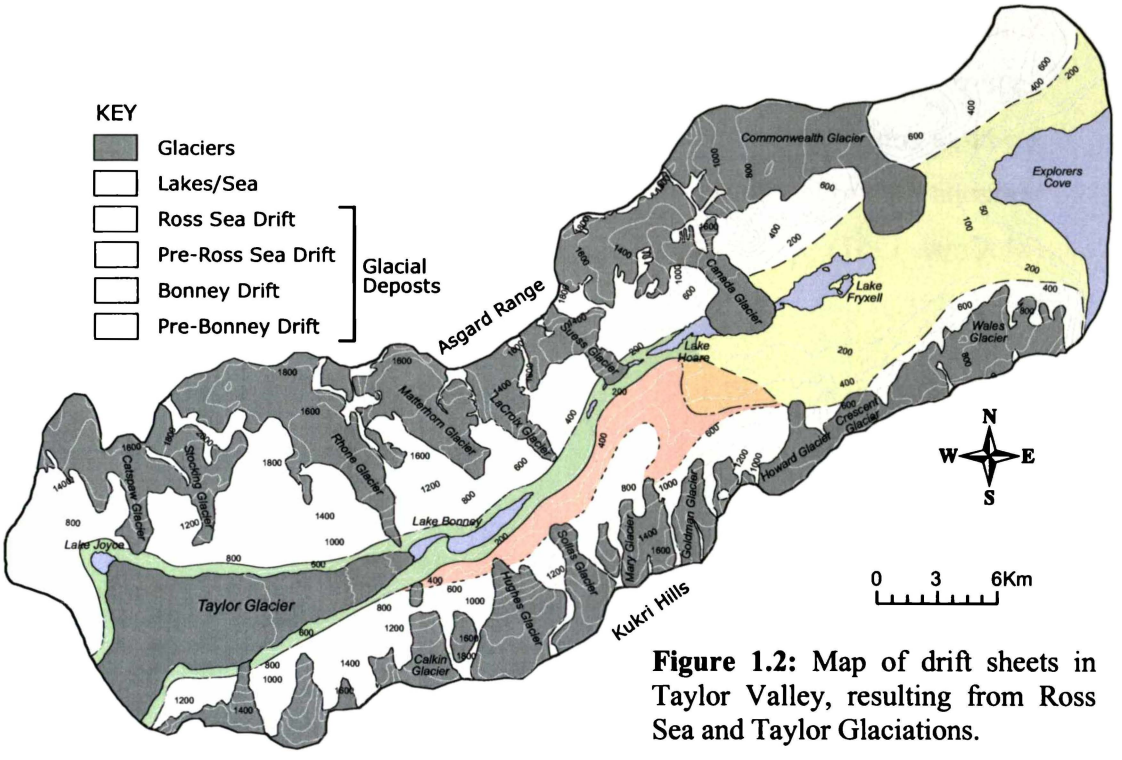

Figure 1.2: Map of drift sheets in Taylor Valley, resulting from Ross Sea and Taylor Glaciations.

These drift sheets can be divided into two types:

(1) Drift deposited by glaciations associated with the expansion of the outlet glacier (Taylor Glacier) draining the inland ice plateau. These deposits are generally light in colour, being made up primarily of the basement granite. Higgins et al. (2000) showed that deposits of Taylor Glaciations are comprised of units of yellow sand, silt

and diamicton. Units of lacustrine origin are present, some being *in situ*. Volcanic ash and marine microfossils are rare within the Taylor drift sheets.

(2) Drift deposited by glaciations associated with expansions of grounded Ross Sea ice. These deposits are rich in dark basaltic material derived from the McMurdo Sound region. The drift is rich in kenyte clasts, the only known local source of which is the Ross Volcanic Complex. This implies that the ice has moved in a circulatory direction from the west, around and over Ross Island and the McMurdo Sound into the Dry Valleys (Stuiver et al., 1981; Judd, 1986). The most recent of these is the Ross Sea Ice Sheet. Deposits formed from this type of glaciation have common units of lacustrine origin, along with deltaic beds and strandlines. There is also an abundance of marine microfossils found within the sediment (Hall et al., 2000).

Soils developed on the glacial deposits have little clay and little variation in colour or texture. The texture is gravelly sand or, less commonly, gravelly loamy sand. There are large zones of calcium carbonate or gypsum accumulations which occur as either horizons or surface crusts, underlain at a depth of about 30 cm by frozen ground (McCraw, 1967).

CHAPTER TWO:

LITERATURE REVIEW

2.0 INTRODUCTION

This chapter looks into work previously undertaken into the glacial history of Taylor Valley. This will involve looking at the development of ideas, starting with the pioneering work of Péwé (1960) to present ideas on the subject. This will be followed by an investigation into the formation of lacustrine carbonates. These involve precipitation induced by algal activity and evaporitic carbonates. The solute concentration required for evaporitic carbonates can be due to either evaporation or freezing. Finally this chapter will investigate the contentious subject of the origin of salts in the Taylor Valley. Many origins have been proposed such as atmospheric precipitation, weathering of surrounding rocks and incursion of sea water into the valley.

2.1 GLACIAL HISTORY OF TAYLOR VALLEY- PAST WORK

2.1.1 MULTIPLE ANTARCTIC GLACIATIONS

Péwé (1960) was the first to describe evidence for multiple glaciations in Antarctica. He described four major Quaternary glaciations in the McMurdo Sound region, focusing on evidence from the Taylor Valley. Previous workers had recognized that the ice cap and other glaciers were more extensive in the past, known as "glacial flooding". They did not however acknowledge more than one advance, or determine that the "glacial floods" were the same events at different locations around Antarctica (Scott, 1905; David and Priestly, 1914; Taylor, 1914; Nichols, 1968). By investigating the glacial chronology in the ice-free regions surrounding McMurdo Sound, Péwé (1960) found evidence of at least four major glacial fluctuations of the ice cap, each successively less extensive than the previous one.

McMurdo Glaciation

The oldest of these advances was named the McMurdo Glaciation. Patches of this drift were found on ridges 610 m a.s.l. on the west side of Koettlitz Glacier, and in Taylor Valley 760 m above the valley floor, near the top of Nussbaum Riegel. The deposits near Koettlitz Glacier contained some kenyte. The boulders in the drift are planed to the ground, and morainal form is absent. Péwé (1960) proposed that during

the McMurdo Glaciation, the Taylor Glacier filled Taylor Valley to a height of 915 m and coalesced with the expanded Koettlitz Glacier in McMurdo Sound, along with the Ferrar Glacier.

- Taylor Glaciation

The next glacial advance was termed the Taylor Glaciation. Drift resulting from the alpine glaciers is light coloured and consists mainly of granite, marble, gneiss and some dolerite. The Koettlitz Glacier drift is rich in dark volcanic rock, mainly kenyte (the source of the kenyte was not recognized, though it was specified not to have come from the only known source at Mt Erebus). The drift in the Taylor Valley is made up of a subdued morainal blanket of granite and metamorphic rocks, with some Beacon Sandstone. The boulders are ventifacted, and desert pavement has developed on them. Péwé (1960) proposed that during the Taylor Glaciation the Taylor Glacier filled the Taylor Valley to an elevation of 610 m a.s.l., though it did not cover Mount Nussbaum (Nussbaum Riegel) as it did in the McMurdo Glaciation. He also described large glacial lakes in the Dry Valleys, which formed as the west side of McMurdo Sound was blocked by ice or moraines from the expanded outlet glaciers during, and immediately after the Taylor Glaciation. The formation of Glacial Lake Washburn was proposed to have occurred as the ice retreated upvalley and glacial ice or a large ice-cored moraine held the water in place.

- Fryxell Glaciation

The next youngest deposit is that of the Fryxell Glaciation. The evidence for this glaciation comes from drift and loop or lateral moraines from the alpine glaciers in Taylor Valley. The moraines of the Commonwealth Glacier are rich in kenyte and Beacon Sandstone. Péwé (1960) proposed that the alpine glaciers extended down to the floor of the valley, overriding and coalescing with the lacustrine deposits of Glacial Lake Washburn. A measure of the age of this deposit was supplied by a series of raised marine benches occurring in front of the Wilson Piedmont Glacier, formed at the close of the Fryxell Glaciation and since uplifted. Two glacial lakes were considered to have formed during this glaciation. The first, between the Canada and

Commonwealth Glaciers was named Glacial Lake Rivard, of which Lake Fryxell is a remnant. A lake blocked by the Suess or Canada Glacier was named Glacial Lake Llano, of which Lake Bonney is a remnant. Both of these lakes were identified by the presence of weakly developed shoreline sediment.

- Koettlitz Glaciation

The latest major glaciation was termed the Koettlitz Glaciation and is the least extensive of the major advances, with only the outlet glaciers having left extensive deposits. These deposits are easily differentiated from the older drifts, as the moraines are ice-cored. During this glaciation the alpine glaciers were only a few hundred metres more extensive than at present. Dating of algae in old buried kettle lakes in the ice-cored moraines near the Hobbs Glacier yield ages of 5,900 ± 120 years. This indicates a minimum age of 6,000 years for the Koettlitz Glaciation.

As a summary of the work, Péwé (1960) presented a working hypothesis for the correlation of the Antarctic glaciations with those identified in New Zealand and North America (Table 2.1).

Table 2.1: Correlation of Antarctic glaciations with glaciations of New Zealand and North America (Péwé, 1960)

McMurdo Sound, Antarctica (Péwé, 1960)	New Zealand (Gage and Suggate, 1958)		North America
6000 year +		Kumara-3	
Koettlitz Glaciation	Otiran	Kumara-2 (22,300 years)	Wisconsin
		Kumara-1	
Fryxell Glaciation		Hohonu	
Taylor Glaciation		Waimaungan	Illinoian
Long interval		Interglacial	Yarmouth
McMurdo Glaciation		Ross	

Armstrong et al. (1968) investigated the glacial chronology proposed by Péwé (1960) by looking at the small cinder cone-lava flow complexes that have been erupted on the broad benches and outer walls of the valley to a height of at least 1500 m a.s.l. The basalts lie on surfaces within glacially eroded Taylor Valley, and thus postdate the last extensive glaciation. Below a height of 800 m the basalt has been eroded by advances of the Taylor Glacier and is now incorporated into irregular mounds and moraines. K-Ar dates on some of the lavas yielded ages of around 2.7 Ma. At the

time of publishing, field work by the authors had confirmed that till deposited by Taylor Glacier underlies the dated volcanics, and that subsequent advances of the glacier have overrun the volcanics to a height of around 1250 m.

2.1.2 OPPOSING GLACIAL SYSTEMS

Work by Denton and Armstrong (1968) showed that the four advances of the Taylor Glacier described by Péwé (1960) were not completely accurate, and that along with advances of the Taylor Glacier, expansion of the Ross Ice Shelf into the mouth of the Taylor Valley also contributed to the accumulation of glacial deposits. Along with mapping of the glacial deposits, K-Ar dates were obtained from 40 volcanic units interbedded with the glacial drift in Taylor Valley, and 11 ^{14}C dates were obtained for the youngest moraine, deposited by the Ross ice sheet along the west coast of McMurdo Sound.

It was discovered that the Taylor Valley had experience three major advances of the Taylor Glacier, followed by a significant recession. K-Ar dates of volcanic rocks that occur between the first and second advance have ages ranging from 2.7 to 3.3 ± 0.2 Ma (Armstrong et al., 1968). K-Ar dates of a cinder cone erupted in the interval between the second and third advance of the Taylor Glacier yielded an age of 1.8 ± 0.2 Ma (Denton and Armstrong, 1968).

More recent glacial activity in Taylor Valley has been characterized, not by advances from West Antarctica, but by ice advances from the Ross Ice Sheet to the west. During these expansions, the Ross Ice Shelf transformed into a predominantly grounded ice sheet. There have been at least four of these expansions into the Taylor Valley. The younger two postdate all major advances of the Taylor Glacier. During these younger two advances, fluctuations in the down-valley extent of the Taylor Glacier were confined to the upper part of the valley and during the last advance, the Taylor Glacier was much smaller than at present (Denton and Armstrong, 1968). Denton and Armstrong (1968) also recognised that fluctuations of alpine glaciers in

Taylor Valley have been out of phase with expansions and contractions of the Ross Ice Sheet in McMurdo Sound.

Denton et al. (1970) confirmed that the fluctuations of the three glacial systems (Ross Sea ice, outlet glaciers and alpine glaciers) in Taylor Valley and the McMurdo Sound region were not synchronous, allowing each of the systems to be dealt with separately in investigating the glacial chronology in the region (Table 2.2).

Table 2.2: Schematic correlation and chronology of glacial events in the McMurdo Sound region. The K/Ar dates given here are averages of numerous age determinations made over a period of several years (the dates are recorded as published in 1970) (Denton et al., 1970).

Taylor Glaciations (Ice Sheet in East Antarctica West of Taylor and Wright Valleys)	Ross Sea Glaciations (Ross Ice Shelf)	Alpine Glaciations
	4450 yrs. B.P. (L-627; Marble Point)[1] 5900 yrs. B.P. (L-462; Hobbs Glacier)[2] 6100 yrs. B.P. (Y-2401; Hobbs Glacier)	
Taylor I	9490 yrs. B.P. (Y-2399; Hobbs Glacier)	*Alpine I*
		12,200 yrs. B.P. (I-3019; Hobbs Glacier)[3]
	Ross I	
	34,800 yrs. B.P. (no laboratory number given, Cape Barne)[4]	*Alpine II*
	> 47,000 yrs. B.P. (Y-2641; Cape Barne; same locality as sample dated 34,800 yrs. B.P.) >49,000 yrs. B.P. (Y-2642; Cape Barne)	K/Ar dates; 2.1 to ~0.4 m.y. B.P. (Walcott Glacier area)
Taylor II	*Ross II*	
	Ross III	
	Ross IV	
Taylor III	K/Ar dates; 3.1 to 1.2 m.y. B.P. (Walcott Glacier area)	
K/Ar dates; 1.6 to 2.1 m.y. B.P. (Taylor Valley)		
		K/Ar dates; 2.1 m.y. B.P. (Taylor Valley)
Taylor IV		*Alpine III*
K/Ar dates; 2.7 to 3.5 m.y. B.P. (Taylor Valley) and 3.7 m.y. B.P. (Wright Valley)		K/Ar dates; 3.5 m.y. B.P. (Taylor Valley)
Taylor(s) V		

[1] Nichols (1968, p. 471); (Olsen and Broecker, 1961) p. 150). The C^{14} date given in the chart and text is corrected. The uncorrected date is 5650 ± 150 yrs. B.P. (L-627).
[2] Péwé (1960). [3] (Black and Bowser, 1969) Black and Bowser (1969). [4](Hendy et al., 1969)

The work by Denton et al. (1971) supports the division of glacial advances in Taylor Valley into Taylor, Ross Sea and Alpine Glaciations, with the Taylor and Ross Sea Glaciations occurring out of phase with each other. Age limits have been established for the earlier valley-cutting Taylor Glaciations by K-Ar dating of basaltic cones, which were either eroded by the glacier or erupted since deglaciations. On the four occasions where the Ross Ice Shelf expanded, it became a grounded ice sheet, which extended up the mouth of the Taylor Valley. During the Ross Sea Glaciations, the ice in the McMurdo Sound attained a thickness of more than 1000 m. The expansion of the ice sheet into the mouth of the Taylor Valley dammed large lakes, the strand lines of which are ~310 m a.s.l. in altitude for the Ross Sea I and reach 400 m a.s.l. for the Ross Sea II Glaciation (Denton et al., 1971). The recessional phase of the Ross Sea I Glaciation correlates with the rapid rise in sea level at the end of the late Wisconsin (Würm) Glaciation (MOIS 2).

K-Ar dating of lava flows indicates that the Taylor Valley has undergone major glaciation, and essentially attained its present profile prior to about 4 m.y. ago. The glaciation that resulted in the carving of the valley is classed as Taylor(s) V glaciations. While the valley was being carved the ice sheet must have been substantially thicker and the ice surfaces substantially higher that at present. As subsequent Taylor Glaciations have been considerably less extensive, it is assumed that the glaciers that carved the valley were wet-based, as opposed to the present dry-based glaciers (Denton et al., 1971).

2.1.3 TAYLOR GLACIER EVENTS

Hendy et al. (1979) presented views about the late Pleistocene glacial chronology of the Taylor Valley by investigating the carbonate-rich lacustrine and deltaic deposits. Analysis of these algal carbonates indicated that they originated from water derived from the EAIS via the Taylor Glacier at a time which corresponded to the previous three global interglacial periods. U/Th and ^{14}C dating of the lacustrine carbonates has provided a chronology for periods of high lakes levels and glacier advances. These

have been divided into a series of events, which can be correlated with the Taylor Glaciations of Denton et al. (1970) (Fig. 2.1).

- *Event I.* Taylor Glacier advanced to its present position, flooding two lobes of Lake Bonney and occupying the third. This event can be correlated to Taylor I Glaciation. Geochemical evidence indicates that this glacial advance contributed water to Lake Bonney approximately 15,000 yr B.P. and that flooding is continuing. U/Th dates of sediment from the East Lobe indicate that the current phase of rising lake level is younger than 5000 years old. Recent moraines close to the present margin of Taylor Glacier indicate there were some fluctuations in the extent of ice during Taylor I Glaciation (Hendy et al., 1979).
- *Event II.* The expanded rising Lake Bonney appears to have overflowed to occupy the Lake Hoare basin. The former lake levels in the area between Lacroix and Suess Glaciers coincide with advances of these glaciers. The oldest lacustrine sediments in the vicinity of the Lacroix Glacier occur on the crests of moraine ridges (90,000-95,000 yr B.P.), and younger carbonates occur close to the glacier on the floors of kettle holes between the moraine ridges (80,000-87,000 yr B.P.). This would occur during glacial retreat, falling lake levels, and the ablation of buried ice. Further evidence for falling lake levels comes from the presence of progressively lower deltas, associated with streams flowing westward into Lake Bonney. Older carbonates show the presence of an earlier event, or initial flooding during Event II (120,000-130,000 yr B.P.). Low $\delta^{18}O$ values for the carbonates, as well as geochemical contrasts to the Ross Sea carbonates to the east, indicate that they originated from water from the Taylor Glacier. This means that the mapping results of Denton et al. (1971) may need to be revised, as they show the strandlines around the Lacroix Glacier and Lake Hoare as being associated with the Ross Sea I Glaciation (Hendy et al., 1979).
- *Event III.* Lacustrine carbonates in the Lake Bonney and Lake Henderson basins have been dated within the range of 180,000-220,000 yr B.P., indicating high lake levels during this time, probably correlative with the ice advance of the Taylor II Glaciation (Denton et al. 1971). Event III carbonates that lie to the west of the

maximum ice limit of the Taylor II Glaciation were probably deposited during the retreat stage of this glaciation (Hendy et al., 1979).

- *Event IV. In situ* lacustrine carbonates found in Dry Valley Drilling Project (DVDP) cores indicate a period of high lake levels at ~300,000 yr B.P. The carbonates found in the DVDP cores also occur as clasts in more recent deposits. Event IV probably correlates with the Denton et al. (1971) Taylor III Glaciation (Hendy et al., 1979).
- *Older Events.* Two DVDP samples were found to be in radiometric equilibrium for the U-Th system, indicating an age greater than 400,000 years old (Hendy et al., 1979).

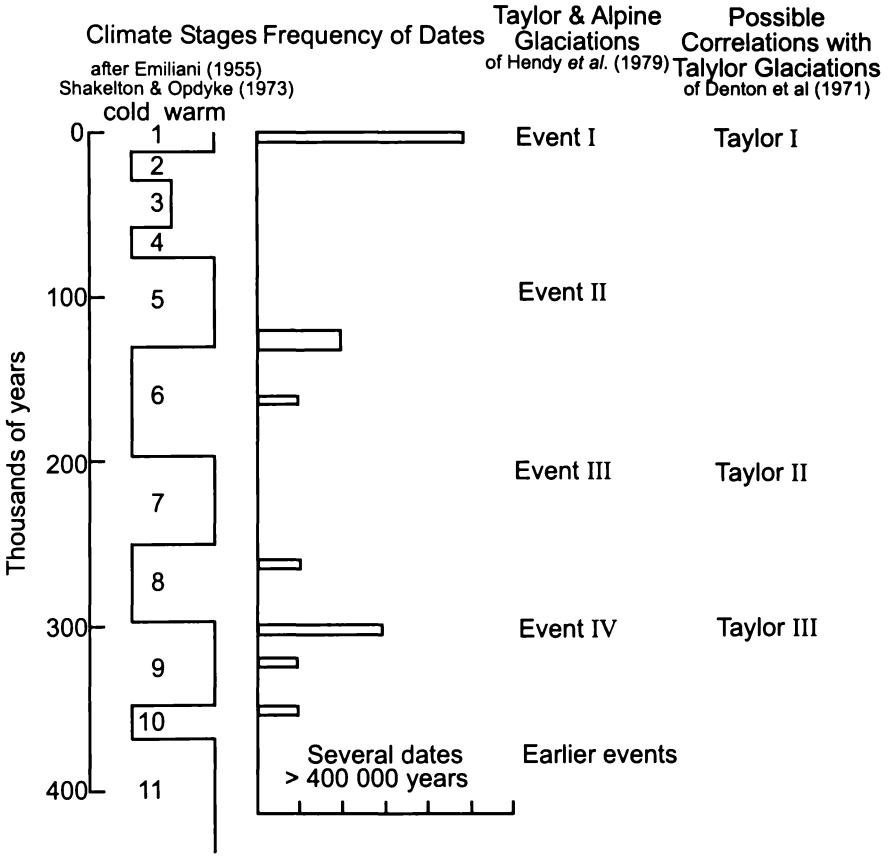

Figure 2.1: Nomogram of all U/Th dates on Taylor Valley proglacial lakes and related sediments; in intervals of 5000 years (Hendy et al., 1979).

Higher lake levels associated with Taylor/Alpine Glaciations coincide with worldwide warm periods. During these periods, there is increased precipitation due to a higher moisture capacity, and increased ablation is probably due to increased temperatures. In high latitudes this acts to increase the activity of the glaciers. As

long as the net increase in precipitation is greater than the net increase in ablation rate, this will result in advance of the glaciers. The lakes result from both the partial occupation of the lake basin by the glacier and an increase in the available water (Hendy et al., 1979). This theory is supported by ice cores taken at McMurdo Dome, which show that recession of Taylor Glacier and local alpine glaciers is concurrent with full expansion of grounded Ross Sea ice (Denton et al., 1989).

- **Bonney Drift**

The Bonney Drift in central and lower Taylor Valley represents the penultimate advance of Taylor Glacier. The glacier has previously been less extensive than present, and currently occupies its most extensive Holocene position since the deposition of the Bonney Drift. The Taylor Glacier has remained frozen-based during the late Quaternary, which means that its movements are in response to changes in ice volume rather than changes in basal thermal conditions. The drift deposited by the Taylor Glacier gives an ideal chance to examine changes in the volume of the EAIS (Higgins et al., 2000b; Higgins et al., 2000a). The outer limit of the penultimate advance of Taylor Glacier is marked by abandoned ice-margin channels, lateral moraines, drift remnants, and terraces of Bonney Drift at 300 m elevation. Algal carbonate clasts deposited in a shallow proglacial lake and associated with Bonney Drift in central Taylor Valley, yield U/Th dates ranging from 70-130 ka, indicating the Bonney advance of Taylor Glacier falls within the penultimate global interglaciation of marine oxygen isotope stage (MOIS) 5. The presence of *in situ* and reworked carbonate clasts of similar ages indicate that the position of the glacier snout fluctuated within this interval (Higgins et al., 2000b; Higgins et al., 2000a).

- **Taylor Glaciations**

There are drifts in central and lower Taylor Valley that are interpreted as older than Bonney Drift. These have been termed the Taylor II (MOIS 7), Taylor III (MOIS 9), and Taylor IVa (~MOIS 11) Glaciations. Evidence for these expansions of the Taylor Glacier come from portions of lateral moraines between 300 to 500 m in elevation in central Taylor Valley, and from U/Th ages on carbonate clasts from DVDP core #12 in lower Taylor Valley, and other reworked carbonate clasts in the Bonney Drift. Drift younger than the Bonney Drift is termed Taylor I, which is primarily the ice-

cored drift surrounding the margin of Taylor Glacier. The successive advances of Taylor Glacier from interglacial MOIS 11 to MOIS 5 have become increasingly less extensive (Higgins, 1993).

2.1.4 ROSS SEA DRIFT

During the last glaciation in McMurdo Sound, the Ross Ice Sheet expanded in to the mouth of the Taylor Valley, damming Glacial Lake Washburn. This high level lake occupied the coastal Fryxell and the Bonney basins of the valley. Stuiver et al. (1981) provided a comprehensive description of the Ross Sea Drift, which resulted from this incursion of a grounded Ross Ice Sheet. This drift largely covers the floor of the lower Taylor Valley, with the outer limit on the north wall of the valley being marked by an ice-cored moraine on the side of Hjorth Hill. This slopes from an altitude of 400 m a.s.l. down towards Lake Hoare at about 58 m a.s.l. On the southern valley wall, moraine segments, as well as a change in morphology to a more subdued moraine features on an older drift, mark the extent of the drift. The western extent of the drift occurs near the Canada Glacier. Trachyte basalt and kenyte erratics are common on this drift surface, becoming less common as the drift grades into glaciolacustrine sediment deposited by the lake-ice conveyor of Glacial Lake Washburn (Stuiver et al., 1981; Denton and Marchant, 2000). Radiocarbon dating of fossil blue-green algae in relict deltas on the valley walls provide a chronology of former lake levels in the two basins occupied by this drift. The dating shows that a high-level lake existed between 23,800-11,820 yr B.P. in late Wisconsin time. This agrees with available radiocarbon dates from minor Ross Sea moraines in lower Taylor Valley. Radiocarbon dates of perched lacustrine deltas in Explorers Cove at the mouth of Taylor Valley indicate that grounded ice remained in western McMurdo Sound between 8,900-8,340 years ago (Denton et al., 1985; Denton et al., 1989).

Algae in deltas record a dam of grounded Ross Sea ice in eastern Taylor Valley, otherwise the lake would not have risen above the valley floor thresholds. The existence of Glacial Lake Washburn must have therefore coincided with the deposition of Ross Sea Drift at the valley mouth. 119 dates of deltas indicate that

grounded ice dammed the valley between 8340 and 23,800 ^{14}C yr BP. This advance is hence coeval with the global Last Glacial Maximum (LGM) (Denton and Marchant, 2000; Hall and Denton, 2000; Higgins et al., 2000b).

The kenyte-bearing nature of the Ross Sea Drift indicates that the ice flowed westward across McMurdo Sound from western Ross Island by a grounded ice sheet, as this is the only source of kenyte in the area (Hall and Denton, 2000). The nature of the glacial deposits in eastern Taylor Valley is addressed in Table 2.3.

Table 2.3: Late Quaternary deposits in eastern Taylor Valley and on adjacent Cape Bernacchi and Hjorth Hill (Hall et al., 2000).

Deposit	Basis for relative age	Ice configuration
Alpine I Drift	Cross-cuts Ross Sea Drift and Glacial Lake Washburn deltas; little weathering.	Current configuration of alpine glaciers and Taylor Glacier; maximum extent of ice since the LGM.
Raised1 marine benches	Cut into and composed of reworked Ross Sea and Wilson Drifts.	No grounded ice along the shore between Explorers cove and Gneiss Point.
Relict deltas	Formed in Glacial Lake Washburn, which was dammed by ice that deposited Ross Sea Drift.	Ice-free at location of each delta at the time it was deposited; deltas >78 m elevation in the Fryxell basin; >118 m elevation in the Bonney basin, and at any elevation in the Explorers Cove basin require that grounded ice blocked the valley mouth at the time each delta was deposited.
Ross Sea Drift	Cross-cut by raised marine deposits; together with Wilson Drift, forms an interlobate moraine, and thus is contemporaneous with Wilson Drift, overlies Bonney Drift; overlies some deltas, but underlies others.	Grounded ice lobe, fed by an ice sheet in the western Ross Sea, extends westward to the valley-mouth threshold on Glacial Lake Washburn.
Wilson Drift	Cross-cut by raised marine deposits; together with Ross Sea Drift, forms and interlobate moraine, and thus is contemporaneous with Ross Sea Drift.	Expansion of eastern margin of the Wilson Piedmont Glacier over the Scott Coast.
Bonney Drift	Overlain by Ross Sea Drift.	Expansion of Taylor Glacier and alpine glaciers.

Figure 2.2 shows an interpretation of the surficial deposits in eastern Taylor Valley.

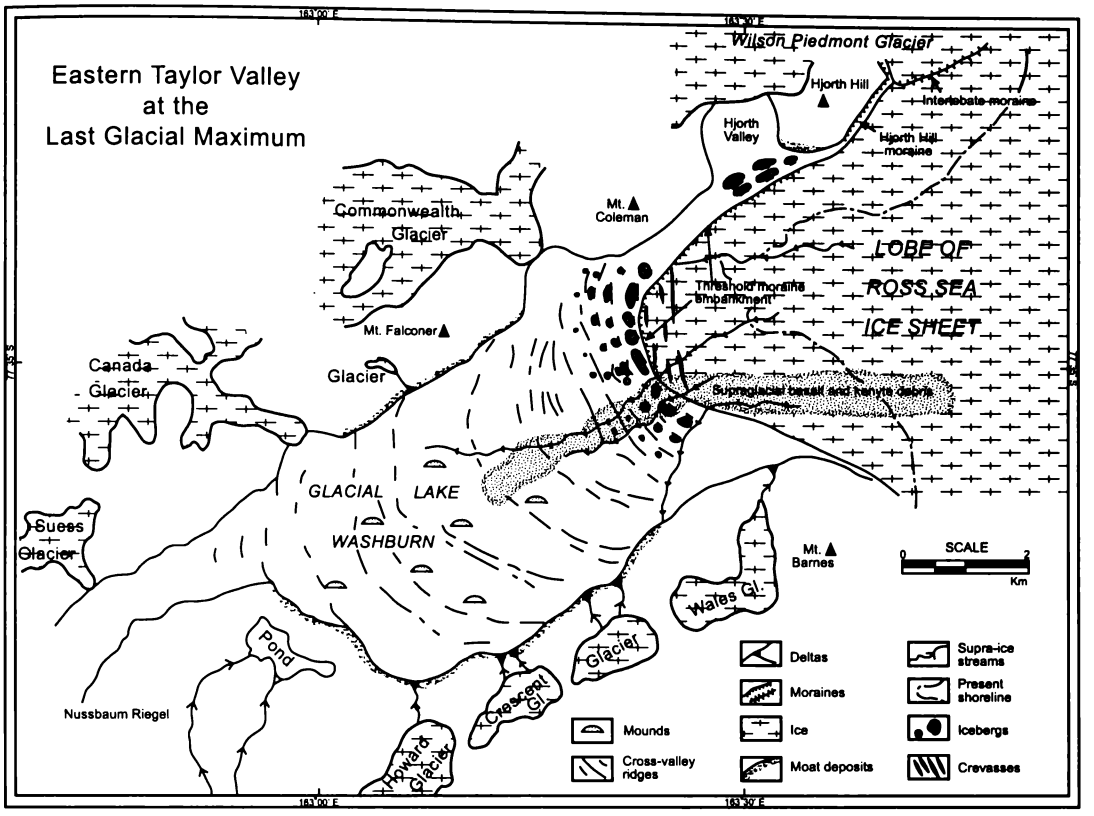

Figure 2.2: Map of eastern Taylor Valley showing the interpretation of surficial deposits. A lobe of the grounded Ross Sea ice sheet terminated at the valley-mouth threshold in Glacial Lake Washburn. A lake-ice conveyor operated on the perennially ice-covered surface of the lake, transporting debris westward beyond the grounding line. Debris that melted out of icebergs above the level of the lake ice formed low ridges and mounds on the lake-ice surface. Fine-grained sediment melted though the lake ice and fell on to the lake floor, but most coarse-grained debris was rafted across the lake and deposited in the marginal moat as ridges and mounds. Small meltwater streams from alpine glaciers formed deltas in the moat. Supra-glacial streams flowed on to the lake ice forming supra-lake-ice streams. These streams eroded though the lake ice and cut headward toward the glacier. In this process, they deposited well-sorted sand and gravel in longitudinal ridges on the lake floor. Outlines of alpine glaciers are generalised, because their actual extent at the LGM are unknown (Hall et al., 2000).

The chronology of high-level lakes in the Taylor Valley over the late Quaternary indicates an out-of-phase relationship between the advances of grounded Ross Sea ice from the east, and expansions of Taylor Glacier from the west (Fig. 2.3). The expansion of the Ross Sea ice caused by lowered sea level and mean lower annual temperatures would have meant a reduction in local precipitation in the Dry Valleys region and on the EAIS. As storms would not have penetrated into the region as frequently as at present, the aridity would have been higher causing a retreat of the Taylor Glacier and alpine glaciers. The presence of kenyte is a main indicator of drift

deposited by the eastward expansion of Ross Sea ice, as kenyte is only known to crop out on Mt. Erebus on Ross Island. A reversal of these conditions during interglacial periods means that the Ross Sea ice retreats from the Taylor Valley, and the Taylor Glacier and alpine glaciers expand.

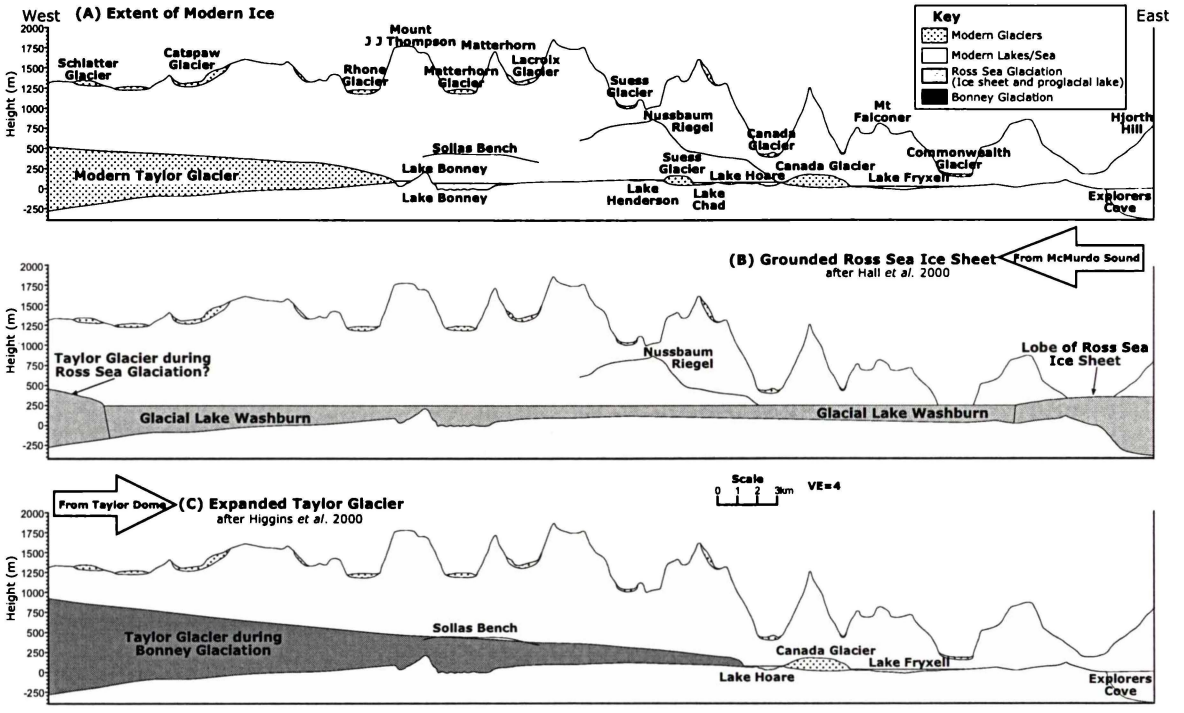

Figure 2.3: Model of glaciation in Taylor Valley involving alternate glacial advance down the Taylor Valley (Taylor Glacier) versus ice sheet advance up the valley (Ross Sea Ice Sheet).(A) Modern extent of glacial ice and positions of lakes. (B) An ice sheet builds in McMurdo Sound as sea levels are lowered and dams the mouth of Taylor Valley, trapping Glacial Lake Washburn. (C) Expansion of the EAIS causes Taylor Glacier to advance into the Lower Taylor Valley.

2.2 LACUSTRINE CARBONATES

Lacustrine carbonates are a relatively common part of the sediment in the Taylor Valley. Lacustrine carbonates deposited in the proglacial lakes formed during the deposition of the Ross Sea and Bonney Drift beds have been successfully dated using U/Th and/or ^{14}C methods. These carbonates result from three types of depositional systems. Two are the result of algal activity and take the form of stromatolitic deposits or deep-water suspension sedimentation. The third type forms as the result of evaporitic concentration of the lake water. Lake Fryxell can be used as an analogue for the deposition of carbonate in the palaeo-lacustrine systems.

The lakes of the Dry Valleys are saline in nature. There are several conditions that need to be met for a saline lake to occur: (i) evaporation must exceed inflow, and (ii) the basin should be hydrologically closed. These conditions are met in the Taylor Valley (Hardie et al., 1978).

2.2.1 LAKE FRYXELL

Lake Fryxell acts as an analogue for behavior of lakes in the Dry Valley. Within cores taken from Lake Fryxell there are three phase of carbonate deposition (Lawrence, 1982). The lake sediments are made up of five units with unit A being the lowermost and unit E the uppermost. Carbonate deposition in Lake Fryxell can be subdivided into two systems:

(1) Deposition during a period of alpine glacier advance. This includes the present Lake Fryxell water column and unit E calcites.

(2) Deposition during a period of Ross Sea advance and retreat, including the deposition of units D and B.

Lake Fryxell is typical of many Dry Valley lakes in having a permanent ice cover and being thermally and chemically stratified. The permanent ice cover is unusual for lakes and is the reason that stratification can occur, as the ice prevents stirring and mixing by wind. The summer melt water from surrounding alpine glaciers is the only significant source of water to the lake, and there are no surface outlets. A chemical diffusion cell exists between the saline bottom waters and essentially fresh surface water. This type of chemically induced density gradient is common in Dry Valley lakes, resulting from the mixing of residual evaporitic brines with inflowing fresh water. The mixing process occurs via molecular diffusion, where the residual brine diffuses upwards into the overlying fresh water, creating a diffusion cell (Hendy et al., 1977; Lawrence and Hendy, 1985; Lawrence and Hendy, 1989; Hambrey, 1994). The compositional history of closed basin saline lakes such as Lake Fryxell consists of two phases: (i) the acquisition of solutes, and (ii) brine evolution and subsequent precipitation of salts (Eugster and Hardie, 1978).

2.2.2 ALGAL CARBONATES

Biological activity also has an effect on the chemistry of the lake. The P_{O_2} data indicates that Lake Fryxell has an upper euphotic zone and a lower anaerobic zone (Fig. 2.4). The removal of CO_2 by algal photosynthesis causes an increase in pH. This causes the precipitation of calcite as supersaturation with respect to calcite has been reached (shown as ion activity products (IAP) in Figure 2.4). This is primarily occurring in the lower euphotic zone (8-9 m), where algal activity is at its highest (Fig. 2.4). The precipitated calcite, along with seston, settles out as a pelagic rain, giving rise to the layered deposit common in Dry Valley lakes. The pH of the bottom water is lowered as the CO_2 fixed by photosynthesis is released during the decay of the algae. This causes the dissolution of the precipitated calcite, and only where the accumulation rate is sufficiently high will the calcite be preserved. This is the depositional regime currently active in the lake, with well-sorted sand with flakes of $CaCO_3$ being deposited. This deposit is typically 30-35 cm thick and laminated with thin silt horizons, this unit has been accumulating for ~6000 years (Lawrence, 1982; Lawrence and Hendy, 1985; Lawrence and Hendy, 1989; Whittaker et al., 2003).

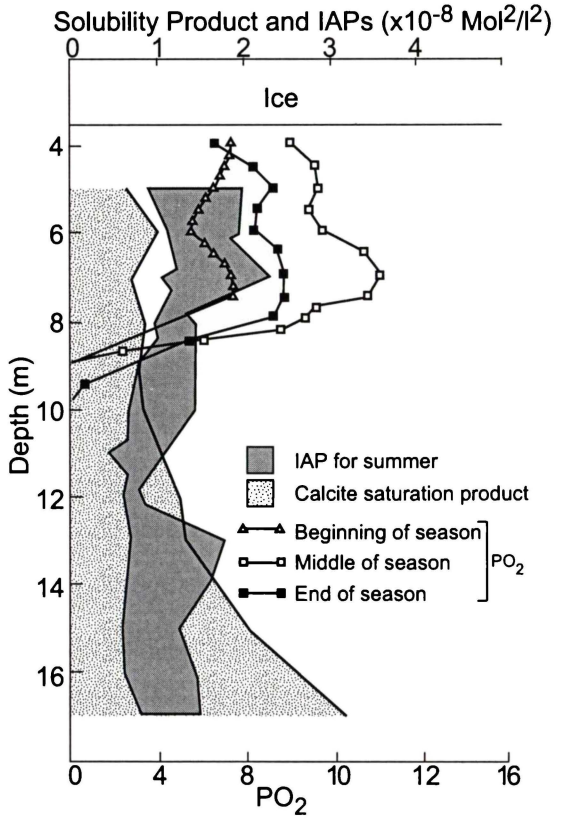

Figure 2.4: Lake Fryxell solubility profile. The stippled area indicates range where calcite is unstable. Where the shaded zone exceeds the stippled zone, calcite can be precipitated. The lines are P_{O_2} profiles for Lake Fryxell. The saturation of O_2 occurs above 9.5 m, showing where algal activity is most vigorous (Lawrence and Hendy, 1985; Lawrence and Hendy, 1989).

An additional mode of deposition occurs where the lake bed lies within the euphotic zone, where there are benthic communities of algae covering the bottom. Here calcite is precipitated in response to CO_2 removal by the algal mat, and is intercalated within the algal mat to form deposits that have been described as stromatolites. Where these algal mats have been described in Lake Hoare, the shallow water mats had columnar protrusions containing internal laminations. The columnar shapes are caused by photosynthetically produced oxygen gas that is entrapped beneath the mucilaginous matrix of the algal mat. At times this can cause lift off from the substrate, and each austral summer, part of the mat tears loose and floats upwards in the water column. This freezes in the new ice formed at the season's end, and due to the annual ablation at the surface and freezing at the base of the ice, mat pieces frozen in the ice pass though until they reach the surface and are scattered by the wind. In Lake Fryxell, much of the gas-charged mat is stabilized by the precipitated calcite and does not tear loose from the substrate, initiating a vertical growth habit of the calcite. In deeper parts of the lake, photosynthetic activity is insufficient to accumulate trapped oxygen, resulting in a flat mat growth habit (Parker et al., 1981; Lawrence, 1982; Wharton et al., 1982; Lawrence and Hendy, 1985; Lawrence and Hendy, 1989).

The presence of algal carbonates in temperate and warm region lakes is well documented, though it is not as common in glacially influenced lakes for the deposition of carbonate-dominated sediments to occur. This is due to the high influx of siliciclastic sediment overwhelming the carbonate that is deposited. The Antarctic lakes are therefore a special case, where siliciclastic sedimentation is low, predominantly occurring at deltas and in the moat region in the summer periods, and minimal turbulence allows algae to grow undisturbed (Reading, 1986; Hambrey, 1994).

A common feature in lacustrine systems dominated by carbonate sedimentation is the presence of varved deposits. Late spring and summer diatom and algal blooms can cause blankets of carbonate to cover the lake-bottom. This leads to the production of a finely laminated, organic-rich limestone. These light layers produced in spring can

be followed by the deposition of dark carbonate-poor laminae in the winter. These consist of organic matter, diatom frustules and fine siliciclastic material. This spring/summer and winter alternation of sedimentation in some lakes can produce varves, representing one years accumulation of sediment. The presence of varves is most common in glacially influenced lakes and will be discussed in greater detail later in the report. This annual sedimentation has been recorded in Lakes Zurich and Greifensee, Sweden, along with other temperate-zone lakes (Reading, 1986; Gomez Fernandez and Melendez, 1991; Platt and Wright, 1991). The annual sedimentation sequence of Lake Zurich can be seen in Fig. 2.5.

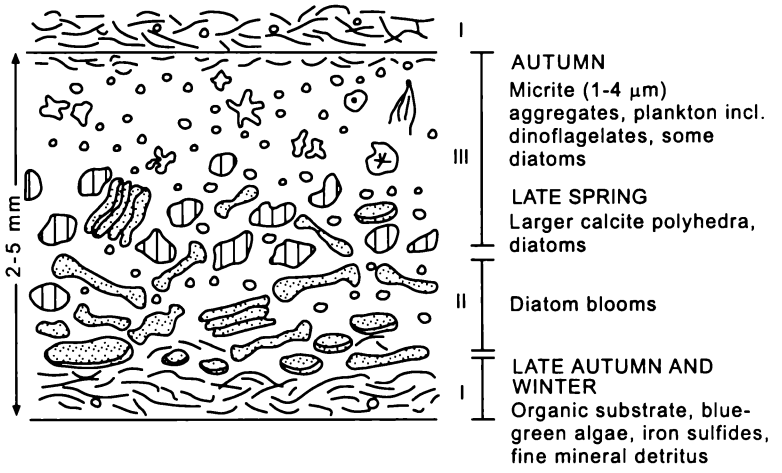

Figure 2.5: Schematic representation of a typical non-glacial varve from Lake Zurich, Switzerland (From Reading, 1986).

A similar type of varved deposit can be found in the Antarctic lakes, caused by the annual precipitation of carbonate and then the fallout of dead algae, which can form varves of alternating carbonate and organic rich material.

2.2.3 EVAPORITIC CARBONATES

Unit D in Lake Fryxell is an example of a carbonate deposited under evaporitic conditions. At c. 10,000 years ago there was a marked reduction in lake level, probably occurring when the lake was no longer dammed by the retreating Ross Sea ice. The lake spread, allowing for a larger ablation surface. This resulted in evaporitic concentration of the lake waters, producing a carbonate precipitate. This period of calcium carbonate deposition is probably responsible for the initial Ca^{2+} depletion of the salts dissolved in the present Lake Fryxell water (Lawrence, 1982; Lawrence and Hendy, 1985; Lawrence and Hendy, 1989).

Saline lakes are dominated by relatively few major solutes, namely: SiO_2, Ca, Mg, Na, K, HCO_3. CO_3, SO_4 and Cl (Eugster and Hardie, 1978; Hardie et al., 1978). Depending on the concentrations of these solutes, saline waters can be described in terms of a brine evolution system (Fig. 2.6). The brine evolution system depends on the evaporitic concentration of the brine, though the final composition of the brine is inherited from the earliest stages of water evolution, which are the weathering reactions in the watershed. The weathering of plagioclase-rich igneous or metamorphic rocks can contribute as much Ca^{2+} and HCO^- to the inflow waters as dissolution of limestone (Hardie and Eugster, 1970; Eugster and Hardie, 1978; Hardie et al., 1978).

Under evaporitic conditions, as the solutes begin to concentrate in the water, supersaturation with respect to the least soluble chemical precipitates is reached. There are the alkaline earth carbonates, calcite or aragonite or Mg-calcite are early precipitates (Fig. 2.6). The early removal of Ca, Mg and CO_3 by precipitation has a large effect on the brine chemistry. If HCO_3>>Ca + Mg at the point that the alkaline earth carbonates form, the subsequent evaporitic concentration will produce waters rich in CO_3+HCO_3 and depleted in Ca + Mg. For water initially with Ca + Mg>>HCO_3, a brine rich in alkaline earth and depleted in CO_3+HCO_3 will result. As concentration proceeds, the waters next become concentrated with respect to gypsum, which is still an early precipitation product. Depending on the Ca/SO_4 ratio, a Na-Cl-SO_4 or Ca-Na-Mg brine will be produced (Fig. 2.6). In an evaporating basin, the less soluble carbonates are often precipitated on the outside where there is contact with more dilute waters, with gypsum closer to the center. The next minerals to form are more soluble. The final stages of mineral precipitation can occur at the surface of open water brine or within the sediment from occluded brine. Common products include mirabilite ($Na_2SO_4.10H_2$), thernardite (Na_2SO_4) and halite (NaCl) in the center (Eugster and Hardie, 1978; Hardie et al., 1978).

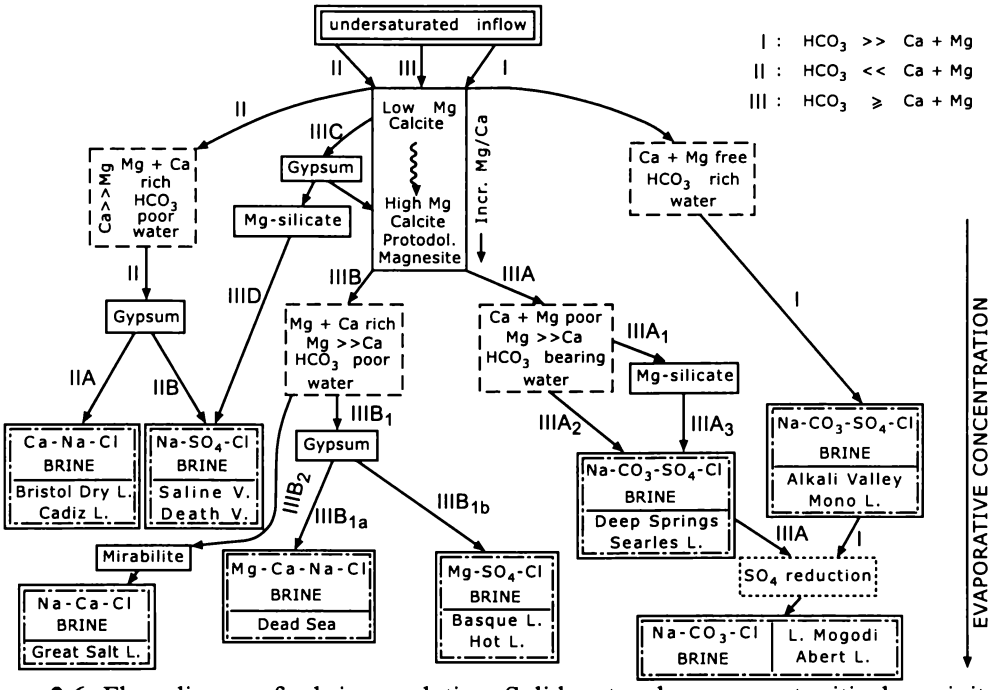

Figure 2.6: Flow diagram for brine evolution. Solid rectangles represent critical precipitates; rectangles with dashed borders are typical water compositions. Final brine types together with examples of salt lakes are surrounded by dash-dot rectangles (Eugster and Hardie, 1978).

As seen in Figure 2.7, as described by Thompson and Nelson (1956), the lake waters should approach the composition of sea water and then move to the right on Figure 2.7 as a result of freeze concentration. This implies that later stages of precipitation and salt concentration should be the same irrespective of the original water composition.

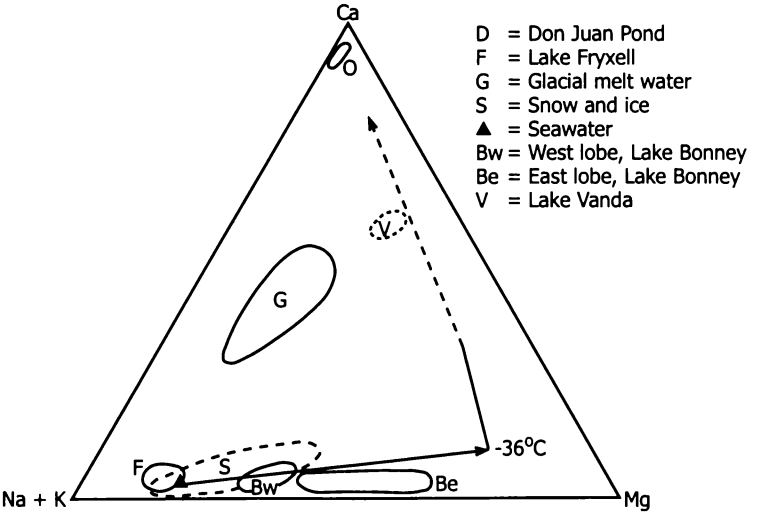

Figure 2.7: Ternary plot showing the relation of lake and seawater compositions. Arrow and dotted line indicate the compositional change of seawater under frigid conditions as described by the Thompson and Nelson (1956) model (Hardie and Eugster, 1970)

The order of deposition of minerals in the evaporation of sea water is $CaCO_3$ – $CaSO_4$ (gypsum) – NaCl – ($MgSO_4$) and the resulting brine contains large quantities of

$MgCl_2$ and $MgSO_4$. When brines are concentrated under frigid conditions, the order of salts being deposited changes to ($CaCO_3$) – $Na_2SO_4.10H_2O$ (mirabilite) – $NaCl.2H_20$ – potassium and magnesium salts (probably $MgSO_4$), and the remaining brine contains large amounts of CaCl, both types of deposition have probably occurred in the Dry Valleys. Most likely in summer the former is important, while in winter the latter becomes dominant (Nishiyama, 1979).

2.3 ORIGIN OF SALTS IN THE TAYLOR VALLEY

The origin of the salts in Taylor Valley has been a subject of contention since the discovery of saline lakes in the valley in the early 1960s. Early work by Boswell (1967) indicated several possibilities for the source of the salts. If sea water was discounted as a source, the salts could come from:

(1) Atmospheric precipitation. The idea that rain water can transport inorganic ions a great distance from the sea is well accepted and the possibility that the salts in the lakes are sourced from melted snow is suggested. It is also suggested that wind blown sea spray could be an appreciable source of salts for Lake Fryxell.

(2) Thermal springs. These have been suggested as the source of heat in Lakes Vanda, Bonney and Fryxell, and could thus also be a source of salts. Boswell (1967) concluded that there was little evidence for this.

(3) The surrounding rocks. The Antarctic environment causes widespread alteration of rocks and minerals, converting normally stable forms into those that are readily soluble. Weathering of rocks allows elements to be released into lakes and pools during times of flushing, such as the annual thaw. Melt water of glaciers also contains a small amount of dissolved rock. Since the lakes are fed by this melt water, it would contribute to the salts in the lakes.

Boswell (1967) suggested that atmospheric precipitation would be only a minor contribution and thermal springs are not a proven source, so therefore the last source is the most probable. This would mean that the relative concentrations of trace elements in the lakes would reflect possible regions of mineralisation in the area. Along with these sources, Angino (1962) suggested that for Lake Fryxell, relict sea

water could be a source for the salts. Angino (1962) stated that determining one source of the salts is not possible, and is likely to come from several different sources.

Jones and Faure (1968) used strontium isotopes to examine the source of the salts. They found that the water in Lake Bonney was relatively high in radiogenic strontium compared with marine strontium, suggesting that it has been derived from chemical weathering of bedrock, therefore not having a purely marine source. The strontium in the soil surrounding Lake Fryxell and the lake waters appeared however to be predominantly marine in origin. Jones and Faure (1968) suggest that as the floor of Taylor Valley opened to McMurdo Sound in the past, the sea had extended up into the valley (the evidence given for this is strandlines, which are now known to be lacustrine in origin). When the sea retreated, the remaining seawater evaporated, causing the deposition of salts. Hendy et al. (1977) refuted that the salt in Lake Bonney came primarily from weathering. To produce the minimum 20 million tonnes of sodium chloride present in the waters and sediment of Lake Bonney from weathering processes, vast amounts of clay minerals and other weathering products should also have been produced. These products are almost absent from the Taylor Valley sediments. They did however acknowledge that weathering could have been the source of some of the salts in other lakes such as Joyce and Hoare.

2.3.1 LAKE BONNEY

Jones and Faure (1978), using strontium isotopes, found that the strontium composition in the soil salts near Lake Bonney, and the saline discharge at the snout, were similar isotopically to the lake water. The $^{87}Sr/^{86}S$ ratios of soil salts and meltwater decrease from Lake Bonney towards the coast. The water of Lake Fryxell (the closest lake to the coast) has a $^{87}Sr/^{86}S$ ratio of 0.7090, which is identical to sea water.

Hendy et al. (1977) considered that the salt in Lake Bonney has been derived from sea water and modified by:

(1) Leaching of soils. This adds more soluble components such as oxidation products and daughter products of radioactive decay.

(2) Precipitation of calcium sulfate and carbonates. This results from concentration via evaporation and freezing, which finally leads to precipitation of sodium chlorides.

(3) Addition of atmospheric aerosols. Salts will be added in this way through the runoff of meltwater into the lake.

2.3.1.1 BLOOD FALLS

Black et al. , (Black, 1969) and Black and Bowswer(1969) suggest that at least some of the salts in Lake Bonney come from saline discharge from beneath Taylor Glacier. In 1962 it was noticed that red ice cone was situated at the terminus of the glacier. The colour was attributed to iron oxides such as goethite. Along with other minerals, there was aragonite precipitated in the ice cone. Black and Bowser (1969) concluded that the discharge came from brine situated beneath the Taylor Glacier, but they were not sure of the brine's origin. They also suggested that the salts in the valley can be partially attributed to wind-blown salt from the Ross Sea, though this would not account for the wide variety of deposits in the valley. The presence of saline ponds in the upper Taylor Valley at heights of 1000-1200 m a.s.l. was considered not likely to be concentrations from sea water. The possibility of glacial reworking of playa salts or marine evaporates has been considered for these water bodies (Black and Bowser, 1969).

Keys (1979) did further work on the saline discharges at the snout of Taylor Glacier. He noted that during "non-summer" months, thousands of cubic ms of saline waters flow from a crevasse at the terminus of Taylor Glacier or a source near the crevasse (now known as Blood Falls). By looking at geothermal gradients, the subglacial profile and ice thickness and ice velocity, it has been suggested that the glacier is over-riding a saline depression of about $5x10^5$ m^2, located 1-2 km up from the terminus. Keys (1979) used the theory that the Taylor Valley had been flooded with sea water at least as far west as Lake Bonney, as the salts in the lake have in his opinion been derived from sea water. This would have occurred during a time when

the Taylor Glacier had retreated, allowing the subglacial depression near the snout of the glacier to be filled with sea water. This would have evaporated to dryness, with the base of the glacier currently melting on contact with this salt. Freezing of surface sediment would prevent normal subterranean flow, causing a damming of the melted saline water, which would burst in late winter or early spring. Weand et al. (1975) believe that subterranean flow is an important inflow into Lake Bonney, as when lake levels rise, only 40% can be accounted for by surface flow. This theory is supported by Wilson (1979), who states that in calcium chloride type lakes, the salts can be largely derived from groundwater leaching of the surrounding rock. In contrast, the salts in sodium chloride type lakes are likely to be marine in origin. Carlson et al. (1990) support the theory of a marine origin of salts in Lake Bonney. From looking at $^{36}Cl/Cl$ ratios they determined the low ratios in Lake Bonney are due to sea water (relict or marine-derived salts), ground water, or both, in addition to higher ratio meltwater. The low $^{36}Cl/Cl$ ratio of the saline discharge at the Taylor Glacier snout supports Keys (1979) theory that marine evaporites are contributing to Lake Bonney.

2.3.2 OTHER SOURCES

Nishiyama (1979) suggested that the variation in distribution of evaporite minerals may be due to differences during the complex process of evaporation from sea water along with an influence of local topographical and meteorological conditions.

Torii et al. (1979) and Torii and Yamagata (1980) agree with other authors about the trapped sea water theory, though believe that modification of this water cannot be the only explanation for the composition of the salts in the valley. They suggest that the water is significantly modified by the accumulation of atmospheric salts over long periods of time.

Keys and Williams (1981) looked at the presence of salts on the surface as well as in the saline lakes. They concluded that there were two main sources for salts to the valley, these being a marine source and weathering of local rock. An important conclusion made in this work was that different sources are important for different

areas, and no single source can account for all the salts. The importance of marine salts is indicated by the abundance of chloride, sulfate and sodium salts, the widespread distribution of the salts and the strong trends they show (such as sodium levels decreasing away from the coast). Chemical weathering is the main source of ions such as magnesium, calcium and carbonate. These weathering reactions, although proceeding at a slow rate, are the same as normal chemical decay. The high levels accounted for by this can be explained by the long periods over which weathering has occurred (over 4 Ma in places). In the Antarctic environment easily weathered minerals such as pyroxenes will contribute most of the ions. Reactions such as that for pigeonite are common in soils derived from dolerite (Green et al., 1988):

$$(Ca_{0.2}, Mg_{0.9}, Fe_{0.9})Si_2O_6 + 2.2CO_2 + 5.1H_2O + 0.225O_2 \rightarrow$$
$$0.2Ca^{2+} + 0.9Mg^{2+} + 0.45Fe_2O_3 + 2.2HCO_3^- + 2H_4SiO_4$$

The Ca^{2+} and some of the $HCO3^-$ would combine to form $CaCO_{3(s)}$. According to Lyons et al (1998a) the dissolution of evaporite salts within stream channels, along with the weathering of silicate minerals, appears to be an important geochemical process in the valleys, especially those with longer streams.

Green et al. (1988) looked at the chemistry of inflowing streams into Lakes Fryxell, Hoare, Joyce (Pearse Valley) and Miers (Miers Valley) to help determine from where the salts in the lake originated. The most important solute acquisition processes for this flowing water are dissolution of marine-derived salts, dissolution of calcite coatings from chemical weathering of parent rock and direct weathering of silicates. They found that the waters of Pearse Valley are sodium-rich and though the most distant valley from Ross Sea, have a strong marine influence, suggesting that either marine aerosols or past contact with seawater have had an important influence on their chemistry. The streams of the Lake Fryxell system have higher sodium/calcium ratios than the streams derived from Canada and Commonwealth Glaciers with longer streams inflowing from the Kukri or Asgard Range. Lake Fryxell water shows depletion in both potassium and magnesium. The magnesium loss can be explained by the deposition of magnesian calcite, and the potassium loss to reverse weathering

and sulfide mineral precipitation in the sediment pore waters. (Green et al., 1988) believe that the composition of the lakes discussed can be explained largely in terms of present inflow, without invoking relict seawater or other salt sources.

Though chemical weathering in the Dry Valleys is slow, the long time over which it has been operating has allowed it to be a major source of Mg^{2+}, Ca^{2+} and CO_3^{2-} as these ions are rapidly dissolved from soils as liquid water becomes available in the austral summer (Keys and Williams, 1981). The seasonal melt water from alpine glaciers can also supply dissolved material to the lake (Parker et al., 1981).

2.3.3 CHLORINE RATIOS

There are only a few sources of Cl^- to the lakes which are recorded in Table 2.4. The $^{36}Cl/Cl$ ratio can be used to determine where the salts in the valley have come from.

Table 2.4: Sources of Cl^- to Taylor Valley lakes (Carlson et al., 1990).

Source of Cl^-	$^{36}Cl/Cl$ (x 10^{-5})
Glacial melt	100 to 500
Weathering from surficial soils	250 to 450
Deep groundwater	20 to 40
Ancient marine salts	~0 to 10

Carlson et al. (1990) found a low $^{36}Cl/Cl$ ratio of 178 x 10^{-15} in Lake Fryxell that could not be explained by just the addition of atmospheric aerosols and weathering by-products. Two inflows from Commonwealth Glacier have ratios of 828 and 929 x 10^{-5}. The presence of marine-derived salts and sea water could lower the ratios of the lake water relative to the surface inflow.

Lyons et al. (1998b) also used $^{36}Cl/Cl$ ratios to follow the source of the salts. They found that the salt discharge at Blood Falls has a ratio of ~10 x 10^{-5}, which places it in the region of sea water. It is estimated that ~95% of the current Cl^- flux to Lake Bonney comes from Blood Falls. The low ratio of this water will 'dilute' the higher ratio sources, which are dominated by glacial melt water (ie. sea salt aerosol) or surface weathering. The low surface water ratios of Lake Bonney reflect this source. The extremely low ratios in the bottom waters reflect either much older water or salts from a different source, with the low ratios suggesting a marine source.

CHAPTER 3:

FIELD LOCATION AND OBSERVATIONS

3.0 Introduction

This chapter introduces the field area from which carbonate samples were collected. A general field description of the collection areas of Nussbaum Riegel, Sollas Bench and Pearse Valley is made, including maps showing the location of the sample sites within these areas. A description of each sample site is made, along with the description of the hand specimen collected at the site. An outline will also be given of the lake-ice conveyor system and the facies deposited within this model.

3.1 Field Methods

The main aim of the field work was to map the extent of lacustrine carbonates in the vicinity of Nussbaum Riegel, on the Sollas Bench, and through the Pearse Valley and to collect representative samples from these three areas. At Nussbaum Riegel the extent and variation of the carbonates was established by mapping the area. Samples were collected where there were changes in the sedimentology or morphology of the carbonates, and the collection sites were marked by measurement with a GPS (Global Positioning System).

At the Sollas Bench and through Pearse Valley, where the carbonates were part of the till on moraine sequences, samples were collected wherever they were found. Where sites were found with deposits of different lithology and morphology, samples were collected to represent all the types. Again the sample sites were marked with GPS. At one locality, where different horizons were cropping out, a pit was dug through the deposit to enable collection from the depth sequence.

3.2 Field Descriptions

The three sample localities are represented in Figure 3.1.

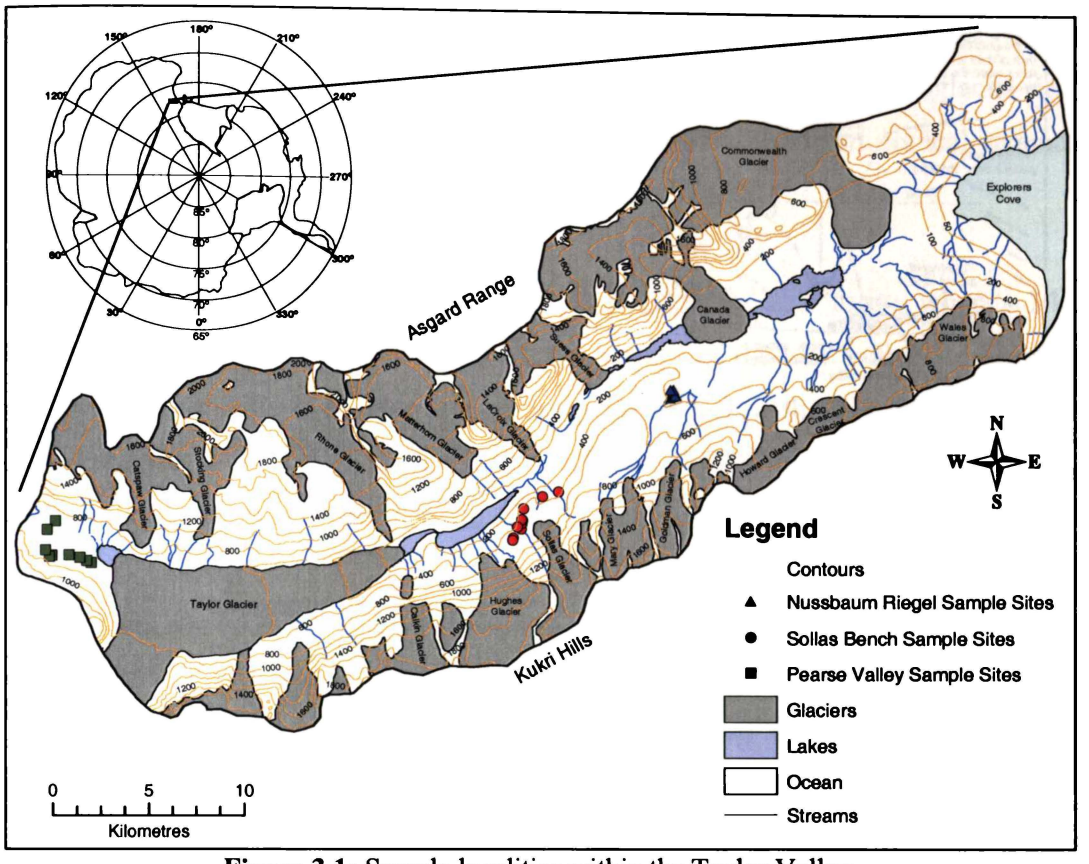

Figure 3.1: Sample localities within the Taylor Valley.

3.2.1 LAKE-ICE CONVEYOR SYSTEM

In Antarctic lakes, where the thickness of the ice is less than the depth of the water column of the lake, incoming solar radiation can hit the sediment/ice interface and cause melting. This causes the annual development of a moat (ice-free zone) around the perimeter of the lake. Where the glacier enters the lake, lines of icebergs are periodically calved off and become locked into the lake ice. This pressure causes the lake ice to move away or relax towards the moat at the opposite end of the lake, moving both the icebergs and sediment along the lake. This was named by Hendy et al. (2000) as the lake-ice conveyor system. The facies model summarising the mechanisms and sediment types of this system is shown in Figure 3.2.

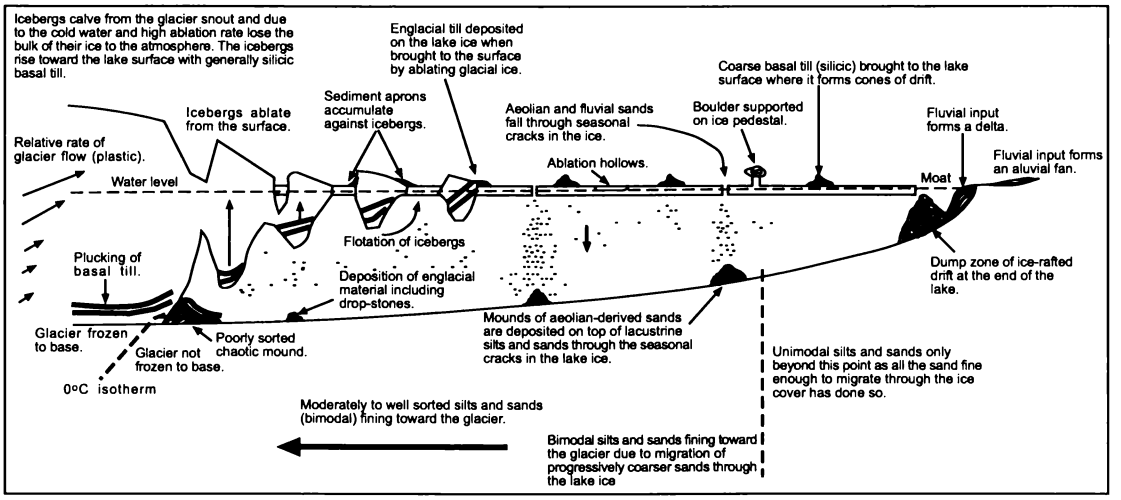

Figure 3.2: The conveyor-belt model of drift deposition from a polar proglacial lake (Hendy et al., 2000).

The regular calving events cause rows of icebergs to be entrained in the lake ice. As the icebergs move away from the glacier front they begin to ablate and release the englacial material either onto the lake surface or directly into the lake water. The material released onto the lake surface forms steep-sided debris cones. As the iceberg ridges disappear, they are replaced by clear lake ice through which the surface sediments are able to melt more readily, as solar radiation can transmit to a greater depth. Only sediment less than 1 mm in size is able to melt through the lake ice (due to balance in heating), giving an apron of fine silt sized material over the lake bottom (Hendy et al., 2000).

The coarse material is slowly moved along the lake surface until it reaches the moat zone, where in the next summer melt it will be deposited as moat drift. This is often in the form of cones deposited by the icebergs. Some of this material can make its way into the sediment earlier by dropping through cracks in the ice (Hendy et al., 2000).

In places rapid glacier movement can cause the lake ice to buckle. This forces ice below the 0°C isotherm, causing it to melt. Any sediment on the surface will fall to the lake bottom, usually in a sinuous ridge parallel to the glacier snout. This material known as unsorted melt-through drift has a variety of grain sizes (Hendy et al., 2000).

Another facies in this proglacial system forms at the ground line of the glacier (where it detaches from the ground and enters the lake). Here any basal and englacial drift melts out of the glacier falling to the lake bottom as a chain on conical mounds (Hendy et al., 2000).

The final facies of this system is that of let-down drift. This forms when a lake eventually drains. Any drift remaining on the surface of the lake will be lowered to the lake bottom. This is usually thin, though can consist of the debris cone. In this case, the patches of silt exposed will deflate more rapidly than the coarser debris, leaving a 'cup and saucer' morphology (Hendy et al., 2000).

When these features are deposited on top of lacustrine carbonate, the carbonate, which normally disintegrates, can be preserved (as in Fig. 3.2). A summary of the proglacial conveyor-belt facies and associated morphologies is recorded in Table 3.1.

Table 3.1: Proglacial conveyor-belt facies and morphologies (Hendy et al., 2000).

Drift Type	Texture	Morphology
Moat drift	Coarse sand to boulders overlying and incorporating lake sediment	Discontinuous cones located slightly below lake level; cones can be aligned to form features that resemble shorelines
Deltas	Sorted, graded gravels, sands and silts with or without cross-bedding	Flat-topped features located at lake level at stream mouths
Grounding-line drift	Sorted to poorly sorted silts to boulders overlying and incorporating lake sediments	Chain of cones located a few hundred meters beyond grounding line
Stress-crack drift	Sorted sands and gravel overlying and incorporating lake sediments	A series of parallel ridges several meters wide, several tens of metres apart
Melt-through drift (sorted)	Sorted fine sand to silt	Bedded sediments thinning away from glacier front
Melt-through drift (unsorted)	Poorly sorted sand to boulders overlying lake sediment	Series of ridges parallel to glacier front beyond grounding line drift areas of lake compression
Let-down drift	Poorly sorted sand to boulders overlying lake sediment	Hummocky drift, possibly cored with lake ice, with dropstones, ridges and low mounds overlying lake sediment; 'cup and saucer' morphology

3.2.2 NUSSBAUM RIEGEL

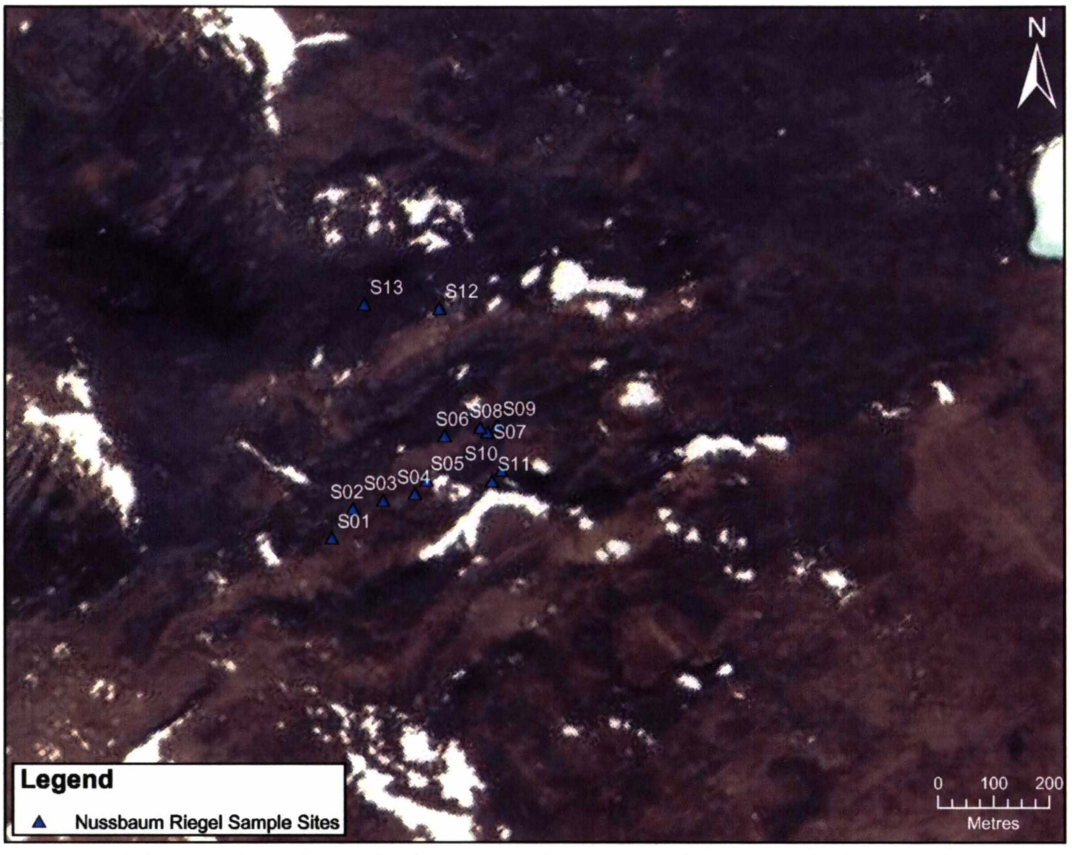

Figure 3.3: Location of sample sites at Nussbaum Riegel. Taylor Glacier is to the west.

At Nussbaum Riegel most of the carbonates are sandy, ranging from plates to knobbly fragments. The locations of samples sites at Nussbaum Riegel are shown in Figure 3.3. The deposits are quite patchy in distribution, though where found, cover much of the surface. The carbonates are underlain by sand and silty lacustrine deposits. They are overlain by inferred lake conveyor deposits (deposition envisaged in the model described in (Hendy et al., 2000)), though the carbonate protrudes from beneath conveyor deposits in places.

The conveyor deposits are comprised of several types of granite, vesicular basalt (sourced from the McMurdo volcanics in the Ross Sea region), basalt (possibly dyke rocks), dolerite and metasedimentary rocks. There is also some coral within the formation in places.

The surface of the till is not highly weathered. There are some well developed dolerite ventifacts and the granites show pitting from variable weathering. The clasts show some fractures but they are not disintegrating. The surface is relatively fresh, being possibly dated as part of MIOS Stage 6.

The landscape is hummocky, with the hills rising from underlying till deposits (Fig. 3.4). The underlying tills are much more weathered, with rocks starting to disintegrate (planed to ground level). Some conveyor deposits are constructional (mounds) and in other places are thin deposits. The larger hills are possibly moraines, and have old till at the top. The streams follow the relief between these hills.

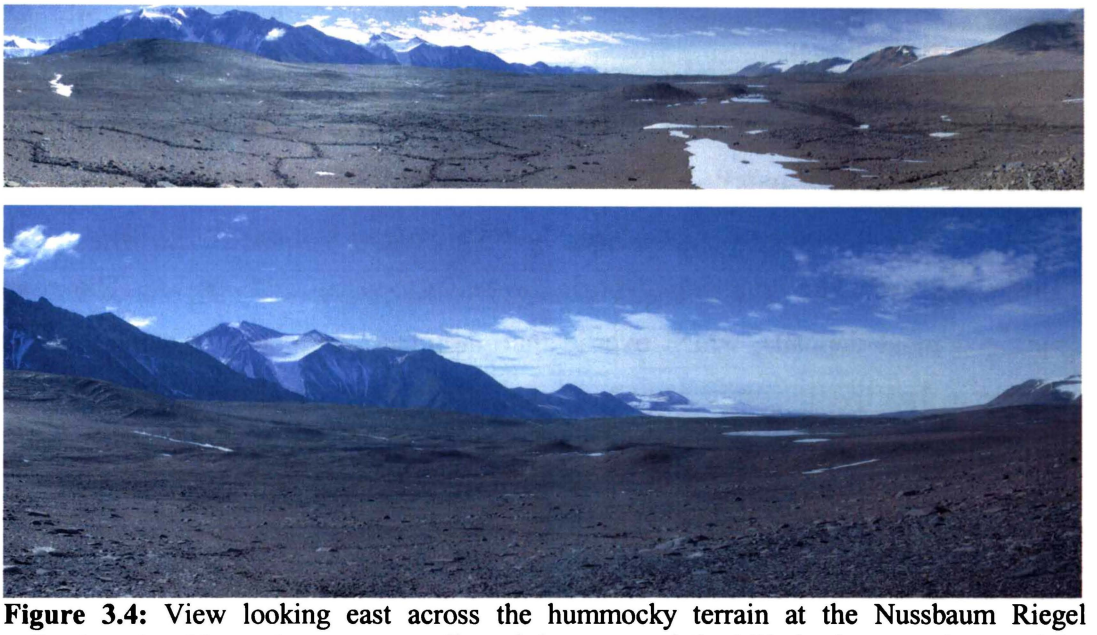

Figure 3.4: View looking east across the hummocky terrain at the Nussbaum Riegel collection site. The carbonate was collected from around the hills in the central part of the photo.

FIELD DESCRIPTION OF SAMPLE SITES AT NUSSBAUM RIEGEL

Following is a description of each site from which carbonate samples were collected. Also included is a brief description of the hand specimens collected at the site. Numbers 0203 refer to the 2002/2003 season in which the samples were collected. This shall be left off the sample numbers in the rest of the chapters for simplicity.

Site 0203S01

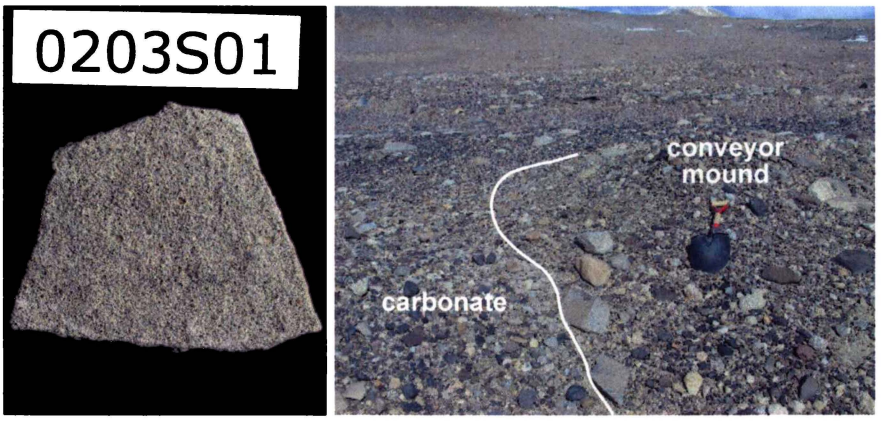

Figure 3.5: Far left: hand specimen of carbonate plates found at site 0203S01; left: site 0203S01, where platy carbonate was exposed from under the overlying conveyor mound. The spade for scale (also in following images) is approximately 110 cm in length.

The carbonate found at this site was platy and had relatively flat upper and lower surfaces (Fig. 3.5a). The plates were ~0.5 cm in thickness and were made up of carbonate cemented detrital material that consists of fine to medium sand. The carbonate plates were found in association with 50 cm to 1 m conveyor mounds. The conveyors deposits overlie the carbonate allowing their preservation. Figure 3.5b shows that around the margins of the conveyor mound the underlying carbonate had been exposed. The conveyor deposits were very sandy with gravel. The coarser grained moat deposits, which overlie that carbonate, were not as sandy and were richer in dark basaltic material.

Site 0203S02

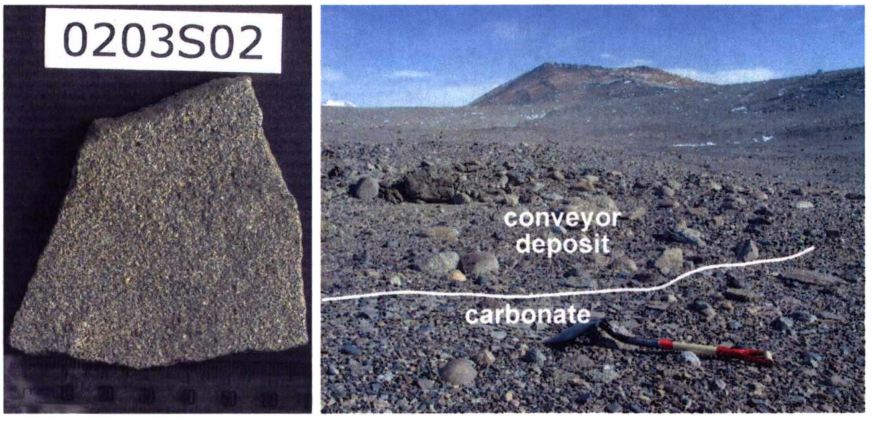

Figure 3.6: Far left: hand specimen of carbonate plates found at site 0203S02; left: site 0203S02, where platy carbonate was exposed from under the overlying conveyor deposits.

The carbonate at this site was platy, with flat upper and lower surfaces (Fig. 3.6a). The detrital material ranged from fine to coarse sand and the plates were on average 0.7 cm in thickness. The carbonate was underlain by a till surface and overlain by conveyor deposits (Fig. 3.6b). When viewed to the west the carbonate deposit was

terminated to the left by a basalt strip. This would have been deposited on top of the carbonate as let-down drift when the lake drained.

Site 0203S03

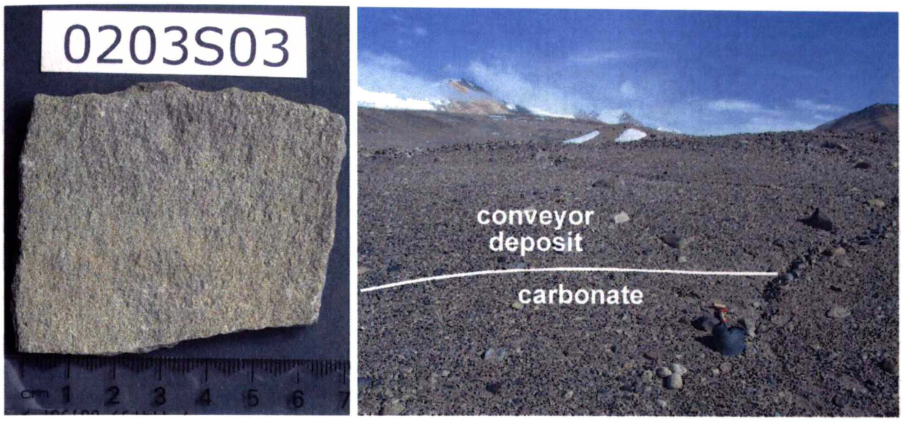

Figure 3.7: Far left: hand specimen of carbonate plates found at site 0203S03; left: site 0203S03, where platy carbonate was exposed from under the overlying conveyor mound.

The carbonate from this site was platy but had irregular surfaces (Fig. 3.7a). In places the edges of the plates were slightly turned-up in places. The plates varied in thickness from ~0.3 to 0.9 cm. The detrital material was very fine to fine sand. The carbonate overlaid sandy sediment that was approximately medium, well sorted sand. The carbonate plates were overlain by conveyor deposits (Fig. 3.7b)

Site 0203S04

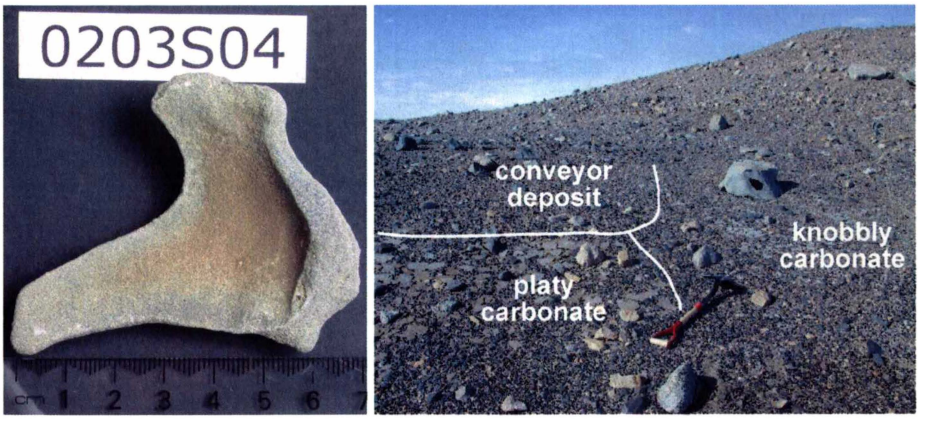

Figure 3.8: Far left: hand specimen of carbonate plates found at site 0203S04; left: site 0203S04, where platy carbonate was exposed from under the overlying knobbly carbonate. Conveyor deposits overlay both of the carbonates.

The carbonate at this site was comprised of irregular plates. The edges were curled up in a manner similar to mud cracks (Fig. 3.8a). The plates vary in thickness from 0.3 cm for much of the area to 0.6 cm along the curling edges. The detrital material is fine sand. The carbonate overlaid an older till surface that was indicated by cavernously weathered boulders. The till was overlain by a sandy, well-sorted, very fine deposit that was rich in basaltic material. The carbonate plates overlay this. At

this site there were two generations of carbonate present. The platy carbonate was overlain by a more knobbly carbonate. All of the carbonate was overlain by conveyor deposits (Fig. 3.8b).

Site 0203S05

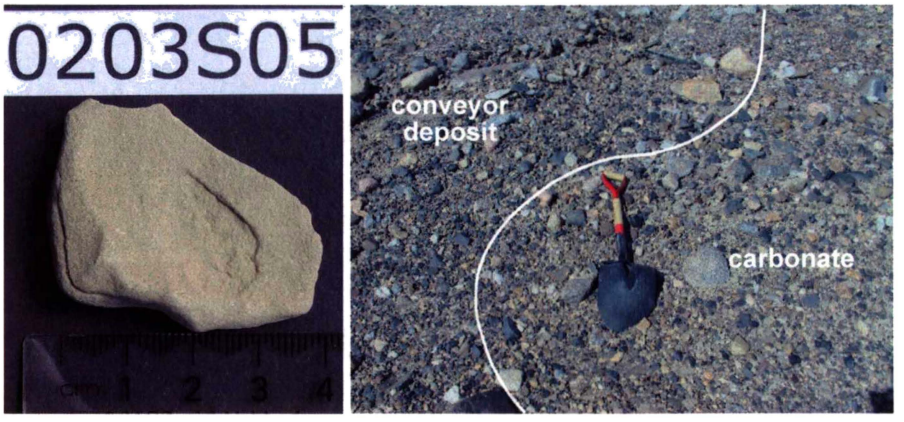

Figure 3.9: (a) Hand specimen of carbonate pieces found at site 0203S05; (b) site 0203S05, where the carbonate was exposed from under the overlying conveyor deposits.

The carbonate at this site comprised irregular pieces that ranged in thickness from 0.3 cm to 1 cm (Fig. 3.9a). The grain size of the detrital material ranged from coarse silt to very fine sand. This site was very close to site S04, but at a slightly higher elevation. The carbonate was overlain by conveyor deposits (Fig. 3.9b) and underlain by coarse silt which graded down into fine sand.

Site 0203S06

Figure 3.10: Above left: hand specimen of knobbly carbonate found at site 0203S06; above right: site 0203S06, where knobbly carbonate was exposed amongst the overlying conveyor deposits.

The carbonate is knobbly in appearance, varying in thickness from 1.5 cm to 3.5 cm (Fig. 3.10a). The carbonate has varying grain size, with layers that are fine sand, while others are very coarse sand to granule. The carbonates also contain gravel sized drop-stones that are mostly pieces of granite. The carbonate layer is underlain by silt.

The carbonate is found scattered amongst conveyor deposits, which would have been deposited on top (Fig. 3.10b).

Site 0203S07

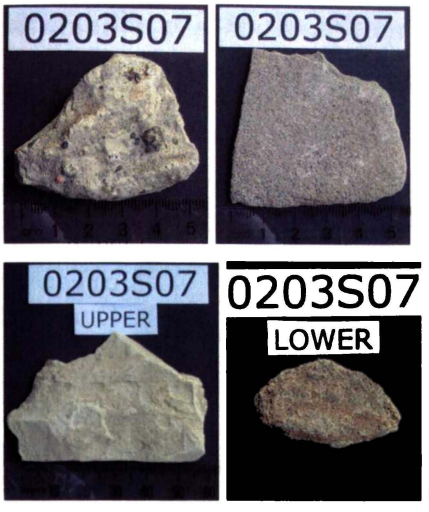

(a)

(b)

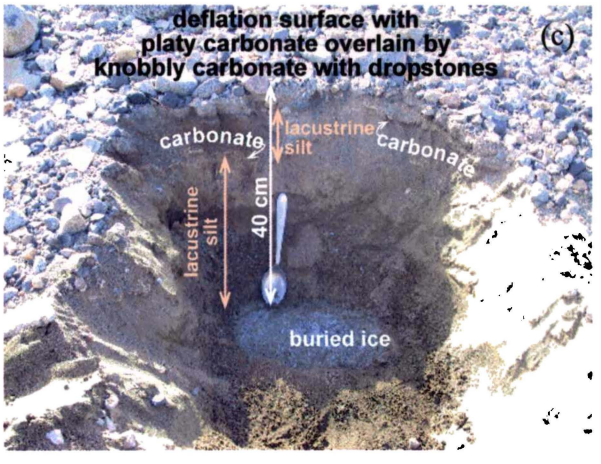

Figure 3.11: (a) Hand specimens of carbonate found at site 0203S07: top left- surface knobbly carbonate; top right- surface platy carbonate; bottom left- upper buried carbonate; bottom right- lower buried carbonate; (b) site 0203S07, plates of carbonate overlain by a small mound of drift, forming the 'cup-and-saucer' morphology typical of let-down drift. The spade for scale is approximately 110 cm in length; (c) the stratigraphy beneath the site.

The carbonate sampled at this site has been protected by a "cup-and-saucer" mound of let-down drift (Fig. 3.11b). Underlying the surface "cup-and-saucer" drift are two carbonates. The upper carbonate is knobbly, at its thickest, being 1.5 cm (Fig. 3.11a). The carbonate has varying grain size, with layers that are fine sand, while others are very coarse sand to granule. The carbonates also contain gravel sized drop-stones that are mostly pieces of granite. The underlying carbonate is platy (Fig. 3.11a). The plates are ~0.4 cm thick and the detrital material is medium sand. A pit dug at the site revealed two layers of subsurface carbonates (Fig. 3.11c). The upper carbonate is thin plate ~ 0.3 cm in thickness. The plates are predominantly very fine sand, but the surface of them has a thin layer of coarse sand. The lower carbonate is made up of

plates that are ~ 0.2 cm thick. The detrital material is medium sand. The two surface carbonates are separated from the subsurface carbonates by a layer of lacustrine silt. The two subsurface carbonates are also separated by lacustrine silt. (Fig. 3.11c). Forty cm below the surface was buried ice (potentially deposited when lake level lowered, stranding the lake ice, the lake refilled and sedimentation occurred over the ice).

Site 0203S08

Figure 3.12: Far left: hand specimen of carbonate plates found at site 0203S08; left: site 0203S08, where knobbly carbonate was exposed on the surface amongst conveyor deposits.

The carbonate at this site was knobbly in appearance, ranging in thickness from 0.3 cm to 2.5 cm in thickness (Fig. 3.12a). The detrital material was predominantly coarse sand, though there were patches of very coarse sand to granule. The carbonate also contained drop-stones that were pebble in size (Fig. 3.12a). The drop-stones ranged in composition from granite pieces, to volcanic rock fragments that appeared to be olivine basalts. Some of the detrital material was comprised of hardened mud clasts. The carbonate is underlain by medium to fine sand and overlain by conveyor deposits.

Site 0203S09

Figure 3.13: Far left: hand specimen of carbonate plates found at site 0203S09; left: site 0203S09, where platy carbonate was exposed amongst overlying conveyor deposits.

The carbonate at this site was platy in nature, with the plate being around 0.5 cm thick. The grain size of the detrital material for the lower 0.2 cm was medium sand. This graded up in to fine sand over the upper 0.3 cm. The carbonate plates at this site were different from other sites, as the surface of the plates was crossed with a series of strips of detrital material that was much coarser than the rest of the sample, being predominantly very coarse sand. These strips also contained small drop-stones that were granule in size. It appears that the coarser material was infilling cracks in the surface of the carbonate. Potentially this carbonate was subaerially exposed and partially dried to form "mud cracks". When the lake level was raised, these cracks were infilled with the coarser material. The carbonate was found on the surface amongst the overlying conveyor deposits (Fig 3.13b).

Site 0203S10

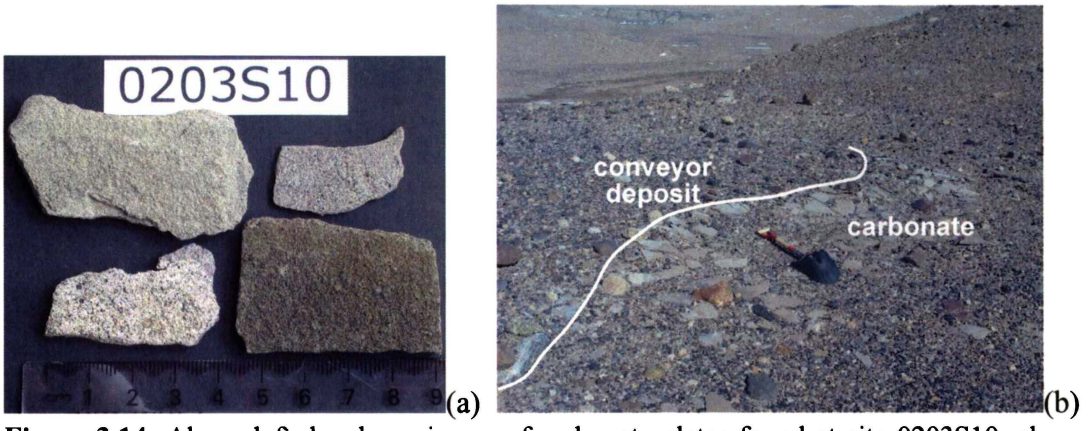

(a) (b)

Figure 3.14: Above left: hand specimens of carbonate plates found at site 0203S10; above right: site 0203S10, where platy carbonate was exposed from under the overlying conveyor mound.

The carbonate at this site was made up of plates that seemed to be made up of individual layers. The plates as a whole were ~1 cm thick. The detrital material of the three lower layers was comprised of medium sand, each layer being ~0.2 cm thick. The upper layer was coarse to very coarse sand and was ~0.4 cm thick. In many places these four layers were not well cemented together, and the plates easily split into their individual layers. The four layers found in the carbonate plate are represented in Fig. 3.14a. The carbonate is underlain by fine sand and protrudes from beneath the overlying conveyor deposits (Fig. 3.14b).

Site 0203S11

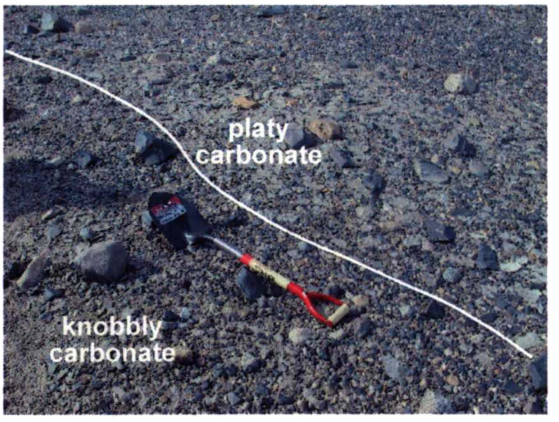

Figure 3.15: Above: hand specimens of carbonate found at site 0203S11; right: site 0203S11, where platy carbonate was exposed from under the overlying knobbly carbonate.

There were two types of carbonate present at this site (Fig. 3.15a). Firstly there were plates that range in thickness from 0.3 cm to 1.2 cm in thickness. The detrital material of the lower 1 cm of the plate was medium sand, while in the upper 0.2 cm it was fine sand. The plates had an uneven upper and lower surface. Also at this site was knobbly carbonate, which at its thickest was around 2.5 cm thick. The detrital material ranged from medium sand to granule. The knobbly carbonates also contained drop-stones that were granule in size and were composed of granite pieces and volcanic rock fragments. The two carbonate layers were underlain by medium sand. The platy carbonate is overlain by knobble carbonate and conveyor deposits overlay both carbonate layers (Fig. 3.15b).

Site 0203S12

Figure 3.16: Far left: hand specimen of carbonate plates found at site 0203S12; left: site 0203S12, where platy carbonate was exposed amongst the surface conveyor deposits.

The carbonate at this site was platy, with rough upper and lower surfaces (Fig. 3.16a). The plates were ~0.5 cm thick. The detrital material was coarse to very coarse sand. The carbonate did not cover a large area at this site (~5 m^2). The carbonate layer was

underlain by medium sand and overlain by a basalt rich conveyor deposit. The site was terminated to the south (left of Figure 3.16b) by a basalt strip.

Site 0203S13

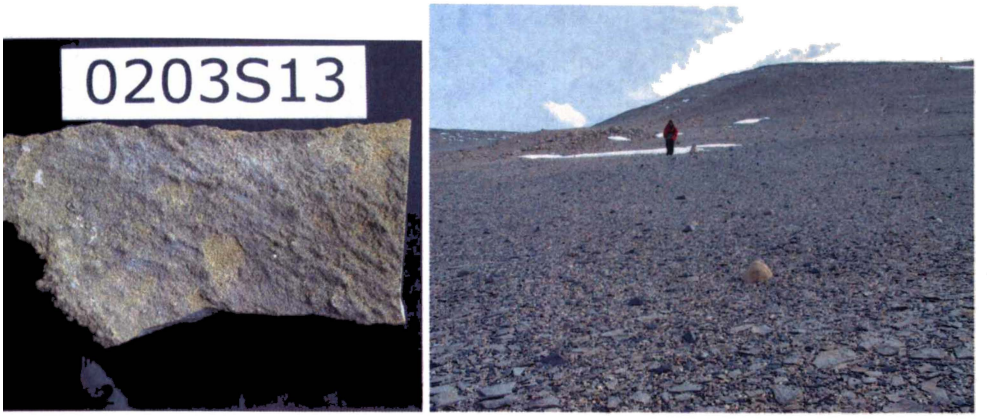

Figure 3.17: Far left: hand specimen of carbonate plates found at site 0203S13; left: site 0203S13, where platy carbonate was exposed on the surface.

The carbonate at this site was made up of irregular plates (Fig. 3.17a). These had small protrusions on the upper and lower surfaces. The plates were ~ 1 cm thick and in places seemed to be splitting along defined planes. There did not appear to be any change in grain size between these boundaries. The detrital material ranges from medium to coarse sand. The carbonate was underlain by coarse sand and was overlain by a thin layer of conveyor deposits. This was the site where carbonate covered the largest surface area. In Figure 3.17b the carbonate covered the entire slope up to the person in the background.

3.2.3 SOLLAS BENCH

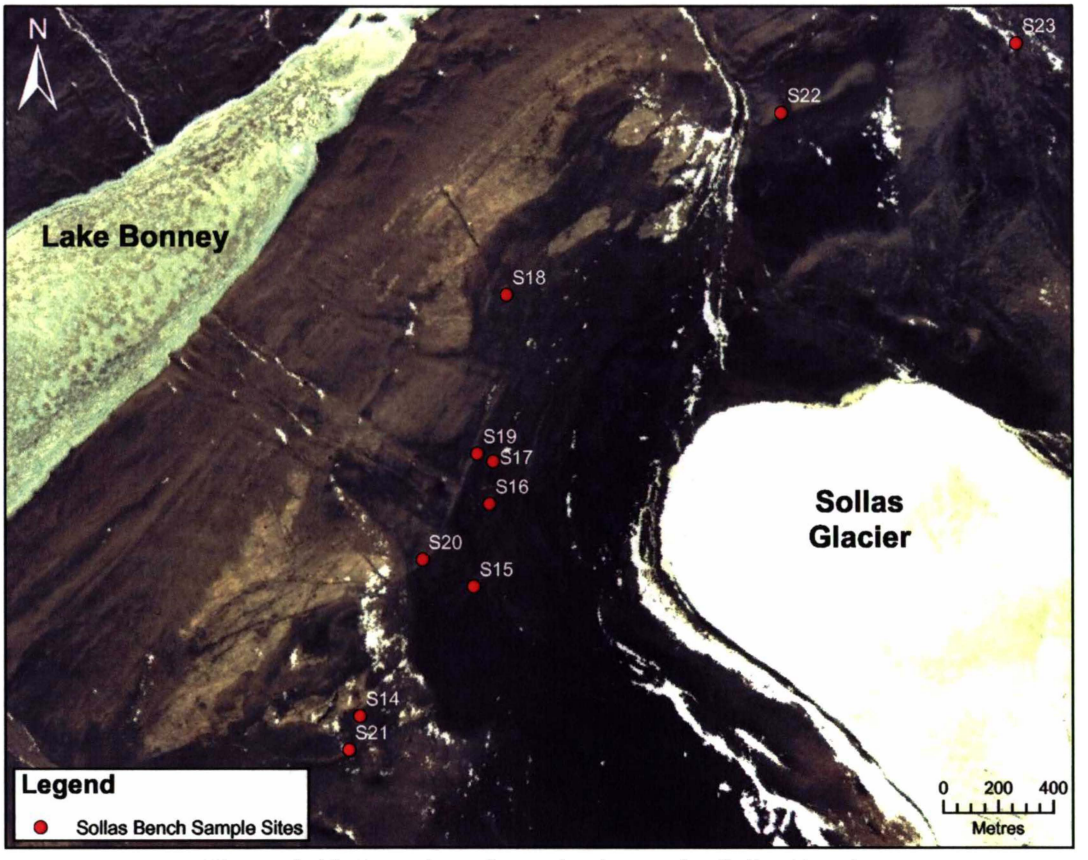

Figure 3.18: Location of sample sites at the Sollas Bench.

At Sollas Bench the carbonate is incorporated into moraines (Fig. 3.18). Most moraines are dominated by granite clasts, which in many places gave the moraines an orange colour due to weathering of the clasts. Many of the moraines also have large pieces of gypsum scattered amongst the carbonate plates (Fig. 3.19). At Sollas Bench the carbonates contain little detrital material, and are mostly in plate form.

Figure 3.19: Examples of gypsum clasts recovered from the Sollas Bench moraines associated with the carbonate deposits.

FIELD DESCRIPTION OF SAMPLE SITES AT SOLLAS BENCH

Site 0203S14

Figure 3.20: Far left: hand specimen of carbonate found at site 0203S14; left: the large moraine mound at site 0203S14 from which the carbonate was collected in the surface till (pack by large boulder for scale).

The carbonate at this site had plates ranging in thickness from 0.5 cm to 2 cm and was comprised of very fine sand. Some of the plates show laminations (Fig. 3.20a). The carbonate was found to be incorporated in the surface till on a moraine (Fig. 3.20b). The moraine was predominantly ground planed granite. There were also small amounts of gypsum in the moraine.

Site 0203S15

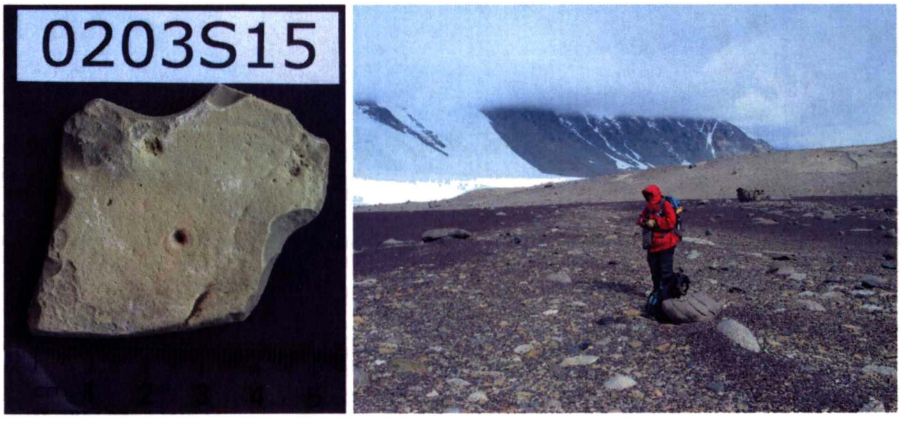

Figure 3.21: Far left: hand specimen of carbonate found a site 0203S15; left: the sinuous moraine at site 0203S15 from which the carbonate was collected.

The carbonate at this site was platy, and ~1 cm thick. The carbonate within the plates was very fine sand size (Fig. 3.21a). The carbonate was collected from the surface of a subdued sinuous moraine (Fig. 3.21b). There was only a small amount of carbonate at this site, but a large amount of gypsum was found. The moraine was partially covered by a basalt fan from a small scoria cone.

Site 0203S16

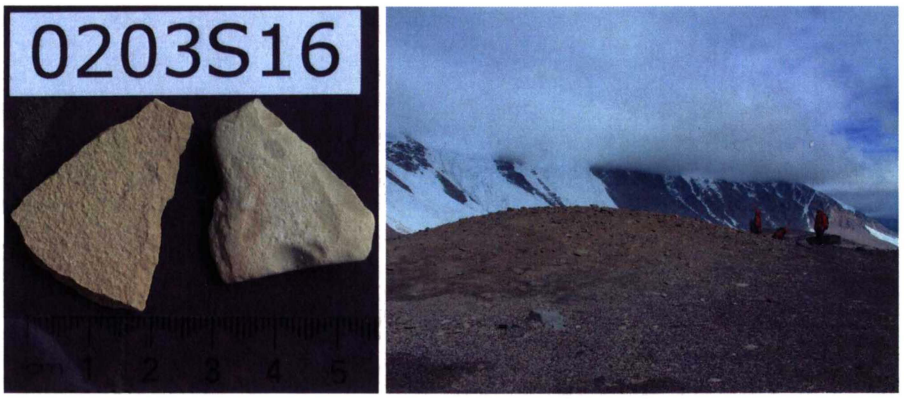

Figure 3.22: Far left: hand specimens of carbonate found at site 0203S16; left: the isolated moraine mound at site 0203S16 from which the carbonate was collected in the surface till.

Two morphological types of carbonate were found at this site. The first were plates that were ~0.7 cm thick and comprised of fine sand (Fig. 3.22a; left). The second were lighter coloured plates that were ~1 cm thick and very fine sand, with a more irregular surface (Fig. 3.22a; right). The carbonate and gypsum were collected from an isolated moraine mound (Fig. 3.22b). The orange colour of the moraine is due to weathering of granite.

Site 0203S17

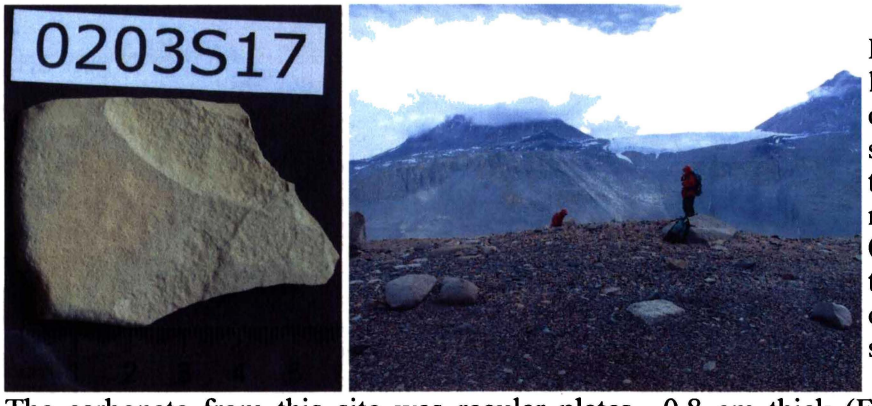

Figure 3.23: Far left: hand specimen of carbonate found at site 0203S17; left: the small moraine mound at site 0203S17 from which the carbonate was collected in the surface till.

The carbonate from this site was regular plates ~0.8 cm thick (Fig. 3.23a). They graded from medium sand in the top 0.15 cm to very fine sand at the top of the plates. A small amount of carbonate was collected from a moraine mound (Fig. 3.23b). Thin flakes of gypsum were also found, though these could have been wind blown.

Site 0203S18

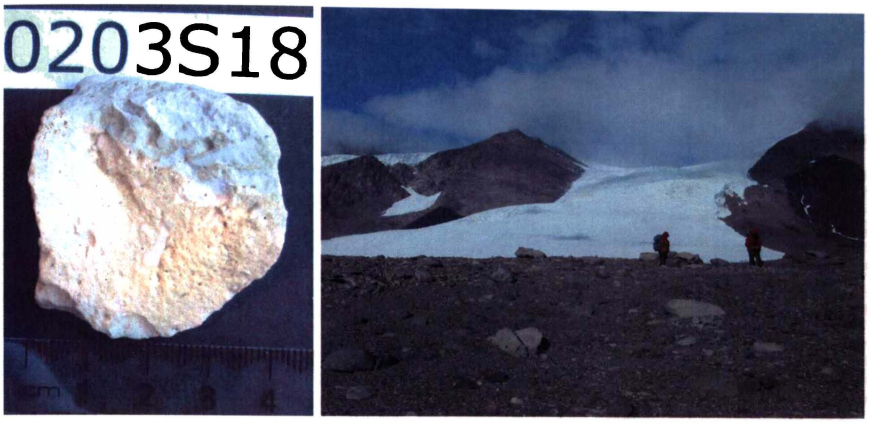

Figure 3.24: Far left: hand specimen of carbonate found at site 0203S18; left: the large moraine mound at site 0203S18 from which the carbonate was collected in the surface till.

The carbonate at this site was irregular clasts up to 2.5 cm thick and very fine sand. The carbonate contained pieces of lighter coloured carbonate, which can be observed on the surface of the clast in Figure 3.24a. Carbonate was collected from a small patch of orange moraine (Fig. 3.24b). The carbonate is knobbly rather than platy.

Site 0203S19

Figure 3.25: Far left: hand specimen of carbonate found at site 0203S19; left: the sinuous moraine at site 0203S19 from which the carbonate was collected in the surface till.

There was a range of carbonate found at this site. Firstly there were plates that were ~0.8 cm thick and comprised of fine sand (Fig. 3.25a). Secondly there were irregular pieces that were very white and comprised of very fine sand. Then there were thin plates ~ 0.3 cm thick that had very irregular surfaces and were medium to coarse sand. These plates contained drop-stones. Lastly there was one piece that contained very fine laminations less than a millimeter thick for the lower 0.8 cm of the samples, while the upper 0.4 cm had no laminations, but contained many pore spaces. Gypsum and carbonate were collected from a sinuous moraine (Fig. 3.25b). The weathering of granite gave the moraine an orange colour. The moraine surface had boulders planed

to ground level indicating advanced weathering, while in some places there was cavernous weathering of the granite indicating intermediate weathering.

Site 0203S20

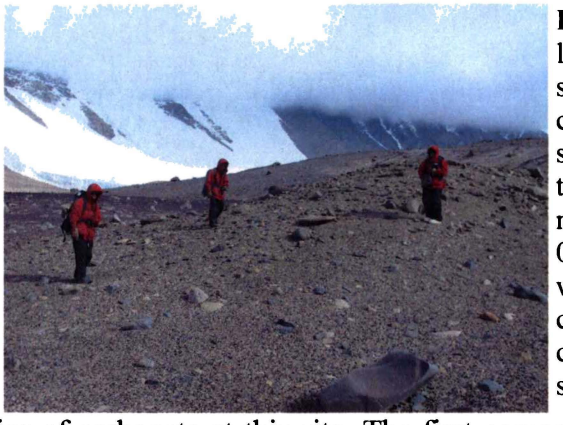

Figure 3.26: Far left: hand specimen of carbonate found at site 0203S20; left: the large moraine mound at site 0203S20 from which the carbonate was collected in the surface till.

There were two morphologies of carbonate at this site. The first comprised plates ~ 1.2 cm thick and comprised of medium sand (Fig. 3.26a). These plates contained laminations that were different in colour, but not grain size. The second type of carbonate was irregular pieces that were very white and made up of fine sand. The carbonate and gypsum were collected from a sinuous moraine (Fig. 3.26b). This moraine crossed the moraine of site S19, but was a different moraine. Again the moraine was orange from weathering of granite.

Site 0203S21

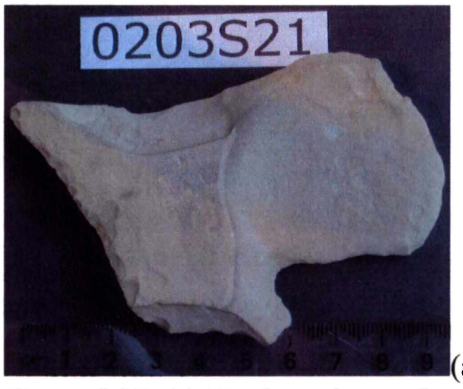

(a)

(b)

Figure 3.27: (a) Hand specimen of carbonate found at site 0203S21; (b) the large moraine mound at site 0203S21 from which the carbonate was collected in the surface till.

The carbonate at this site was comprised of irregular plates that were up to 1.4 cm thick and made up of fine sand (Fig. 3.27a). Carbonate and gypsum was collected from a sinuous moraine that crossed perpendicular to the moraine of site S14 (Fig.

3.27b). The till showed a mix of weathering with some boulders planed to the ground, while others were intact.

Site 0203S22

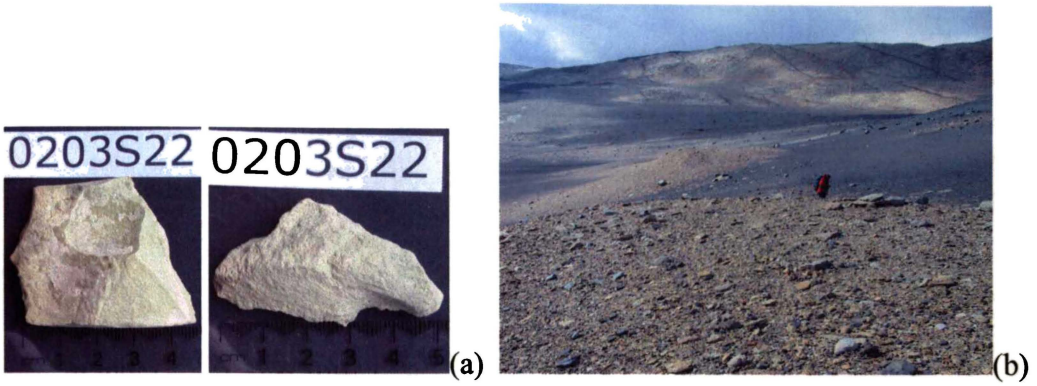

Figure 3.28: (a) Hand specimens of carbonate found at site 0203S22; (b) the large moraine mounds at site 0203S22 from which the carbonate was collected in the surface till.

There were two carbonate morphologies found at this site. The first was comprised of plates up to 1.8 cm thick and made up of medium sand (Fig. 3.28a; left). The second was irregular pieces ~ 1.2 cm thick that were made up of very fine sand (Fig. 3.28a; right). These carbonate clasts were lighter in colour than others found at Sollas Bench. The carbonate was collected from large moraine mounds (Fig. 3.28b). These were situated west of Sollas Glacier and below a volcanic cone.

Site 0203S23

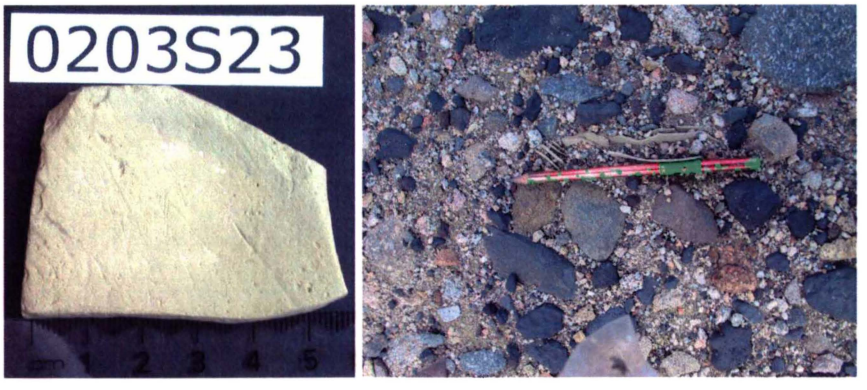

Figure 3.29: (a) Hand specimen of carbonate found at site 0203S23; (b) carbonate plates found in the surface till at site 0203S23. Pencil for scale is approximately 14 cm in length.

The carbonate plates collected from this site were ~0.8 cm thick and comprised of fine sand (Fig. 3.29a). There were also plates that were much whiter and finer in grain size. The carbonate was collected from a till surface. The plates potentially could be *in situ*, with frost action having worked the plates out of the ground into a vertical

position. The carbonate was sampled beside a stream channel at the lowest extent of a field of large cavernously weathered boulders.

3.2.4 PEARSE VALLEY

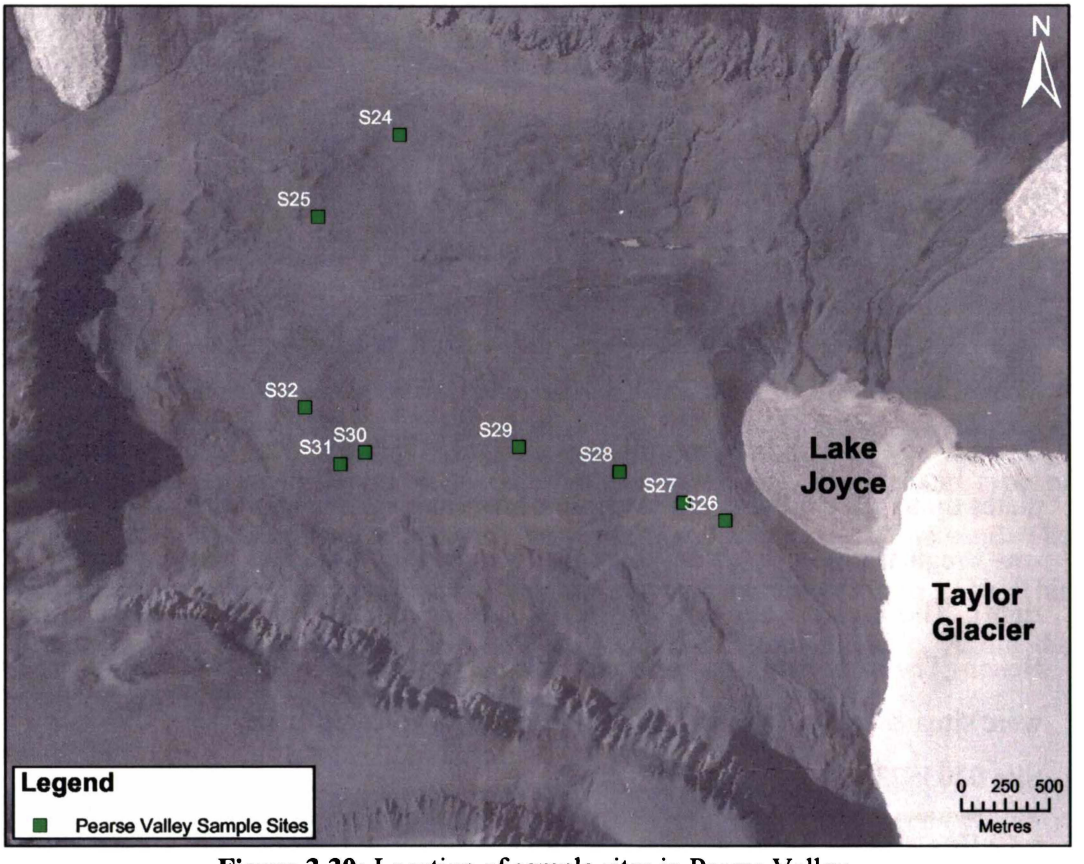

Figure 3.30: Location of sample sites in Pearse Valley.

In Pearse valley, as with the Sollas Bench, the carbonate was incorporated in the surface till of moraines (Fig. 3.30). The moraines were much less subdued than in other parts of Taylor Valley, being up to several metres high. The more subdued moraine form is the most common in Antarctica, as frozen base glaciers entrain very little sediment. This results in only small moraines developing. This is in contrast to moraines of temperate "wet" glaciers, which entrain much sediment, resulting in moraines many metres in height. As at the Sollas Bench, the carbonates were very clean (little detrital material) and were mostly in plate form.

FIELD DESCRIPTION OF SAMPLE SITES IN PEARSE VALLEY

Site 0203S24

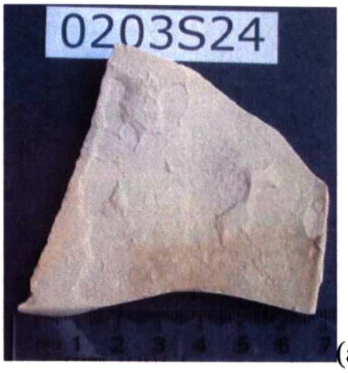

(a)


(b)

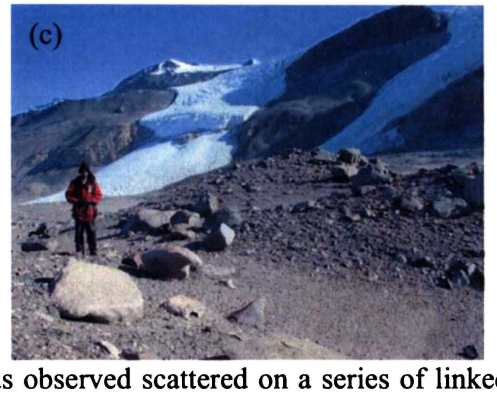

Figure 3.31: (a) Hand specimens of carbonate found at site 0203S24; (b & c) the series of linked moraine mounds at site 0203S24 from which the carbonate was collected in the surface till.

The carbonate from this site was platy, being ~ 0.4 cm thick and comprised of medium sand (Fig. 3.31a). The carbonate was observed scattered on a series of linked large moraine mounds (Fig. 3.31 b&c). The rocks were exfoliating, with some planed to ground level, while some were cavernously weathered. The moraine was dominantly dolerite, with some granite.

Site 0203S25

(a)


(b)

Figure 3.32: (a) Hand specimen of carbonate found at site 0203S25; (b) the large moraine mound at site 0203S25 from which the carbonate was collected in the surface till.

The carbonate at this site was made of small pieces ~ 1 cm thick and comprised of fine sand (Fig. 3.32a). The carbonate was collected from the surface till of a series of

recessional moraines that appeared to be recessional to the large moraine of site S24 (Fig. 3.32b). The moraine was predominantly composed of dolerite clasts along with cavernously weathered granite. The carbonate at this site was very scattered.

Site 0203S26 to 0203S32

Figure 3.33: (a) Hand specimens of carbonate found from sites 0203S26 to 0203S32; collected from along the southern margin of Pearse Valley.

The carbonate clasts collected from sites 0203S26 through to 0203S32 were collected by other members of the field party and hence have no associated site photos. The carbonate was collected from a till surface with a mixed lithology of granite, beacon sandstone, and dolerite. The weathering was strong, with cavernously weathered granite and ventifacts.

3.3 FIELD INTERPRETATION OF DEPOSITS

- **NUSSBAUM RIEGEL**

The samples collected from Nussbaum Riegel were *in situ* deposits that covered large portions of the ground surface. The deposits were composed predominantly of volcanic clasts cemented by carbonate. From the morphology and sedimentology of the carbonate plates, it is likely that there were several generations of cementation. Some sites had plates that were knobbly in appearance and contained granite dropstones. These were distinct from other sites where the carbonates were flat plates that contained only alkaline volcanic material and no granitic or metasedimentary material.

At site 7 there was a moat deposit with a cup and saucer morphology. On the surface around the margins of the mound there were three distinct morphologies of carbonate plates. There was knobbly carbonate with granite dropstones, and two platy carbonates with different thicknesses. A pit (Fig. 12h) showed two layers of carbonate, one near the surface, and one further down. The absence of the knobbly carbonates beneath the surface possibly means that they are part of a deflated deposit left on the surface. If this is the case, the knobbly deposits represent a younger generation of carbonate precipitation than for the flat plate-like deposits. The carbonate layers were ultimately only preserved if other lacustrine deposits were laid on top. These would either have resulted from continued sedimentation of lacustrine silts and sands, or the deposition of conveyor deposits from the lake-ice conveyor system. Many of the deposits were likely to be preserved with the final draining of the lake and the deposition of let-down drift.

- **SOLLAS BENCH**

The samples collected from Sollas Bench were not *in situ*, but were incorporated into the surface till on moraines. These moraines were likely to have been deposited during expansion of the Taylor Glacier. The carbonates at this site were all comprised of flat plates and associated with large pieces of fishtail gypsum. It is likely at this site that the Taylor Glacier advanced through a lateral or proglacial lake in which the carbonate was being deposited. The varying appearance of the carbonate could be due to bulldozing of several layers of carbonate deposited in the lake, which were then all incorporated into moraines by the advancing glacier.

- **PEARSE VALLEY**

The Pearse Valley carbonates were also part of a moraine sequence. In this valley, the existing proglacial Lake Joyce is an example of a lake through which the Taylor Glacier could advance and incorporate the lake sediments along its lateral and terminal moraines. As with the Sollas Bench samples, the varying morphology of the carbonate could have been due to multiple generations of carbonate deposition in the proglacial lake that were later incorporated into the Taylor Glacier and deposited in moraines.

CHAPTER FOUR:

SCANNING ELECTRON MICROSCOPIC AND X-RAY DIFFRACTION ANALYSES

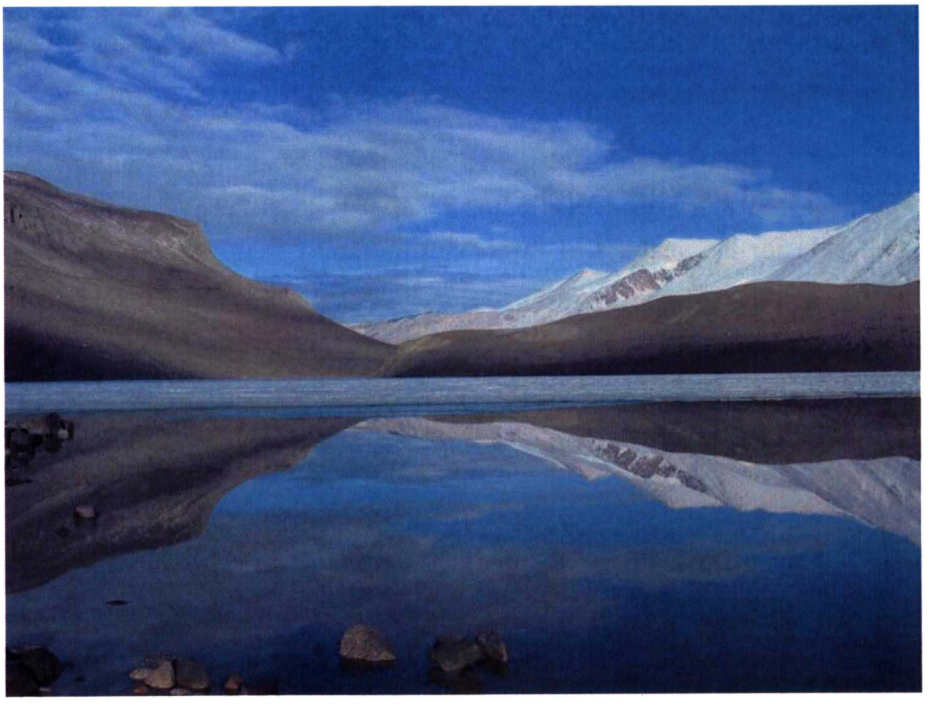

4.0 INTRODUCTION

This chapter investigates the mineralogy of the carbonates collected from Nussbaum Riegel, Sollas Bench and Pearse Valley by interpretation of their XRD (x-ray diffraction) diffractograms using the method of Smith and Nelson (1993). The information gathered on their mineralogy in this way has been compared with the crystal morphology by examination of SEM (scanning electron microscope) images. The information gathered is used to determine the origin of the crystal morphology observed. The controls on the mineralogy of the carbonate samples will be addressed in chapter five (trace element chemistry).

4.1 METHODS

4.1.1 X-RAY DIFFRACTION ANALYSIS (XRD)

Carbonate samples collected from the Taylor Valley were analysed by X-ray diffraction to determine their aragonite-calcite ratios.

The method used for XRD analysis was developed by Smith and Nelson (1993), and is applicable for the analysis of carbonates. Samples were ground in a ring mill to <200 μm and the resulting powder was back-filled into Philips aluminium sample holders. This avoids any direct pressure or handling of the powder face being exposed to the x-rays. It also produces a face of unoriented crystals, which is necessary for quantitative analysis.

Analyses were carried out on a Philips XPERT PW 3046/00 X-ray diffractometer using copper K α radiation (λ = 1.54Å) at 1600 W. The flat surface of the unoriented powder mount was scanned from 25 to 33 °2θ. Smith and Nelson (1993) developed a standard curve that relates mineral abundance to peak intensity, from known mixtures of powdered aragonite and calcite. This curve (Fig. 4.1) was used to determine the aragonite-calcite ratio.

Each trace is graphically examined to determine the exact location of the calcite [110], and both aragonite [021] and [111] peaks and their peak heights were measured.

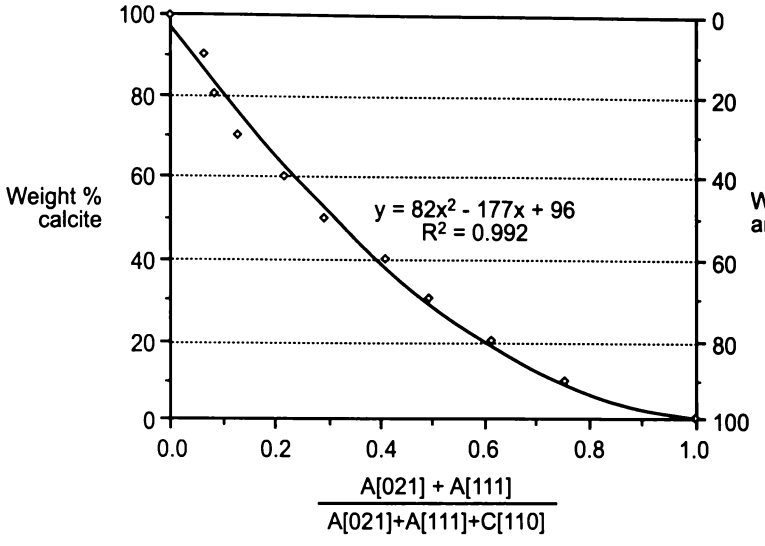

Figure 4.1: Graphical determination of aragonite-calcite content (Smith and Nelson, 1993).

- **Carbonate Percentage**

Additionally, the $CaCO_3$ percentage was calculated dissolving a known weight of powdered sample in 30 ml of ~10% (v/v) analytical grade HCl and run through the auto tritrator against ~10% (v/v) analytical grade NaOH. Preweighed filter papers were used to filter the samples before analysis, and the percentage $CaCO_3$ was determined by weight difference and compared with the results obtained by back titration.

4.1.2 SCANNING ELECTRON MICROSCOPY (SEM)

SEM can be useful in providing an insight into the crystallisation patterns of calcite and aragonite by looking at the crystal morphology and orientation. SEM analysis can also give information into the degree of weathering of a sample and in the case of lacustrine samples, show the presence of biological structures such as those in diatoms and algae.

Small pieces of samples were mounted on carbon tape on stubs, which were then coated with platinum-palladium by a Hitachi E-1030 Sputter Coater to make them

conductive. The samples were then analysed with a Hitachi S-4000 Field Emission Scanning Electron Microscope.

4.2 RESULTS AND DISCUSSION

4.2.1 XRD

Along with the diffractograms from the XRD analyses, charts showing the main peak heights and the background reading were produced. In combination, these were used to determine the heights of the A(021), A(111) and C(110) peaks. These values were used to determine the aragonite/calcite (arag/cal) ratio, by way of the graph in Figure 4.1. Three representative examples of the diffractograms are shown in Figure 4.2. A summary of the arag/cal ratio and carbonate percentage is shown in Table 4.1.

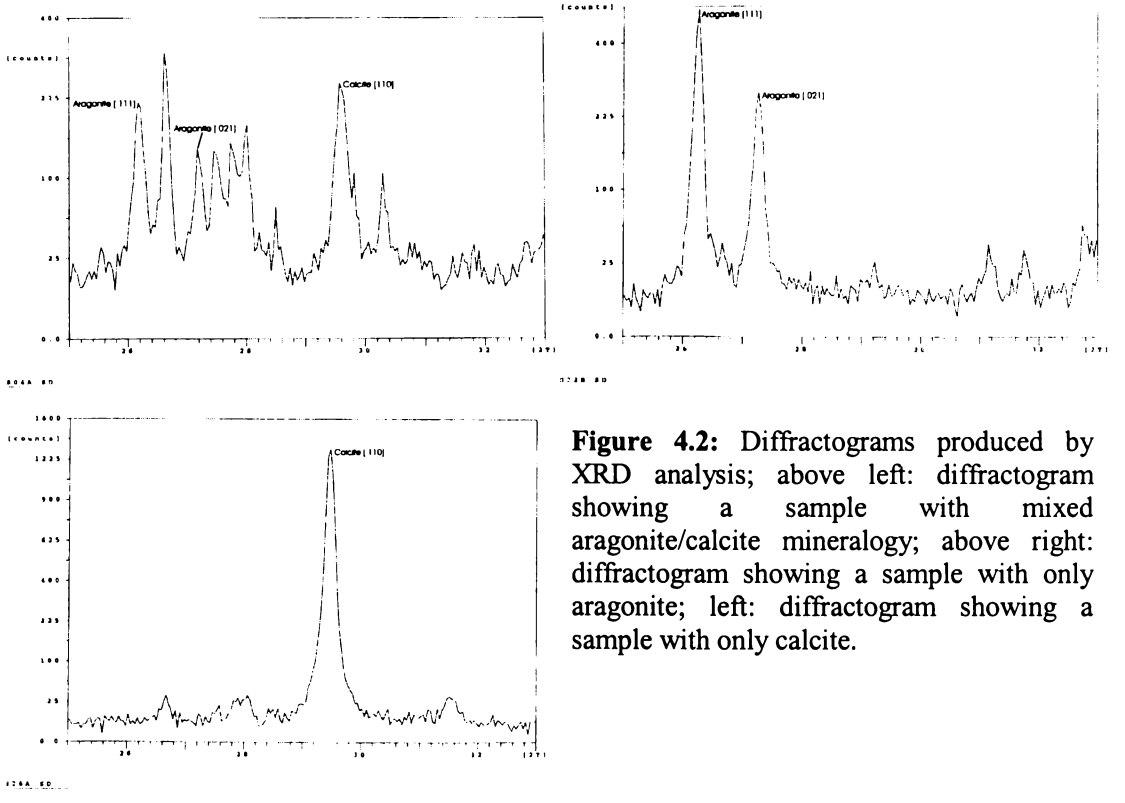

Figure 4.2: Diffractograms produced by XRD analysis; above left: diffractogram showing a sample with mixed aragonite/calcite mineralogy; above right: diffractogram showing a sample with only aragonite; left: diffractogram showing a sample with only calcite.

Table 4.1: Carbonate percentage and aragonite/calcite (arag/cal) ratio for Nussbaum Riegel, Sollas Bench and Pearse Valley samples.

Nussbaum Riegel			Sollas Bench			Pearse Valley		
	carbonate %	arag/cal		carbonate %	arag/cal		carbonate %	arag/cal
S01a	40	0.49	S14a	84	1.00	S24a	75	0.98
S02a	44	0.04	S14b	83	1.00	S25a	79	1.00
S03a	40	0.70	S15a	84	0.99	S26a	91	0.02
S04a	43	0.58	S16a	86	0.99	S27a	96	0.96
S05a	34	0.67	S17a	79	0.99	S27b	87	0.88
S06a	31	0.88	S18a	89	1.00	S27c	96	0.91
S07a	46	0.93	S19a	89	1.00	S28a	87	0.95
S07b	45	0.99	S20a	80	1.00	S29a	-	-
S07La	54	0.97	S21a	81	0.99	S30a	76	-
S07Ua	48	0.94	S22a	73	0.97	S31a	90	0.96
S08a	48	0.90	S22b	88	1.00	S32a	93	0
S09a	50	0.92	S23a	91	1.00			
S10a	43	0.97						
S11a	43	0.95						
S11b	53	0.96						
S12a	41	0.39						
S13a	44	0.70						

From the carbonate percentage the samples can be split into detrital rich and detrital poor carbonate. Samples from Nussbaum Riegel average 44% carbonate, whereas the Sollas Bench and Pearse Valley samples are much more pure, with an average of 84% and 87% carbonate, respectively.

As observed in the XRD diffractograms in Figure 4.2 and the arag/cal ratio in Table 4.1, there are three main groups of mineralogies for the carbonate in the samples. The first group have mixed mineralogy, with carbonate in the form of both calcite and aragonite, and were mainly found at Nussbaum Riegel. The next group have a mineralogy that was predominantly aragonite, and were found at all three locations. Finally there are samples that consist of entirely calcite, which were found only in the Pearse Valley.

4.2.2 SEM

When the SEM images from the three sample sites were examined, they showed a wide range in crystal morphology both between and within the collection locations.

4.2.2.1 NUSSBAUM RIEGEL

The SEM images captured from the Nussbaum Riegel samples show that they consist of carbonate cemented detrital material. A common component of the detrital material is glass shards, many of which are vesicular. Examples of these are illustrated in Figure 4.6 B and R. Despite XRD indicating that many of these samples are of mixed mineralogy, with both calcite and aragonite making up the cement, it was difficult to distinguish these in the SEM images. Many of the samples containing both aragonite and calcite have acicular or fibrous crystal morphology throughout the sample, indicating that both carbonate forms exhibit similar crystal morphologies (Fig. 4.6). The carbonate cement could have precipitated during freezing or evaporation of pore waters following a drop in lake level.

Also observed in the samples from Nussbaum Riegel were sponge spicules (Fig. 4.3), recognised by their characteristic parallel-sided internal canal. The presence of sponge spicules supports an argument for the carbonates having been deposited in a palaeo lake proglacial to an expanded Ross Ice Sheet (discussed in chapter 6). The sponge spicules would have been sourced from marine sponges, before being entrained in the grounded ice and deposited into the lake environment by the lake-ice conveyor system.

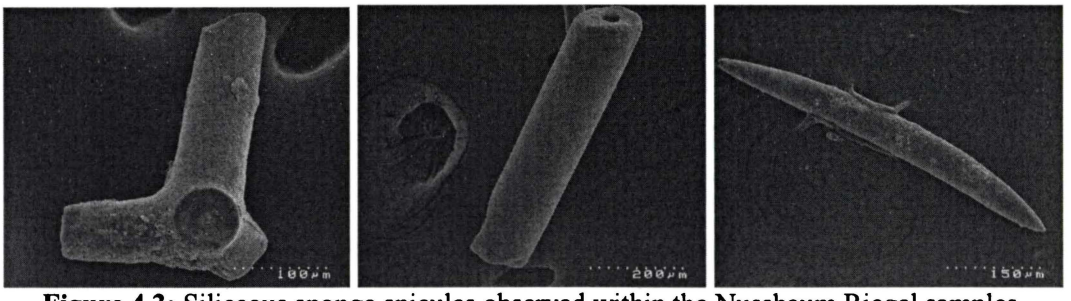

Figure 4.3: Siliceous sponge spicules observed within the Nussbaum Riegel samples.

Figure 4.4 records SEM images from the samples collected at Nussbaum Riegel.

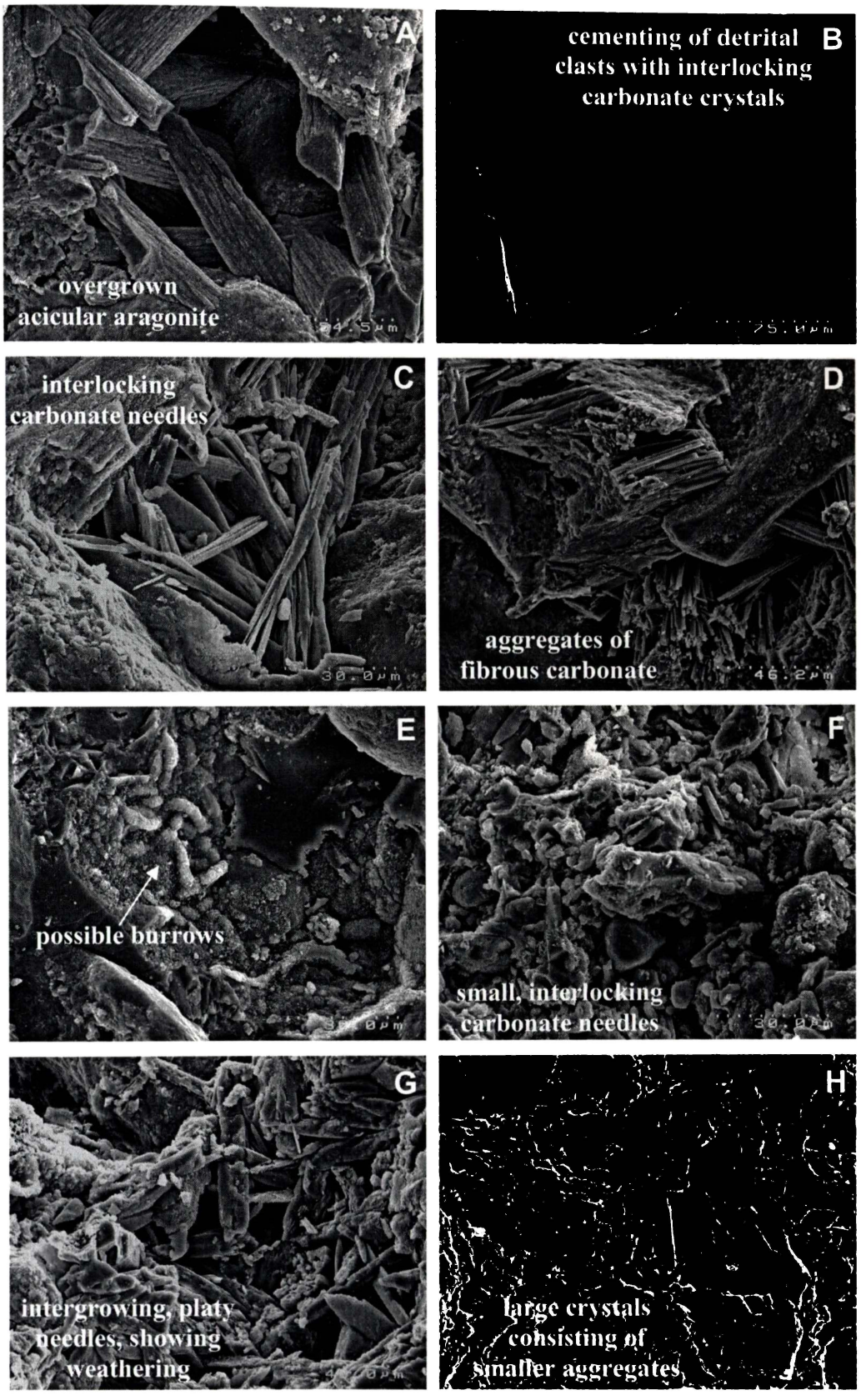
A
overgrown
acicular aragonite
B
cementing of detrital
clasts with interlocking
carbonate crystals
C
interlocking
carbonate needles
D
aggregates of
fibrous carbonate
E
possible burrows
F
small, interlocking
carbonate needles
G
intergrowing, platy
needles, showing
weathering
H
large crystals
consisting of
smaller aggregates

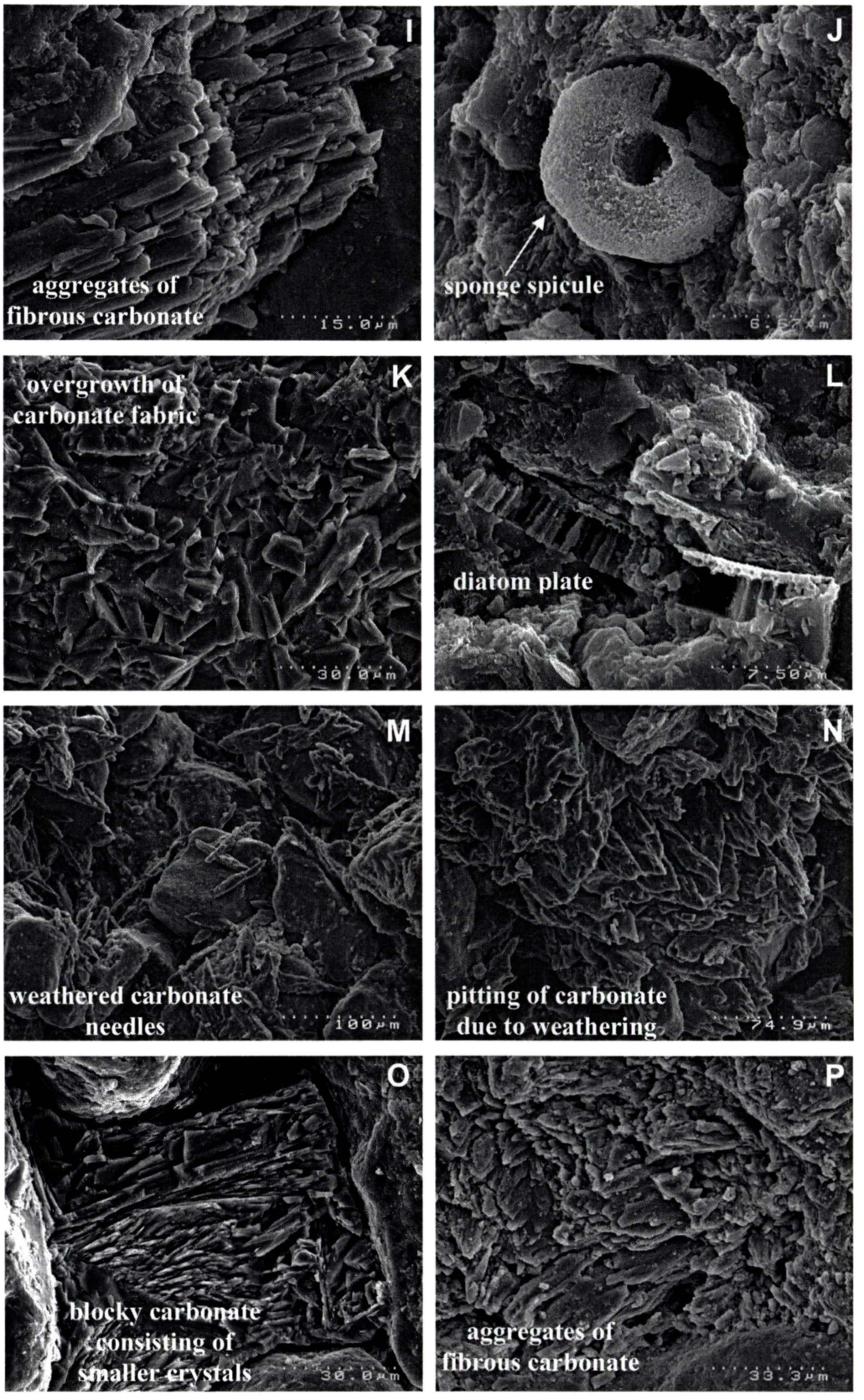
I
aggregates of
fibrous carbonate
15.0µm
J
sponge spicule
6.67µm
K
overgrowth of
carbonate fabric
30.0µm
L
diatom plate
7.50µm
M
weathered carbonate
needles
100µm
N
pitting of carbonate
due to weathering
74.9µm
O
blocky carbonate
consisting of
smaller crystals
30.0µm
P
aggregates of
fibrous carbonate
33.3µm

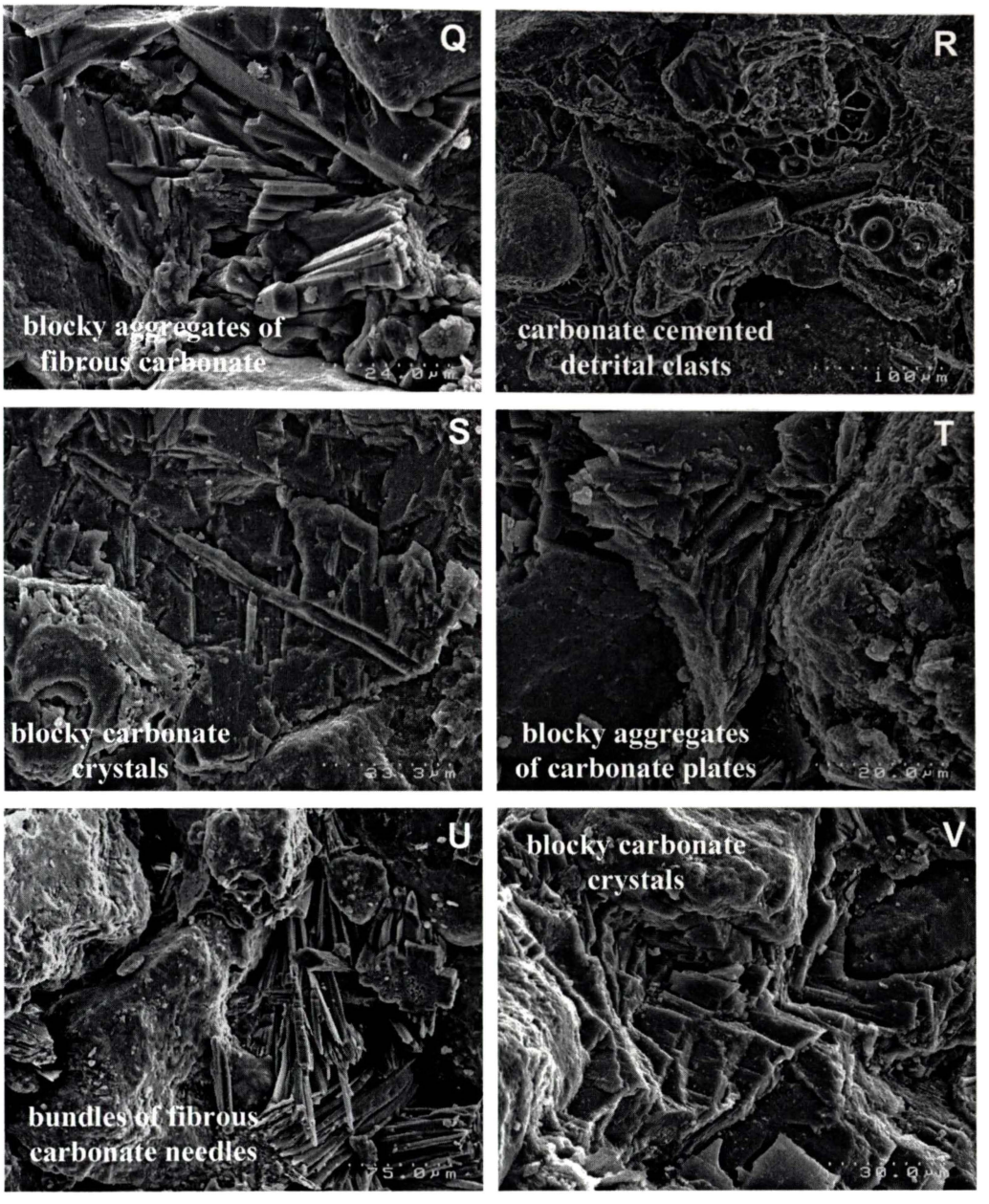

Figure 4.4: SEM images of carbonate samples collected from sites at Nussbaum Riegel. The descriptions of crystal morphology and the site where the sample was collected are recorded in Table 4.2.

Table 4.2: Description of crystal morphologies found within SEM images of samples collected from Nussbaum Riegel.

Image	Site	Description
A	S01a	The sample is acicular aragonite, possibly with overgrowths of calcite. This would have formed by aragonite precipitating first, followed by the calcite. Many of the crystals also show intergrowth. There is a large amount of pore space between the cement crystals.
B	S02a	This sample contains detrital clasts cemented with interlocking fine calcite crystals. There is little pore space when compared to other

		samples.
C	S03a	This sample contains inter-growing plates and needles of aragonite and calcite. Both the aragonite and calcite show fibrous crystal morphology.
D	S04a	The sample contains large carbonate crystals made up of aggregates of fibrous carbonate crystals.
E	S04a	This indicates possible evidence of biological activity in the form of burrows.
F	S05a	There are small needles of carbonate that showed little intergrowth. The fabric of the sample is very open, with many pore spaces.
G	S06a	The carbonate is intergrowing platy needles. These show a degree of weathering, with many having rough surfaces and ragged crystal ends.
H	S07a	This sample contained large carbonate crystals that were aggregates of fibrous crystals. The samples had very little pore space.
I	S07a	This is a magnification of the samples in image H, showing the aggregates of fibrous carbonate.
J	S07b	This shows the end of a sponge spicule, indicated by the characteristic internal canal.
K	S07Ua	The carbonate in this sample shows a large amount of overgrowth, which almost obscures the original crystal fabric.
L	S07Ua	This potentially is a cross section of a diatom plate, indicating the salinity of the palaeo lake was low enough to allow the growth of diatoms.
M	S07La	The aragonite needles found in this sample appear to have been weathered to a greater degree than in other samples. The surfaces of the needles show pitting.
N	S07La	This image shows an enlargement of the sample in image M. The pitting of the needles is clear, with the crystals showing steeper terminations than in other samples.
O	S08a	The crystals in this sample are blocky, with large crystals appearing to be comprised of aggregates of smaller crystals. It appears that the carbonate crystals have become detached from the detrital clasts in places
P	S09a	This sample consists of aggregates of smaller fibrous crystals. The crystals show some weathering, with pitting on their surface.
Q	S10a	The aragonite crystals are blocky aggregates of fibrous crystals, also showing intergrowth.
R	S11a	The image indicates the carbonate cementing the detrital clasts.
S	S11a	This image is an enlargement of image Q, showing the large blocky crystals that are acting as cement.
T	S11b	The carbonate is blocky aragonite crystals, that in places appears to be comprised of aggregates of plates (top left of image).
U	S12a	The carbonate consists of bundles of fibrous needles that are a mix of aragonite and calcite.
V	S13a	The carbonate is large blocky crystals that closely cement the detrital clasts.

4.2.2.2 SOLLAS BENCH

Figure 4.5 records SEM images for the samples collected at Nussbaum Riegel.

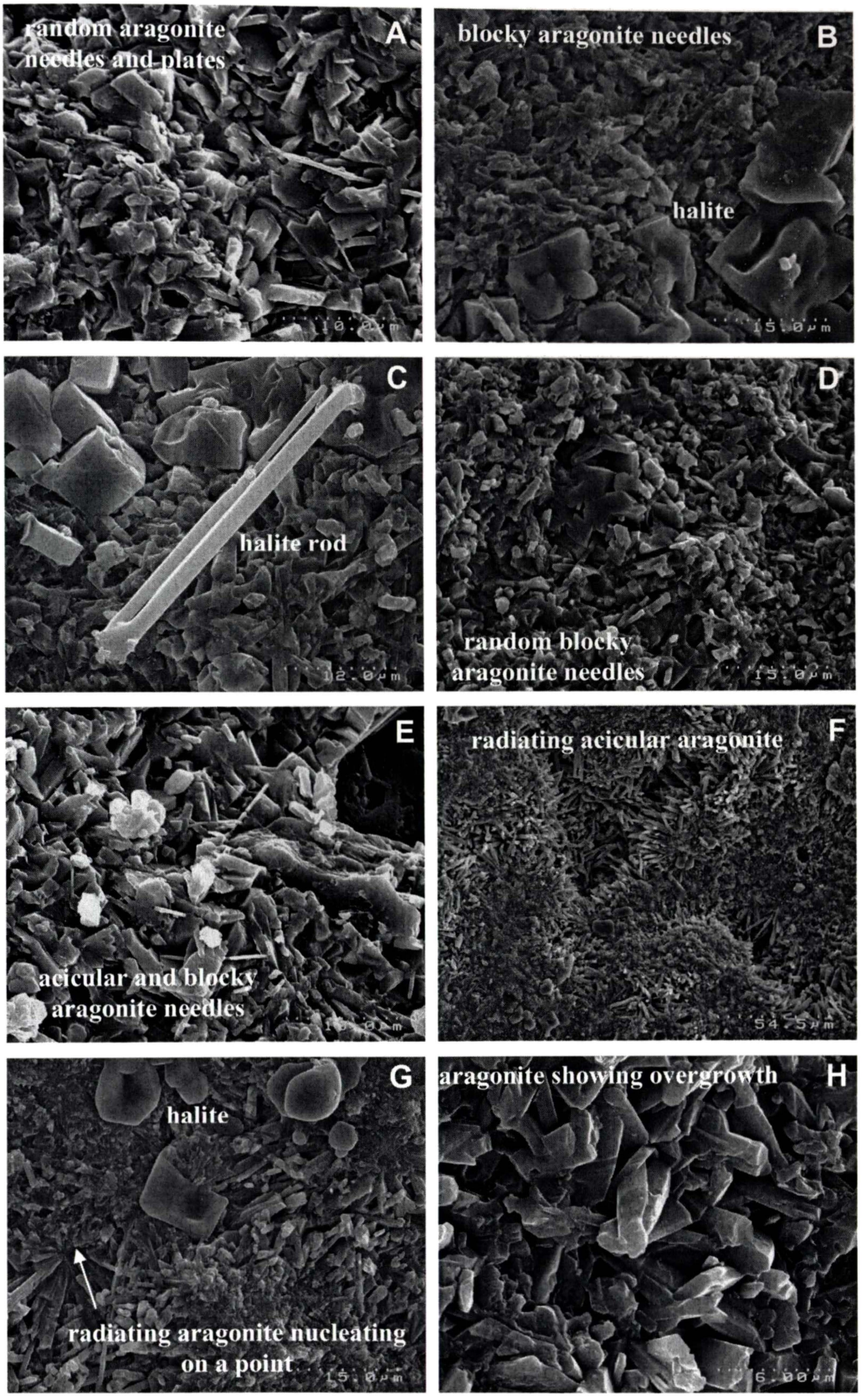
random aragonite needles and plates
A
blocky aragonite needles
B
halite
C
halite rod
D
random blocky aragonite needles
E
acicular and blocky aragonite needles
F
radiating acicular aragonite
G
halite
radiating aragonite nucleating on a point
H
aragonite showing overgrowth

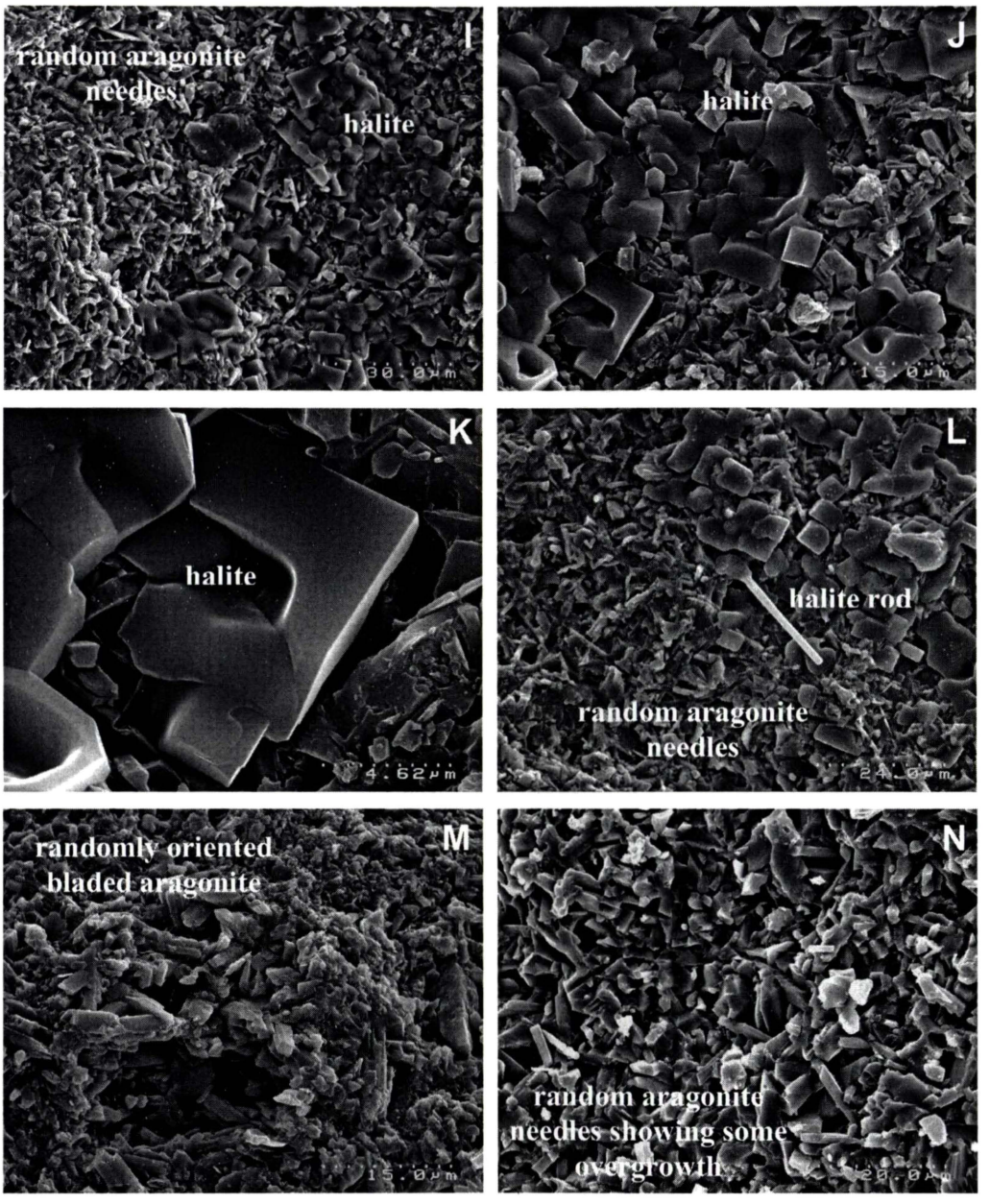

Figure 4.5: SEM images of carbonate samples collected from sites at the Sollas Bench. The description of crystal morphology and the site from which the respective sample was collected is recorded in Table 4.3.

Table 4.3: Description of crystal morphologies found within SEM images of samples collected from the Sollas Bench.

Image	Site	Description
A	S14a	The aragonite in this sample is in the form of needles and plates that fall in a random array.
B	S15a	The aragonite is in the form of short, blocky needles. There are patches of halite that partially fill pore spaces (bottom right of image).
C	S15a	This image shows a rod of halite found amongst the cubic halite within the sample.
D	S16a	The carbonate in this sample consists of randomly orientated blocky aragonite needles.
E	S17a	This sample is a mix of randomly oriented acicular aragonite and blocky aragonite needles
F	S18a	The sample contains acicular aragonite that is in botryoidal form.
G	S18a	This image is an enlargement of the sample in image F. The sample contains cubic halite. The aragonite appears to have nucleated at a common point before growing into botryoids.
H	S19a	The carbonate in this sample consists of aragonite needles that appear to have been overgrown by more aragonite.
I	S20a	The sample contains aragonite needles with many of the pore spaces containing cubic halite crystals.
J	S20a	This image is an enlargement of one of the patches of halite found in the sample in image I, indicating how it infills pore spaces.
K	S20a	This is an enlargement of the bottom left of image J.
L	S21a	The sample shows a random array of aragonite needles with halite infilling some of the pore spaces. A rod of halite can be observed in the centre of the image.
M	S22a	The carbonate in this sample consists of bladed aragonite, which shows some evidence of dissolution.
N	S23a	This sample consists of a random array of aragonite that appears to have been overgrown.

An unusual feature in these carbonate samples is the presence of halite crystals. In many cases these partially fill the pore spaces. The presence of gypsum associated with the carbonate in the moraine, along with the presence of halite, indicates that these carbonates were precipitated from supersaturated brine. When the samples were prepared for SEM analysis, they were rinsed in water to remove surface detritus. It was suspected that the halite could be due to reprecipitation of salts dissolved in the water during the rinsing process. When further samples were selected for analysis, they were not rinsed in water. One of these unrinsed samples contained abundant halite, which indicates that the halite is a primary precipitation product (Fig. 4.6)

Figure 4.6: Halite observed within a carbonate sample from site 19.

From examination of the SEM images, it is evident that two crystal morphologies dominate within the carbonate samples, these being:

(1) randomly orientated carbonate needles and blades (Fig. 4.5, images a- e, h-n).

(2) acicular carbonate, needles and blades that have a radiating crystal habit in the form of either botryoids or spherules (Fig. 4.5, images f & g).

The random orientation of carbonate needles and blades could result from crystals forming in suspension within the water column of saturated brine, before settling out to form beds of interlocking carbonate needles. This crystal morphology is similar to that found by Lawrence and Hendy (1989) in cores taken from Lake Fryxell. These carbonates were described as algal precipitates, as explained in Chapter Two. The presence of halite within the samples at Sollas Bench precludes this being the mechanism of formation, as very high salinity would not allow the growth of sufficient algae to cause a whiting effect.

The radiating crystals appear to have nucleated on small particles and grown outwards. These could either be silt sized detrital clasts or small crystals of carbonate. A likely point of growth would be at the sediment-water interface. Along this interface there would be an abundance of small particles available for nucleation of carbonate.

When a further range of samples were selected from within the Sollas Bench samples sites, it became apparent that the two crystal morphologies were associated with two different appearances in hand specimen. The hand specimens with randomly orientated crystals observed in Figure 4.5 (images a-e, h-n) were regular plates that

were light brown in colour. The hand specimen of sample 18 (Fig. 4.5, images f & g), which contained the radiating acicular aragonite, was an irregular piece of carbonate that was white in colour and much harder than the other samples. When more of these hard, irregular, white carbonates were investigated using SEM, it was observed that these also contained radiating acicular aragonite (Fig. 4.7).

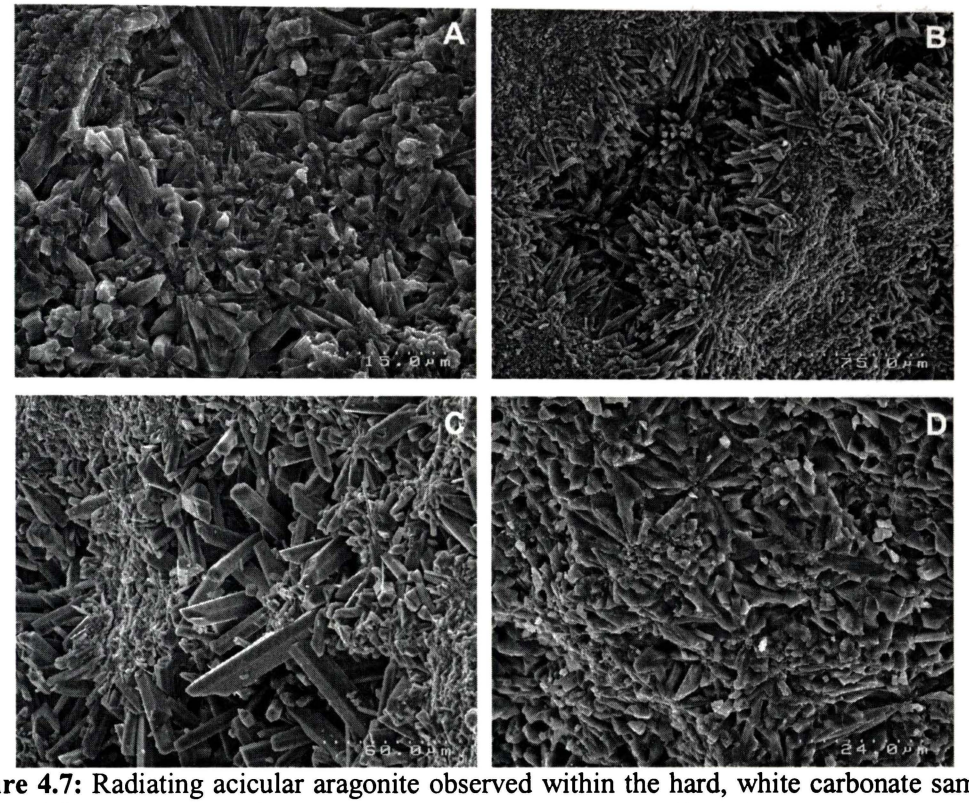

Figure 4.7: Radiating acicular aragonite observed within the hard, white carbonate samples collected from Sollas Bench. A-C: collected from site 16, D: collected from site 23.

As observed in Figure 4.8 B & C, where the aragonite has grown into pore spaces, spherules occur. An excellent illustration of this can be observed in the top right corner of image B, where the aragonite has nucleated on a point and grown outwards into a sphere.

4.2.2.3 PEARSE VALLEY

Figure 4.8 records SEM images from the samples collected at Nussbaum Riegel.

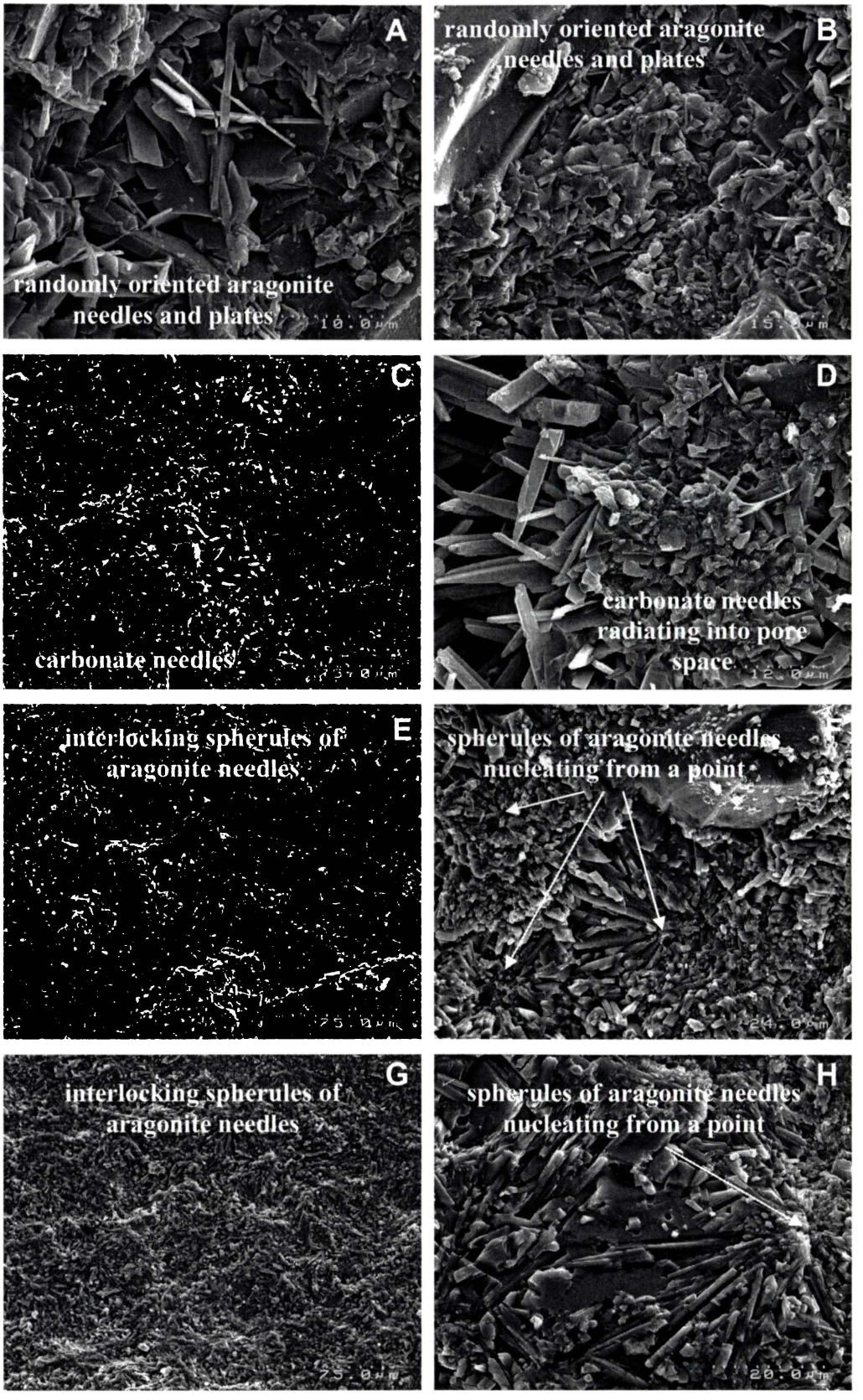
A
randomly oriented aragonite needles and plates
B
randomly oriented aragonite needles and plates
C
carbonate needles
D
carbonate needles radiating into pore space
E
interlocking spherules of aragonite needles
F
spherules of aragonite needles nucleating from a point
G
interlocking spherules of aragonite needles
H
spherules of aragonite needles nucleating from a point

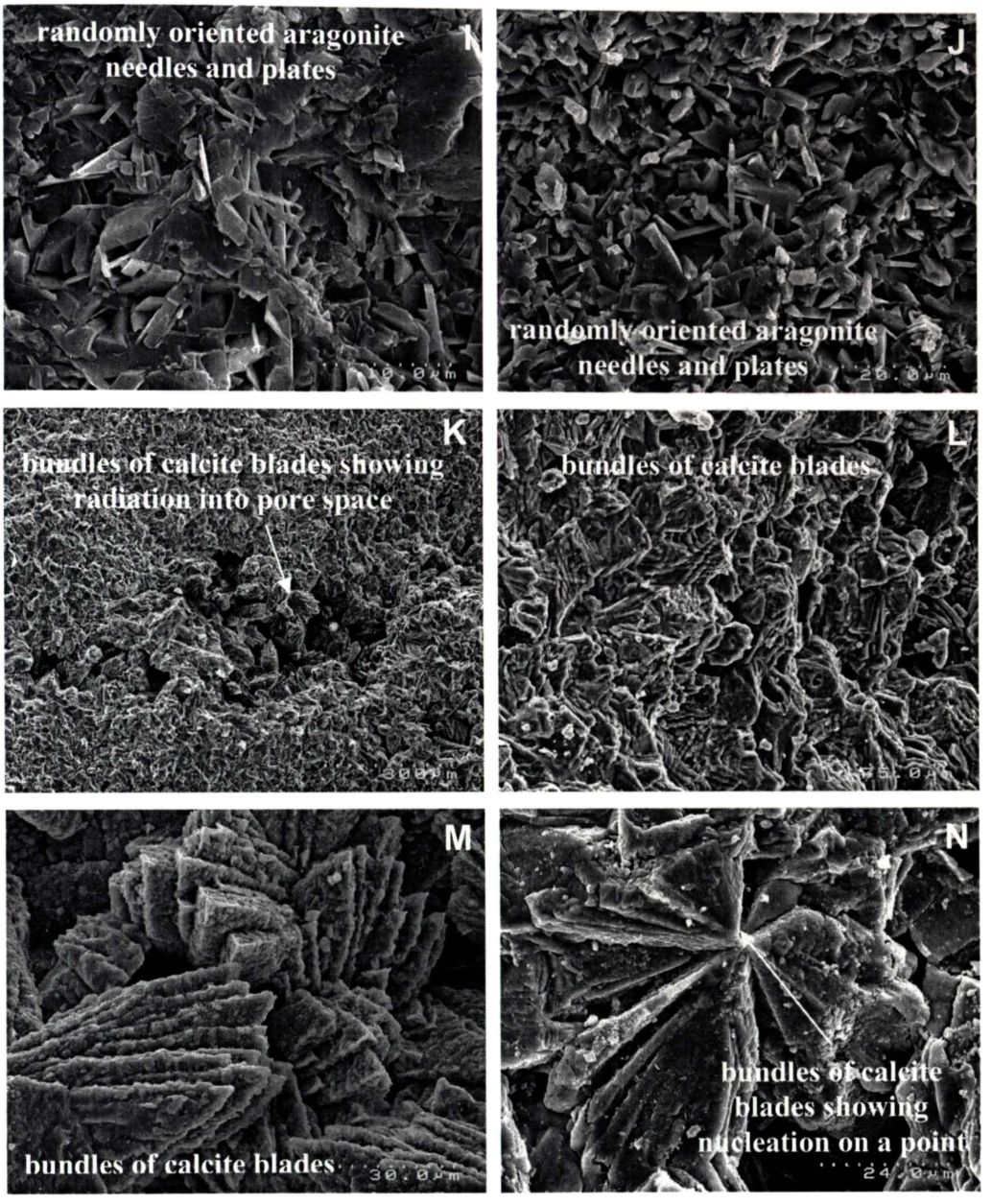

Figure 4.8: SEM images of carbonate samples collected from sites in Pearse Valley. The description of crystal morphology and the site from which the samples were collected is recorded in Table 4.4.

Table 4.4: Description of crystal morphologies occurring within SEM images of samples collected from Pearse Valley.

Image	Site	Description
A	S24a	The carbonate in this sample is a mix of plates and needles that have a random orientation.
B	S25a	The sample consists of aragonite plates and needles that have a random orientation. There are a higher percentage of detrital clasts in this sample than others from this location.
C	S26a	According to XRD this sample is calcite, which is in the form of blades and needles. These radiate into pore spaces and commonly nucleate from a point.
D	S26a	This is an enlargement of the edge of a pore space of the sample in image C, indicating the radiating nature of calcite needles.
E	S27a	The aragonite in this sample is in the form of interlocking spherules.
F	S27a	This image is an enlargement of interlocking spherules observed in image E. The spherules appear to have nucleated from a common point.
G	S28a	The carbonate in this sample consists of interlocking spherules of aragonite needles.
H	S28a	This image is an enlargement of interlocking spherules observed in image G, with growth originating from a common point.
I	S30a	The carbonate in this sample is made up of a mix of aragonite needles, plates and blades that fall in a random orientation.
J	S31a	This sample consists of a random array of aragonite needles. There is some evidence of overgrowth, with some of the needles becoming interlocked.
K	S32a	This sample consists of bladed calcite. There are regularly spaced bands of pore spaces, as observed along the centre of the image.
L	S32a	This is an enlargement of the surface of the sample in image K, showing the interlocking blades of calcite.
M	S32a	This is an enlargement of a pore space of the sample in image K, indicating the bundles of bladed calcite that are common in the sample.
N	S32a	Many of the calcite bundles appear to have nucleated on a point, as observed in an enlargement of a pore space in the sample in image K.

Unlike the samples from Sollas Bench, those collected from Pearse Valley contained no halite. There was also no gypsum associated with the carbonates in the moraines. The samples from Pearse Valley were similar, in that they consisted of the same two crystal morphologies with randomly oriented crystals (Fig. 4.8, images a-b, i-j) and radiating acicular needles (Fig. 4.8, images c-h).

The hand specimens of samples from Pearse Valley also reflected their crystal morphology. As for the Sollas Bench samples, the hand specimens of carbonates with random crystals were regular, light brown plates. The carbonates with radiating crystal morphology were hard, white and irregular in shape. The hardness could be due to greater strength imparted by the interlocking fans of radiating aragonite.

Within Figure 4.9 it can be observed how the radiating aragonite crystals are nucleating on surfaces. Figure 4.9, A & B show crystals radiating from common points of origin, which are likely to be small clasts. Figure 4.9, C & D indicate how the aragonite has grown out from the surfaces of detrital clasts.

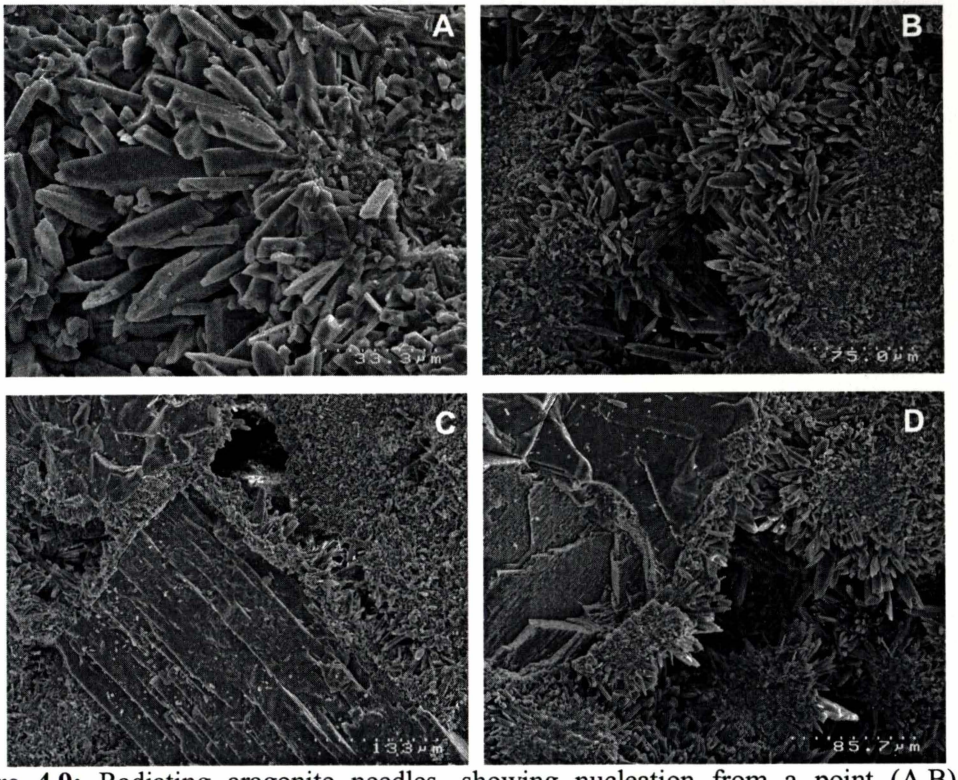

Figure 4.9: Radiating aragonite needles, showing nucleation from a point (A,B) and aragonite needles growing outwards from the surface of detrital clasts (C,D).

An unusual feature of the carbonates collected from Pearse Valley was that the samples collected from site 32 consisted entirely of calcite (Fig. 4.9, K-N). These carbonates also show a radiating morphology, but rather than being acicular aragonite, they consist of blades of calcite. These blades occur in bundles or sheaths, with each bundle growing from a common point (Fig. 4.10)

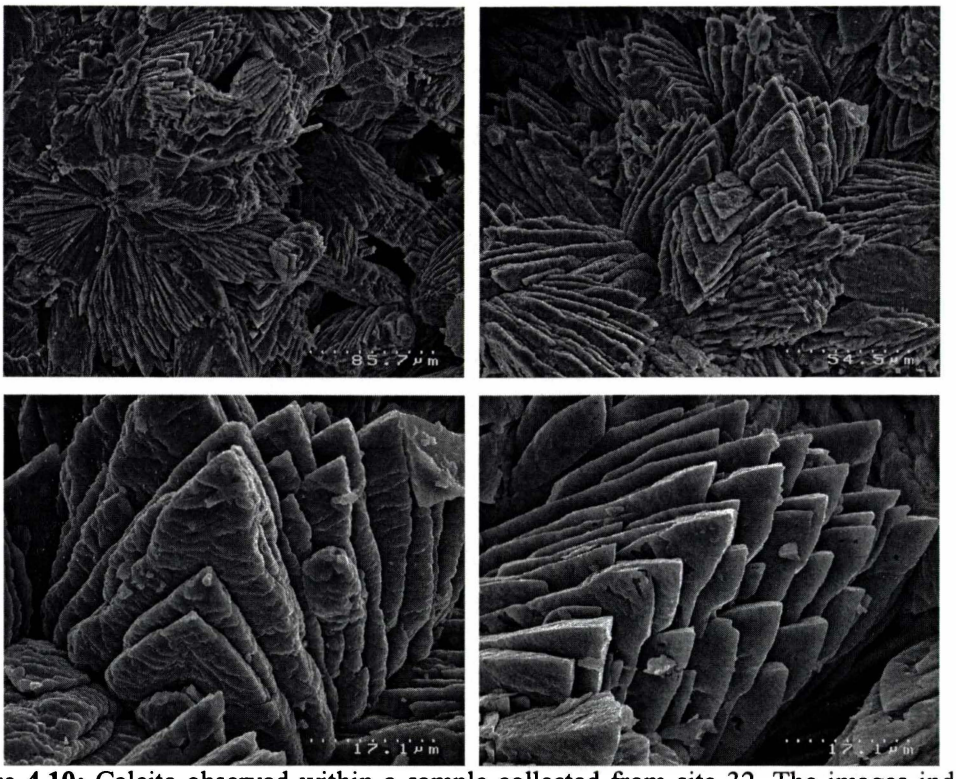

Figure 4.10: Calcite observed within a sample collected from site 32. The images indicate how the carbonate consists of bundles of calcite blades growing from common points of nucleation. The lower two images are enlargements of calcite bundles.

The carbonate samples collected from Sollas Bench and Pearse Valley were likely to have formed as a result of concentration of a water body to saturated brine. This would have resulted in precipitation of minerals such as carbonate, gypsum and halite. The concentration of the water could have been due to either evaporation or freezing. The crystal morphologies observed within the samples could result from either of these processes. A means of distinguishing the two origins could be achieved through investigation of their stable isotopic composition. This aspect will be addressed in the following chapter.

CHAPTER FIVE:

CARBONATE CHEMISTRY:

TRACE ELEMENTS

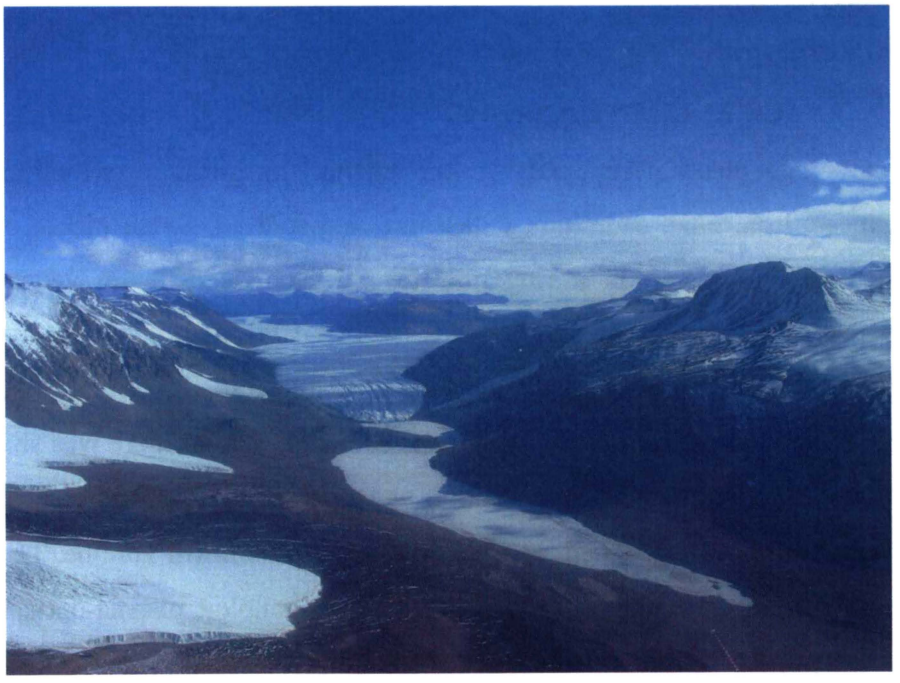

5.0 INTRODUCTION

Chemical investigation of the carbonates from the field area have been made in an attempt to establish the geochemical regime prevailing at their time of deposition. For example, the inclusion of Sr^{2+} and Mg^{2+} into the carbonate can have a temperature dependence (Wolf et al., 1967; Bathurst, 1975). The chemistry can also be controlled by post-depositional (diagenetic) effects. These processes can be tracked by changes in isotopic ratios and by the concentration of trace elements. Chilingarian et al. (1979) state that the expulsion of elements, such as strontium and magnesium, occurs during recrystallisation. Manganese and barium are commonly associated with inversion, recrystallisation and possibly grain growth. As carbonate is precipitated, various trace elements will substitute in differing degrees for Ca^{2+} in the crystal lattice. This chapter investigates the trace element composition of the carbonate and what controlled its composition.

5.1 TRACE ELEMENT ANALYSES

The carbonate pieces were analysed for calcium, magnesium, strontium, barium, manganese, iron, zinc, cadmium, potassium, and sodium. Small pieces of air-dried sample were powdered in a ring mill for 20 seconds. Known weights of each powdered sample were dissolved in 30 ml of ~10% (v/v) analytical grade HCl. Tucker (1988) determined that the leaching of manganese, strontium, or sodium was no more than 1M for HCL and 0.1M for acetic acid, though there was slightly more leaching of Fe. Once all visible reaction had stopped the solution was run through 0.45 m millipore filter papers and then made up to a known volume. The solutions were then analysed using ICP-OES (inductively coupled plasma-optical emission spectroscopy) for calcium, magnesium, strontium, barium, manganese, iron, and zinc. The same solutions were also run by AAS (atomic absorption spectroscopy) for potassium and sodium.

Along with the samples from Nussbaum Riegel, Sollas Bench and Pearse Valley, archived samples collected from other sites in past field seasons were also analysed (Table 5.1). These samples were collected before analytical techniques allowed for

accurate measurements of trace element concentration, or trace element analyses were not included in the relevant theses. These samples were analysed to give a fuller picture of the partitioning of trace elements in carbonates in the Dry Valleys.

Table 5.1: Location of archived carbonate samples analysed for trace elements. Publications containing information of these samples are included.

Location	Publication
Taylor Valley: Bonney Drift (Fig. 5.1)	Collected by Higgins (1993)
DVDP Cores 8 & 12 (lower Taylor Valley)	Dated by Hendy et al. (1979)
Miers Valley	Collected by Clayton-Green (1986)
Marshall Valley	Collected and dated by Judd (1986)

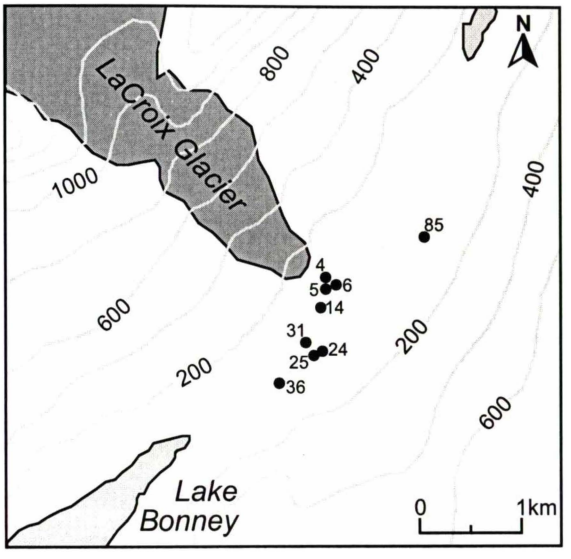

Figure 5.1: Location of analysed samples from the Bonney Drift in central Taylor Valley. Sample locations from (Higgins et al., 2000).

5.2 TRACE ELEMENT CHEMISTRY

The data from the trace element analyses for Nussbaum Riegel, Sollas Bench, Pearse Valley, and the archived samples is recorded in Appendix 1.

5.2.1 CALCIUM

The composition of the majority of samples collected were dominated by calcium carbonate, mostly in the form of aragonite. The concentrations of all acid soluble cations would be related to the abundance of calcium carbonate, unless high magnesium calcites were present. Thus there is little point in considering the calcium concentrations by themselves, except as a measure of the carbonate purity. Likewise, the concentrations of all other acid soluble cations are best considered by examining the ratios of their abundance to that of calcium. The carbonate percentages vary

greatly between the sites, with an average of 43% for Nussbaum Riegel, 84% for Sollas Bench and 87% for Pearse Valley samples.

Much of the chemical separation identified in plots of calcium against other ions is due to the differences in calcium concentration. The trace element composition will be controlled by the carbonate mineralogy and the lake water composition. The latter will have been complicated by progressive changes in trace metal concentrations in the remaining brine as evaporation/freezing and precipitation proceeded, resulting in changing concentrations in the carbonates.

Some of the trace element variability between the sites can be explained by changes in carbonate mineralogy. Trace elements will substitute to differing degrees in calcite and aragonite due to their different crystal structure. The orthorhombic crystal lattice of aragonite is relatively open. This allows the larger cations, such as strontium and barium, to substitute for calcium (Fig. 5.2). The more closed rhombohedral crystal lattice of calcite favours substitution of the small cations such as magnesium, manganese and iron. The degree to which an ion will substitute for calcium can be accessed by their ionic radius and distribution coefficients (Fig. 5.2). The distribution coefficient is the ratio of the amounts of a substance distributed between two immiscible phases at equilibrium (Milliman, 1974; Tucker and Wright, 1990).

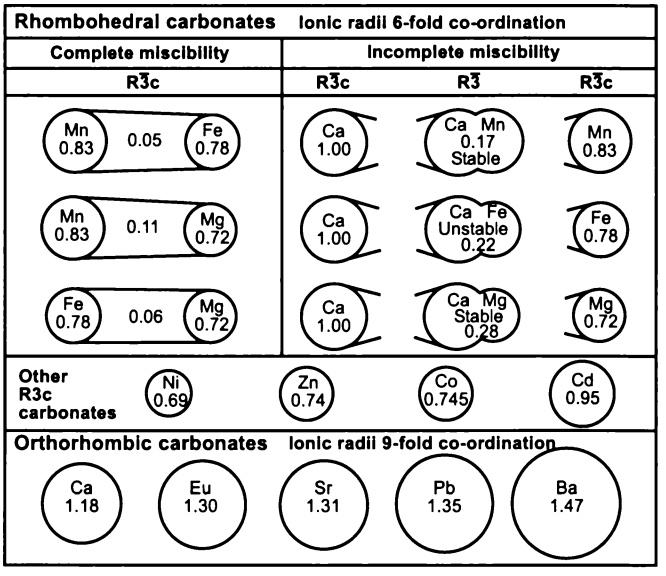

Figure 5.2: Cationic radii and carbonate space groups. The diameters of 'cation' circles are proportional to their radii. Linked cations show the extent of miscibility for some rhombohedral carbonates. Central figures in these solid solution series are differences (in Å) between end-member radii (Tucker and Wright, 1990).

There is a large variation in the experimentally determined distribution coefficients, making their use in determining trace element incorporation difficult. A summary of various research on the topic of distribution coefficients is discussed in (Rimstidt et al., 1998). Some of the commonly accepted distribution coefficients for aragonite are listed in Table 5.2.

Table 5.2: Commonly accepted distribution coefficients for the incorporation of trace elements in aragonite. Kd' is the experimental distribution coefficient (Moore, 1989)

Element	Kd'	Reference
Sr	0.9 - 1.2 (1.6)	Kitano et al. (1968, 1973), Holland et al. (1964), Kinsman and Holland (1969)
Na	~ 0.00014 (3-4 = $\underline{D}^{Na}_{calcite}$)	Calculated from Fig. 1 of White (1977), Kitano et al. (1975)
Mg	~ 0.0006 - 0.005	Brand and Veizer (1983)
Mn	0.86 (1/2-1/3 = $\underline{D}^{Mn}_{calcite}$)	Raiswell and Brimlecombe (1977), Brand and Veizer (1983)

An additional complication to the trace element composition is the presence of a second competing phase (gypsum) in some of the lacustrine environments. While gypsum is observed within the Sollas Bench deposits, they are not *in situ* and it is not obvious that they formed concurrently with the carbonate phases, however they do occur as intimately mixed deposits in recent Lake Bonney and Lake Vanda sediments. Where gypsum is also depositing from a brine, there will be competing partitioning for calcium and trace elements (especially strontium and barium). Unfortunately the distribution coefficients of strontium and barium between gypsum and brines are not as well understood as those for carbonate phases.

5.2.2 MAGNESIUM

The magnesium concentrations show similarities between Sollas Bench and Pearse Valley beds, but there is a distinct difference in origin for the Nussbaum Riegel carbonates (Fig. 5.3).

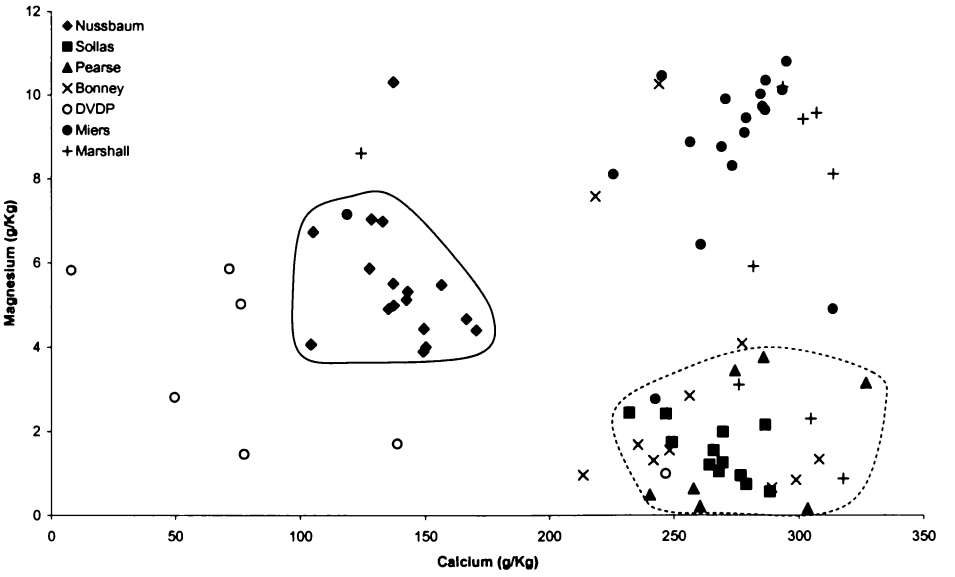

Figure 5.3: Magnesium concentrations in carbonate samples plotted against calcium concentration. Nussbaum refers to Nussbaum Riegel samples. Sollas refers to Sollas Bench samples, Pearse refers to Pearse Valley samples. Bonney refers to samples collected from the Bonney Drift in Taylor Valley. DVDP refers to samples from the Dry Valley Drilling Project Core 12. Miers refers to samples from Miers Valley, and Marshall refers to Marshall Valley samples. This will remain the same for the following graphs. The solid line denotes the field containing Nussbaum Riegel samples and the dashed line denotes the field containing Sollas Bench and Pearse Valley samples. This will also remain the same for the following graphs in this chapter.

The effect of mineralogy can be observed when the magnesium/calcium ratio is plotted against the aragonite/calcite ratio for the Nussbaum Riegel, Sollas Bench and Pearse Valley samples (Fig. 5.4). The results of XRD analysis of the Marshall Valley samples undertaken by Judd (1986) were combined with chemical analyses from this thesis and added to the plot. These results indicate that with increasing calcite abundance relative to aragonite, there is an increase in magnesium. The samples collected from Miers Valley contained only calcite (Clayton-Green, 1986). When compared to the samples of mixed mineralogy, the Miers Valley carbonates contain a much higher concentration of magnesium.

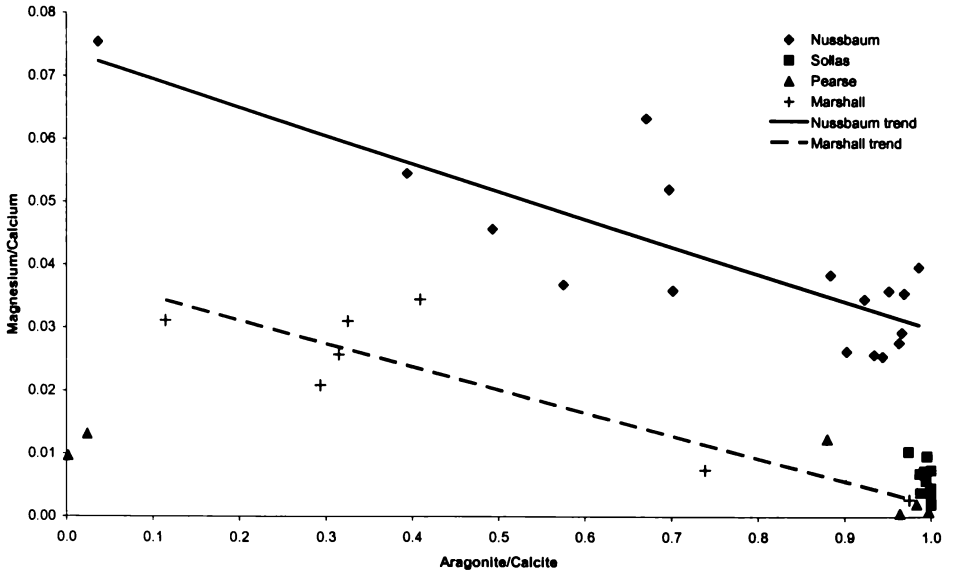

Figure 5.4: Magnesium/calcium ratio plotted against the aragonite/calcite ratio.

Mineralogy is not the only control on the magnesium concentration. When the correlations were extrapolated, they trend back to a different lake water composition. The samples from Marshall Valley and Nussbaum Riegel were fed by water originating from Ross Sea ice, which appears to have been higher in magnesium than water originating from Taylor Glacier, which sourced water from which the Sollas Bench and Pearse Valley carbonate samples precipitated. The sources of the waters for the palaeo lakes will be addressed in the following chapter.

5.2.2.1 MAGNESIUM CONTROL ON CARBONATE MINERALOGY

It has long been held in the literature that the composition and morphology of inorganically precipitated sedimentary carbonate crystals is controlled largely by the magnesium/calcium ratio of the precipitation solution. Müller et al. (1972) found that for the lacustrine environment the mineralogy of the carbonate would change with increasing magnesium/calcium ratio, though no attempt was made to explain why this occurs (Table 5.3).

Table 5.3: Control of Mg/Ca ratio on mineralogy of precipitates (Müller et al., 1972).

Mg/Ca ratio of the precipitating solution	Mineralogy of precipitate
<2	Low-Mg calcite
2-12	High-Mg calcite (±aragonite)
>12	Aragonite
Very high values	Hydrous Mg-carbonates

Folk (1974) argued that the magnesium/calcium ratio controlled the composition of calcium carbonate. Previously it was held that carbonate precipitated as aragonite if the rate of precipitation was very fast, if the degree of supersaturation was higher, or the temperature was high. Folk (1974) considered that the presence of Mg^{2+} favoured the production of aragonite in an acicular form, and lack of Mg^{2+} allowed calcite to crystallise in fibrous or rhombic forms. Folk (1974), supported by Bathurst (1975), proposed that the Mg^{2+} acted to selectively poison crystal growth in all directions other than the c-axis, forcing magnesian carbonate to assume a fibrous or steep rhombic form.

The crystal lattice has alternating layers of Ca^{2+} and CO_3^{2-}. At the "c" end of the growing crystal, a sheet of Ca^{2+} ions is added and is then overlapped by another sheet of CO_3^{2-} groups. If a Mg^{2+} lands in the Ca^{2+} sheet, it easily fits in and the next sheet will cover the mistake and the crystal will continue to grow in the c-axis direction. If the Mg^{2+} attaches itself to the edge of the Ca^{2+} sheet it will tend to block growth in that direction (it cannot be covered over by a CO_3^{2-} sheet) and being of small ionic radius it will make the overlying and underlying CO_3^{2-} sheets 'scrunch' together to accommodate it (Fig. 5.5). Thus contracted, the structure can no longer accept the large Ca^{2+} ion, and sideways growth is slowed (Folk, 1974). This distortion has been used to explain why inorganic magnesian calcite forms only as small fibers or micritic crystals with curved faces and steep rhombic faces, and never forms large crystals as only so much distortion can be tolerated before sideways growth is completely stopped (Folk, 1974).

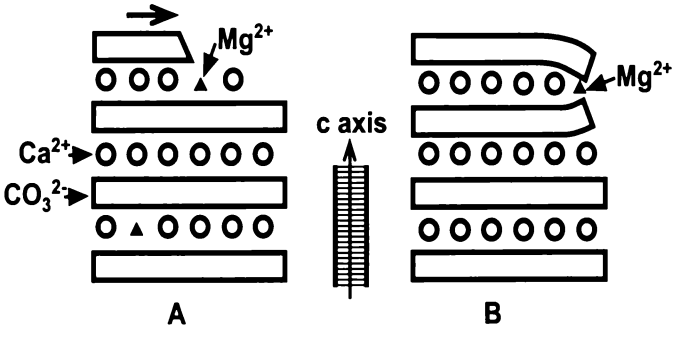

Figure 5.5: Diagrammatic representation of the effect of Mg^{2+} on $CaCO_3$ crystal growth. (A) shows the effect of adding Mg to the end growth surface, while (B) shows how addition of magnesium to the side of the crystal causes "scrunching" of the crystal structure (Folk, 1974).

This effect would mean that it is difficult for any Mg-calcite to form, and carbonate would more readily crystallise as aragonite, especially as the magnesium/calcium

ratio increased. Any Mg-calcite that does form would be as small fibrous crystals, or ones with steep crystal faces. Thus the presence of Mg^{2+} in sea water prevents the formation of equant, sparry crystals of low-Mg calcite (Fig. 5.6).

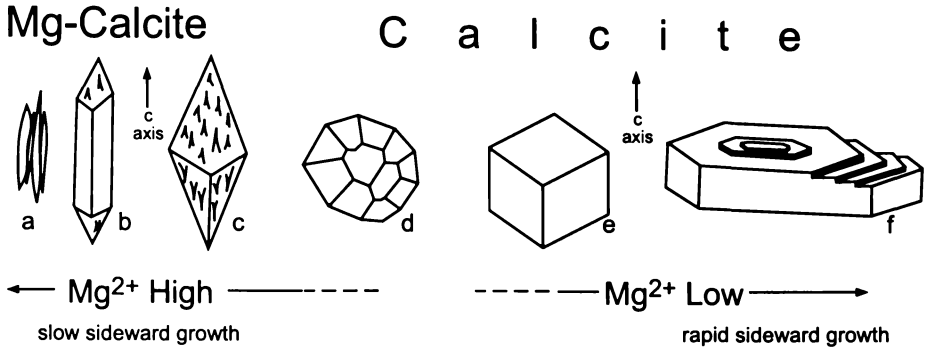

Figure 5.6: Crystal habit of $CaCO_3$ as controlled by Mg/Ca ratio. Where Mg is abundant it selectively poisons sideways growth so that fibrous crystals or elongate rhombs develop. Subsurface waters, often a mixture of sea water with fresh water, have a low Mg content and complex polyhedra form. In fresh waters either the elemental rhomb forms, or (if growth is very rapid and the Mg/Ca ratio is very low), calcite may form mica-like books (Folk, 1974).

Berner (1975) supported the concept that the favouring of precipitation as aragonite from supersaturated sea water and other Mg-rich solutions, as Mg^{2+} was not readily absorbed on to the surface of aragonite, nor was Mg^{2+} taken up to any extent into the aragonite crystal lattice, meaning its growth was relatively unaffected by the presence of Mg^{2+}. In contrast Mg^{2+} was readily absorbed on to the surface of calcite and incorporated into its crystal structure. As a result, the crystal growth of calcite in sea water was strongly inhibited by Mg^{2+}. He believed that most of the magnesium inhibition was due to the non-equilibrium incorporation of magnesium into growing calcite (Berner, 1975).

Lahann (1978) suggested that the growth inhibition mechanism of Folk (1974) should lead to poisoning of crystal growth on c-axis faces as well as on faces perpendicular to c. Emplacement of a CO_3^{2-} layer over a relatively smaller Mg^{2+} ion absorbed on a c-axis face of calcite should also cause the two CO_3^{2-} layers to "scrunch together". This distortion, shortening along the c-axis, of the CO_3^{2-} spacing, would shorten the edges of the co-ordination octahedra of the cations adjoining the Mg^{2+} ion, which was exactly the same lattice stress created by Mg^{2+} incorporation on edge faces. The distortion of the co-ordination octahedral, which was assumed to be sufficient to

prevent incorporation of Ca^{2+} ions on edge faces, should now prevent incorporation of CO_3^{2-} ions co-ordination to the offending Mg^{2+} ions, thereby poisoning growth in the c-axis direction.

The lattice deformation created by Mg^{2+} incorporation into calcite should increase the solubility of the phase. As the growing crystal is considered to be constantly dissolving and growing, any process that increases the dissolution rate should reduce the net growth rate. In this way, the Folk (1974) mechanism could inhibit calcite growth but, as shown, should be independent of orientation. This mechanism may be important as a means of Mg^{2+} induced calcite growth poisoning, but is inadequate as an explanation for morphology variation (Lahann, 1978).

Lahann (1978) believed that the morphology of calcite crystals grown in different environments might be explained on the basis of double-layer theory and a surface-controlled calcite growth mechanism, rather than the magnesium/calcium ratio of the precipitating fluid. If one precipitating ion is present in solution in great excess, it may be absorbed into the growing surface to a greater degree than the deficient ion, thus imparting its charge to the surface of the growing crystal. Thus the crystal growth is controlled only by the concentration of the deficient ion since the surface concentration of the abundant ion will be relatively constant. The $m_{Ca^{2+}}/m_{HCO_3^-}$ ratio of sea water is about 4.3, and if Mg^{2+} ions are considered, the cation/anion ratio of surface-absorbed species rises to 26.5. These cation/anion ratios suggest that calcite crystallisation from sea water should be dependant on the availability of bicarbonate or carbonate ions, as these ions are deficient in the solution (Lahann, 1978).

The dependency of calcite crystallisation on the availability of carbonate or bicarbonate ions becomes even more significant as the presence of carbonate ions is required to dewater surface absorbed Ca^{2+} ions. Ca^{2+} and Mg^{2+} in aqueous solution contain six water molecules in their inner hydration spheres, each being bonded in octahedral co-ordination to six carbonate groups, in layers perpendicular to the c-axis. The incorporation of Ca^{2+} and Mg^{2+} ions into the calcite lattice implies therefore,

replacement of the six water molecules from the inner hydration sphere with bonds to six different carbonate groups (three above and three below) (Lahann, 1978).

On an edge face, there will be both carbonate and calcium layers exposed. The great excess of surface-active cations over surface-active anions in seawater implies that in normal circumstances a c-axis face will be saturated on the surface with cations. In contrast, very few or no carbonate ions will be exposed on the c-axis face. The absence of exposed carbonate groups and saturation of the surface with Ca^{2+} and Mg^{2+} ions should create a strong potential on c-axis faces. The greater availability of carbonate groups will facilitate dewatering of surface-absorbed Ca^{2+} ions and preferential growth of the crystal in this direction will result, resulting in needle-like crystals. If the ratio of surface-active cations to anions is nearer to unity, equant crystals will develop. The m_{Ca2+}/m_{HCO_3-} ratio of freshwater is about 0.4. Intermediate crystal types such as scalenohedrons and prisms should result from water types giving cation/anion ratios between those for sea water (needles) and fresh water (equant) (Lahann, 1978).

Although little is known about the kinetics or mechanisms of aragonite crystallisation, analogy with calcite would suggest that aragonite crystallising from sea water should be elongated in the c-axis direction. The surface charge control on $CaCO_3$ morphology would appear to be applicable to aragonite as well as calcite (Lahann, 1978).

Lahann (1978) assumed the rate-determining step for crystal growth in the $CaCO_3$-H_2O system is the dehydration of surface absorbed Ca^{2+} ions, meaning the substitution of Mg^{2+} ions for Ca^{2+} ions on the growing calcite surface would markedly slow the rate of crystal growth because of the greater energy demand for dehydration. The data contained in Lippman (1960), (cited in Lahann, 1978) indicate that the free energy of dehydration for Mg^{2+} is 17% greater than for Ca^{2+}, meaning the calcite growth would be "poisoned".

Mucci and Morse (1983) supported the theory that magnesium/calcium ratios of the precipitating liquid controlled the composition of the precipitate. Their kinetic data was consistent with Lahann's kinetic data (Lahann, 1978) indicating that Mg^{2+} strongly inhibited carbonate precipitation.

Through the excess of cations to anions for the $CaCO_3$ system in sea water, the surfaces of the calcite crystals have a net positive charge. The highest charge density is on the c-axis faces and so these attract the largest number of anions resulting in fastest growth in the c-axis direction. The availability of CO_3^{2-} ions becomes the rate-limiting step in crystal growth.

- Morphology

The initial work undertaken by Lahann (1978) was developed further by Given and Wilkinson (1985), who pointed out that there is a full spectrum of acicular to equant crystal morphologies, found for both calcite and aragonite in waters with a large range of magnesium/calcium ratios. They argued that this alone discounted the magnesium/calcium ratio as the control on mineralogy and morphology. They found that there was a strong relationship between the rate at which crystals grew and their morphology. When levels of CO_2 are decreased (ie. by degassing) acidity is low and supersaturation with respect to carbonate species occurs. This leads to fast crystal growth rates and acicular crystal form. With increased levels of CO_2, the opposite occurs, leading to slow crystal growth rates, and equant crystals. As explained by Lahann (1978), the rate of precipitation in the c-axis direction is controlled by the availability of CO_3^{2-} (Given and Wilkinson, 1985).

- Calcite Composition

It is reasonable to consider that incorporation of magnesium on a side face is solely a function of the magnesium/calcium ratio of the precipitating fluid, and that on these faces magnesium incorporation may be controlled by distribution coefficients. However on c-axis faces, where the charged surface facilitates cation dehydration, growth is controlled by the local availability of carbonate ions. The final magnesium

content of natural calcites is a function of (a) the magnesium/calcium ratio of ambient fluids and (b) the rate of crystal growth as determined by fluid Ca^{2+} and CO_3^{2-} concentrations (Given and Wilkinson, 1985).

- Mineralogy

The rate of precipitation and supply of carbonate ions also controls the mineralogy of the precipitate (Fig. 5.7). High CO_3^{2-} availability gives rise to aragonite, whereas lower availability gives rise to calcite (Given and Wilkinson, 1985).

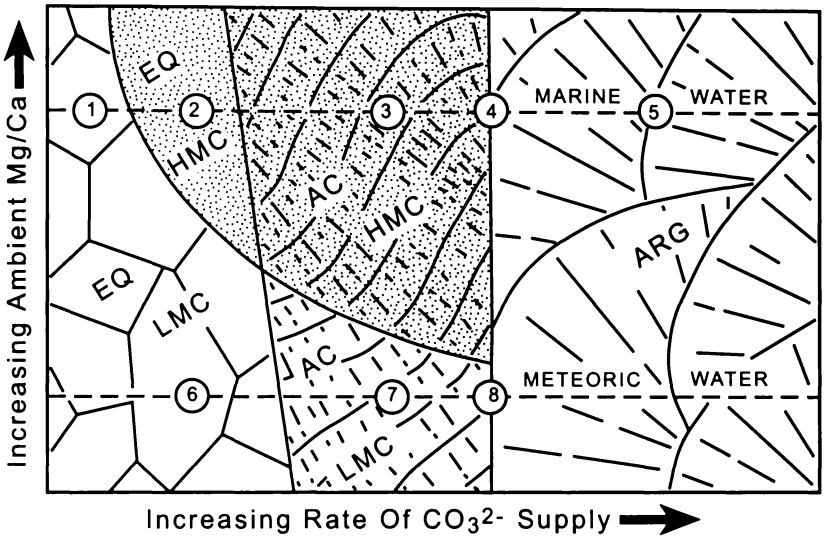

Figure 5.7: Schematic illustration of relation between fluid Mg/Ca ratio, rate of carbonate ion supply, crystal morphology and mineralogy of inorganic precipitates (low-Mg calcite, high-Mg calcite or aragonite). Mg/Ca ratio of the meteoric line is 0.3 and of the marine line 5.2. Low-Mg calcite is up to 9 mole % $MgCO_3$ and high-Mg calcite is above. The positions of modern, naturally occurring precipitates shown are (1) equant calcite spar cement in cold deeper-water, low latitude sediment and shallow water temperate sediments, (2) cements in reefs (rare), (3) cements in reefs and lime sands, (4) cements in reefs and lime sands, (5) spar cements in meteoric environments, (6) speleothems and travertines, and (7) speleothems (rare) (Given and Wilkinson, 1985).

5.2.3 STRONTIUM

Strontium, like magnesium is an important trace element component in carbonates, showing a wide variation in the samples. The Miers Valley samples show the lowest concentrations, with Nussbaum Riegel samples being predominantly lower than the Sollas Bench and Pearse Valley samples (Fig. 5.8).

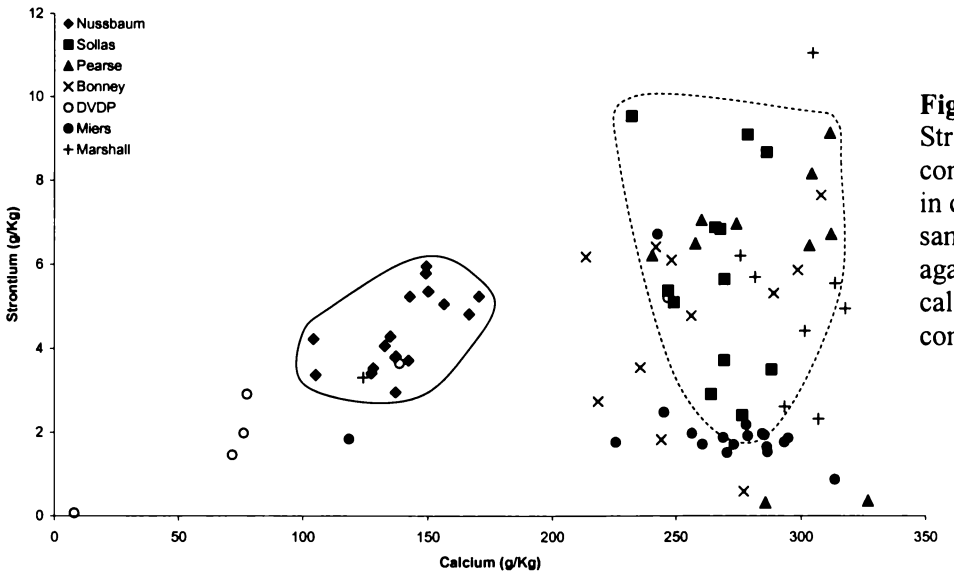

Figure 5.8: Strontium concentrations in carbonate samples plotted against the calcium concentration.

As with magnesium, much of the variation observed in strontium concentration can be explained by changes in mineralogy. The larger cation of strontium fits more easily into the aragonite lattice, allowing it to substitute for calcium to a greater degree than it does in calcite. As the concentration of calcite relative to aragonite increased, the concentration of strontium dropped (Fig 5.9). This could explain why the calcite samples from DVDP cores and Miers Valley had lower level strontium concentrations than many of the samples, and why the aragonite samples from Sollas Bench had the highest concentrations. The samples of mixed mineralogy from Nussbaum Riegel plotted with an intermediate strontium concentration.

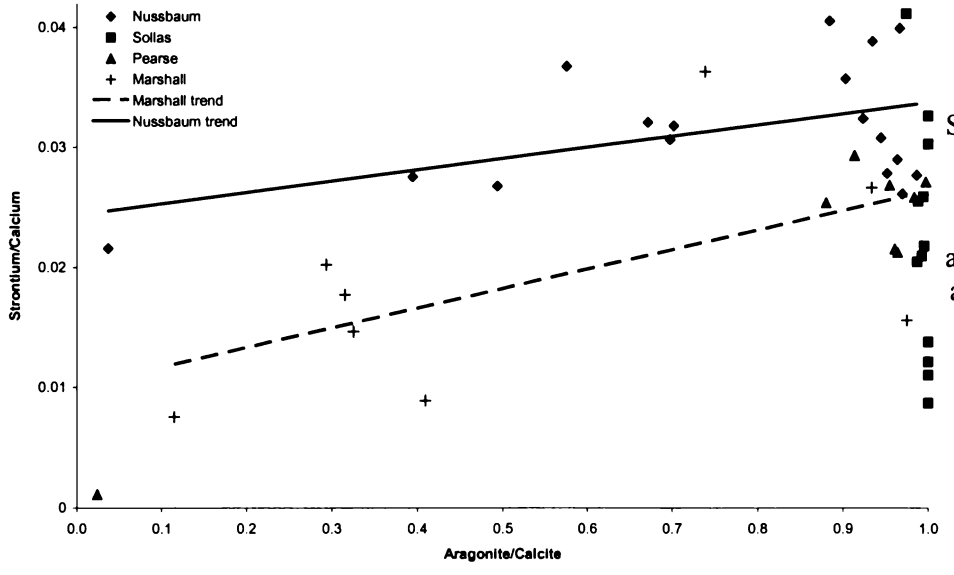

Figure 5.9: Strontium/ calcium ratio plotted against the aragonite/ calcite ratio.

Again, the mineralogy is not the only control on the strontium concentration in the samples. When the trend lines were extrapolated, they showed that the water from which the carbonate was precipitating had different concentrations of strontium. To a certain degree, the ratio of strontium/calcium in the precipitating solution would have played a role in determining the strontium concentration of the precipitated carbonate (Kinsman, 1969; Rathburn and Deckker, 1997).

According to Rathburn and Deckker (1997), the incorporation of strontium is strongly affected by the precipitation rate and magnesium content of calcite, though the degree to which this is occurring is difficult to determine. A considerable distortion will be introduced in the structure of calcite by replacing calcium with magnesium. The distortion may be reduced, in part, by the simultaneous substitution of calcium by some of other larger cations, such as strontium. In this way, small cations such as Fe^{2+}, Mn^{2+} and Zn^{2+} will have the effect of increasing the distribution coefficient for strontium, thus increasing the strontium content of calcite (Ichikuni, 1973; Pingitore, 1978; Mucci and Morse, 1983; Rimstidt et al., 1998).

Diagenetic effects such as recrystallisation and fluid flow tend to decrease strontium concentrations (Kinsman, 1969; Brand and Veizer, 1980). There is little evidence in SEM images of the recrystallisation, indicating that diagenesis is not likely to have played a major role in controlling the strontium concentrations of the carbonates.

5.2.4 BARIUM

Being a larger cation, barium should behave in a manner similar to strontium, substituting to a greater degree for calcium in aragonite and a lesser degree in calcite. The barium concentrations are higher in the Nussbaum Riegel and Miers Valley samples, than the Sollas Bench and Pearse Valley samples, despite the higher concentration of calcite relative to aragonite (Fig. 5.10).

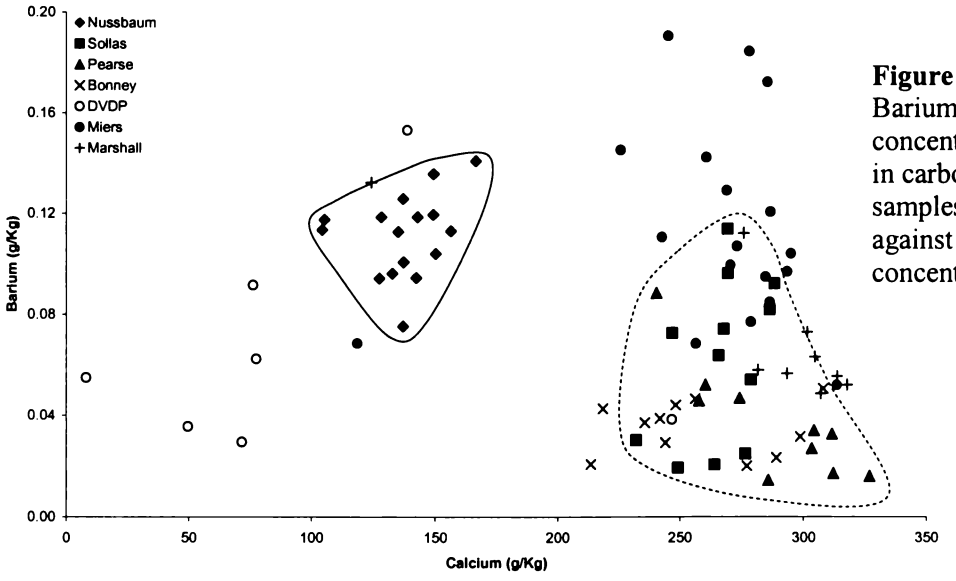

Figure 5.10: Barium concentrations in carbonate samples plotted against calcium concentration.

Despite having a higher concentration of barium than other sites, barium concentrations of the Nussbaum Riegel samples, when plotted against the aragonite/calcite ratio, showed that as calcite concentration increased relative to aragonite, the barium concentration decreased (Fig. 5.11). The same trend is evident in the Marshall Valley samples.

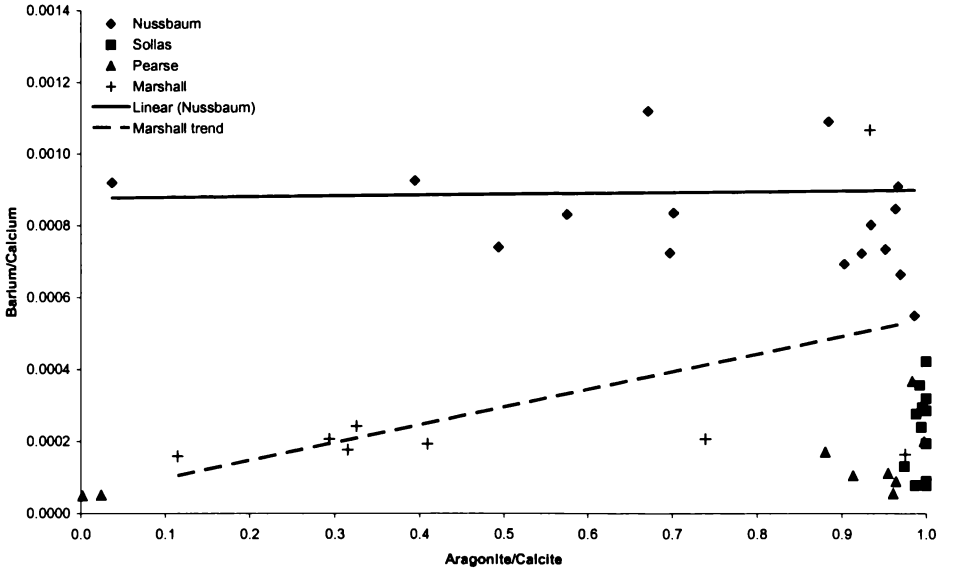

Figure 5.11: Barium/calcium ratios plotted against the aragonite/calcite ratio.

The concentration of barium in the carbonates appeared to be controlled primarily by the composition of the source water. Despite being mainly aragonite, the samples

from the Sollas Bench and Pearse Valley had lower concentrations of barium than the samples with mixed mineralogy from Nussbaum Riegel.

The samples from Nussbaum Riegel and Miers Valley were precipitated in water from the same general source (Ross Sea ice) and had similar concentrations of barium. Even though the source is similar, the Nussbaum Riegel and Miers Valley carbonates were not deposited from the same water as, (i) the deposits are of a different age and, (ii) the lakes would not have been connected. The Sollas Bench, Pearse Valley and Bonney Drift samples were precipitated in water originating from Taylor Glacier, and could be expected to have a similar barium concentration.

The spread in magnesium/calcium, strontium/calcium and barium/calcium ratios for each of the lacustrine deposits fall within narrow ranges, the biggest being Sollas Bench with ranges of 4 to 5 fold for all three ratios. There are no systematic trends in the alkaline earth distributions within the Sollas Bench samples, which could be due to sequestering of these elements in sulfate phases. The alkaline earth ratios for the other sites show distributions that appear to be strongly influenced by the mineralogy of the carbonate phases (higher magnesium and lower strontium and barium with increasing calcite concentration relative to aragonite).

5.2.5 IRON

Nussbaum Riegel and DVDP samples have higher concentrations of iron than the other sites (Fig. 5.12). This could be partly due to leaching of iron by HCL from detrital material during the dissolution of the carbonates, as these two sites have a much greater percentage of detrital material. The iron concentrations for the rest of the sites show little variation (Fig. 5.12).

Iron and manganese distributions have an additional complication not observed with alkaline earth elements. Iron and manganese are susceptible to changes in the oxidation state of the precipitating water, with both being more mobile in reducing conditions. Thus the oxidation state of the water can control the concentration of

these elements incorporated into the precipitating carbonate, with higher concentrations being available in reducing conditions. At the interface between anoxic (reducing) waters and oxic (oxidizing) waters, iron will often precipitate or be absorbed on to mineral surfaces. Two samples of carbonates from the Bonney Drift and one from DVDP Core 12 (Fig. 5.12) showed anomalously high iron content. As these three samples also had the highest manganese content for their classes, it is likely that they were precipitated under reducing conditions.

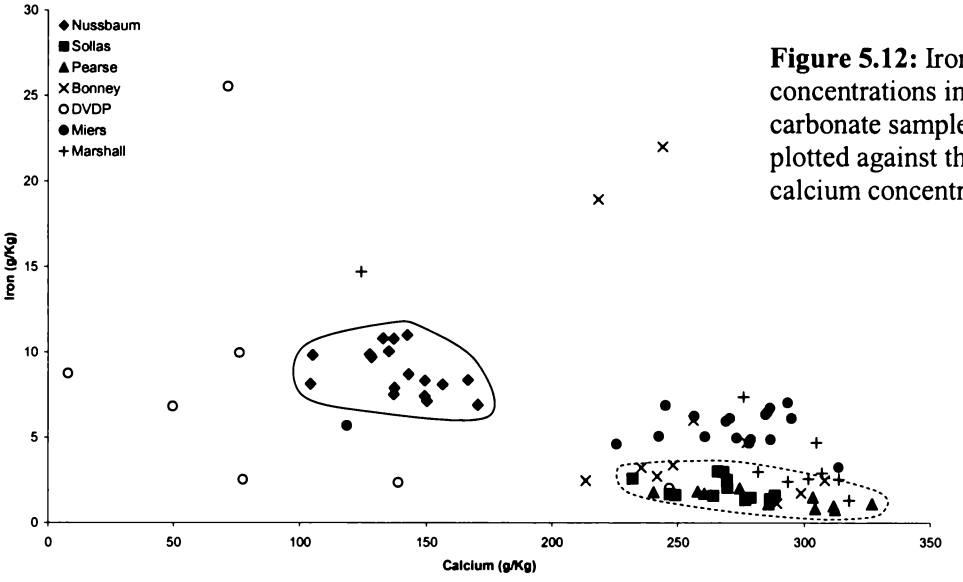

Figure 5.12: Iron concentrations in carbonate samples plotted against the calcium concentration.

As iron has a smaller ionic radius than calcium (Fig. 5.13), it would be expected that it would be more easily incorporated into the calcite lattice. As observed in Figure 5.13, for the Nussbaum Riegel samples, the iron concentration increased with an increase in calcite relative to aragonite. This trend did not occur in the Marshall Valley samples. The difference in the trends could be due to oxidising water conditions in Glacial Lake Péwé (meaning the iron is less mobile), or to the incorporation of more basaltic clasts in the Nussbaum Riegel carbonates.

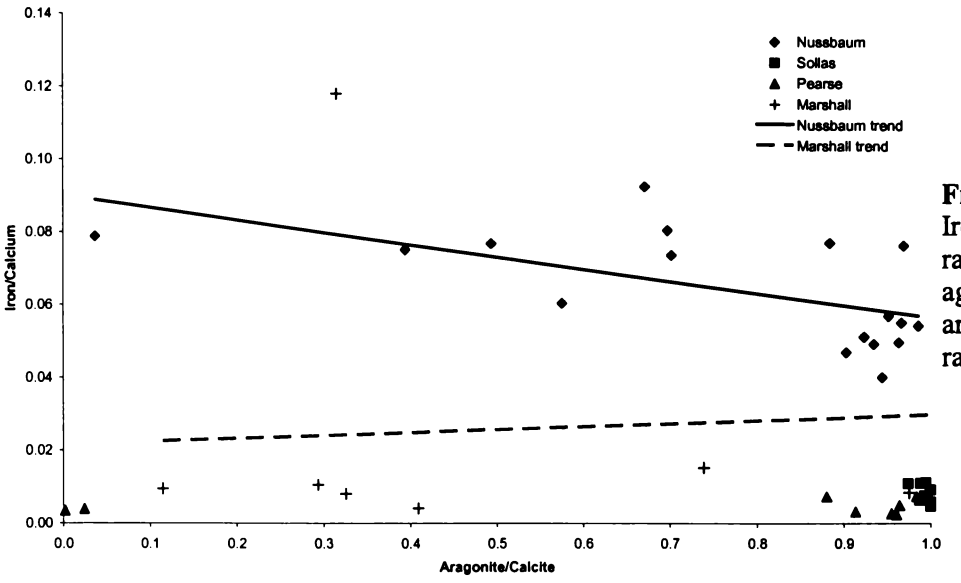

Figure 5.13: Iron/calcium ratios plotted against the aragonite/calcite ratio.

5.2.6 MANGANESE

There is little differentiation between different sites in manganese concentration (Fig. 5.14). The greatest spread in manganese concentrations are evident in the Nussbaum Riegel samples.

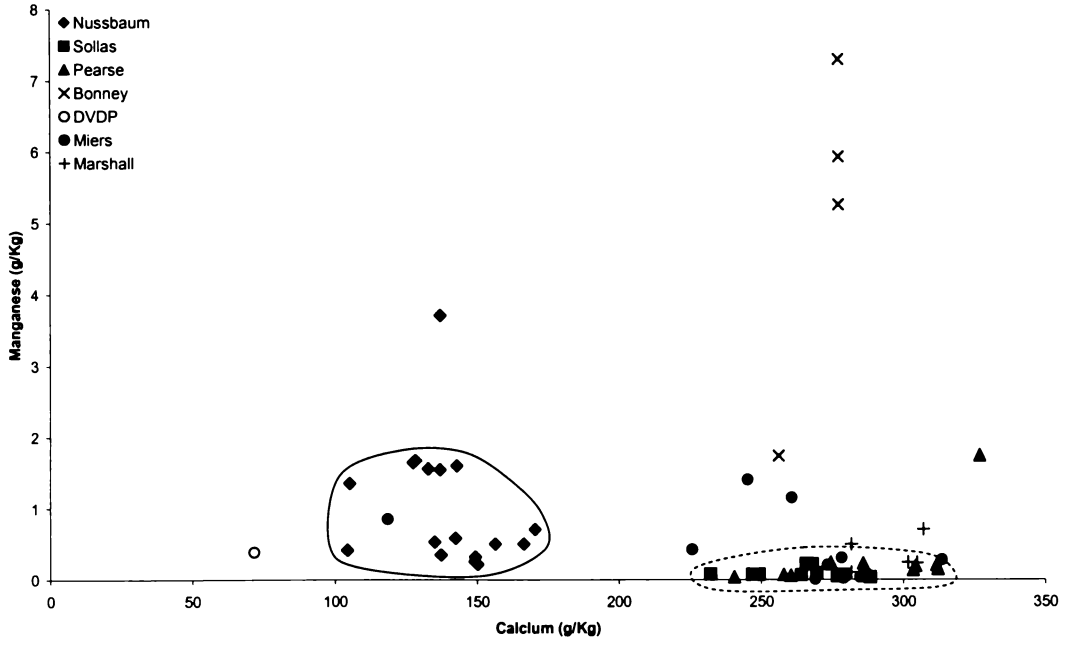

Figure 5.14: Manganese concentrations in carbonate samples plotted against the calcium concentration.

Figure 5.15 indicates that manganese is a stable substitute for calcium in rhombohedral carbonates. This can explain much of the spread in the Nussbaum Riegel samples, with manganese concentrations increasing with increasing calcite concentrations relative to aragonite.

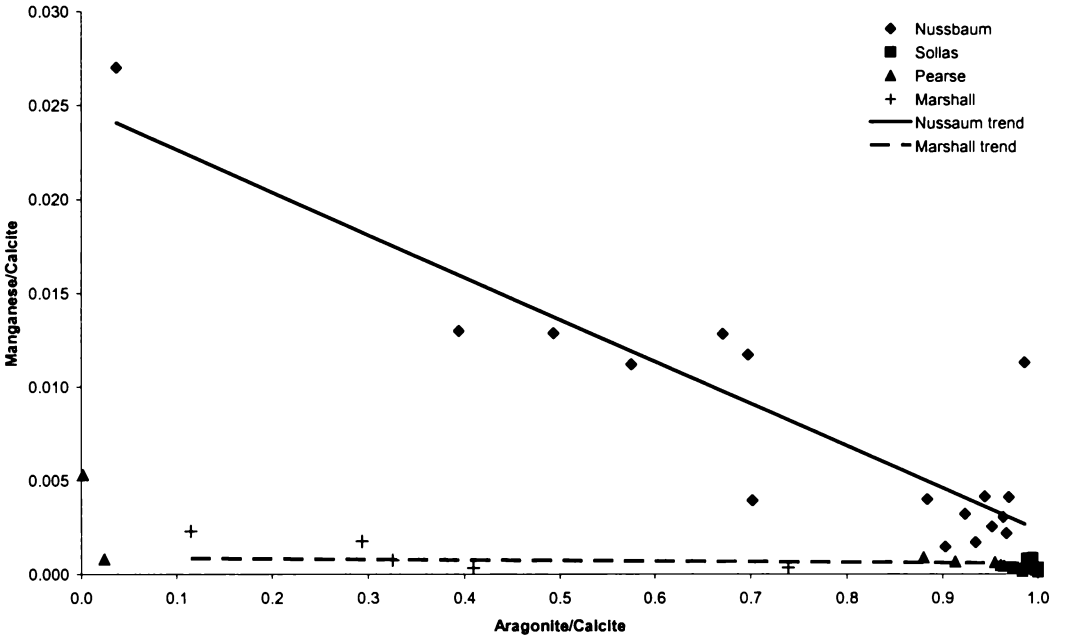

Figure 5.15: Manganese/calcium ratios plotted against the aragonite/calcite ratio.

Again, as with iron, manganese did not show a trend with mineralogy for the Marshall Valley samples, but did show a strong trend with the Nussbaum Riegel samples. The origin could be that oxidising conditions in Glacial Lake Péwé caused the manganese to be less mobile, and therefore incorporated to a lesser degree.

5.2.7 ZINC

The zinc ionic radii of 0.74 Å is very close to that of magnesium of 0.72 Å, and should show a similar trend of trace element substitution to that of magnesium. However, the abundance of zinc in the carbonate samples was far less than that of magnesium. This would be expected, as zinc has a lower abundance in the lake waters than magnesium, so there is less present to be incorporated into the carbonates.

The range of zinc/calcium ratios was very similar to that of the range of manganese/calcium ratios. Like manganese, zinc showed little differentiation between the sites, though greater variability within sites than manganese (Fig.5.16).

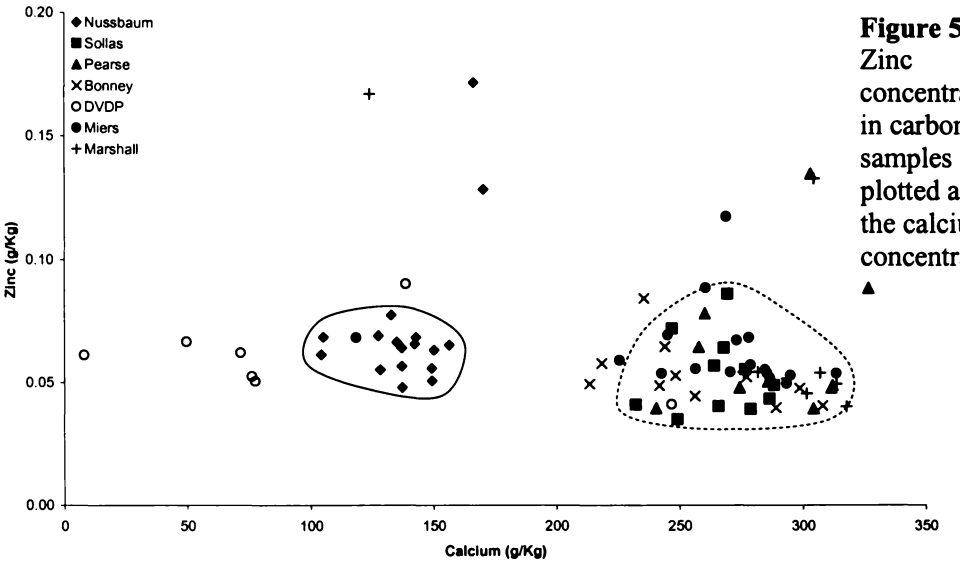

Figure 5.16: Zinc concentrations in carbonate samples plotted against the calcium concentration.

The trend shown by the Nussbaum Riegel samples clearly indicated a slight increase in zinc with increasing aragonite (Fig. 5.17). This is the opposite from that which would be expected from zinc's ionic radius (Fig. 5.17).

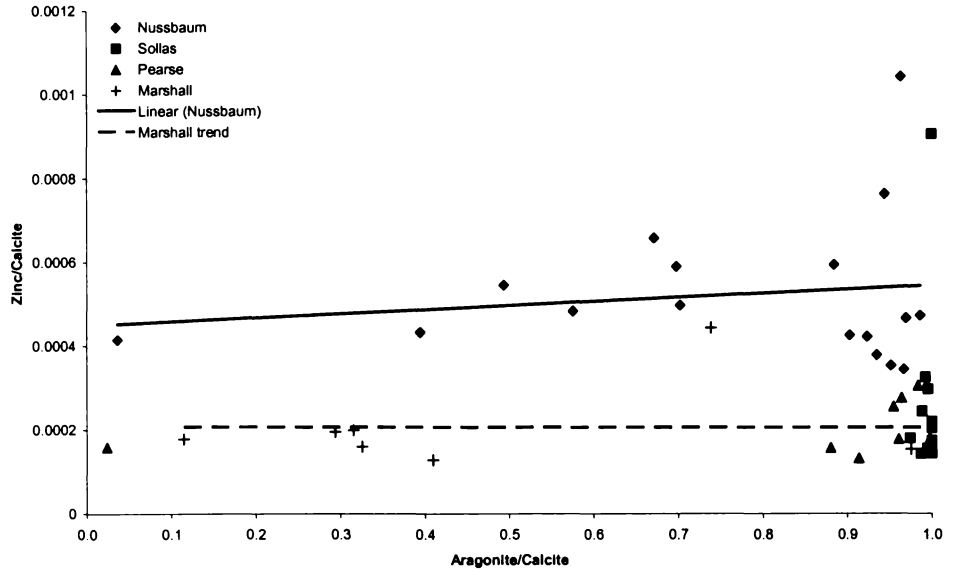

Figure 5.17: Zinc/calcium ratios plotted against the aragonite/calcite ratio.

Increasing diagenetic alteration to equilibration with meteoric waters should lead to an enrichment of magnesium, zinc, iron and a depletion of strontium, sodium and

possibly magnesium in the final product (Pingitore, 1978; Brand and Veizer, 1980). This enrichment/depletion would occur as a result of aragonite/calcite transformation. There was an absence of enrichment in zinc in the Nussbaum Riegel samples with increased calcite abundance relative to aragonite, suggesting that recrystallisation of aragonite to calcite was not likely to be occurring.

5.2.8 POTASSIUM

Potassium and sodium are not easily incorporated into aragonite or calcite. Their presence was likely to be the result of high concentrations in the precipitating water, or the inclusion of acid leachable clastics within the carbonate deposits.

The sites were able to be differentiated by their potassium content, with Nussbaum Riegel samples having higher potassium concentration than the other sites (Fig. 5.18). The Bonney Drift samples showed the least variation in potassium concentration, plotting in a field similar to the other sites.

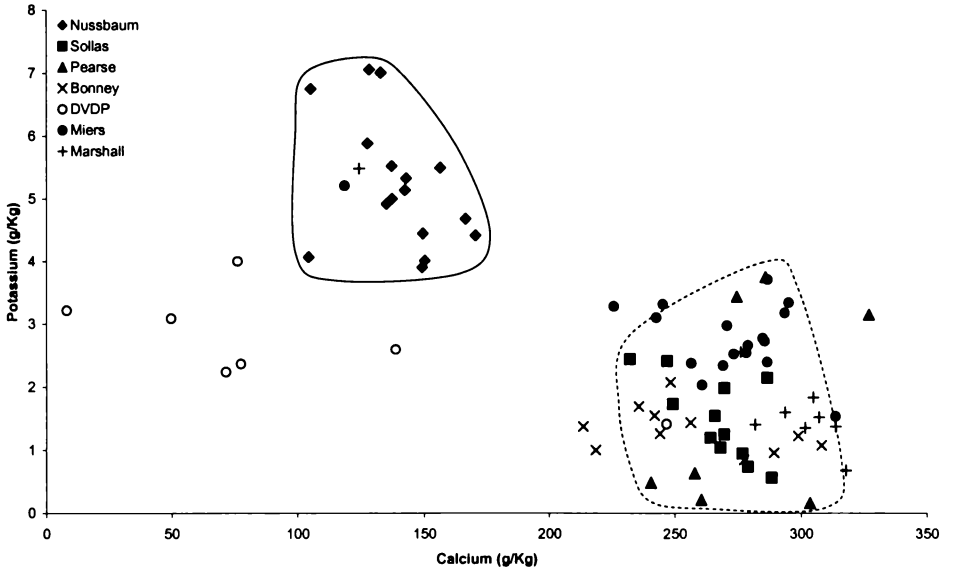

Figure 5.18: Potassium concentrations in carbonate samples plotted against the calcium concentration.

Figure 5.19 showed that there appeared to be no carbonate mineralogical control on the potassium content of the carbonates. This suggests that inclusion of detritus was a more likely source of the variation.

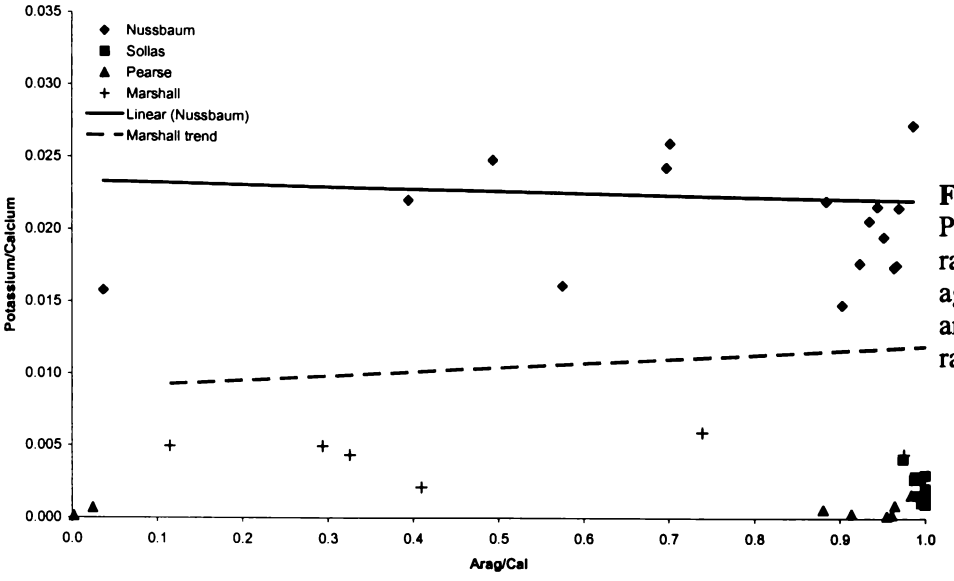

Figure 5.19: Potassium/calcium ratios plotted against the aragonite/calcite ratio.

5.2.9 SODIUM

Unlike potassium, sodium concentrations displayed little differentiation between the sites (Fig. 5.20), but as with potassium there was no variation with changes in the carbonate mineralogy (Fig. 5.21). The variation displayed in sodium is most likely a result of variation in sodium concentration in the precipitating waters as can be observed within and between modern Taylor Valley lakes. There was no evidence for significant direct sea water contribution to the salts of any of the lakes examined, or there would be large observed differences in sodium content.

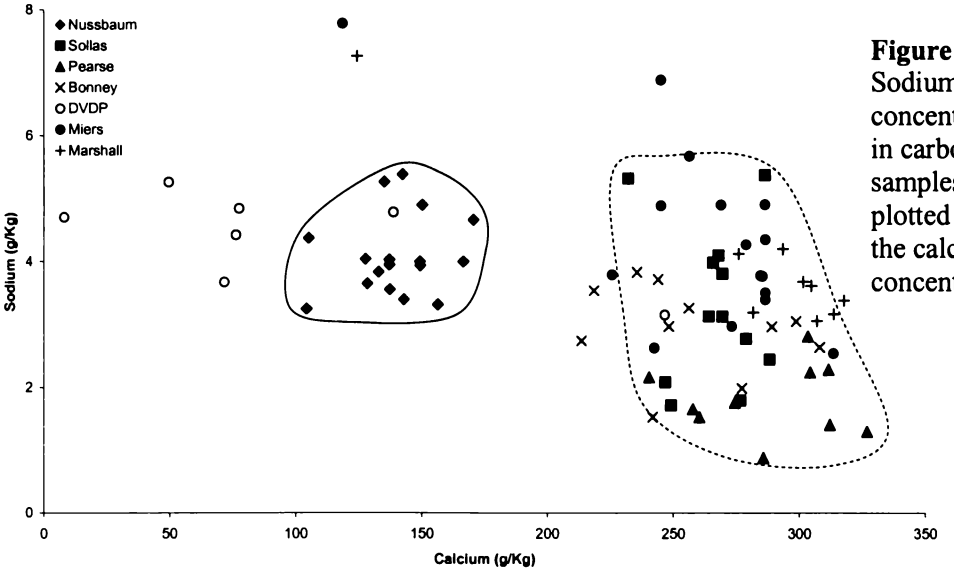

Figure 5.20: Sodium concentrations in carbonate samples plotted against the calcium concentration.

It is interesting that the Sollas Bench carbonates have a lower sodium/calcium ratio than the other carbonates, as this is the only site that contains halite within the carbonate samples. It is possible that the Nussbaum Riegel carbonates contain a higher than expected concentration of sodium due to leaching from the detrital sediment within the carbonates.

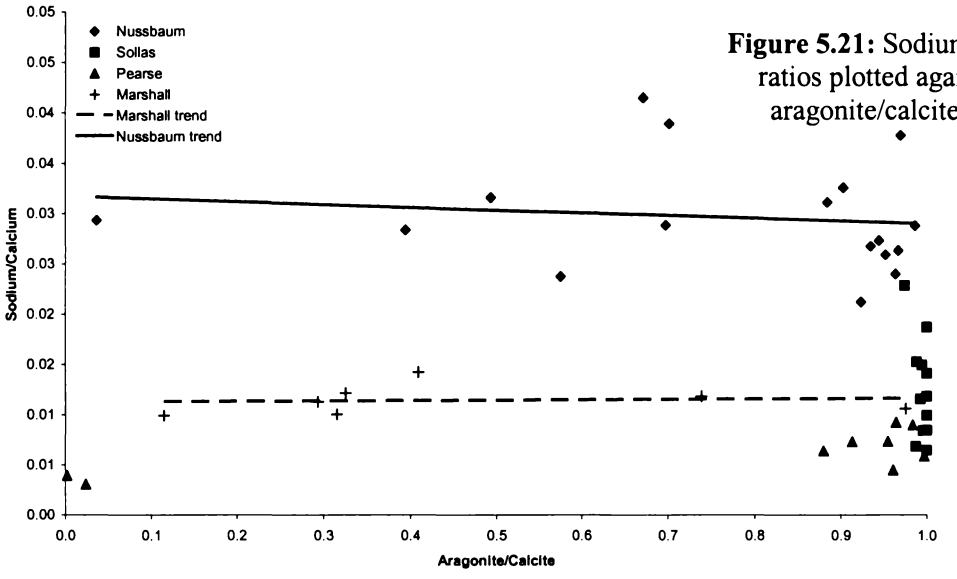

Figure 5.21: Sodium/calcium ratios plotted against the aragonite/calcite ratio.

5.3 SUMMARY OF CONTROLS ON CARBONATE MINERALOGY, MORPHOLOGY, AND TRACE ELEMENT CHEMISTRY

The carbonate mineralogy, morphology, and trace element composition was predominantly controlled by several factors (Tucker and Wright, 1990):

(1) The composition of the precipitating fluids (especially magnesium/calcium ratio). The magnesium/calcium ratio will not control the mineralogy or morphology of the precipitating carbonates.

- Magnesium ions have a marked retarding effect on the precipitation of calcite out of seawater, but not on aragonite. The reason is the Mg^{2+} ions fit more easily into the calcite lattice, but as Mg^{2+} ions are smaller than Ca^{2+} ions, they have a higher surface charge and this attracts a larger hydration sphere. The inhibitory effect relates to the high energy required to dehydrate the Mg^{2+} ions as they are incorporated into the calcite crystals.

- Incorporation of magnesium on a side face is solely a function of the magnesium/calcium ratio of the precipitating fluid, and that on these faces magnesium incorporation may be controlled by distribution coefficients (Lahann, 1978).

(2) The carbonate supply rate

- High CO_3^{2-} availability gives rise to aragonite, whereas lower availability gives rise to calcite (Given and Wilkinson, 1985).
- When levels of CO_2 are decreased (ie. by degassing) acidity is low and supersaturation with respect to carbonate species occurs, leading to fast crystal growth rates and acicular crystal form. The rate of precipitation in the c-axis direction is controlled by the availability of CO_3^{2-} (Given and Wilkinson, 1985).
- The final magnesium content of natural calcites is a function of (a) the magnesium/calcium ratio of ambient fluids (on side faces) and (b) the rate of crystal growth as determined by fluid Ca^{2+} and CO_3^{2-} concentrations (on c-axis faces (Given and Wilkinson, 1985).

(3) Rate of precipitation

- Rate of crystal growth can be affected by P_{CO_2}, rates of fluid flow and temperature, which can in turn determine cement morphology (Chafetz et al., 1985).

Other factors that need to be taken into account when considering the mineralogy of carbonates:

- Dissolved phosphate inhibits both calcite and aragonite precipitation (the former more so), by adsorption on to the crystal surface and blocking of nucleation and growth sites (Berner, 1975; Tucker and Wright, 1990).
- Sulfate in seawater apparently inhibits calcite precipitation considerably more than aragonite, possibly in the manner described from Mg^{2+} poisoning (Folk, 1974; Tucker and Wright, 1990).
- Dissolved organic compounds can inhibit the precipitation of calcite (Berner, 1975)

- Carbonate precipitates can be a function of temperature, with lower temperatures favoring the formation of calcite over aragonite (Burton and Walter, 1987; Morse et al., 1997).
- An increase in P_{CO_2} will cause decreases in Mg incorporation into carbonate (Burton, 1993).
- Oxidation state of the precipitating water can control mobility of some ions.
- Co-precipitation of other phases (ie. gypsum) can change the partitioning of elements such as barium, strontium and magnesium.

Common views that aragonite will precipitate if the rate of precipitation is very fast if the degree of supersaturation is high or at higher temperatures (Folk, 1974) do not seem to hold for this environment. Though saturation levels may be high in many cases, the temperatures in this environment will be low. When examining the reasons for differences in mineralogy, morphology and trace element chemistry, interactions of all of the factors need to be taken into account. Very rarely will one factor be acting to solely control the chemistry, though some may play dominant roles.

For the carbonates collected from Nussbaum Riegel, Sollas Bench and Pearse Valley, there appears to be two main controls on their trace element chemistry, (1) the composition of the precipitating water body, and (2) the mineralogy of the carbonate (aragonite or calcite). It is difficult to determine which of these two factors play the more dominant role. The degree to which these two factors influence different elements is demonstrated in Table 5.4.

Table 5.4: Degrees to which the composition of the precipitating water and mineralogy of carbonate have an effect on the incorporation of different trace elements.

Element	Composition of water	Mineralogy of carbonate
Calcium	×	×
Magnesium	✓	✓✓
Strontium	✓	✓✓
Barium	✓	✓
Iron	×	×
Manganese	×	✓
Zinc	×	×
Potassium	✓	××
Sodium	✓	××

✓= has an effect ✓✓= has a major effect × = has little effect ×× = has no effect

CHAPTER SIX:

CARBONATE CHEMISTRY:

STABLE ISOTOPES

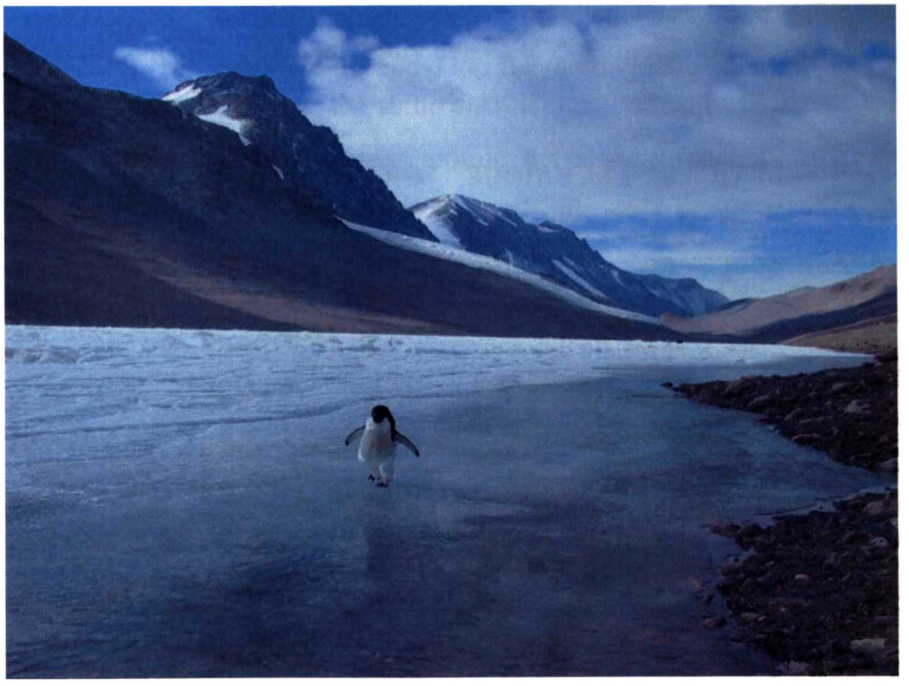

6.0 INTRODUCTION

This chapter investigates the stable isotope composition of the lacustrine carbonates. It looks into how oxygen isotopes can be used to distinguish the source of the water in the palaeo lakes. This can be undertaken as water sourced from either the Ross Sea Ice Shelf or the Taylor Glacier has a different $\delta^{18}O$ signature.

The various potential processes occurring in the palaeo lakes that could have influenced the $\delta^{13}C$ values of the carbonates have been investigated. These can include (Leng and Marshall, 2004):

- rates of precipitation, i.e. non-reversible kinetic fractionation, which occur in authigenic and biogenic precipitation;
- pH effects- speciation control;
- biochemical fractionation;
- growth in microenvironments not typical of the water body as a whole.

6.1 ANALYTICAL TECHNIQUE FOR DETERMINATION OF STABLE OXYGEN AND CARBON ISOTOPE COMPOSITIONS

After the dry carbonate samples were prepared by crushing in a ring mill for 20 seconds, they are reacted in the Europa CAPS (Carbonate Automatic Preparation System) using the individual acid dosing or 'drip' method, in which the sample is reacted with a small amount of orthophosphoric acid and the resulting CO_2 frozen out.

The samples are loaded into individual reaction vessels, which in turn are placed in a 24-position carousel. Each sample is analysed sequentially. The vessel is evacuated and a predetermined dose of orthophosphoric acid is dispensed. While the sample is reacting the evolved CO_2 is frozen into a dedicated cold finger, positioned close to the mass spectrometer inlet, to minimise sample transfer time. Water is removed during the reaction by passing the CO_2 through a loop that is maintained at -90°C, which freezes the water, but not the CO_2.

After the reaction is complete (after 10 minutes), the sample CO_2 is introduced to the Europa Geo 20-20, where gas pressures are balanced, and the sample gas run against an internal reference gas. This reference gas is calibrated daily by running an internal standard, WCS, against it. WCS is calibrated against NBS-19, and cross-checked against NBS-20. External precision for replicate analyses of WCS is better than 0.05‰ for both carbon and oxygen.

$\delta^{13}C$ and $\delta^{18}O$ isotope ratios are presented in the usual delta (δ) notation, normalised, and expressed in per mille (‰), relative to Vienna Peedee belemnite (VPDB) (Coplen, 1988; Coplen, 1994).

6.2 THEORETICAL CONSIDERATIONS

By using the natural fractionation of oxygen in the water of the hydrosphere and atmosphere, stable isotopic analysis can be used to distinguish water masses. Isotopes of the same element take part in the same chemical reactions, but because the atoms of different isotopes are of different atomic mass they react at different rates. Differences in the mass of isotopes in a molecule will result in differences in vibrational frequencies. These lead to differences in the thermal properties (including free energies) so that substitution of one isotope for another will result in changes in equilibrium constants. When two or more phases containing the same isotopic element are formed in equilibrium with each other, the isotopes will be partitioned between the phases with the heavier isotope favouring the phase with the highest vibrational frequency. Physical processes such as evaporation discriminate against heavy isotopes. This equilibrium can result in reaction products that are isotopically heavier or lighter than their precursor materials. An example of this is the ice from the snout of Taylor Glacier, which has a $\delta^{18}O$ value of around –42‰ as a result of the precipitation falling at the South Pole. The precipitation at the South Pole has $\delta^{18}O$ values of between –55‰ and –40‰ (Urey, 1947; Epstein et al., 1963; Epstein et al., 1965; Drewry, 1979).

Stable isotopes at or near natural abundance levels are commonly reported in the form of delta values, given in parts per thousand or per mille (‰). Delta values are not absolute isotope abundances, but differences between sample readings and one or another of the widely used natural abundance standards, which are considered delta = 0. (e.g. air for N, At%^{15}N = 0.3663033; Peedee Belemnite for C, At%^{13}C = 1.1112328 (Craig, 1957)). Absolute isotope ratios (R) are measured for sample and standard, and the relative measure delta is calculated (Craig, 1957):

$$\delta = \left(\frac{R_{sanple} - R_{std}}{R_{std}} \right) (1000\delta‰)$$

The standard used in the analysis of $\delta^{18}O$ and $\delta^{13}C$ is the PDB (Peedee Belemnite). This is solid carbonate from a belemnite *Belemnitella americana,* collected from the Cretaceous Pee Dee formation, South Carolina, U.S.A. As the original PDB standard has been exhausted, IUPAC recommended that isotope abundances be reported relative to VPDB (Vienna PDB, the new primary reference for carbon isotope ratios having a $\delta^{13}C$ of 0‰), by assigning an exact $\delta^{13}C$ values of +1.95‰ and exact $\delta^{18}O$ of 2.2‰ on the VPDB scale to the IAEA reference material NBS 19 calcium carbonate (Friedman and O'Neil, 1977; Bowen, 1988; Coplen et al., 2003).

There are a number of causes of fractionation between isotopes. In the case of oxygen, the process that has the biggest effect is temperature in the form of evaporation and condensation. From the vapour pressure data for water, it is evident that the lighter molecular species are preferentially enriched in the vapor phase, the extent depending on the temperature. The opposite will occur during condensation, the heavier molecular species being preferentially removed. The isotopic separation caused by this process under equilibrium conditions is an example of a Rayleigh Distillation (Dansgaard, 1964). A summary of this is given in Fig. 6.1. Fractionation of oxygen can also occur in processes such as the precipitation of calcium carbonate (McCrea, 1950; Epstein et al., 1953).

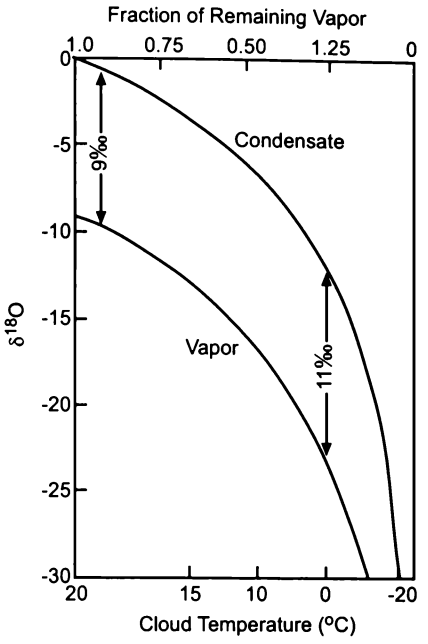

Figure 6.1: $\delta^{18}O$ in a cloud vapour and condensate plotted as a function of the fraction of remaining vapour in the cloud for a Rayleigh process. The temperature of the cloud is shown on the lower axis. The increase in fractionation with decreasing temperature is taken into account (Hoefs, 1987).

There are two main carbon reservoirs, organic matter and sedimentary carbonates. These two are isotopically different, due to two different formation mechanisms (Craig, 1953):

(1) a kinetic effect during photosynthesis. This leads to the depletion of ^{12}C in the remaining CO_2 and concentration of the light ^{12}C in the organic matter formed.

(2) a chemical exchange effect. Here exchange occurs between atmospheric CO_2 and dissolved HCO_3^-, which leads to an enrichment of ^{13}C in the bicarbonate.

The reactions which distribute ^{13}C and ^{18}O into carbonates are (Milliman, 1974):

$$H_2{}^{18}O_{(l)} + CaC^{16}O_{3(s)} \leftrightarrow H_2{}^{16}O_{(l)} + 1/3CaC^{18}O_{3(s)}$$

$$^{13}CO_3{}^{2-}{}_{(aq)} + {}^{12}CO_{3(s)} \leftrightarrow {}^{12}CO_3{}^{2-}{}_{(aq)} + {}^{13}CO_{3(s)}$$

For oxygen and carbon isotopes, the carbonate mineralogy is important in fractionation. At 25°C, the $\delta^{18}O$ content of aragonite is 0.6‰ higher than co-precipitated calcite, and increases by 0.06‰ for each mol% of $MgCO_3$ (Tarutani et al., 1969). Calcite is enriched in $\delta^{13}C$ relative to HCO_3^- in water by 0.9‰, and aragonite is enriched by 1.8‰ relative to calcite (Rubinson and Clayton, 1969).

6.3 RESULTS

Samples collected at the Nussbaum Riegel, Sollas Bench and Pearse Valley show a large range of $\delta^{18}O$ and $\delta^{13}C$ values between the locations, while samples from within each location show less variability (Table 6.1 and Fig 6.2).

Table 6.1: Oxygen and carbon stable isotopes for Nussbaum Riegel, Sollas Bench and Pearse Valley samples.

Nussbaum Riegel			Sollas Bench			Pearse Valley		
	$\delta^{18}O_{vpdb}$	$\delta^{13}C_{vpdb}$		$\delta^{18}O_{vpdb}$	$\delta^{13}C_{vpdb}$		$\delta^{18}O_{vpdb}$	$\delta^{13}C_{vpdb}$
S01a	-30.74	-0.94	S14a	-35.51	4.37	S24a	-37.73	2.70
S02a	-29.14	-3.10	S14b	-36.76	6.61	S25a	-38.26	2.52
S03a	-28.24	-0.60	S15a	-35.75	6.51	S26a	-33.69	0.64
S04a	-31.49	-2.30	S16a	-35.89	6.42	S27a	-36.34	7.10
S05a	-31.44	-1.96	S17a	-37.18	8.32	S27b	-33.50	3.17
S06a	-30.51	-1.18	S18a	-34.21	7.16	S27c	-35.42	7.35
S07a	-30.24	-0.18	S19a	-37.15	7.29	S28a	-35.81	7.16
S07b	-30.49	0.02	S20a	-37.33	8.31	S29a	-	-
S07La	-30.63	0.03	S21a	-35.28	7.40	S30a	-38.19	2.59
S07Ua	-32.64	-1.28	S22a	-33.88	8.19	S31a	-38.00	2.87
S08a	-30.40	0.20	S22b	-34.32	7.50	S32a	-33.58	3.78
S09a	-30.88	-0.66	S23a	-37.15	4.92			
S10a	-31.95	-0.67						
S11a	-31.24	-0.35						
S11b	-30.88	0.00						
S12a	-30.43	-1.52						
S13a	-31.46	-0.53						

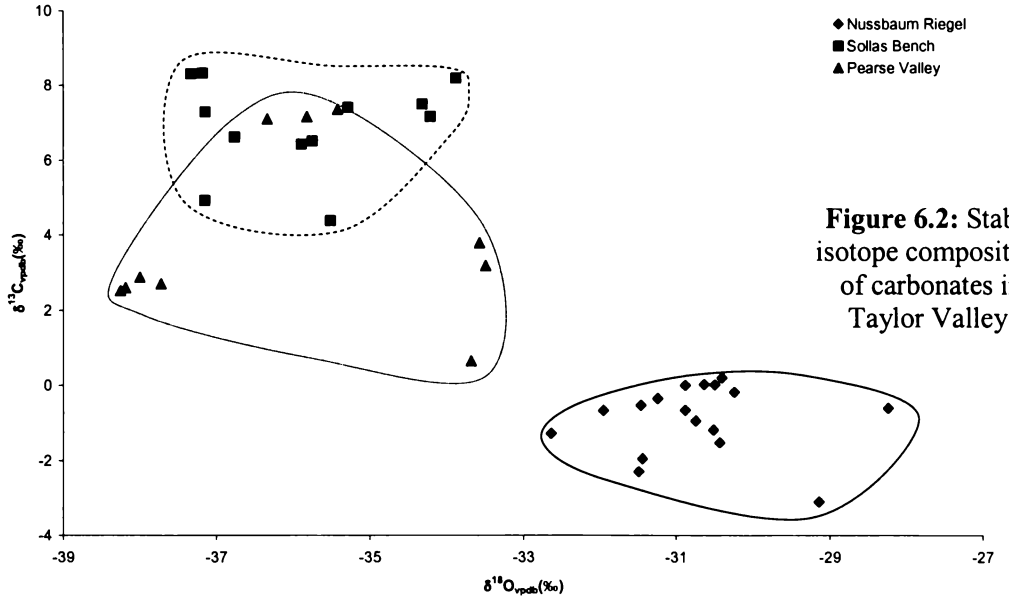

Figure 6.2: Stable isotope composition of carbonates in Taylor Valley.

The carbonate samples collected from Sollas Bench (■) and Pearse Valley (▲) have strongly depleted $\delta^{18}O$ values when compared with the Nussbaum Riegel samples (♦), with values ranging from -33.69‰ to -38.26‰ for Pearse Valley and -33.88‰ to

-37.33‰ for Sollas Bench. The $\delta^{18}O$ is less depleted for the Nussbaum Riegel samples compared with the other two collection locations, with values ranging from -28.24‰ to -32.64‰.

The carbonate samples collected from Sollas Bench and Pearse Valley have strongly enriched $\delta^{13}C$ values when compared to the Nussbaum Riegel samples, with values ranging from +0.64‰ to +7.35‰ for Pearse Valley and +4.37‰ to +8.32‰ for Sollas Bench. There is an overlap with these two localities, with the more enriched Pearse Valley samples plotting in the Sollas Bench field. The $\delta^{13}C$ is less enriched for the Nussbaum Riegel samples compared to the other two collection locations, with values ranging from -3.10‰ to +0.20‰.

6.4 DISCUSSION

The source of the water from which the carbonate was precipitated can be determined using stable isotopes. Overall the isotopic composition of the lacustrine carbonates will reflect the nature of the water from which they were precipitated, and hence can be used to determine the processes taking place and source(s) of the contemporaneous waters in the palaeo lake.

6.4.1 $\delta^{18}O$

The $\delta^{18}O$ values of the carbonates are controlled by the isotopic composition of the water feeding the lakes from which they were precipitated and the temperature of precipitation. As shown in Fig. 6.2, the carbonates deposited at Nussbaum Riegel have $\delta^{18}O$ of -32‰ to -28‰. Ice from the Ross Sea Ice Shelf has an average $\delta^{18}O$ of -35‰, which makes it a likely source for the water of this palaeo lake. Ice from the snout of Taylor Glacier has $\delta^{18}O$ values of around –42‰. The $\delta^{18}O$ of approximately -38‰ to -34‰ for samples from Sollas Bench and Pearse Valley (Fig. 6.2) reflect water sourced from this glacier ice. The difference in delta values between the precipitating water and the carbonate is due to fractionation as the carbonate is precipitated. This fractionation causes the carbonate to be ~4‰ heavier than the water at 0°C according to the equation:

$$t°C = 19.7 - 4.34(\delta cc - \delta w)$$

where δw is the $\delta^{18}O$ value of CO_2 gas at equilibrium with the water at 25°C and δcc is the $\delta^{18}O$ value of the CO_2 gas released from the aragonite when it is reacted with orthophosphoric acid (Grossman and Ku, 1986).

Carbonates precipitated from an evaporating water body tend to show enrichment in $\delta^{18}O$. The enrichment will continue until a steady state is achieved. In this way the $\delta^{18}O$ reflects the salinity, temperature and relative humidity. In polar environment, where lakes have permanent ice cover, this evaporation effect does not occur to any great extent. "Evaporation" of a water body in this environment occurs by ablation of the ice surface and freezing of water on to the bottom of the ice. As there is little isotopic fractionation between $H_2O_{(l)}$ and $H_2O_{(s)}$, evaporitic enrichment will therefore have been minimal.

6.4.2 $\delta^{13}C$

The carbon isotope composition of the carbonate reflects the nature of carbon dioxide cycling within the host lakes. Carbonates do not precipitate in equilibrium with their environments. Disequilibrium effects can be caused by the following (Leng and Marshall, 2004):

- rates of precipitation, i.e. non-reversible kinetic fractionation, which occur in authigenic and biogenic precipitation;
- pH effects- speciation control;
- biochemical fractionation;
- growth in microenvironments not typical of the water body as a whole.

The main factors influencing the $\delta^{13}C$ composition of carbonate precipitated in Antarctic lakes may be (i) temperature, (ii) $\delta^{13}C$ in CO_2 trapped in the Antarctic ice sheet, (iii) CO_2 exchange with the atmosphere, (iv) algal productivity; or (v) the circulation of lake water.

6.4.2.1 SOLLAS BENCH AND PEARSE VALLEY

The strongly positive $\delta^{13}C$ values observed in the Sollas Bench and Pearse Valley samples (from 4.37‰ to 8.32‰, Fig. 6.2) indicate low temperature equilibrium with atmospheric CO_2. Here, exchange of carbon occurs between atmospheric CO_2 and dissolved HCO_3^-, which leads to an enrichment of ^{13}C in the bicarbonate (Hoefs, 1987).

Pre-twentieth century atmospheric CO_2, at 25°C, had a $\delta^{13}C$ of -6.9‰. Aragonite in isotopic equilibrium will be enriched in ^{13}C by 7.8‰ at 25°C and further enriched by 1.2‰ in $\delta^{13}C$ for every 10°C change in the temperature. At 0°C, this gives a $\delta^{13}C$ value of +6‰, and at -10°C a $\delta^{13}C$ value of +7‰ (Friedman and O'Neil, 1977). $\delta^{13}C$ values of +6‰ to +7‰ would only be possible with an ice-free lake surface, allowing equilibration with the atmosphere. Halite dominated lakes can reach temperatures as low as -20 °C before all of the brine freezes, while $CaCl_2$ dominated lakes can reach -40°C before the brine freezes. Hypersaline lakes in Antarctica record temperatures down to -40°C because their salinities are high and commonly range up to about 250‰ (Rao et al., 1998). This is consistent with the presence of halite crystals in some of the Sollas Bench samples, as water cannot maintain an ice cover once the salt concentration reaches saturation point and halite precipitation occurs.

The lighter, though still positive $\delta^{13}C$ values, of some of the Pearse Valley samples (ranging from +0.64‰ to +3.78‰, Fig. 6.2) could be at equilibrium with the atmospheric CO_2 at higher temperatures than the samples with more positive $\delta^{13}C$. Carbonates are not a major part of the bedrock around the three collection sites (they only occur as vein fills in dykes), making contribution of carbon from this source unlikely.

6.4.2.2 NUSSBAUM RIEGEL

When the carbonate carbon isotopic values from this site are compared with the mineralogy for the Nussbaum Riegel samples (Fig. 6.3), it can be observed that $\delta^{13}C$

composition becomes depleted as the aragonite/calcite ratio changes in favour of calcite.

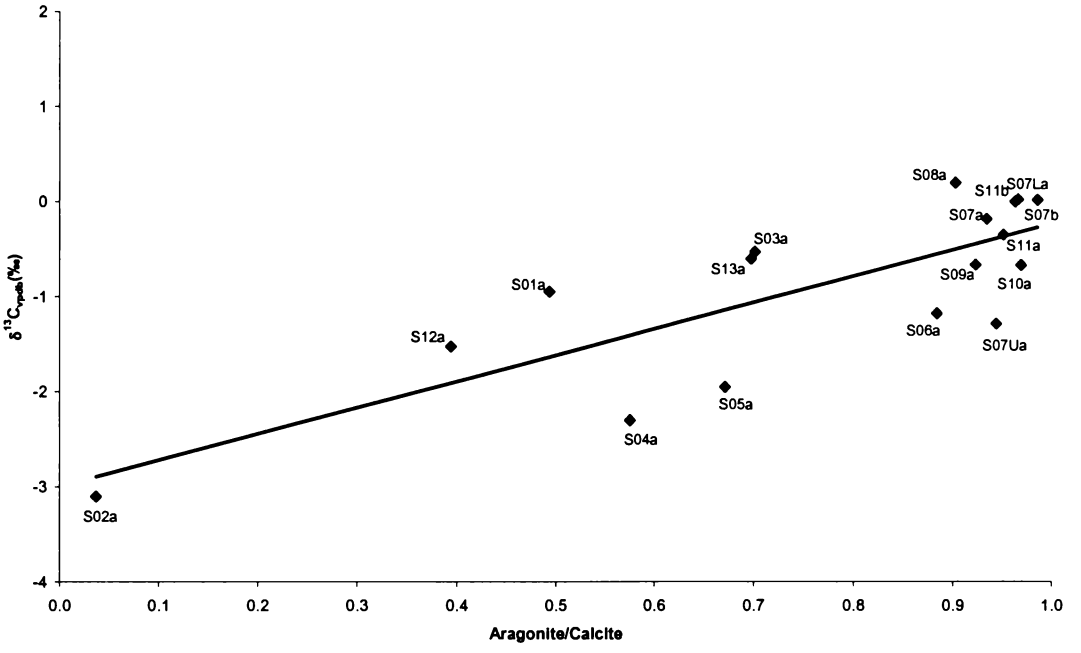

Figure 6.3: $\delta^{13}C$ values for Nussbaum Riegel samples plotted against change in mineralogy (aragonite/calcite ratio).

- Carbonate Mineralogy

Rubinson and Clayton (1969) found experimentally an enrichment of $\delta^{13}C$ in calcite and aragonite relative to bicarbonate of 0.9‰ and 2.7‰, respectively. González and Lohmann (1985) also found a 1.0‰ to 1.4‰ enrichment in $\delta^{13}C$ in inorganic marine aragonite cement compared with equilibrium calcite. Romanek et al. (1992) investigated this phenomenon further by looking at the effect of temperature, concluding that the calcite-bicarbonate and aragonite-bicarbonate fractionation is essentially independent of temperature (over the range of 10-40°C). Aragonite therefore has generally heavier $\delta^{13}C$ values than calcite. This can explain only some of the variability seen in Fig. 6.3, as the range of 3.3‰ across the values is greater than the enrichment factor between aragonite and calcite. Thus it can be concluded that the effect of carbonate mineralogy on $\delta^{13}C$ in these carbonates is small.

- pH

There is considerable fractionation of carbon isotopes between the species of the carbonate system prior to precipitation of carbonate. For a given isotopic composition of the total dissolved carbon (ΣCO_2), the isotopes will not be evenly distributed between CO_2, HCO_3^-, and CO_3^{2-}, though the sum of all of the isotopes in the different species must equal the sum of all the isotopes in ΣCO_2. As the percentage of CO_2, HCO_3^-, and CO_3^{2-} are a function of the pH of the solution, the $\delta^{13}C$ values of each carbonate species changes as a function of pH (Zeebe and Wolf-Gladrow, 2001). The effect that pH has on the $\delta^{13}C$ of the carbonate species can be seen in Figure 6.4.

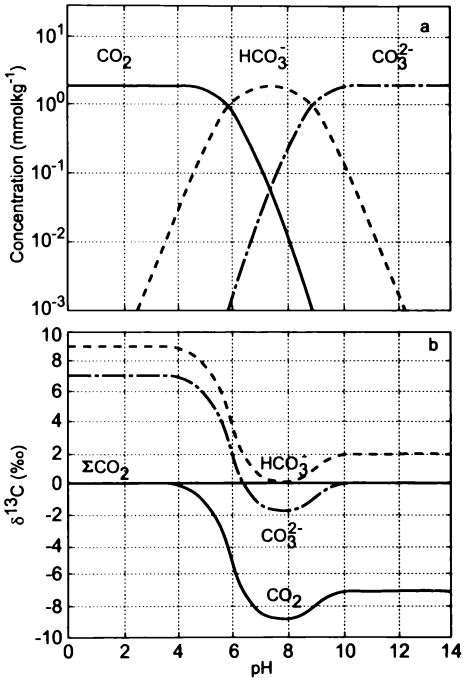

Figure 6.4: This figure shows carbon isotope partitioning in a closed sea water carbonate system as a function of pH. (a) Concentrations of the dissolved species at ΣCO_2 = 2 mmolkg^{-1}, T = 25°C, and S = 35 salinity units. (b) $\delta^{13}C$ of the dissolved species for $\delta^{13}C_{\Sigma CO2}$ = 0‰ (Zeebe and Wolf-Gladrow, 2001).

- Biochemical Fractionation

The effect of biological activity also needs to be taken into account when considering the $\delta^{13}C$ values. Photosynthesis by algae will preferentially remove CO_2 enriched in ^{12}C, which will then be sequestered in the organic matter as it dies and falls to the bottom of the lake. This will leave waters enriched in ^{13}C, from which the carbonate will precipitate. However, calcium carbonate precipitated under equilibrium conditions will contain relatively more ^{13}C than ^{12}C, compared with the aqueous CO_2, as the heavier carbon is preferentially included during precipitation. In this way, continued removal of organic carbon and inorganic carbon will result in steadily

increasing $\delta^{13}C$ values, as long as the carbon pool is not replenished from an outside source. This effect can be quite marked in Antarctic lakes where stratified water columns and permanent ice cover prevent recharge of the CO_2 reservoir from which the algae are removing the CO_2. The calcium carbonate precipitated in this reaction will reflect the changing fractionation of the CO_2 (Lawrence and Hendy, 1985).

Potential Explanation for Stratigraphy

The pit dug at site 7 (Fig. 6.5) is being investigated to determine which processes have been influencing the carbonate precipitated in this system.

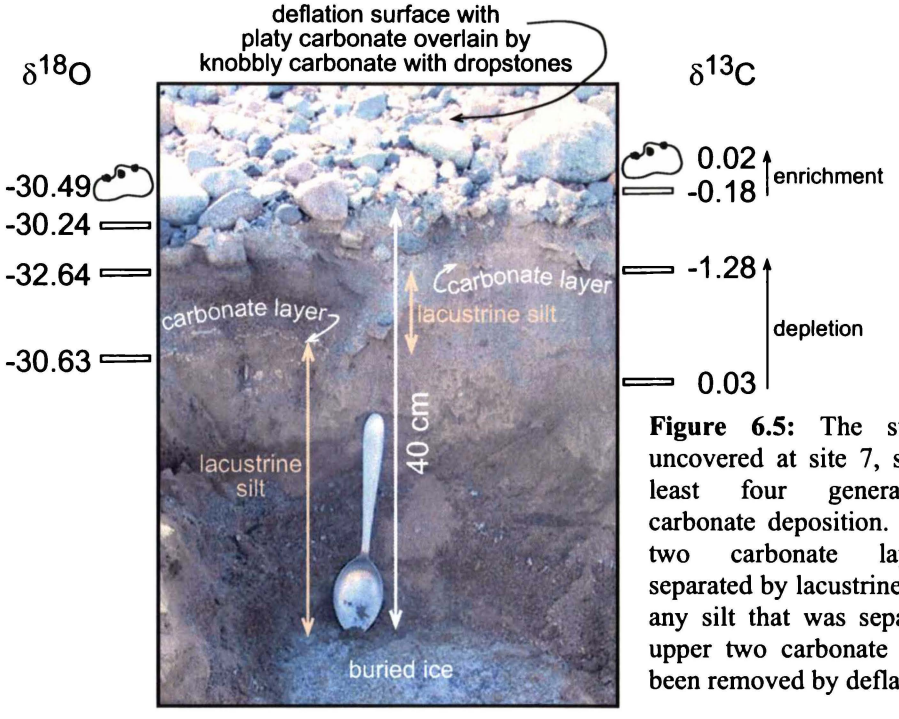

Figure 6.5: The stratigraphy uncovered at site 7, showing at least four generations of carbonate deposition. The lower two carbonate layers are separated by lacustrine silt, while any silt that was separating the upper two carbonate layers has been removed by deflation.

- Depletion in both carbon and oxygen isotopes between lower subsurface carbonate and upper subsurface carbonate:

The depletion in $\delta^{13}C$ values from the bottom carbonate to the overlying carbonate layer can be explained by the progressive removal of $CaCO_3$. Inorganically precipitated $CaCO_3$ removes ^{13}C preferentially to ^{12}C. If the carbon source is in the form of $CO_{2(aq)}$ the fractionation will be ~10‰, whereas if the carbon is in the form of CO_3^{2-} or HCO_3^-, the fractionation will be ~2‰. As observed in Figure 6.4, at a pH above 6, the CO_3^{2-}/HCO_3^- system is "in play". As the pH of the lake water is most

likely to be above 6 (Lawrence, 1982), this will be what is affecting the precipitation of carbonate. If half of the CO_3^{2-} is removed, it will result in the remainder becoming depleted by ~1‰. If the lower carbonate layer was precipitated with a $\delta^{13}C$ value of +0.03‰, and this removed around half of the CO_3^{2-} in the lake, the next carbonate precipitated with a measured $\delta^{13}C$ value of -1.28‰, would have $\delta^{13}C$ depleted by ~1‰, which appears to be the case.

If the precipitation of the second carbonate involved freezing of the water, the oxygen isotopes would become depleted, which could explain the more negative $\delta^{18}O$ value of -32.64‰.

- Enrichment in carbon and oxygen isotopes between upper subsurface carbonate and the platy and knobbly carbonates of the deflation surface:

It appears that the average $\delta^{13}C$ value of carbonate precipitated from the Nussbaum Riegel lake is around 0.03‰. After the depletion of the $\delta^{13}C$ values from the precipitation of the lower two carbonate beds, flooding of the lake with meltwater could bring the water composition back to the average value of 0.03‰ before the precipitation of the upper two carbonates. Addition of meltwater could also account for the lighter $\delta^{18}O$ values of the upper two carbonates.

If all of the Nussbaum Riegel samples are considered (Fig. 6.3), it is likely that the two buried carbonate layers uncovered at site 7 will be underneath the carbonates at the other sites as well. This can only be assumed as pits were not dug at the other sites. The carbonates of mixed mineralogy (sites 1-5,12,13) also have depleted $\delta^{13}C$ values. It is possible these were deposited after the two buried carbonates (the precipitation of buried carbonates causing the depletion in $\delta^{13}C$ values). This could have been followed by an influx of meltwater bringing the composition of the Nussbaum Riegel lake from which these carbonates precipitated back to its average value, allowing the deposition of carbonates with more enriched $\delta^{13}C$ values observed at the other sites. The more depleted values at sites 1-5, 12 and 13 are also possibly partly due to the fractionation factor between aragonite and calcite.

CHAPTER SEVEN:

PETROGRAPHY

7.0 Introduction

This chapter investigates the provenance of the detrital material contained within the carbonate samples. This is achieved by examining petrographic thin sections of the carbonate plates and determining the most abundant mineral components. The likely sources of these minerals are then identified.

7.1 Method

Samples of carbonate were prepared by cutting the carbonate plates into small pieces ~2 cm in length that could be mounted on frosted glass microscope slides. Many of the plates were not hard enough to mount directly on the slides, so thoroughly dried samples were first set in epoxy resin. The resin blocks were cut to size and mounted onto glass slides, then cut and polished to a thickness of 0.3 m. The carbonate plates were mounted as a vertical section through the plate.

7.2 Results

Samples from Nussbaum Riegel contain carbonate cemented detrital material. Varying percentages of carbonate can be observed in the various samples. E-F in Figure 7.1 show an example of a small amount of cement, while S-T in Figure 7.1 shows a sample with high amounts of cement (in places the detrital material is cement supported). The samples from Sollas Bench and Pearse Valley are predominantly carbonate components, with a small amount of detrital minerals. The sample observed in Figure 7.1, U-V has a higher proportion of detrital material than other samples, though shows the predominance of carbonate. The grain size of the detrital material varies greatly, with the samples collected from Sollas Bench and Pearse Valley having the smallest grain size. The samples from Nussbaum Riegel vary in grain size between samples, but also show variation within samples, observed in Figure 7.1, I-J and O-P.

The detrital material in the Nussbaum Riegel samples is dominated volcanic glass fragments and anorthoclase (Fig. 7.1, S-T), with olivine crystals (Fig. 7.1, A-B) and volcanic rock fragments being relatively common. Subordinate to these components

are biotite (Fig. 7.1, C-D), aegerine-augite (Fig. 7.1, I-J), brown amphibole (possibly kaersutite) (Fig. 7.1, I-J), muscovite (Fig. 7.1, E-F), and plagioclase. The detrital minerals in the Sollas Bench and Pearse Valley samples are dominated by anorthoclase and plagioclase, along with small amounts of biotite.

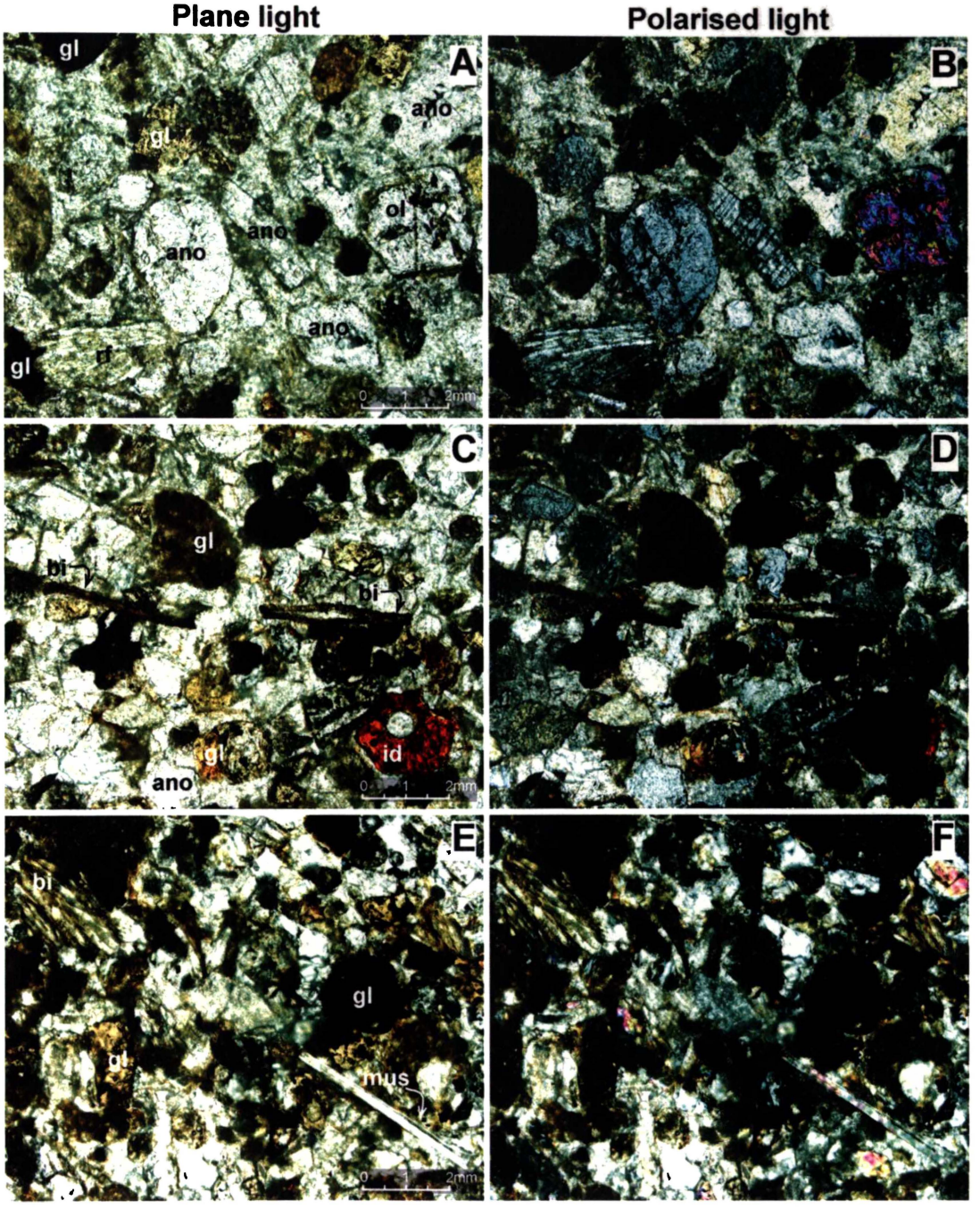

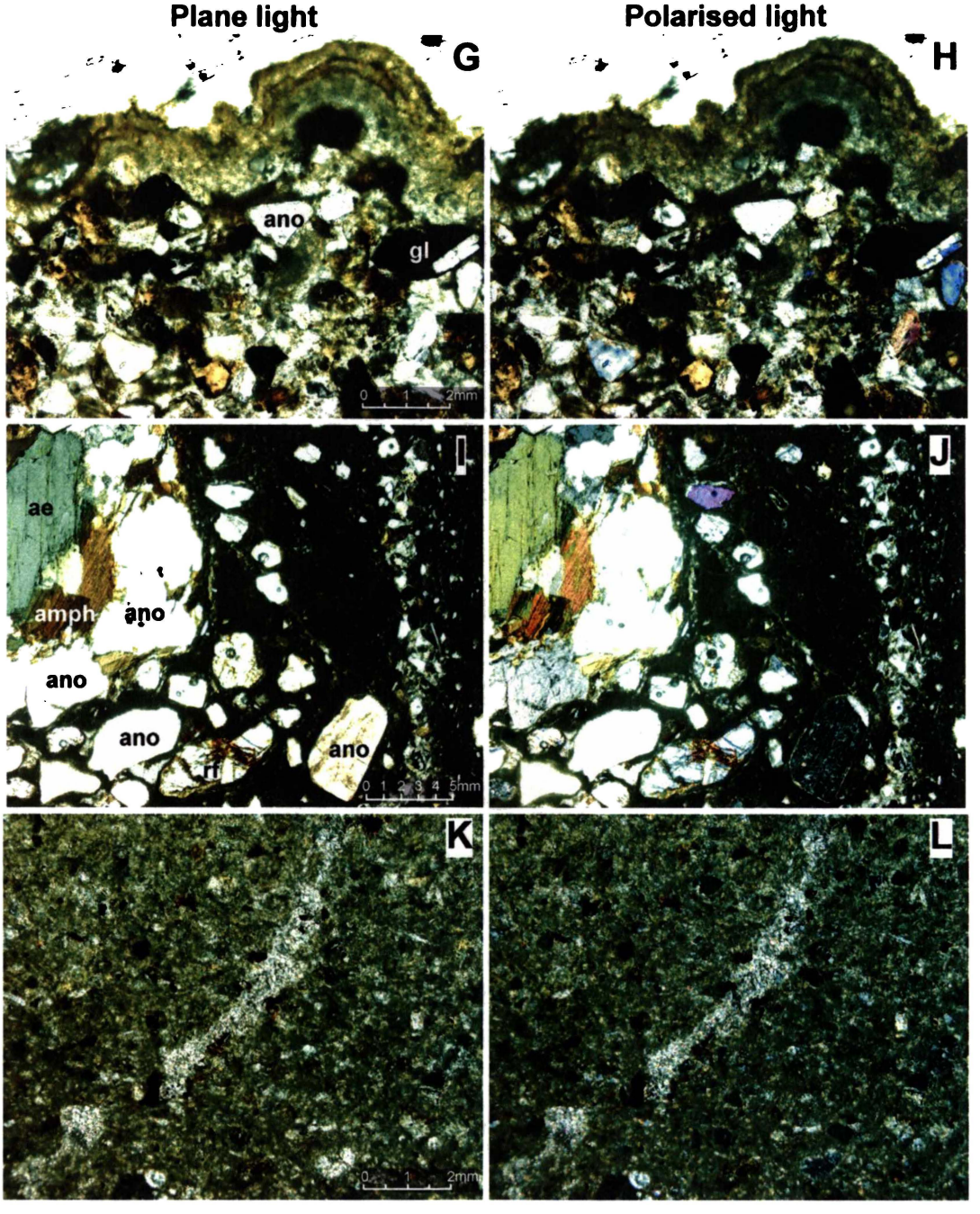
Plane light
Polarised light
G
H
ano
gl
0 1 2mm
I
J
ae
amph
ano
ano
ano
ano
rf
0 1 2 3 4 5mm
K
L
0 1 2mm

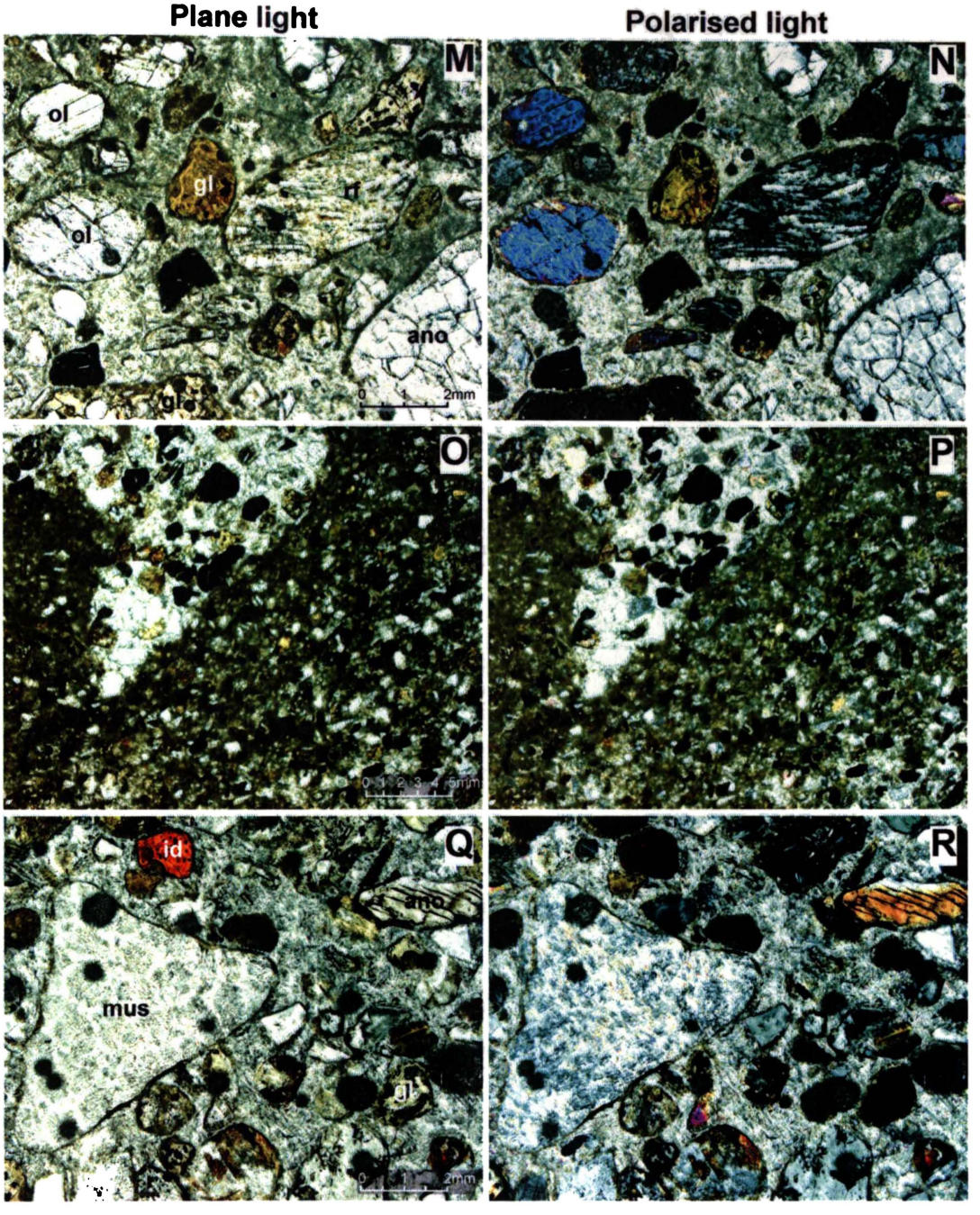
Plane light
Polarised light
M
N
ol
gl
ol
ano
gl
0 1 2mm
O
P
0 1 2 3 4mm
Q
R
id
ano
mus
gl
0 1 2mm

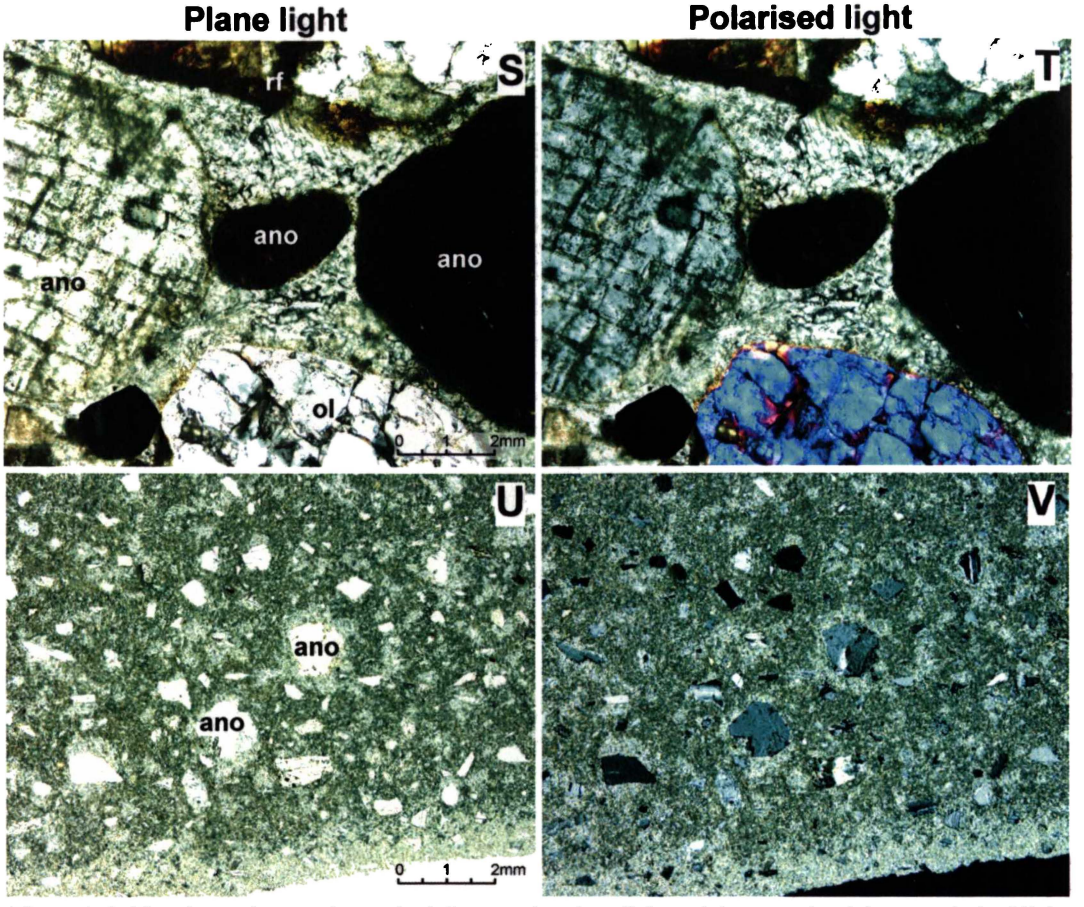

Figure 7.1: The photomicrographs on the left are under plane light and those on the right are polarised light. ano: anorthoclase; ol: olivine; mus: muscovite; ae: aegerine; bi: biotite; amph: brown amphibole; id: iddingsite; rf: rock fragment; gl: volcanic glass. (A-B) S01a; the sample has abundant anorthoclase. Note the alteration of some of the glass fragments to yellow smectite. Note the trachytic texture of the rock fragment; (C-D) S02a; sample contains rods of flaking biotite. The iddingsite has an unaltered core of olivine; (E-F) S03a; the sample contains rare rods of muscovite; (G-H) S03a; note the rind of carbonate that contains no detrital material; (I-J) S07b; this sample contains coarse and fine layers, with the coarse layers containing abundant anorthoclase with some aegerine and brown amphiboles. The fine layers alternate between micritic carbonate and fine volcanic material; (K-L) S07Ua; this sample contains fine grained volcanic material cemented by micritic carbonate; (M-N) S08a; note the abundance of carbonate cement; (O-P) S09a; this sample has cracks in fine grained volcanic material infilled with coarser material of similar composition; (Q-R) S11a; this sample has rare rock fragments of muscovite; (S-T) S11a; note the carbonate cement supporting the volcanic material and the difference in grain size within the same sample of (Q-R); (U-V) S24a; the $CaCO_3$ has a micritic nature with scattered crystals of anorthoclase.

7.3 Discussion

7.3.1 Nussbaum Riegel

The mineral assemblage and presence of volcanic rock fragments and volcanic glass, points to a volcanic source for much of the detrital material in the samples. Along with the volcanic material are sediments sourced from basement rock. The source of this volcanic material is likely to be the McMurdo Volcanics occurring in the McMurdo Sound region.

underlying finer material (Fig. 7.1, O-P). Figure 7.1, I-J is an example of multiple depositional events. The left of the photomicrograph is the top of the sample, where a coarse layer overlies a micritic layer, representing two depositional events. Within this photomicrograph, there are four depositional events represented. These were likely to have occurred before the deposit was cemented by carbonate, thus would be sedimentation episodes within the palaeo lake.

7.3.2 Sollas Bench and Pearse Valley

The samples collected from the Sollas Bench and Pearse Valley show little variation in texture and composition in the photomicrographs. The carbonate is micritic, though shows small changes in grain size within samples (Fig. 7.4). The changes in grain size are likely to relate to different depositional events as depositional conditions changed. Some of the samples also contain intraclasts (Fig. 7.4). (Rao, 1997) attributed this to the penecontemporaneous reworking of the deposit followed by the infilling of intergranular pore space with micrite cement.

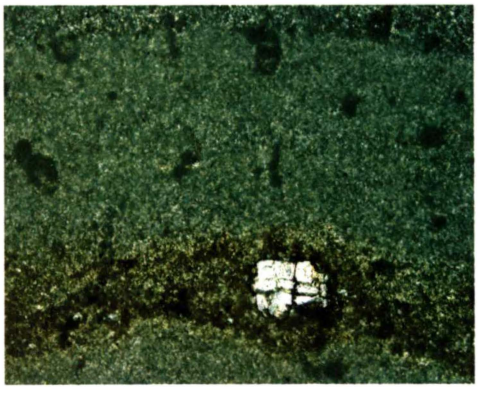

Figure 7.4: Sample S23a from Pearse Valley showing the micritic carbonate with intraclasts and rare detrital material.

Similar deposits of micritic aragonitic carbonate have been observed by Rao (1997) in Radok Lake, East Antarctica (Fig. 7.5).

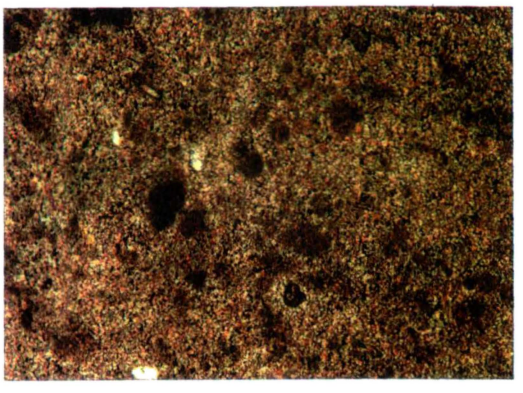

Figure 7.5: Modern polar freshwater carbonate, Radok Lake, East Antarctica. Micrite with intraclasts. Intraclasts are dark micrite and surrounded by coarsely crystalline micrite, because they were reworked penecontemporaneously and the intergranular pore space was later filled by micrite cement. XRD analysis of this carbonate indicates that it is entirely aragonite, which precipitates as micrite and intraclasts in cold freshwater (Rao, 1997).

In the deposits from Sollas Bench and Pearse Valley, the detrital material is distributed in two ways. The most common distribution is as scattered grains throughout the carbonate matrix. These grains could have been incorporated into the carbonate either as windblown sediment directly on to an open lake surface, or as melt-through on an ice surface. Secondly there can be concentrated bands of detrital material. These could represent wind storm events causing a greater sediment load in the water column. They could also be due to periods where ice cover had re-established on the lake surface as its salinity decreased slightly. This would have allowed the accumulation of sediment on the ice surface, which would then have been released into the water column when the ice melted.

- **McMurdo Volcanics**

Along the western and south-eastern sides of the Ross Sea, are chains of Pliocene to Recent alkali basalt volcanic centres, with an active centre on Ross Island, Mt. Erebus. Mount Erebus has in the past produced kenyte lava flows such as those at Cape Evans and Cape Barnes, which are the source of the kenyte found in the Ross Sea drift in Taylor Valley. Other areas of volcanic activity include Observation Hill, Mt. Terror, White Island, Black Island, Brown Island, Mt. Discovery and Mt. Melbourne. Collectively, the eruptives are known as the McMurdo Volcanics (Fig. 7.2). The volcanic rocks of Ross Island and Victoria Land are nepheline-normative alkali basalts and include trachytes and phonolites (Kovach and Faure, 1977; Kyle, 1990).

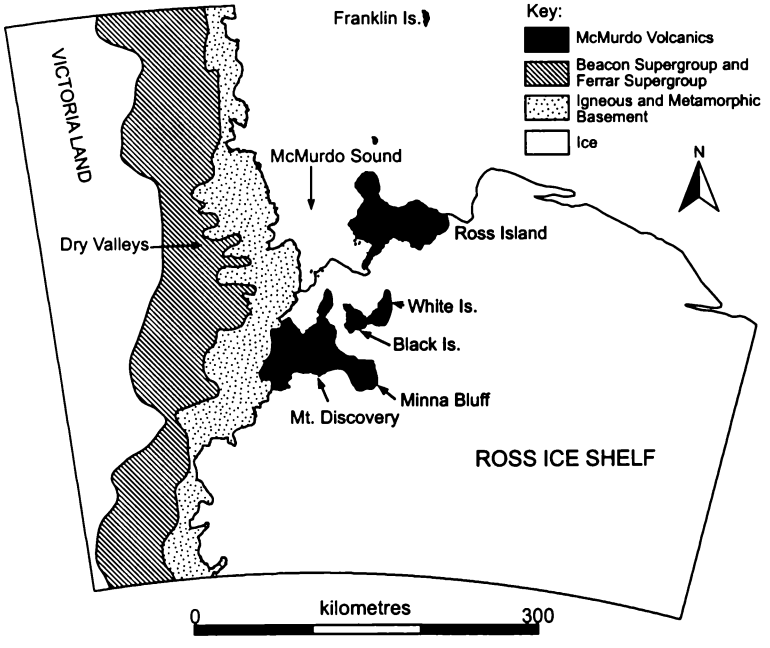

Figure 7.2: Generalised geologic map of McMurdo Sound showing the location of Cenozoic McMurdo Volcanics in the Erebus volcanic province, close to the Dry Valleys region.

The alkali volcanics in the region consist of an older olivine basalt-basalt-trachyte series and a younger olivine basalt-basalt series (Treves, 1968). The predominant rock outcropping on Mt. Erebus is Antarctic kenyte. This has been described as anorthoclase trachyte by Treves (1968), or anorthoclase phonolite by Gibbenbach et al. (1973) and Kyle (1977). The anorthoclase phonolites of Mt. Erebus have been erupting, and are probably differentiated from a basanite parent, as this is the most common volcanic rock on Ross Island. Other common rocks include nepheline

hawaiite and nepheline benmorite, which represent intermediate products of the differentiation process. Common phenocrysts occurring in the anorthoclase phonolite include anorthoclase, olivine, clinopyroxene, and magnetite (Kyle, 1977; Caldwell and Kyle, 1994).

Trachytes from Observation Hill on Hutt Point Peninsula contain phenocrysts of anorthoclase, aegerine-augite and amphibole. $^{40}K/^{40}Ar$ of these rocks give an age of 1.18 ± 0.03 m.y., which establishes a minimum age for the onset of Ross Island volcanism (Forbes et al., 1974).

Volcanic activity in Taylor Valley has produced around 30 scoriaceous basanite cones up to 60 m high, each representing an eruptive centre. These rocks are porphyritic basanites with olivine, clinopyroxene and labradorite phenocrysts. Thirty one K-Ar age determinations (Fig. 7.3) fall within 4.76-1.57 Ma and is no evidence of Holocene activity (Kyle, 1990).

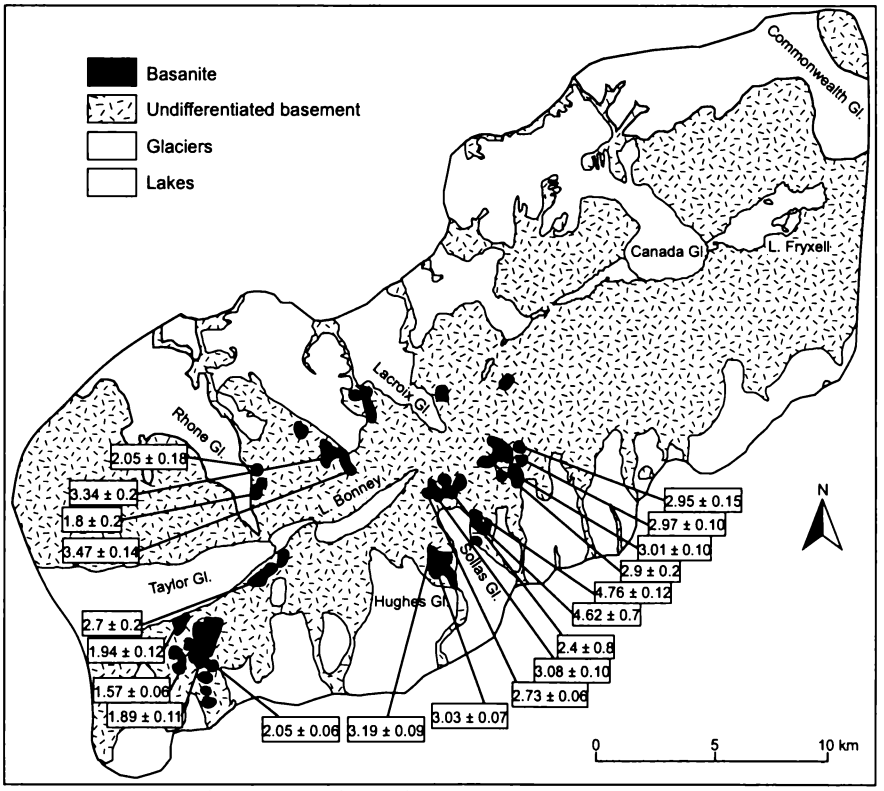

Figure 7.3: Locations of the McMurdo Volcanic Group rocks exposed in the Taylor Valley. Boxed numbers refer to K-Ar ages in millions of years (dates from (Angino et al., 1962; McCraw, 1962; Kurasawa, 1978; Porter and Beget, 1981) (adapted from Kyle (1990)).

Mineralogical investigations have been made of a number of suites of Erebus volcanic province rocks. The dominant phenocrysts in many of the rocks are anorthoclase. Within the basic and ultrabasics rocks, clinopyroxene, olivine, apatite, aegerine-augite, kaersutite, and aenigmatite are present. Alkali amphiboles and micas are uncommon. Nepheline is an incipient groundmass phase, and thus is not seen in thin section (Kyle, 1990).

The mineral assemblage of the anorthoclase + olivine ± biotite ± aegerine-augite ± kaersutite in the detrital minerals of the Nussbaum Riegel carbonate samples is consistent with a source from the alkali McMurdo Volcanics. In many of the samples, the olivine has been partially altered to iddingsite, often with only a core in the centre of unaltered olivine. Many of the glass fragments have crystal inclusions, which are commonly olivine. There is evidence of some weathering, with some of the volcanic glass being altered to smectite (shown as a yellow colour in the photomicrographs of Fig. 7.1).

Although there was no quartz evident in the thin sections, when the minerals were separated using a franz magnetic separator and examined under a microscope, there were quartz grains in the non-magnetic separates. Many of the anorthoclase crystals were not fresh volcanic crystals, but rather slightly weathered plutonic crystals. Along with non-magnetic minerals, there was sponge spicules, meaning a component of the sample was sourced from the marine area of the McMurdo Sound.

There are two key means of deriving the sediment into the lakes environment:

(1) Erosion and transport by a grounded ice sheet with deposition into the lake.
(2) Deposition as airfall tephra, either directly on to the lake surface, or on to the ice sheet.

For ice to move up the Taylor Valley, it had to move over areas of metasedimentary rocks. Some sediment from these rocks would likely be eroded and incorporated into the detrital material in the carbonates. The presence of plutonic quartz, feldspar and anorthoclase, along with muscovite indicate that at least some of the sediment was

derived from the basement metasediments and granites. A variation on this possibility is sediment being attained by basal freezing and surface ablation, where marine sediments and macrofossils are frozen on to the base of the Ross Sea ice shelf and subsequently moved up through the ice. Some of the volcanic sediment could also have been attained by this mechanism from the submarine McMurdo Volcanics. This sediment, once incorporated into the ice shelf would have been moved up the valley into the lake environment by the ice-conveyor system envisaged by Hendy et al. (2000)

A component of the volcanic sediment was likely sourced from airfall tephra. In support of this interpretation is the freshness of the minerals. Crystal edges are relatively unabraded and glass fragments still show vesicles, showing that little modification by erosion has taken place. There are two likely scenarios for the addition of airfall tephra to the deposits, the first being the deposition of volcanic airfall tephra directly on to the palaeo lake surface. This could either have had ice cover or have been ice-free. The airfall could also have been deposited on to the ice shelf, followed by deposition into the lake system by the ice-conveyor system envisaged by Hendy et al. (2000). The airfall could have been erupted from any of the alkali-volcanic centres of the McMurdo Volcanics.

Once deposited into the lake, the sediment was cemented by a carbonate of mixed aragonite/calcite mineralogy. The samples that have a small amount of muscovite also contain dropstones on the surface of the sample, not present in most of the samples. The drop stones and muscovite are likely to be deposited from glacially eroded metasediments after the volcanic material is deposited. The thin flakes of muscovite could also easily be a windblown component of the sediment. The rock could be termed a volcaniclastic carbonate or a carbonate cemented volcaniclastic sandstone.

The varying grain size within the samples could be due to different depositional events. In some cases it appears that coarser material is infilling cracks in the

CHAPTER 8:

SYNTHESIS

8.0 INTRODUCTION

This chapter synthesizes the data addressed in the previous chapters, leading to the testing of alternative hypotheses/models and identification of the preferred explanation. To achieve this, the information obtained for each sampling location will be addressed within a depositional model. There are two main models under which the data are investigated. One is based on a palaeo proglacial lake associated with expansion of a grounded ice sheet in McMurdo during glacial periods, and the second involves a palaeo proglacial lake either terminal or lateral to an expanded Taylor Glacier, forming during interglacial periods.

For each model an attempt is made to interpret the observed mineralogy and crystallography in relation to the trace element chemistry. Key information discriminating between the two models are stable isotope data, bearing upon the source of the waters.

8.1 DEPOSITIONAL MODELS

8.1.1 NUSSBAUM RIEGEL

A summary of the pertinent results from the Nussbaum Riegel carbonates is recorded in Appendix 2. The oxygen isotope compositions for the Nussbaum Riegel carbonates indicate that they were deposited in water that was sourced from a marine based ice sheet similar to the Ross Sea Ice Sheet, suggesting that they were deposited during a glacial period when the ice shelf was grounded in McMurdo Sound. The ice grounding is indicated by the presence of sponge spicules within the carbonate layers, and coral fragments and bivalves associated with the carbonates. This makes these deposits similar to the Ross Sea Drift, deposited during MOIS 2.

The palaeo lake would have been proglacial to the grounded, expanded ice in McMurdo Sound. A likely extent of the expanded ice sheet and proglacial lake can be observed in Figures 8.1 and 8.2. We propose to refer to the palaeo lake as "Glacial Lake Nussbaum". The evidence for this lies within the till surface associated with the carbonates. The surface till are conveyor deposits. These were probably deposited by

the lake-ice conveyor described by Hendy et al. (2000). Much of this surface till is likely to be let-down drift, deposited as the lake finally drained. Hendy et al. (2000) described let-down drift as being hummocky, possibly cored with lake ice, with dropstones, ridges and low mounds overlying lake sediment, and 'cup and saucer' morphology. These are the surface morphologies commonly observed at Nussbaum Riegel. It would have been the deposition of this drift that allowed the preservation of the underlying carbonate layers.

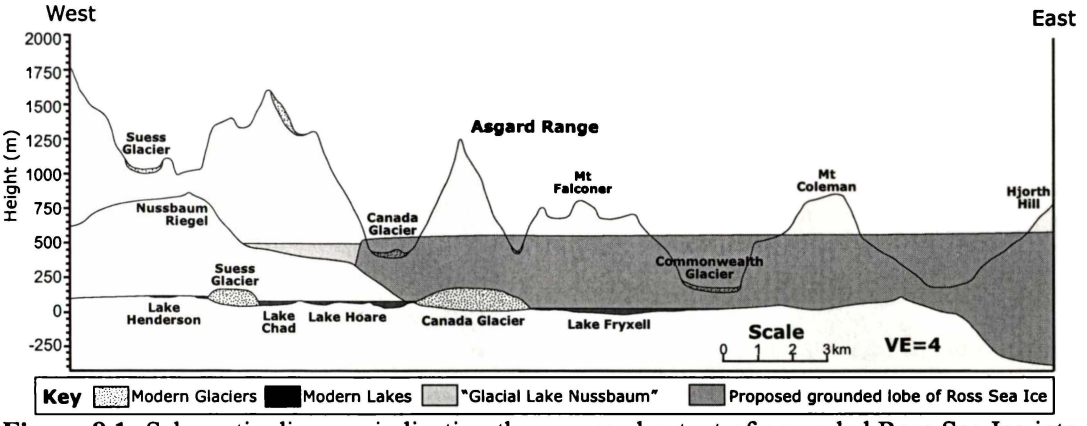

Figure 8.1: Schematic diagram indicating the proposed extent of grounded Ross Sea Ice into the mouth of Taylor Glacier. The expanded ice would have dammed "Glacial Lake Nussbaum", the extent of which was on the slopes of Nussbaum Riegel.

It is likely that the ice would have extended up the Taylor Valley through the depression currently occupied by Lake Hoare and the Suess Glacier. At the snout of this glacier there potentially could have been another proglacial lake at a similar elevation to "Glacial Lake Nussbaum" (Fig. 8.2). This can only be inferred, as there is no obvious evidence for its existence. The valley has steep sides at this point, and any lake sediment deposited on these slopes would have been easily reworked and moved down-slope. This area could also have been scoured by subsequent advances of the Taylor Glacier (Higgins et al., 2000). During the expansion of the Ross Sea ice, the alpine glaciers would also have retreated with their extent suggested in Figure 8.2.

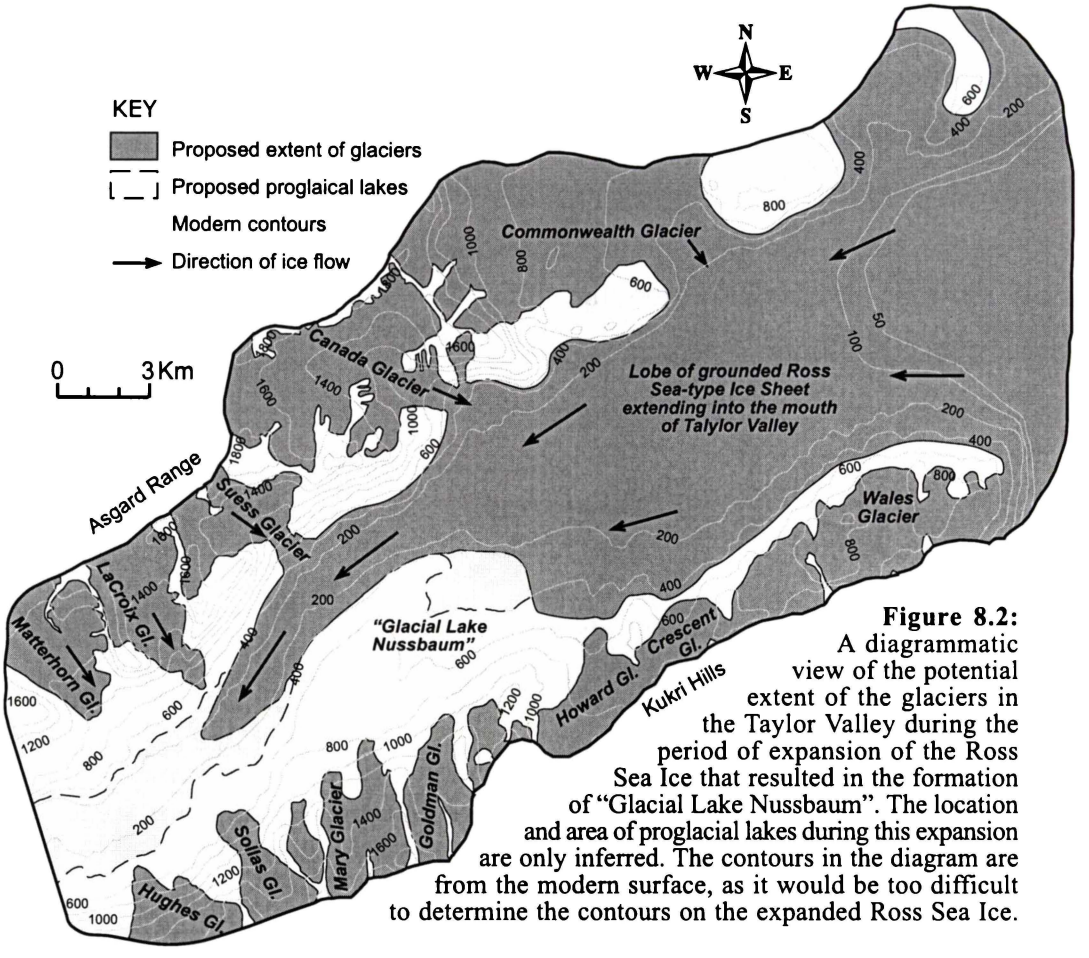

Figure 8.2: A diagrammatic view of the potential extent of the glaciers in the Taylor Valley during the period of expansion of the Ross Sea Ice that resulted in the formation of "Glacial Lake Nussbaum". The location and area of proglacial lakes during this expansion are only inferred. The contours in the diagram are from the modern surface, as it would be too difficult to determine the contours on the expanded Ross Sea Ice.

Petrographic analysis of the carbonates indicates that the detrital component of the carbonate consists of alkali volcanic rock fragments, probably sourced from the McMurdo Volcanics occurring in the McMurdo Sound region, and material eroded from metasedimentary and granitic basement rocks. The two main mechanisms of introducing the volcanic material into the lake environment are possibly:

(1) Erosion and transport by a grounded ice sheet with deposition into the lake.

(2) Deposition as airfall tephra, either directly on to the lake surface, or on to the ice sheet.

As much of the detrital sediment is volcanic, this supports the theory of a palaeo lake dammed by an expanded ice sheet occupying McMurdo Sound. The material would have been fed from the seaward end of the valley by the grounded ice sheet, followed by transport via the lake-ice conveyor system.

Further investigation of the carbonate sediment by SEM indicates that it cements the detrital sediment. The carbonate has acicular or fibrous crystal morphology, often with larger crystals being composed of bundles of carbonate fibers. XRD indicated that these samples were of a mixed mineralogy, containing both aragonite and calcite. The volcanic nature of the detrital sediment was also evident in the SEM images. Taking into account the nature of the carbonate, the rock could be termed a volcaniclastic carbonate or a carbonate cemented volcaniclastic sandstone.

A common type of erratic found within drift deposits of the Ross Sea Glaciations is kenyte, which records westward flowing ice across McMurdo Sound from Ross Island. This phonolite occurs in place only at Cape Barne on Ross Island. The lava flow here has been dated at 0.94 Ma and is unlikely to be older than 1.5 Ma (Kyle, 1976). This puts an upper age limit on moraines containing kenyte erratics. The absence of kenyte in the drift at Nussbaum Riegel could indicate that these deposits are either older than 0.94 to 1.5 Ma, or the ice flow into the mouth of Taylor Valley may not have passed through the source area of kenyte.

The trace element chemistry of the carbonates indicates that the origin of their composition is primarily controlled by the composition of the precipitating fluid and the mineralogy of the carbonate. Samples containing higher proportions of aragonite have higher concentrations of the larger ions such as barium and strontium, while those with more calcite in the mineral structure are higher in the smaller ions such as magnesium. The high percentage of detrital sediment within the Nussbaum Riegel carbonate has probably lead to significant leaching of many ions from this material during chemical analysis.

As described in Chapter Five, much of the literature argues that the mineralogy of carbonate precipitated is controlled by the magnesium/calcium ratio of the precipitating water, with high ratios yielding aragonite over calcite. This does not fit with the results recorded for the Nussbaum Riegel carbonates, as these samples have a higher magnesium/calcium ratio than the other two sites, but this is the site with

carbonate of mixed mineralogy (calcite and aragonite). An explanation for this can be provided by Given and Wilkinson (1985), who explained that mineralogy and morphology can be controlled by the availability of CO_3^{2-} ions, with high availability leading to fast precipitation of acicular aragonite. The predominance of aragonite requires the Nussbaum Riegel carbonates have to have been dominated by rapid precipitation. To allow this there has to be a change in the availability of CO_3^{2-} ions (ie. more of them). A mechanism for this would be degassing of CO_2, thereby increasing the pH, and hence the availability of the CO_3^{2-} ions.

The model conditions under which this could occur are as follows (Fig. 8.3):

- Sustained high lake level thereby allows infiltration of water into the pore spaces of the underlying sediment.
- Subsequent drop in lake level, enabling freezing of the lacustrine sediments.
- Movement of deep pore waters down slope, following a hydrostatic head towards the new lower lake level surface.
- Pore waters follow more permeable layers in the lacustrine sediment and on reaching the surface evaporate or freeze.
- Evaporation/freezing would cause CO_2 degassing and concentration of brine. The degassing would change the pH, forcing precipitation of carbonate. The precipitation would be restricted to areas close to the lake margin, forming a ring up to possibly 20 m distance from the lake.
- The $\delta^{13}C$ values for the Nussbaum Riegel carbonates are close to atmospheric equilibrium supporting this model. Evaporation would lead to enrichment in the $\delta^{18}O$ values, although this would not be significant until the late stages of evaporation.

The carbonate would be precipitated along the sediment/atmosphere interface thereby cementing the sediment, before reaching a critical thickness at which the water flow would be restricted and would move in a different direction. This would explain why most of the carbonate plates are less than 1.5 cm thick. This also could explain why there are changes in grain size within a carbonate plate, as the cementation is occuring in whatever is in the surface stratigraphy.

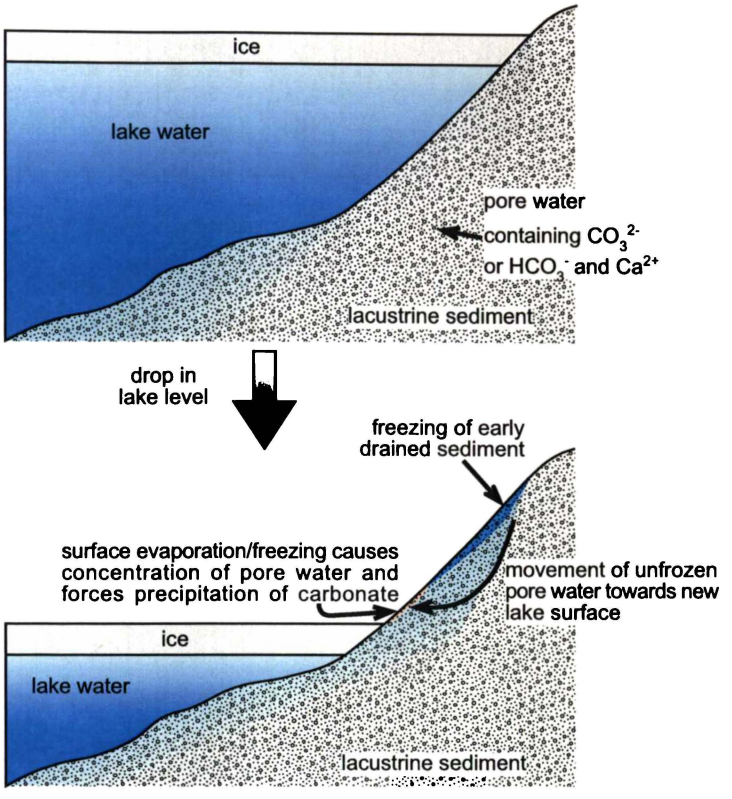

Figure 8.3: Depositional model for the Nussbaum Riegel carbonates. The upper diagram shows original lake conditions, followed by precipitation of carbonate in the lower diagram and lake level falls.

The rapid degassing of the pore water as it reached the surface would account for the aragonite mineralogy and the presence of smaller carbonate fibers. The calcite found in some of the carbonate samples of mixed mineralogy could have occurred as a final precipitate, once the degassing had taken place and the precipitation rate had slowed down. Alternatively the calcite could be due to cementation from freezing of the remaining pore water (no CO_2 loss, pH falls, CO_3^{2-} less available). The magnesium/calcium ratio is higher in samples with more calcite, possibly due to the magnesium/calcium ratio increasing as calcium was preferentially removed by carbonate precipitation.

To explain the different morphologies and mineralogy of carbonate in hand specimen, several episodes of lake level fall and precipitation followed by lake level rise would have occurred. With the two subsurface platy carbonate, there were at least three generations of surface carbonates:

- Knobbly carbonate with dropstones (predominantly aragonite).

- Platy carbonate (predominantly aragonite). The platy carbonate was associated with knobbly carbonate at sites S11 and S07.
- Platy carbonate (mixed calcite and aragonite).

According to the position of the carbonates on the surface relative to other carbonates and conveyor deposits, a sequence of deposition in "Glacial Lake Nussbaum" could have developed, as follows (see Figure 8.4 for a visual representation):

- **Carbonate 1:** A drop in lake level would have resulted in the lower most subsurface carbonate layer in pit 7 being deposited, followed by a rise in lake level (Fig. 8.4, ①). If the lake level change was the result of fluctuation of the ice damming the valley mouth, the rise would not have to involve additions of large amounts of melt water. With the rising lake water, a layer of lacustrine silt and sand was deposited.
- **Carbonate 2:** Another drop in lake level could cause the deposition of the upper subsurface carbonate layer in pit 7 (Fig. 8.4, ②). If the lower carbonate layer was precipitated with a $\delta^{13}C$ value of +0.03‰, and this removed around half of the CO_3^{2-} in the lake, the next carbonate precipitated with a measured $\delta^{13}C$ value of -1.28‰, would have $\delta^{13}C$ depleted by ~1‰, which appears to be the case (little addition of melt water between the deposition of the two, meaning the CO_3^{2-} in the water would not have been replenished). The deposition of the carbonate would have been followed by a rise in lake level, again as a result of ice fluctuations. A layer of lacustrine silt was then deposited.
- **Carbonate 3:** A fall in lake level resulted in the deposition of a platy carbonate of mixed aragonite and calcite mineralogy (Fig. 8.4, ③). The sites at which this carbonate layer was found were S01, S02, S03, S04, S05, S12, and S13. The removal of CO_3^{2-} from the lake water by the two underlying carbonates caused these to have more depleted $\delta^{13}C$ values (-0.60‰ to -3.10‰). An influx of melt water caused the lake level to rise, replenishing dissolved ions such as CO_3^{2-} and Ca^{2+}.

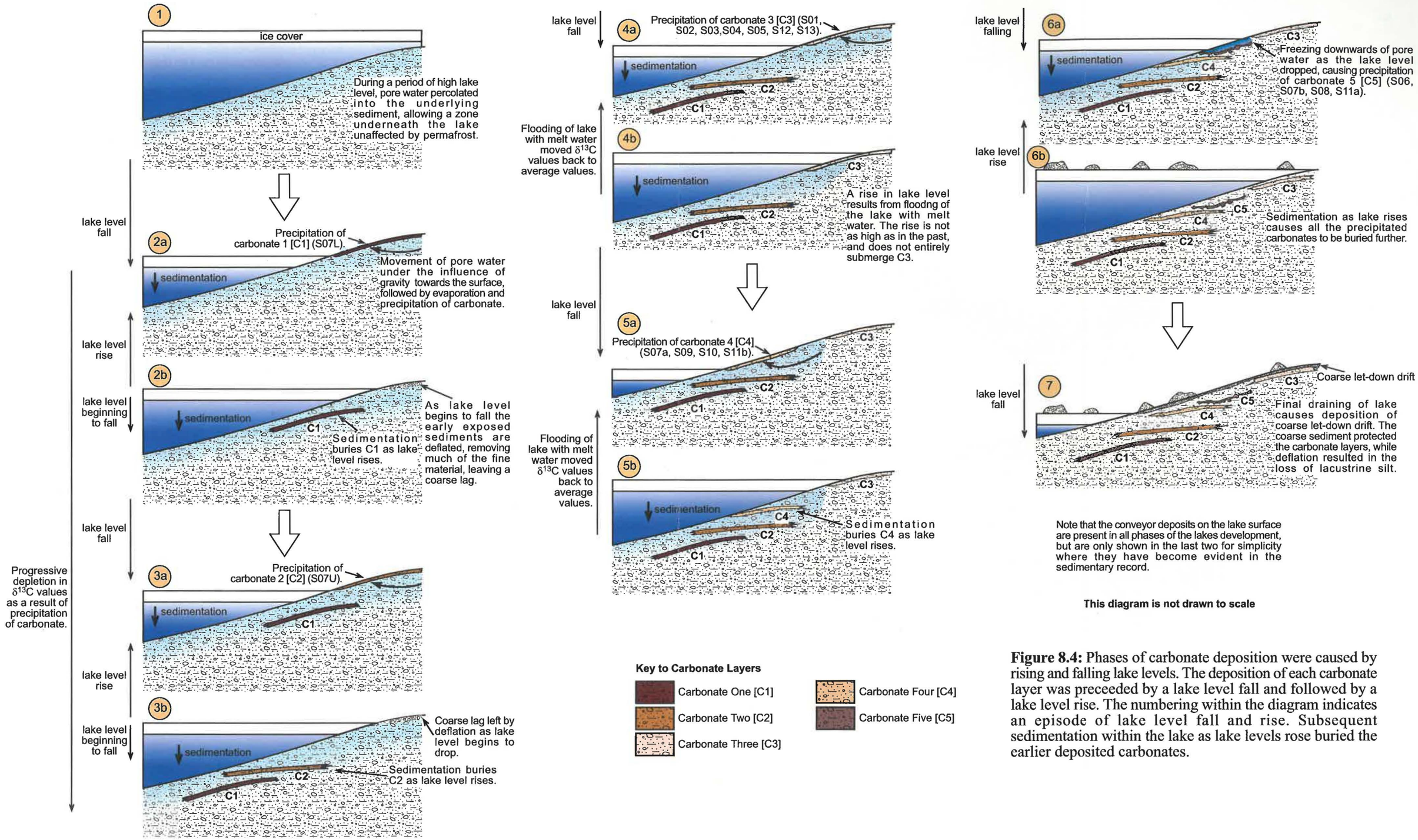

Figure 8.4: Phases of carbonate deposition were caused by rising and falling lake levels. The deposition of each carbonate layer was preceeded by a lake level fall and followed by a lake level rise. The numbering within the diagram indicates an episode of lake level fall and rise. Subsequent sedimentation within the lake as lake levels rose buried the earlier deposited carbonates.

- **Carbonate 4:** Another fall in lake level caused the precipitation of another platy carbonate, this time only consisting of aragonite (Fig. 8.4, ④). The replenishing of the CO_3^{2-} by melt water returned the $\delta^{13}C$ values to its original value (~+0‰ to +0.6‰). The water level would have fallen to a lower altitude than the previous drop, as these carbonates are found down slope from the plates of mixed mineralogy. Further additions of melt water and/or ice fluctuations caused another rise in lake level. There would have been deposition of lacustrine sediments during this time.
- **Carbonate 5:** The final carbonate layer to be deposited was the knobbly carbonate (Fig. 8.4, ⑤). As this has a different morphology to the other carbonates, and has a much coarser grain size, a different mechanism needs to be invoked for its deposition. This carbonate has an irregular appearance, with many protrusions, indicating that it has grown in three dimensions. This is in contrast to the platy carbonates which, when precipitated at the sediment/atmosphere interface, grew only in two dimensions. The three dimensional growth of these carbonates indicates they were probably precipitated at depth within the sediment, rather than at the surface. The concentration of the solute required for this to have occurred could have been due to progressive freezing downwards of the pore water. The saturated solution, on reaching a coarse, porous layer, was able to degas CO_2 (possibly this coarse layer did not have water-filled pore spaces), inducing the carbonate to precipitate. As there would have been no limits to the direction of cementation, the growth was in all directions, causing the irregular appearance of the carbonates. The carbonate cemented the existing sedimentary sequence, which is why the dropstones were incorporated throughout the carbonate layer.
- **Draining of lake:** The final event taking place in the sequence of deposition was the draining of the lake, resulting in the deposition of coarse let-down drift (Fig. 8.4, ⑥). This would have helped protect the underlying carbonate. Subsequently, windstorm events would have caused the ablation of much of the intervening lacustrine silt, causing the carbonates to become exposed on the surface.

Some of the carbonate samples thicken along the edges of the plates, appearing to curl upwards. This could have occurred as the carbonate plates were being formed, as cracks may have been caused by frost cracking. These cracks would have given a conduit through which more pore water could escape and precipitate carbonate. In this way, the continued growth along these cracks would have cause thickening in these zones. At another site, the carbonate contained cracks that were infilled by sediment coarser than the rest of the samples. Again, the cracks could have formed from frost cracking. These could have been infilled by the coarser sediment, which potentially could have been wind blown. The coarser sediment would then have been cemented by further evaporation of pore water moving up the cracks.

8.1.2 SOLLAS BENCH

A summary of the pertinent results for the Sollas Bench carbonate samples is included in Appendix 2. The oxygen isotope composition for the Sollas Bench carbonate samples indicate that they were deposited in water sourced from Taylor Glacier ice. This suggests that they were deposited during a time of expansion of outlet glaciers from the EAIS. The palaeo lake could either have been a lateral or terminal proglacial lake to an expanded Taylor Glacier.

As the carbonates have been incorporated in moraines, it cannot be determined how many episodes of carbonate deposition are represented. The sample collected from site S18 has been dated by the U/Th method to 208 ± 1.7 ka, placing it within MOIS 7. This moraine is the lowest in the series of moraines from which the carbonates were collected, making it likely to be from a younger advance. The carbonates from the other moraines are older than can be dated by the U/Th, making them older than ~350 ka (Hall, 2004). This makes it likely that there are at least two palaeo proglacial lake systems represented in the carbonate samples collected from Sollas Bench. As the Taylor Glacier expanded, it would have advanced through its own proglacial lake. When this occurred, soft lake sediment would have been entrained in the basal ice. As the glacier advanced down-valley, this lacustrine sediment would have been

deposited within the lateral moraines, which are observed to slope down-valley (Fig. 3.1).

XRD analysis shows that these carbonates are aragonitic, while SEM analysis indicates that there are two different crystal morphologies present within the carbonate samples, one with random orientation and another with radiating needles. As there are these differing carbonate crystal morphologies, it is likely that several generations of carbonate cementation have been incorporated in the moraines.

The trace element chemistry of the carbonate is controlled by two main factors, being (i) the composition of the precipitating fluid, and (ii) the mineralogy of the carbonate. The higher purity of the carbonate in the Sollas Bench carbonate samples, compared with the Nussbaum Riegel samples, meant there was less leaching of ions from detrital grains incorporated in the carbonate during chemical analysis.

A search of the literature failed to provide adequate models to explain the mechanism for deposition of these carbonates. The carbonates could have been formed in one of three ways:

(1) Precipitation was driven by algal consumption of CO_2 from a stratified lake. Carbonates deposited in this manner are known as **whitings**.
(2) Alternatively, precipitation was driven by concentration of solutes due to evaporation. These deposits are known as **evaporites**.
(3) Alternatively, precipitation was as a result of solute concentration under freezing conditions. Minerals precipitated under these conditions do not have a name.

We proposed to refer to minerals formed as a result of freezing of water as **"cryorites"**. In the McMurdo Oasis, there are a variety of source water compositions. Where freezing sea water is involved, large quantities of mirabilite are often found, but where low sodium waters are involved (eg. Marshall Valley and mid-Miers Valley), sodium salts are absent but aragonite and gypsum result.

There is a possibility that the precipitation of "cryorites" may be identified by their carbon isotope values. In a case presented by (Clark and Lauriol, 1992), samples from karst caves within the permafrost region of northern Yukon, Canada, had $\delta^{13}C$ values as high as +17.0‰. In this environment, rapid freezing forces CO_2 degassing and calcite precipitation as a cryptocrystalline powder within the ice, later released through sublimation or melting. Via freezing and sublimation of calcium bicarbonate solutions under laboratory conditions, the rate of reaction was shown to preclude isotopic equilibration being obtained during precipitation of calcite, resulting in the partitioning of ^{13}C between CO_2 and $CaCO_3$. As freezing proceeds, the light CO_2 is degassed and lost from the system, resulting in the precipitation of calcite with heavy $\delta^{13}C$ values. The degassed CO_2 is lost via diffusion to the atmosphere or becomes trapped in the ice with the fine-grained carbonate precipitate as an intercrystalline contaminate, and later released through sublimation or melting. This concept is supported by (Niles et al., 2004), who examined the suitability of cryogenically formed calcites as an analog for martian meteorite carbonates. These carbonates also had enriched $\delta^{13}C$ values. Their experiments showed that in precipitation via freezing, the kinetic fractionation factor was more important than an equilibrium fractionation factor.

In the Antarctic environment, it is likely that many of the carbonates precipitated would have been as a result of freezing, making them "cryorites". This potentially could be recognised by their $\delta^{13}C$ values. Though $\delta^{13}C$ values as positive as +7‰ can be as a result of low temperature equilibration with the atmosphere, in many situations, contact with the atmosphere may not have been long enough for this equilibration to occur. It is possible that many of the more positive $\delta^{13}C$ values could be as a result of freezing processes. For this to have occurred, the CO_2 degassing during the precipitation of carbonate would have to be removed from the system to account for the removal of the light ^{13}C. If this can occur in an ice-covered lake, which is effectively a closed system, the production of "cryoritic" carbonates could be recognised by very positive $\delta^{13}C$ values.

An example of whitings is the carbonate sediment located in the Lake Fryxell system. The carbonate collected from Sollas Bench is not likely to have been whitings. The presence of halite and gypsum indicates that the minerals were precipitated due to concentration by removal of water (evaporation/freezing), rather than by algal activity.

Two models need to be developed to account for the two differing crystal morphologies observed within the carbonates (random and radiating). The first of these models will account for the randomly oriented aragonite needles, in which three different scenarios will be presented.

(1) A concentrated brine existing as an ice-free water surface in summer would have undergone progressive concentration as water was removed by evaporation (Fig. 8.5). During winter, water was removed from the brine by freezing of the water surface. As freezing progressed, further concentration of the brine would occur as more water was removed (Fig. 8.5). During this time there would have been continued ablation from the ice surface. Upon reaching the saturation point for Ca^{2+} and SO_4^{2-}, gypsum ($CaSO_4.2H_2O$) would have precipitated (Fig. 8.4):

$$Ca^{2+} + SO_4^{2-} + 2H_2O \rightarrow CaSO_4.2H_2O$$

If $[Ca^{2+}] > [SO_4^{2-}]$, the $[Ca^{2+}]$ would have increased as water was removed. As CO_2 could not escape due to the ice cover, the P_{CO_2} would rise, forcing the pH down. Upon removal of the ice (ie. during spring thaw), the excess CO_2 would have degassed to the atmosphere suddenly. The P_{CO_2} would have dropped, causing the pH to rise, resulting in the rapid precipitation of carbonate. The change in the pH would have resulted in a greater availability of CO_3^{2-} ions, allowing for rapid precipitation of acicular or fibrous aragonite (Fig. 8.4).

The carbonate produced in this manner would have been a "rain-out" of aragonite needles. These would have accumulated on the lake bottom, resulting in a random array of aragonite needles. These carbonates would be classed as evaporites.

If $[SO_4^{2-}] > [Ca^{2+}]$, the $[Ca^{2+}]$ would have decreased as water was removed, probably faster than the $[CO_2]$ could increase. This would have been unlikely to have caused the precipitation of carbonate when the ice cover was lost.

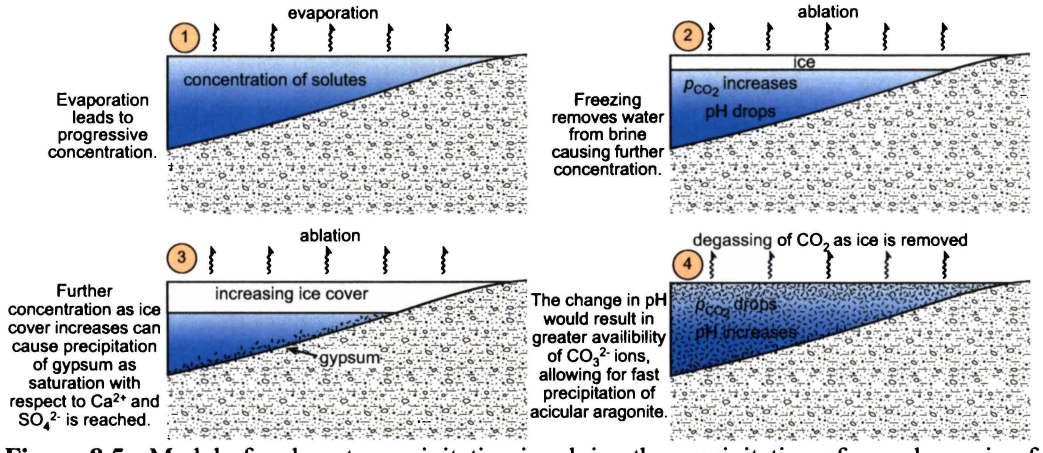

Figure 8.5: Model of carbonate precipitation involving the precipitation of a random rain of acicular aragonite needles.

(2) Starting with concentrated brine, on freezing in winter, gypsum would first have been precipitated. During the freezing of the water column, concentrated brine pockets could have been caught within the ice structure. Further freezing could have caused the brine in these pockets to become saturated with respect to carbonate, causing it to precipitate (Fig. 8.6). When the ice melted in summer, the carbonate precipitated in the brine pockets would have 'rained-out', forming a randomly oriented carbonate bed. These would be classed as "cryorites". To explain why the carbonate precipitated was aragonite rather than calcite, the ratio of CO_3^{2-} ions to Ca^{2+} ions had to be high. The precipitation of gypsum would have pulled both SO_4^{2-} and Ca^{2+} ions in equal amounts, causing the CO_3^{2-} to Ca^{2+} ratio to increase. The greater availability of CO_3^{2-} ions would allow for the fast precipitation of acicular aragonite. Careful consideration would need to be made of the physical chemistry involved, as simple removal of water from a closed system also results in increasing P_{CO_2} and decreasing pH. This could mean than the conditions were never met to cause the precipitation of carbonate.

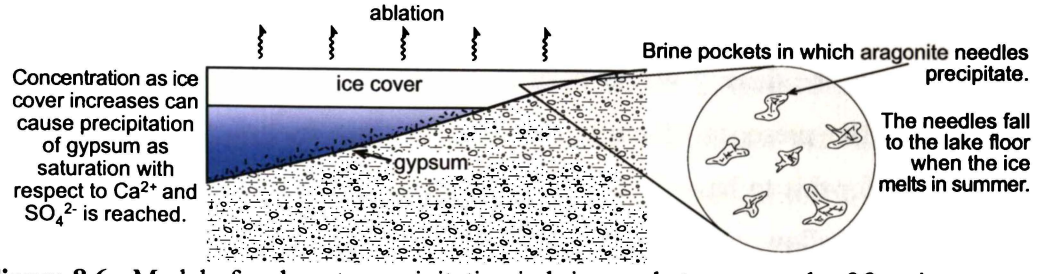

Figure 8.6: Model of carbonate precipitation in brine pockets as a result of freezing.

(3) The precipitation of the carbonate could also have been due to evaporation of an open water body. If the concentration of the brine was sufficient that saturation with respect of halite was reached, the brine could have remained ice free for much of the year as temperatures lower than -20°C would have to have been reached before the brine would begin to freeze. In this case, evaporation would have caused the removal of water until saturation with respect to carbonate was reached, causing its precipitation. In this case the P_{CO_2} would have been constant and the rate of precipitation would have been directly proportional to the amount of water removed. If gypsum was precipitated first and $Ca^{2+}>SO_4^{2-}$, the precipitation gypsum would have stripped all the SO_4^{2-} out of the water. This would have caused the CO_3^{2-} to Ca^{2+} ratio to increase, allowing for the precipitation of aragonite rather than calcite. The precipitation of mirabilite elsewhere in the system could have been a potential mechanism for the removal of SO_4^{2-}. These carbonates would be evaporites.

The next model to be developed would have to account for the presence of the radiating needles of aragonite.

(1) The progressive freezing downwards of brine during winter could have caused the brine to become saturated with respect to carbonate. Where there were points of nucleation, carbonate could begin to grow outward in a radiating habit. This would most likely have occurred at the sediment/water interface, where there would have been an abundance of fine particles to act as nucleation points. The growth outwards from these points would have caused the interlocking growth of the radiating needles (Fig. 8.7). To get growth at the sediment surface, the concentrated brine needs a mechanism to have moved from the freezing ice front

to the bottom of the water column. Potentially, as the concentration of ions in the water rose, the density would have also risen, causing the water to sink to the bottom. The presence of more soluble salts, such as halite, would have been required for this to have occurred. Another possibility is that the water body was relatively shallow, and freezing of the water column could have occurred either through the entire water column, or at least down to a point close to the sediment surface. This would have forced the concentration of solutes at the sediment/water interface, where there were abundant particulates. The precipitation could then have occurred *in situ* along this surface. These would fall into the category of "cryorites".

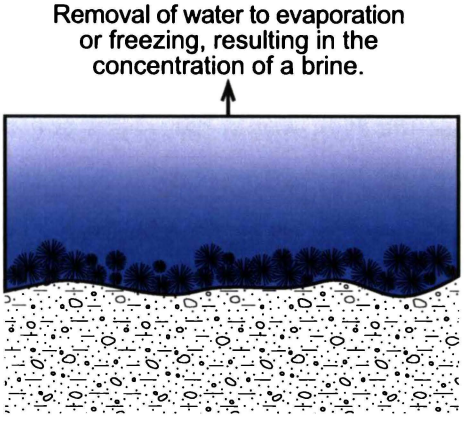

Figure 8.7: Model of carbonate precipitation involving the precipitation of a radiating aragonite needles on nucleation points at the sediment/water interface.

(2) Mechanism (3) from the previous discussion could also have resulted in the precipitation of radiating aragonite. In this mechanism, the brine was being produced at the water surface where evaporation was taking place. For precipitation to occur along the sediment surface, the brine had to be moved to the bottom of the water column. As in the previous mechanism, this could have occurred as the brine increased in density and sank to the bottom. If the evaporation was occuring in a shallow water body, wind could have caused stirring and resulted in mixing of the brine through the water column. As this continued, the concentration would have increased at the sediment/water interface, until precipitation began to nucleate at the particles in this zone. Continued growth would have resulted in the development of radiating, interlocking spheres of aragonite needles. These carbonates would be classed as evaporites.

The $\delta^{13}C$ values established in the Sollas Bench carbonates are all positive, ranging from 4.3‰ to 8.3‰. The sample with a $\delta^{13}C$ value of 4.3‰ could be expected to be as a result of carbonate precipitated from water in equilibrium with the atmosphere. The rest of the carbonates with $\delta^{13}C$ values between 6.5‰ and 8.5‰ could be either due to equilibration with the atmosphere, or precipitation due to freezing. Water in equilibrium with the atmosphere at -10°C results in carbonate with a $\delta^{13}C$ value of +7‰. Carbonate precipitated by freezing processes can also result in positive $\delta^{13}C$ value in this range. This makes it difficult to determine which of these processes is responsible for the $\delta^{13}C$ values. As a consequence, the carbonates located at the Sollas Bench could be a mix of evaporites and "cryorites".

The halite identified within many of the samples was likely to have been deposited as a secondary precipitate. This could have occurred within the lake system or on the surface of the moraines in which the carbonates are incorporated are wet and dried, causing remobilisation of surface salts. There is also a possibility that the halite was precipitated from the water column simultaneously with the carbonate.

8.1.3 PEARSE VALLEY

A summary of the pertinent results from the Pearse Valley carbonates is included in Appendix 2. The oxygen isotope compositions of these carbonates indicate that they were deposited in water sourced from Taylor Glacier ice. This shows that they were deposited during a time of expansion of the EAIS outlet glaciers, meaning that they were deposited during an interglacial period. The palaeo lake in which the carbonates were deposited was likely to have been similar to the present Lake Joyce, which currently is proglacial to a lobe of the Taylor Glacier extending into the mouth of Pearse Valley. This lake will be referred to as "Glacial Lake Pearse".

As the lobe of the glacier expanded, it would have incorporated lake sediments from within "Glacial Lake Pearse" which would have been likely to represent several episodes of carbonate deposition. The carbonates were finally deposited in a moraine

that runs around the margin of Pearse Valley. The moraine occurs at roughly the same elevation around the valley (Fig. 3.30).

SEM analysis of the Pearse Valley carbonates indicated that the crystals had two crystal morphologies of random and radiating needles. XRD analysis showed that in most cases the carbonate was aragonite. Unusual to this location was a site where the carbonate was entirely calcite. The calcite also had a radiating crystal habit, with the calcite nucleating from a point. Unlike the sites at the Sollas Bench there was no halite or gypsum present associated with the carbonates.

As with the other sample locations, the trace element analyses of carbonates from the Pearse Valley indicated that the carbonate chemistry is controlled by two main factors, (i) the composition of the precipitating fluid, and (ii) the mineralogy of the carbonate.

As the carbonates in the Pearse Valley have a similar crystal morphology and chemistry to those on the Sollas Bench, they were likely to have formed in an analogous manner. The problem with these carbonates is accounting for the presence of aragonite rather than calcite. For most of the mechanisms discussed for the Sollas Bench carbonates, gypsum needed to be precipitated first to raise the CO_3^{2-} to Ca^{2+} ratio. As gypsum was not present at this site, this cannot be invoked for changing the ratio of CO_3^{2-} to Ca^{2+}. Mechanism (1) for the randomly oriented needles will still apply at this site, as the increased CO_3^{2-} ion availability is driven by degassing. For the other mechanisms, another means of increasing the CO_3^{2-} ion availability would need to be found, unless just fast precipitation can cause the precipitation of acicular aragonite. The calcite samples are easily explained in this environment with no gypsum. Any of the mechanisms that accounted for the radiating crystal morphology in the Sollas Bench carbonates could apply to the calcite samples in Pearse Valley. As there is no precipitation of gypsum, there was no means of changing the ratio of CO_3^{2-} to Ca^{2+}, this would mean that the precipitation was slower, causing the carbonate precipitated to be bladed calcite.

The $\delta^{13}C$ values of the Pearse Valley carbonates are less positive than the Sollas Bench carbonates, ranging from 0.6‰ to 7.2‰. Other than sample S28a, with a $\delta^{13}C$ value of +7.1‰ and S30a with a $\delta^{13}C$ value of +7.2‰, $\delta^{13}C$ values indicate atmospheric equilibration. This would class most of the carbonates collected as evaporites. The two sample with more positive $\delta^{13}C$ values could also be due to freezing processes, making them "cryorites". These two samples are also the ones with radiating crystal morphology, meaning the mechanism (1), accounting for radiating aragonite is the most likely method of precipitation.

8.2 ORIGIN OF THE SALTS IN WESTERN TAYLOR VALLEY

The presence of more than 20 million tonnes of sodium chloride currently estimated for the Bonney drainage basin, within the water and sediment of Lake Bonney, indicates that there is a substantial source of salt local to the area. The origin of the salts in Taylor Valley have been a subject of contention since the discovery of saline lakes in the valley in the early 1960s. Workers on the subject have suggested that if sea water was discounted as a source, the salts could come from: (i) atmospheric precipitation, or (ii) weathering of surrounding rocks (Boswell et al., 1967). According to Hendy et al. (1977), the salt in Lake Bonney could not come primarily from weathering or atmospheric precipitation. They believed that it was derived from sea water and modified by leaching of soils, precipitation of calcium sulfates and carbonates and by the addition of atmospheric aerosols.

The presence of the saline discharge from Blood Falls at the snout of Taylor Glacier indicates that there is a substantial source of salts beneath Taylor Glacier. Keys (1979) proposed that the glacier is over-riding a saline depression of about $5x10^5$ m^2, located 1-2 km up from the terminus. Keys suggested that the Taylor Valley had been flooded with sea water at least as far west as Lake Bonney, as the salts in the lake have in his opinion been derived from sea water. This would have occurred during a time when the Taylor Glacier had retreated, allowing the subglacial depression near the snout of the glacier to be filled with sea water. This would have evaporated to dryness, with the base of the glacier currently melting on contact with this salt.

It is unlikely that that Taylor Valley could have been flooded with sea water as far up-valley as Lake Bonney, as suggested by Keys (1979). If this had occurred it would be expected that there would be significant quantities of salt in the other drainage basins such as Hoare and Fryxell, which is not the case. The valley morphology also would make it difficult for the sea to extend up the valley to Lake Bonney. Sea level would have needed to rise more than 200 m to reach the Bonney drainage basin and the saline depression beneath the snout of Taylor Glacier proposed by Keys (1979). As a rise of this magnitude is not likely to occur, another mechanism for moving the salts into the Taylor Valley needed to be investigated.

A break-through in the understanding of the origin of the salts in the Bonney drainage basin came from examining radio-echo sounding (RES) measurements and ground-penetrating radar (GPR) subglacial profiles of the Taylor and Ferrar Glaciers obtained by (Morse et al., 2003) over the 2002/03 season. The Ferrar Valley is currently below sea level for much of its extent and during periods of slightly higher sea level, would be below sea level for its whole length. During "super"-interglacials when the EAIS outlet glaciers retreated back into the Transantarctic Mountains, the Ferrar Glacier would retreat far up-valley and the valley would become a fjord. At this time, the Taylor Glacier would retreat beyond the Cavendish Rocks. Beginning with the bottom right profile (F01) in Figure 8.8, the Ferrar Valley has a marked "v" profile. In this part of the valley, the bottom of the "v" is roughly around sea level (errors make it difficult to determine whether it is above or below). Following the profiles into the Taylor Valley (T10, T09, T08, T07), the "v" profile continues, though the elevation rises slightly before dropping down a steep slope into a flat-bottomed depression that is ~280 m below sea level. This basement rock profile can be more clearly examined in the cross section to the right of Figure 8.8. Sea water could overflow the small ridge between the Taylor and Ferrar Valleys and flow into the large depression that is currently beneath Taylor Glacier. This could occur in two ways:

(1) If this flow was less than evaporation/ablation (low flow rate by ground water or slow surface flow), the pooled water would be removed at a rate great enough to

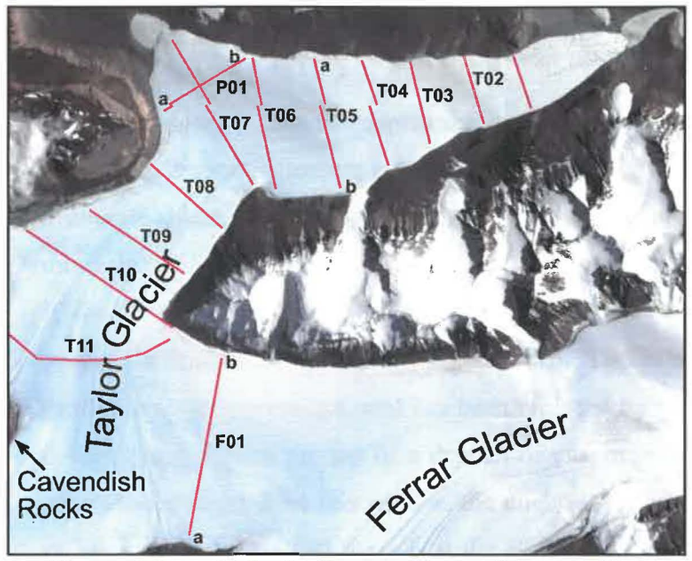

The red lines indicate the positions of the profiles

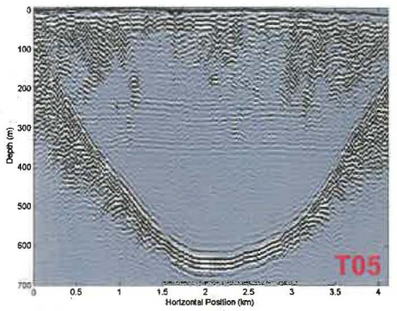

At this point the valley still has a slighlty flattened bottom, indicating that there are still evaporites present.

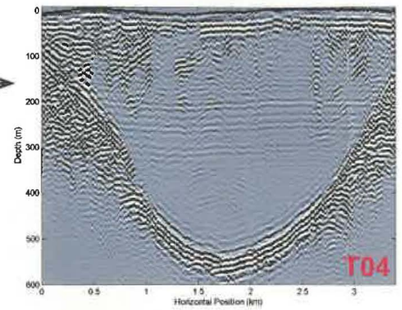

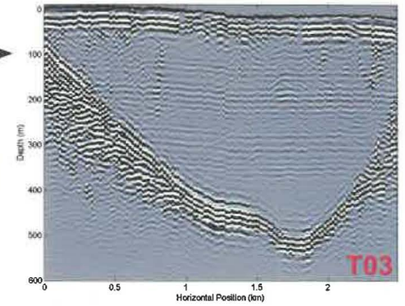

Further down Taylor Valley, beyond the evaporite sequence, the valley profile again becomes a "v", though from here on down the valley the "v" has been greatly modified by glacial action and has taken on the more classic "u" profile common in glaciated regions.

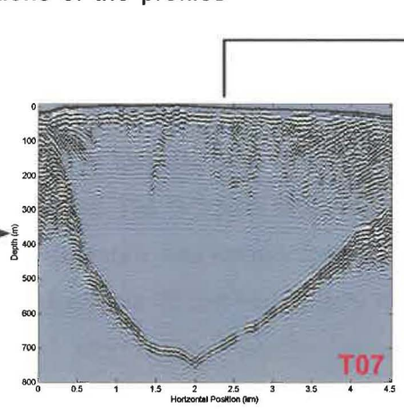

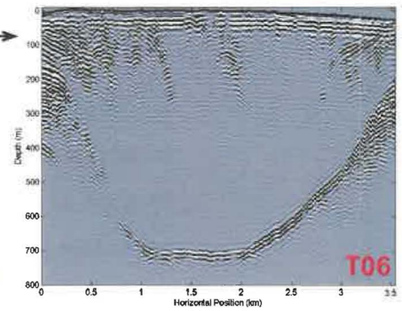

When the evaporation/ablation is greater than the incoming water, a flat-bottomed evaporite sequence developed, obscuring the "v" valley profile.

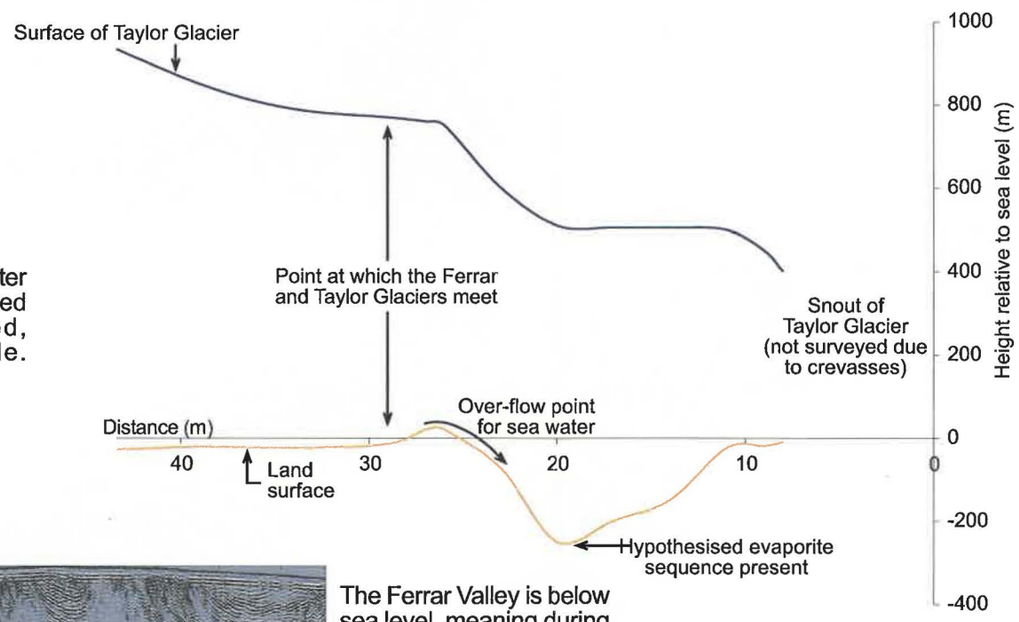

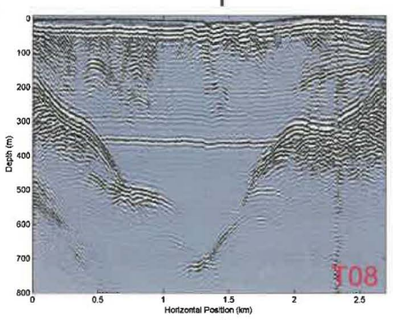

The overflowing water flowed into the Taylor Valley and pooled in a depression that is below sea level.

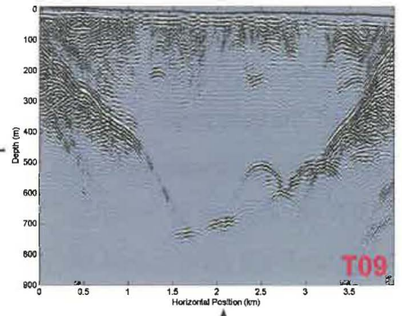

The valley profile in the upper reaches of Taylor Valley is a river carved "v", relatively unmodified by the glacial action.

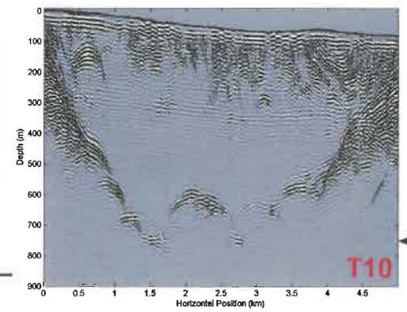

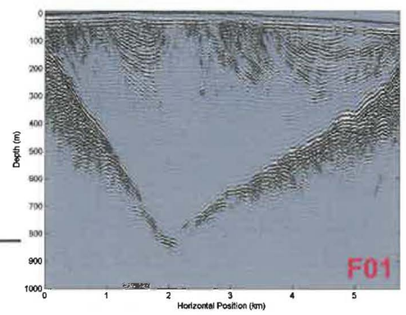

The Ferrar Valley is below sea level, meaning during interglacial periods it becomes a fjord. When the Ferrar and Taylor Glaciers are retreated, water can flood into the Taylor Valley at the point the Ferrar Valley and Taylor Valley meet.

In the profiles, the top of the profile is the glacier surface and the strong reflectors are basement rock.

Figure 8.8: Subglacial radar surveys of the Taylor and Ferrar Glaciers. The surveys indicate a possible evaporite sequence in a subglacial depression beneath the Taylor Glacier.

produce evaporite minerals. As this continued over time, a thick layer of evaporites would be produced.

(2) Water flowing into the depression could produce a large lake. When sea level decreased, the water flowing into the depression would be cut off and the lake would evaporate/ablate, eventually resulting in the deposition of a thick layer of evaporite minerals.

If these were being deposited in a water body, the mineral precipitation would produce a flat-bottomed deposit. When profile T06 is examined (Fig. 8.8), the "v" profile is no longer present, and has been replaced by a flat bottom. This flat bottom is likely to represent the top of a deposit of evaporite minerals. If the "v" profile is extrapolated down from this surface, the thickness of evaporites could easily be ~100 m. Moving to profile T05 there is still a slightly flat bottom to the valley, indicating that this is reaching the edge of the evaporite basin. From profile T04 down the valley, the profile begins to regain its "v" profile.

The "v" profile observed in the images is unusual for a glaciated region, as glacial valleys more commonly have "u" profiles. The "v" seen in these valleys is likely to be a relict river system carved when Antarctica was warmer (potentially carved in the Oligocene to Miocene). As these glaciers are frozen-based, they do not have great erosive power, which could explain why the "v" profile has not been greatly modified. Further down the Taylor Valley, the sinuous "v" profile has been modified to a greater degree and the valley has taken on the more classic "u" profile. This is possibly because the glacier has become wet-based in the past in this part of the valley, thereby allowing for a greater degree of erosion.

The flat-bottomed profile observed in the depression beneath Taylor Glacier indicates that there likely to be is a substantial evaporite deposit present. The basin appears to be ~1 km wide, ~4 km long and ~0.1 km deep. If we assume this deposit fills a "v" valley there is ~ 2 x 10^8 m^3 of salts in the basin. With the density of salt being 2.165 that equates to ~ 433 million tonnes of salt.

The glacier is currently over-riding this hypothesised evaporite sequence. Where it is in contact with the salt bed, melting would be occurring, causing mobilisation of the salt. Presently this reworked salt is entering the Bonney Basin through an outlet at Blood Falls. The presence of salt in the carbonates collected from Sollas Bench indicates that this process has been ongoing. It is likely that these carbonates were deposited in a lake similar to Lake Bonney. Lake Bonney currently has a thickness of at least 1.2 m of halite at its base. The cores collected from Lake Bonney during the 2002/03 season showed the following sequence beneath that halite: an unknown thickness of hydrohalite, ~0.15 m of well sorted sand containing flecks of carbonate, an evaporite sequence ~0.06 m thick underlain by more well sorted sand with carbonate flecks. The evaporite sequence contains laminated carbonate and a small amount of gypsum. The carbonate chemistry and mineralogy is similar to the carbonate samples collected from Sollas Bench and Pearse Valley (Croall, 2005). This fits the models previously described from the Sollas Bench carbonates. It also potentially explains why the Pearse Valley contains little salt. Lake Joyce is currently a chloride brine, but there is not enough salt in the system for halite to precipitate. The ice flow direction over the proposed saline depression beneath Taylor Glacier would mean that little or no salt from the depression is remobilised into the Pearse Valley system. This could be a similar case with the palaeo lake in which the Pearse Valley carbonates were deposited, which would be why there was no halite present within these carbonates.

8.3 CONCLUSIONS

The carbonate samples collected from Nussbaum Riegel have the following proposed origin:

- Deposited in "Glacial Lake Nussbaum", dammed by expanded Ross Sea Ice. The ice was likely to be grounded due the presence of sponge spicules, coral and bivalve fragments.
- Deposited during periods of lake level fluctuation, where draining of ground water towards a lower lake level resulted in evaporation at the surface and cementation of the surficial sediment.

- The sediment cemented by the carbonate was predominantly grains of alkali volcanic minerals and rock fragements, sourced from the McMurdo Volcanics.
- The carbonate had acicular or fibrous crystal morphology, often with larger crystals being composed of bundles of carbonate fibers.
- The carbonate was of mixed mineralogy, containing both aragonite and calcite.
- The trace element chemistry was controlled primarily by the mineralogy of the precipitating carbonate, along with the trace element ratios of the precipitating water.

The carbonate samples collected from Sollas Bench have the following proposed origin:

- Deposited in a lake proglacial to an expanded Taylor Glacier.
- The carbonate was deposited under a regime of water removal, either via evaporation or freezing, making these carbonates a mix of evaporites and "cryorites". In this case they appear to be primarily "cryorites".
- Halite was identified within many of the carbonate samples and gypsum was found associated with them. This indicates that there was a strongly concentrated brine present at the time of precipitation.
- The carbonate had predominantly acicular or fibrous crystal morphology. The needles were either randomly oriented or had a radiating morphology. The samples with radiating crystal morphology were much harder and whiter than those with randomly oriented crystals.
- The carbonate was aragonite.
- The trace element chemistry was controlled primarily by the mineralogy of the precipitating carbonate, along with the trace element ratios of the precipitating water.
- The carbonate samples could represent many episodes of carbonate deposition, as they have been reworked into lateral moraines as the Taylor Glacier expanded.

The carbonate samples collected from the Pearse Valley have the following proposed origin:

- Deposited in "Glacial Lake Pearse" dammed by the Taylor Glacier, as it moved up the mouth of the Pearse Valley.

- The carbonate was deposited under a regime of water removal, either via evaporation or freezing, making these carbonates a mix of evaporites and "cryorites". In this case they appear to be predominantly evaporites.
- The carbonate had predominantly acicular or fibrous crystal morphology. The needles were either randomly oriented or had a radiating morphology. The samples with radiating crystal morphology were much harder and whiter than those with randomly oriented crystals.
- The carbonate was aragonite.
- The trace element chemistry was controlled primarily by the mineralogy of the precipitating carbonate, along with the trace element ratios of the precipitating water.
- The carbonate samples could represent many episodes of carbonate deposition, as they have been reworked into lateral moraines as the Taylor Glacier expanded.

8.4 FURTHER WORK

Through the investigations in this thesis, several aspects have come to light that require further research to be undertaken:

- Work needs to be done on understanding the kinetics involved in the precipitation of aragonite. The investigation needs to be done at a range of temperatures, as this work has highlighted that aragonite can precipitate in freezing conditions, not just in tropical settings
- Physical chemistry involved in the precipitation of carbonate in a closed-system freezing water body could be investigated to determine whether the freezing down of this system would result in the precipitation of aragonite.
- An attempt needs to be made to find a suitable technique to date these carbonate deposits. A possibility is (U-Th)/He dating, as these carbonates are rich in uranium. This would help pin down timing of glacial advances in the Dry Valleys.
- It would be beneficial to compare carbonates from many lakes around Antarctica to see if differing conditions result in carbonates of different mineralogy and chemistry.

- A full investigation needs to be made into the effect freezing conditions have on carbon isotopes. It could be that strongly positive $\delta^{13}C$ could be indicative of carbonate deposited via freezing ("cryorites").
- More work could be undertaken at Nussbaum Riegel. Pits could be dug at a variety of sites allowing more information to be gathered about the subsurface stratigraphy of the carbonate sediment. Another possibility would be to take a series of shallow cores through the area.
- Drilling into postulated evaporite sequences in the subglacial depression beneath Taylor Glacier to ascertain whether it exists. If it does, a variety of work could be undertaken on its geochemistry, chronology and environment of deposition.

Angino, E.E., Armitage, K.B. and Tash, J.C., 1962a. Chemical stratification in Lake Fryxell, Victoria Land, Antarctica. Science, 138: 34-36.

Angino, E.E., Turner, M.D. and Zeller, E.J., 1962b. Reconnaissance geology of the lower Taylor Valley. Victoria Land, Antarctica. Geological Society of America Bulletin, 73: 1553-1561.

Armstrong, R.L., Hamilton, W. and Denton, G.H., 1968. Glaciation in Taylor Valley, Antarctica, older than 2.7 million years. Science(159): 3811.

Bathurst, R.G.C., 1975. Carbonate sediments and their diagenesis. Developments in sedimentology, 12. Elsevier Scientific Pub. Co., Amsterdam, New York, 658 pp.

Berner, R.A., 1975. The role of magnesium in the crystal growth of calcite and aragonite from sea water. Geochimica et Cosmochimica Acta, 39: 489-504.

Black, R.F., 1969. Saline discharges from Taylor Glacier, Victoria Land, Antarctica. Antarctic Journal of the United States, 4(3): 89-90.

Black, R.F. and Bowser, C.J., 1969. Salts and association phenomena of the termini of the Hobbs and Taylor Glaciers, Victoria Land, Antarctica. International Union of Geology and Geophysics. Commission on Snow and Ice, 79: 226-238.

Black, R.F., Jackson, M.L. and Berg, T.E., 1965. Saline discharge from Taylor Glacier, Victoria Land, Antarctica. Journal of Geology, 73(1): 175-180.

Boswell, C.R., Brooks, R.R. and Wilson, A.T., 1967. Trace element content of Antarctic lakes. Nature, 213: 167-168.

Bowen, R., 1988. Isotopes in the earth sciences. Elsevier, London, New York, 647 pp.

Brand, U. and Veizer, J., 1980. Chemical diagenesis of a multicomponent carbonate system-1: trace elements. Journal of Sedimentary Petrology, 50(4): 1219-1236.

Bromley, A.M., 1985. Weather observations Wright Valley, Antarctica. N.Z. Meteorological Service, Information Publication 11: 37p.

Burton, E.A., 1993. Controls on marine carbonate cement mineralogy: review and reassessment. Chemical Geology, 105(1-3): 163-179.

Burton, E.A. and Walter, L.M., 1987. Relative precipitation rates of aragonite and Mg calcite from seawater: Temperature or carbonate ion control? Geology, 15: 111-114.

Caldwell, D.A. and Kyle, P.R., 1994. Mineralogy and geochemistry of ejecta erupted from Mount Erebus, Antarctica, between 1972 and 1986, Volcanological and environmental studies of Mount Erebus, Antarctica. Antarctic Research Series, Volume 66. American Geophysical Union, pp. 147-162.

Carlson, C.A., Phillips, F.M., Elmore, D. and Bentley, H.W., 1990. Chlorine-36 tracing salinity sources in the Dry Valleys of Victoria Land, Antarctica. Geochimica et Cosmochimica Acta, 54: 311-318.

Chafetz, H.S., Wilkinson, B.H. and Love, K.M., 1985. Morphology and composition of non-marine carbonate cements in near-surface settings. In: N. Schneidermann and P.M. Harris (Editors), Carbonate cements. Society of Economic Paleontologists and Mineralogists, Tulsa, Oklahoma.

Chilingarian, G.V., Bissel, H.J. and Wolf, K.H., 1979. Diagenesis of carbonate sediments and epigenesis (or catagenesis) of limestones. In: G. Larsen and

G.V. Chilingarian (Editors), Diagenesis in sediments and sedimentary rocks. Developments in sedimentology, 25A. Elsevier Scientific, Amsterdam, New York.

Clark, I.D. and Lauriol, B., 1992. Kinetic enrichment of stable isotopes in cryogenic calcites. Chemical Geology (Isotope Geoscience), 102: 217-228.

Clayton-Green, J.M., 1986. Proglacial sedimentation of Late Wisconsin age in Miers Valley, Antarctica. Department of Earth Sciences. University of Waikato. MSc Thesis.

Clow, G.D., McKay, C.P., G.M., S.J. and Wharton Jr., R.A., 1988. Climatological observations and predicted sublimation rates at Lake Hoare, Antarctica. Journal of Climate, 1: 715-728.

Coplen, T.B., 1988. Normalization of oxygen and hydrogen isotope data. Chemical Geology (Isotope Geoscience), 72: 293-297.

Coplen, T.B., 1994. Reporting of stable hydrogen, carbon, and oxygen isotopic abundances. Pure and Applied Chemistry, 66: 273-276.

Coplen, T.B. et al., 2003. Compilation of minimum and maximum isotope ratios of selected elements in naturally occuring terrestrial materials and reagents, Water-Resources Investigations Report 01-4222. USGS.

Craig, H., 1953. The geochemistry of the stable carbon isotope. Geochimica et Cosmochimica Acta, 3: 53-92.

Craig, H., 1957. Isotopic standards for carbon and oxygen and correction factors for mass spectrometric analysis of carbon dioxide. Geochimica et Cosmochimica Acta, 12(133-149).

Croall, J., 2005. Antarctic lacustrine carbonates as palaeo climatic indicators, Lake Bonney, Antarctica. Pers. Comm.

Dansgaard, W., 1964. Stable isotopes in precipitation. Tellus, 16(4): 436-468.

David, T.W.E. and Priestly, R.E., 1914. Glaciology, physiography, stratigraphy, and tectonic geology of South Victoria Land, British Antarctic Expedition, 1907-1909. Geology, 1: 1-319.

Denton, G.H. and Armstrong, R.L., 1968. Glacial geology and chronology of the McMurdo Sound region. Antarctic Journal, July-August(99-101).

Denton, G.H., Armstrong, R.L. and Stuiver, M., 1970. Late Cenozoic glaciation in Antarctica: The record in the McMurdo Sound region. Antarctic Journal, Jan-Feb: 15-21.

Denton, G.H., Armstrong, R.L. and Stuiver, M., 1971. The Late Cenozoic glacial history of Antarctica. In: K.K. Turekian (Editor), The Late Cenozoic glacial ages. Yale University Press, New Haven, Connecticut, pp. 267-306.

Denton, G.H., Brockheim, J.G., Wilson, S.C. and Stuiver, M., 1989. Late Wisconsin and Early Holocene glacial history, inner Ross Embayment, Antarctica. Quaternary Research, 31: 151-182.

Denton, G.H. and Marchant, D.R., 2000. The geological basis for a reconstruction of a grounded ice sheet in McMurdo Sound, Antarctica, at the Last Glacial Maximum. Geografiska Annaler, 82A(2-3): 167-212.

Denton, G.H., Stuiver, M. and Austin, K.G., 1985. Radiocarbon chronology of the last glaciation in McMurdo Sound, Antarctica. Antarctica Journal, Review: 59-60.

Doran, P. and Wharton, R.A., 1996. McMurdo Dry Valleys, http://lternet.edu/documents/Publications/climdes/mcm/mcmclim.htm.

Drewry, D.J., 1979. Stable isotope and radio echo sounding investigations of Taylor Glacier, Victoria Land. Antarctic Journal of the United States, 14(5): 93-94.

Epstein, S., Buchbaum, R., Lowenstam, H.A. and Urey, H.C., 1953. Revised palaeotemperature scale. Bulletin of the Geological Society of America, 64: 1314-1325.

Epstein, S., Sharp, R.P. and Goddard, I., 1963. Oxygen-isotope ratios in Antarctic snow, firn and ice. The Journal of Geology, 71(6): 698-720.

Epstein, S., Sharp, R.P. and Gow, A.J., 1965. Six-year record of oxygen and hydrogen isotope variations in South Pole firn. Journal of Geophysical Research, 70(8): 1809-1819.

Eugster, H.P. and Hardie, L.A., 1978. Saline lakes. In: A. Lerman and P. Baccini (Editors), Lakes--chemistry, geology, physics. Springer-Verlag, New York, pp. 237-293.

Folk, R.L., 1974. The natural history of crystalline calcium carbonate: effect of magnesium content and salinity. Journal of Sedimentary Petrology, 44(1): 40-53.

Forbes, R.B., Turner, D.L. and Carden, J.R., 1974. Age of trachyte from Ross Island, Antarctica. Geology, 2: 297-298.

Friedman, E.I., C.P., M. and Nienow, J.A., 1987. The cryptoendolithic microbial environment in the Ross desert of Antarctica: Continuous nanoclimate data, 1984 to 1986. Polar Biology, 7: 273-287.

Friedman, I. and O'Neil, J.R., 1977. Compilation of stable isotope fractionation factors of geochemical interest. In: M. Fleischer (Editor), Data of Geochemistry. US Geol Survey Professional Paper, pp. 440-kk.

Gage, M. and Suggate, R.P., 1958. Glacial chronology of the New Zealand Pleistocene. Geological Society of America Bulletin, 69: 585-598.

Gibbenbach, W.F., Kyle, P.R. and Lyon, G.L., 1973. Present volcanic activity on Mount Erebus, Ross Island, Antarctica. Geology, 1: 135-136.

Given, R.K. and Wilkinson, B.H., 1985. Kinetic control of morphology, composition, and mineralogy of abiotic sedimentary carbonates. Journal of Sedimentary Petrology, 53(1): 109-119.

Gomez Fernandez, J.C. and Melendez, N., 1991. Rhythmically laminated lacustrine carbonates in the Lower Cretaceous of La Serrania de Cuenca Basin (Liberian Ranges, Spain). In: P. Anadon, L. Cabrera and K.R. Kelts (Editors), Advances in lacustrine facies analysis. Blackwell Scientific Publications, Oxford, Boston.

González, L.A. and Lohmann, K.C., 1985. Carbon and oxygen isotopic composition of Holocene reefal carbonates. Geology, 13: 811-814.

Green, W.J., Angle, M.P. and Chave, K.E., 1988. The geochemistry of Antarctic streams and their role in the evolution of four lakes of the McMurdo Dry Valleys. Geochimica et Cosmochimica Acta, 52: 1265-1274.

Grossman, K.L. and Ku, T.L., 1986. Oxygen and carbon fractionation in biogenic aragonite: temperature effects. Chemical Geology (Isotope Geoscience), 59(1): 59-74.

Hall, B.L., 2004. U/Th dates from Sollas Bench carbonates. University of Maine. Pers. Comm.

Hall, B.L. and Denton, G.H., 2000. Radiocarbon chronology of Ross Sea Drift, eastern Taylor Valley, Antarctica: evidence for a grounded ice sheet in the Ross Sea at the Last Glacial Maximum. Geografiska Annaler, 82A(2-3): 305-336.

Hall, B.L., Denton, G.H. and Hendy, C.H., 2000. Evidence from Taylor Valley for a grounded ice sheet in the Ross Sea, Antarctica. Geografiska Annaler, 82A(2-3): 275-303.

Hambrey, M.J., 1994. Glacial environments. UBC Press, Vancouver, viii, 296 pp.

Hardie, L.A. and Eugster, H.P., 1970. The evolution of closed basin brines. Mineralogical Society of America special paper, 3: 237-290.

Hardie, L.A., Smoot, J.P. and Eugster, H.P., 1978. Saline lakes and their deposits: a sedimentological approach. In: A. Matter and M.E. Tucker (Editors), Modern and ancient lake sediments. Blackwell Scientific, Oxford

New York, pp. vi, 290.

Haskell, T.R., Kennet, J.P., Prebble, W.M., Smith, G. and Willis, I.A.G., 1965. The geology of the middle and lower Taylor Valley of South Victoria Land, Antarctica. Transactions of the Royal Society of New Zealand, 2(12): 169-186.

Henderson, R.A. et al., 1965. An ablation rate for Lake Fryxell, Victoria Land. Antarctica Journal of Glaciology, 6: 129-133.

Hendy, C.H., Healy, T.R., Rayner, E.M., Shaw, J. and Wilson, A.T., 1979. Late Pleistocene glacial chronology of the Taylor Valley, Antarctica, and the global climate. Quaternary Research, 11(2): 172-185.

Hendy, C.H., Sadler, A.J., Denton, G.H. and Hall, B.L., 2000. Proglacial lake-ice conveyors: a new mechanism for deposition of drift in polar environments. Geografiska Annaler, 82A(2-3): 249-270.

Hendy, C.H. and Utting, A., 1984. Notes on the occurrence of mixed calcite and aragonite beds in ice free valleys of the Trans Antarctic Mountains, Antarctic Research Unit, University of Waikato. Report No. 13: 29-50.

Hendy, C.H., Wilson, A.T. and Neale, V.E., 1969. Marine deposits 35,000 years old, Cape Barne, Ross Island, Antarctica. New Zealand Journal of Geology and Geophysics, 12(4): 707-712.

Hendy, C.H., Wilson, A.T., Popplewell, K.B. and House, D.A., 1977. Dating of geochemical events in Lake Bonney, Antarctica, and their relationship to glacial and climatic changes. New Zealand Journal of Geology and Geophysics, 20: 1103-1122.

Higgins, S.M., 1993. The glacial geology, geomorphology, and geochronology of Bonney drift central Taylor Valley, Southern Victoria Land, Antarctica: evidence from late Quaternary expansions of the East Antarctic Ice Sheet during interglacial stages 5, 7, and 9. Geology Department. University of Maine. MSc Thesis.

Higgins, S.M., Denton, G.H. and Hendy, C.H., 2000a. Glacial geomorphology of Bonney Drift, Taylor Valley, Antarctica. Geografiska Annaler, 82A(2-3): 365-389.

Higgins, S.M., Hendy, C.H. and Denton, G.H., 2000b. Geochronology of Bonney Drift, Taylor Valley, Antarctica : evidence for interglacial expansions of Taylor Glacier. Geografiska Annaler, 82A(2-3): 391-409.

Hoefs, J., 1987. Stable isotope geochemistry. Springer-Verlag, Berlin, Germany.

Hollin, J.T., 1962. On the glacial history of Antarctica. Journal of Glaciology, 4(32): 173-194.

Hughes, T.J., 1973. Is the West Antarctic Ice Sheet disintergrating? Journal of Geophysical Research, 78(33): 7884-7911.

Ichikuni, M., 1973. Partition of strontium between calcite and solution: effect of substitution by manganese. Chemical Geology, 11: 315-319.

Jones, L.M. and Faure, G., 1968. Origin of salts in Taylor Valley. Antarctic Journal, September-October: 177-178.

Jones, L.M. and Faure, G., 1978. A study of strontium isotopes in lakes and surficial deposits of the ice-free valleys, southern Victoria Land, Antarctica. Chemical Geology, 22: 107-120.

Judd, F.M., 1986. The chronology of the Ross Sea II glaciation, an Antarctic glaciation of Illinoian age. Department of Earth Sciences. University of Waikato. MSc Thesis.

Kennet, J.P. et al., 1974. Cenozoic paleoceangraphy in the Southwest Pacific Ocean, Antarctic glaciation, and the development of the Circum-Antarctic current. In Initial Reports of DSDP LEG 29. U.S. Government Printing Office, 1155-1171 pp.

Keys, J.R., 1980. Air temperature, wind, precipitation and atmosphere humidity in the McMurdo region. Department of Geology Pub. No. 17(Antarctic Data Series No. 9): Victoria University of Wellington, New Zealand.

Keys, J.R.H., 1979. Saline discharge at the terminus of Taylor Glacier. Antarctic Journal of the United States, 14(5): 82-85.

Keys, J.R.H. and Williams, K., 1981. Origin of crystalline, cold desert salts in the McMurdo region, Antarctica. Geochimica et Cosmochimica Acta, 45: 2299-2309.

Kinsman, D.J.J., 1969. Interpretation of Sr^{2+} concentrations in carbonate minerals and rocks. Journal of Sedimentary Petrology, 39(2): 486-508.

Kovach, J. and Faure, G., 1977. Sources and abundance of volcanogenic sediment in piston cores from the Ross Sea, Antarctica. New Zealand Journal of Geology and Geophysics, 20(6): 1017-1026.

Kurasawa, H., 1978. Geochemistry of Ferrar dolerite dikes and Cenozoic volcanics of the Dry Valleys region. Dry Valleys Drilling Project Bulletin, 8: 34-38.

Kyle, P.R., 1976. Geology, mineralogy and geochemistry of the late Cenozoic McMurdo Volcanic Group, Victoria Land, Antarctica. PhD Thesis, Victoria University, Wellington.

Kyle, P.R., 1977. Mineralogy and glass chemistry of recent volcanic ejecta from Mt Erebus, Ross Island, Antarctica. New Zealand Journal of Geology and Geophysics, 20(6): 1123-1146.

Kyle, P.R., 1990. Erebus volcanic province. In: W.E. LeMasurier and J.W. Thomson (Editors), Volcanoes of the Antarctic Plate and Southern Oceans. Antarctic Research Series, Volume 48. American Geophysical Union.

Lahann, R.W., 1978. A chemical model for calcite crystal growth and morphology control. Journal of Sedimentary Petrology, 48(1): 337-344.

Lawrence, M.J.F., 1982. Origin and occurrence of Antarctic lacustrine carbonates, with special reference to Lake Fryxell, Taylor Valley. Department of Earth Sciences. University of Waikato. MSc Thesis.

Lawrence, M.J.F. and Hendy, C.H., 1985. Water column and sediment characteristics of Lake Fryxell, Taylor Valley, Antarctica. New Zealand Journal of Geology and Geophysics, 28: 543-553.

Lawrence, M.J.F. and Hendy, C.H., 1989. Carbonate deposition and Ross Sea ice advance, Fryxell basin, Taylor Valley, Antarctica. New Zealand Journal of Geology and Geophysics, 32: 267-278.

Leng, M.J. and Marshall, J.D., 2004. Palaeoclimate interpretation of stable isotope data from lake sediment archives. Quaternary Science Reviews, 23(7-8): 811-831.

Lyons, W.B. et al., 2000. Importance of landscape position and legacy: the evolution of the lakes in Taylor Valley, Antarctica. Freshwater Biology, 43: 355-367.

Lyons, W.B. et al., 1998a. Geochemical linkages among glaciers, streams and lakes within the Taylor Valley, Antarctica. American Geophysical Union: 77-92.

Lyons, W.B., Welch, K.A. and Sharma, P., 1998b. Chlorine-36 in the waters of the McMurdo Dry Valley lakes, southern Victoria Land, Antarctica: Revisited. Geochimica et Cosmochimica Acta, 62(2): 185-191.

McCraw, J.D., 1962. Volcanic detritus in Taylor Valley, Victoria Land, Antarcitca. New Zealand Journal of geology and geophysics, 5(5): 740-745.

McCraw, J.D., 1967. Soils of Taylor Dry Valley, Victoria Land, Antarctica, with notes on soils from other localities in Victoria Land. New Zealand Journal of Geology and Geophysics, 10(2): 498-539.

McCrea, 1950. On the isotopic chemistry of carbonates and a palaeotemperature scale. Journal of Chemical Physics, 18(1849): 1857.

Milliman, J.D., 1974. Marine carbonates. Recent sedimentary carbonates Part 1. Springer-Verlag, Berlin. Heidelberg. New York.

Moore, C.H., 1989. Carbonate diagenesis and porosity. Developments in sedimentology, 46. Elsevier, Amsterdam ; New York, 338 pp.

Morse, D.L., Conway, H. and Cuffey, K., 2003. Radar surveys of Taylor Glacier, Transantarctic Mountains, East Antarctica, International Glaciological Society Meeting, Milan, Italy.

Morse, J.W., Wang, Q. and Tsio, M.Y., 1997. Influences of temperature and Mg:Ca ratio on $CaCO_3$ precipitates from seawater. Geology, 25: 85-87.

Mucci, A. and Morse, J.W., 1983. The incorporation of Mg^{2+} and Sr^{2+} into calcite overgrowths: Influences of growth rate and solution composition. Geochimica et Cosmochimica Acta, 47: 217-233.

Müller, G., Ition, G. and Forstner, U., 1972. Formation and diagenesis of inorganic Ca-Mg carbonates in the lacustrine environment. Naturwissenschaften, 59: 158-164.

Nichols, R.L., 1968. Coastal geomorphology, McMurdo Sound, Antarctica. Journal of Glaciology, 7(51): 449-178.

Niles, P.B., Leshin, L.A., Guan, Y., Ming, D.W. and Gibson, E.K., 2004. Cryogenic calcite- A morphologic and isotopic analog to the ALH84001 carbonates. Lunar and Planetary Science XXXV.

Nishiyama, T., 1979. Distribution and origin of evaporate minerals from Dry Valleys, Victoria Land. Memoirs of National Institute of Polar Research, 13: 136-147.

Nylen, T.H., Fountain, A.G. and T., D.P., 2004. Climatology of katabatic winds in the McMurdo dry valleys, southern Victoria Land, Antarctica. Journal of Geophysical Research, 109.

Olsen, E.A. and Broecker, W.S., 1961. Lamont natural radiocarbon measurements VII. Radiocarbon, 3: 141-175.

Parker, B.C., Simmons, G.M., Love, F.G., Wharton, R.A. and Seaburg, K.G., 1981. Modern stromatolites in Antarctic Dry Valley lakes. BioScience, 31(9): 656-661.

Péwé, T.L., 1960. Multiple glaciations in the McMurdo Sound region, Antarctica; a progress report. USINC-IGY Antarctic Glaciological Data, Report number 2: Field work 1958-1959.

Pingitore, N.E., 1978. The behaviour of Zn^{2+} and Mn^{2+} during carbonate diagenesis: theory and applications. Journal of Sedimentary Petrology, 48(3): 799-814.

Platt, N.H. and Wright, V.P., 1991. Lacustrine carbonates: facies models, facies distribution and hydrocarbon prospects. In: P. Anadon, L. Cabrera and K.R. Kelts (Editors), Advances in lacustrine facies analysis. Blackwell Scientific Publications, Oxford, Boston.

Porter, S.C. and Beget, J.E., 1981. Provenance and depositional environments of late Cenozoic sediments in permafrost cores from lower Taylor Valley, Antarctica. In: L.D. McGinnins (Editor), Dry Valley drilling project. Antarctic research series, volume 33. American geophysical union, pp. 351-363.

Rao, C.P., 1996. Modern carbonates, tropical, temperate, polar : introduction to sedimentology and geochemistry. Carbonates, Tasmania, 206 pp.

Rao, C.P., 1997. A colour illustrated guide to sedimentary textures. Carbonates, Tasmania, 128 pp.

Rao, C.P., Goodwin, I.D. and Gibson, J.A.E., 1998. Shelf, coastal and subglacial polar carbonates, East Anarctica. Carbonates and Evaporites, 13(2): 174-188.

Rathburn, A.E. and Deckker, P.D., 1997. Magnesium and strontium compositions of Recent benthic foraminifera from the Coral Sea, Australia and Prydz Bay, Antarctica. Marine Micropaleontology, 32: 231-248.

Reading, H.G., 1986. Sedimentary environments and facies. Blackwell Scientific, Oxford, xi, 615 pp.

Rimstidt, J.D., Balog, A. and Webb, J., 1998. Distribution of trace elements between carbonate minerals and aqueous solutions. Geochimica et Cosmochimica Acta, 62(11): 1851-1863.

Riordian, A.J., 1973. The climate of Vanda Station, Antarctica. In: G. Weller and S.A. Bowling (Editors), Climate of the Arctic, pp. 268-275.

Romanek, C.S., Grossman, E.L. and Morse, J.W., 1992. Carbon isotopic fractionation in synthetic aragonite and calcite: Effects of temperature and precipitation rate. Geochimica et Cosmochimica Acta, 56: 419-430.

Rubinson, M. and Clayton, R.N., 1969. Carbon-13 fractionation between aragonite and calcite. Geochimica et Cosmochimica Acta, 33(997-1002).

Scott, R.F., 1905. Results of the National Antarctic Expidition, I, geographical. Geological Journal, 25: 353-373.

Smith, A.M. and Nelson, C.S., 1993. Mineralogical, carbonate geochemical, and diagenetic data for modern New Zealand bryozoans, Occasional Report No. 70, Department of Earth Sciences, University of Waikato.

Stuiver, M., Denton, G.H., Hughes, T.J. and Fastook, J.L., 1981. History of the marine ice sheet in West Antarctica during the last glaciation, as working hypothesis. In: G.H. Denton and T.H. Hughes (Editors), The last great ice sheets. Wiley-Interscience, New York, pp. 319-436.

Tarutani, T., Clayton, R.N. and Mayeda, T.K., 1969. The effect of polymorphism and magnesium substitution on oxygen isotope fractionation between calcium carbonate and water. Geochimica et Cosmochimica Acta, 33: 987-996.

Taylor, G., 1914. Physiography and glacial geology of East Antarctica. Geological Journal, 44: 365-382.

Thompson, D.C., R., C. and Bromley, A., 1971. Climate and surface heat balance in an Antarctic dry valley. New Zealand Journal of Science, 14: 245-251.

Thompson, T.G. and Nelson, K.H., 1956. Concentration of brines and deposition of salts from sea water under frigid conditions. American Journal of Science, 254: 227-238.

Torii, T., Murata, S. and Yamagata, N., 1980. Geochemistry of the Dry Valley lakes. Journal of the Royal Society of New Zealand, 11(4): 387-399.

Torii, T. and Ossaka, J., 1965. Antarcticite: a new mineral, calcium chloride hexahydrate, discovered in Antarctica. Science, 149: 975-977.

Treves, S.B., 1968. Volcanic rocks of the Ross Island area. Antarctic Journal of the United States, 3: 108-109.

Tucker, M.E., 1988. Techniques in sedimentology. Blackwell Scientific Publications, Oxford England ; Boston, ix, 394 , [1] folded leaf of plates pp.

Tucker, M.E. and Wright, V.P., 1990. Carbonate sedimentology. Blackwell Scientific Publications, Oxford, 482 pp.

Urey, H.C., 1947. The thermodynamic properties of isotopic substances. Journal of the Chemistry Society (London): 562-581.

Weand, B.L., Fortner, R.D., Hoehn, R.C. and Parker, B.C., 1975. Subterranean flow into Lake Bonney. Antarctic Journal of the United States, 10(1): 15-19.

Wharton, R.A., Parker, B.C., Simmons, G.M., Seaburg, K.G. and Love, F.G., 1982. Biogenic calcite structures forming in Lake Fryxell, Antarctica. Nature, 295(5548): 403-405.

Whillans, I.M., 1976. Radio-echo layers and the recent stability of the West Antarctic Ice Sheet. Nature, 264: 152-155.

Whittaker, T.E. et al., 2003. Recent and abrupt variations in depositional environment in Lake Fryxell, Dry Valleys, Antarctica, Geological Society of America Seattle Annual Meeting, Seattle.

Wilson, A.T., 1979. Geochemical problems of the Antarctic dry areas. Nature, 280: 205-208.

Wolf, K.H., Chilingarian, G.V. and Beales, F.W., 1967. Elemental composition of carbonate skeletons, minerals and sediments. In: G.V. Chilingarian, H.J. Bissel and R.W. Fairbridge (Editors), Carbonate rocks. Developments in sedimentology, 9. Elsevier, Amsterdam, New York, pp. 2 v.

Zeebe, R.E. and Wolf-Gladrow, D., 2001. CO_2 in seawater: equilibrium, kinetics, isotopes. Elsevier Oceanography Series, 65. Elsevier, Amsterdam.

APPENDIX ONE:
TRACE ELEMENT DATA

Trace element concentrations for Nussbaum Riegel, Sollas Bench and Pearse Valley and archived samples. The concentrations are recorded in mg/Kg or ppm.

	Ba	Ca	Fe	Mg	Mn	Sr	Zn	K	Na
Nussbaum Riegel									
S01a	94.42	127529.58	9874.60	5881.97	1644.32	3412.45	69.42	3.21	4.05
S02a	126.01	137048.79	10789.11	10335.69	3700.30	2957.86	56.85	2.15	3.99
S03a	96.29	132768.41	10807.22	7004.81	1554.86	4070.41	77.93	3.26	3.82
S04a	118.81	142838.41	8703.48	5328.76	1600.50	5246.67	68.76	2.34	3.41
S05a	117.77	105162.65	9833.84	6747.79	1349.20	3372.69	68.88	5.33	4.35
S06a	113.71	104268.53	8135.94	4071.27	414.72	4230.25	61.62	2.29	3.19
S07a	119.84	149193.16	7432.94	3903.81	251.52	5799.22	56.11	3.20	4.08
S07b	75.45	137018.79	7525.05	5524.65	1547.12	3796.52	64.41	3.82	3.97
S07La	136.03	149343.32	8333.30	4445.45	322.06	5965.99	51.01	2.63	3.88
S07Ua	355.29	170426.67	6914.26	4413.29	704.46	5251.89	129.39	3.86	4.80
S08a	104.26	150167.03	7134.46	4010.10	218.42	5366.53	63.56	2.28	4.94
S09a	113.23	156379.39	8105.76	5493.23	499.90	5069.09	65.66	2.78	3.28
S10a	94.69	142328.99	11008.31	5136.52	581.16	3720.68	65.99	3.22	5.56
S11a	100.88	137228.99	7908.17	5002.72	346.01	3821.11	48.15	2.80	3.65
S11b	141.16	166475.90	8370.58	4680.42	503.41	4826.51	172.99	2.93	3.97
S12a	118.79	128292.02	9698.79	7054.04	1669.19	3532.83	55.45	2.82	3.61
S13a	112.88	135042.35	10056.64	4920.12	529.68	4293.36	66.80	3.53	5.22
Sollas Bench									
S14a	113.86	269335.34	2518.78	1250.10	89.96	3718.67	242.87	0.81	3.77
S14b	20.60	264008.50	1577.20	1195.40	63.50	2908.60	57.40	0.55	3.12
S15a	63.75	265705.28	3020.22	1539.94	224.20	6885.46	40.74	0.75	3.98
S16a	74.25	267868.64	2986.06	1039.11	214.33	6842.98	64.86	0.81	4.21
S17a	19.42	249170.97	1620.10	1730.97	71.46	5105.92	35.34	0.70	1.76
S18a	54.04	278772.74	1464.95	735.25	65.82	9100.78	39.63	0.28	2.84
S19a	24.85	276565.29	1331.85	947.73	49.61	2404.34	56.02	0.46	1.81
S20a	72.76	246852.39	1680.12	2413.42	71.97	5378.33	72.76	0.27	2.09
S21a	96.22	269450.87	2063.76	1982.56	86.82	5650.00	87.02	0.45	3.21
S22a	30.33	232129.63	2578.38	2442.34	75.98	9555.96	41.44	0.97	5.29
S22b	81.94	286364.98	1395.16	2146.52	49.24	8674.87	43.90	0.53	5.30
S23a	92.25	288210.59	1608.43	563.14	28.92	3493.14	49.51	0.50	2.48
Pearse Valley									
S24a	88.58	240430.51	1792.42	484.25	37.30	6221.46	39.86	0.40	2.19
S25a	52.09	260326.43	1707.48	212.83	57.53	7060.25	79.01	0.33	1.56
S26a	14.40	285713.81	1105.33	3749.80	226.82	315.58	50.89	0.20	0.89
S27a	17.15	312104.78	762.09	-	144.54	6727.19	49.42	0.09	1.43
S27b	46.85	274331.46	2018.88	3438.33	240.27	6975.02	48.60	0.17	1.81
S27c	32.64	311578.61	990.35	-	205.37	9143.18	48.46	0.10	2.29
S28a	34.06	304278.15	824.53	-	190.37	8172.59	39.82	0.05	2.25
S30a	45.85	257779.67	1834.02	632.26	67.35	6505.77	65.20	0.42	1.68
S31a	26.97	303365.56	1504.34	160.20	133.03	6453.23	136.46	0.27	2.77
S32a	15.98	326809.65	1104.82	3150.25	1731.16	358.59	89.55	0.04	1.28

	Ba	Ca	Fe	Mg	Mn	Sr	Zn	K	Na
Taylor Valley: Bonney Drift									
87-005a	23.27	289078.30	1134.61	654.73	-	5315.05	40.11	958.23	2952.26
87-006-020e	46.52	256201.56	6002.32	2840.11	1728.21	4781.11	44.92	1435.38	3249.55
87-006-17b	20.83	213527.77	2470.42	957.85	-	6193.60	49.77	1373.87	2730.94
87-014a	38.83	241853.34	2727.27	1307.25	-	6424.76	49.23	1546.42	1518.86
87-024a	20.01	277171.46	4697.24	4082.90	7274.12	581.04	52.86	847.04	1976.93
87-025-50c	31.55	298696.07	1736.89	837.83	-	5868.49	48.27	1224.25	3035.58
87-031-69b	42.81	218536.79	18943.35	7592.44	5229.01	2744.08	58.29	999.54	3525.50
87-031-70c	37.18	235613.07	3230.70	1679.43	-	3552.13	85.16	1690.98	3814.08
87-036-094c	29.30	244045.51	22016.21	10271.45	5900.51	1821.17	65.28	1262.15	3700.00
87-004-47b	44.13	248250.05	3384.69	1547.53	-	6110.49	53.35	2074.24	2957.38
87-085a	50.59	308006.53	2486.99	1328.54	-	7653.88	41.00	1075.34	2625.57
Dry Valley Drilling Project									
76-33	38.48	246665.82	2043.45	987.41	-	5215.36	41.57	1414.79	3139.98
76-54	29.60	71611.34	25546.00	5870.91	385.36	1459.43	62.41	2239.78	3669.61
76-56	62.48	77528.02	2531.77	1459.16	-	2909.16	50.77	2366.27	4836.03
76-57	153.43	138667.41	2361.99	1711.32	-	3650.63	90.76	2594.78	4773.21
76-58	54.95	7958.19	8750.23	5824.65	-	70.35	61.19	3215.54	4701.67
76-59	91.66	76227.10	9959.65	5032.91	-	1975.20	52.80	4001.80	4415.24
76-61	35.73	49616.15	6816.95	2811.00	-	-36.22	66.80	3087.71	5255.20
Miers Valley: Glacial Lake Trowbridge									
C295	51.96	313504.22	3255.50	4903.98	274.85	867.93	54.37	1534.87	2528.98
C298	104.16	294859.02	6122.14	10804.16	-	1860.37	53.51	3341.68	-
C301	110.73	242558.17	5070.71	2765.70	-	6730.09	54.31	3103.81	2616.85
C302	68.67	118492.62	5705.18	7175.12	849.16	1838.24	68.67	5206.82	7776.38
C304	129.17	268915.16	5946.17	8766.00	7.36	1870.43	118.84	2341.45	4876.24
C403b	172.34	285323.29	6487.25	9731.02	-	1932.48	54.52	2729.92	3749.00
C403c	94.89	284554.96	6355.35	10026.23	31.58	1963.85	55.89	2774.07	3762.28
C408a	77.01	278752.18	4901.09	9456.31	23.54	1912.56	57.89	2660.87	4247.77
C861	190.79	245143.62	6879.40	10465.33	1398.43	2479.05	70.14	3317.31	-
C862	145.47	225697.56	4607.58	8118.12	420.43	1761.50	59.63	3282.23	6856.27
C878	120.63	286540.57	4874.58	10352.15	-	1527.91	52.44	3711.14	4864.61
C899	107.01	273151.06	4970.28	8314.58	203.73	1702.83	68.11	2523.71	3378.91
C908L	68.43	256420.28	6255.04	8879.77	-	1970.18	56.24	2377.12	3488.01
C908M	84.87	286308.93	6736.33	9651.03	-	1642.76	44.22	2394.74	3775.38
C908U	96.85	293304.45	7037.57	10119.93	-	1766.87	50.14	3181.64	4329.83
C938	142.31	260638.66	5056.84	6436.66	1144.71	1711.14	89.61	2031.47	2958.04
C941	184.57	278099.37	4671.21	9106.95	303.56	2175.99	69.22	2542.87	5648.01
C943	99.55	270490.44	6121.36	9909.43	-	1511.54	54.94	2974.87	4879.71
Marshall Valley: Glacial Lake Péwé									
G12 (bed b)	48.67	306969.15	2909.55	9574.71	700.24	2315.35	54.56	1522.81	3042.30
G13 (bed d)	63.16	304711.97	4699.90	2295.15	102.37	11064.19	134.47	1832.84	3598.42
G14 (bed d)	57.98	281619.46	2985.98	5912.62	492.37	5697.90	54.89	1406.19	3178.14
G18 (bed e)	112.17	275881.77	7368.75	3102.67	-	6209.54	54.87	2556.30	4102.58
G23 (bed b)	132.60	124202.74	14717.55	8633.38	-	3313.05	168.04	5480.45	7254.64
G27 (bed a)	55.45	313635.54	2538.96	8119.21	233.76	5557.28	49.90	1373.76	3151.49
G33 (bed a)	73.00	301535.15	2570.21	9425.17	100.83	4419.12	45.99	1354.09	3661.15
G45 (bed e)	52.07	317619.54	1303.46	869.26	-	4956.54	40.65	678.34	3363.59
G47 (bed a)	56.55	293418.35	2410.97	10199.13	238.59	2610.29	52.18	1600.49	4177.67

APPENDIX TWO:

SUMMARY OF CARBONATE CHEMISTRY

Summary of chemical features of the carbonates collected from Nussbaum Riegel. Ca/Ar refers to the calcite/aragonite ratio in the following tables.

Label	Sample Type	University Collection No.	Grid Reference	^{18}Ovpdb	^{13}Cvpdb	% $CaCO_3$	Ca/Ar
0203S01	Bulk sample	W0500001	S 77°30.765' E 162 °51.866'	-	-	-	-
S01a	Hand specimen (sub sample)	W0500002	"	-30.74	-0.94	30	0.49
0203S02	Bulk sample	W0500003	S 77°3.489' E 162 °52.224'	-	-	-	-
S02a	Hand specimen (sub sample)	W0500004	"	-29.14	-3.10	45	0.04
0203S03	Bulk sample	W0500005	S 77°39.482' E 162 °52.361'	-	-	-	-
S03a	Hand specimen (sub sample)	W0500006	"	-28.24	-0.60	45	0.70
0203S04	Bulk sample	W0500007	S 77°39.477' E 162 °52.506'	-	-	-	-
S04a	Hand specimen (sub sample)	W0500008	"	-31.49	-2.30	54	0.58
0203S05	Bulk sample	W0500009	S 77°39.464' E 162 °52.561'	-	-	-	-
S05a	Hand specimen (sub sample)	W0500010	"	-31.44	-1.96	48	0.67
0203S06	Bulk sample	W0500011	S 77°39.422' E 162 °52.651'	-	-	-	-
S06a	Hand specimen (sub sample)	W0500012	"	-30.51	-1.18	49	0.88
0203S07	Bulk sample	W0500013	S 77°39.397' E 162 °52.918'	-	-	-	-
S07a	Hand specimen (sub sample)	W0500014	"	-30.24	-0.18	50	0.93
S07b	Hand specimen (sub sample)	W0500015	"	-30.49	0.02	43	0.99
0203S07U	Bulk sample	W0500016	S 77°39.397' E 162 °52.918'	-	-	-	-
S07Ua	Hand specimen (sub sample)	W0500017	"	-32.64	-1.28	43	0.94
0203S07L	Bulk sample	W0500018	S 77°39.397' E 162 °52.918'	-	-	-	-
S07La	Hand specimen (sub sample)	W0500019	"	-30.63	0.03	53	0.97
0203S08	Bulk sample	W0500020	S 77°39.416' E 162 °52.823'	-	-	-	-
S08a	Hand specimen (sub sample)	W0500021	"	-30.40	0.20	41	0.90
0203S09	Bulk sample	W0500022	S 77°39.416' E 162 °52.823'	-	-	-	-
S09a	Hand specimen (sub sample)	W0500023	"	-30.88	-0.66	45	0.92
0203S10	Bulk sample	W0500024	S 77°39.467' E 162 °52.856'	-	-	-	-
S10a	Hand specimen (sub sample)	W0500025	"	-31.95	-0.67	31	0.97
0203S11	Bulk sample	W0500026	S 77°39.467' E 162 °52.856'	-	-	-	-
S11a	Hand specimen (sub sample)	W0500027	"	-31.24	-0.35	46	0.95
S11b	Hand specimen (sub sample)	W0500028	"	-30.88	0.00	46	0.96
0203S12	Bulk sample	W0500029	S 77°39.299' E 162 °52.647'	-	-	-	-
S12a	Hand specimen (sub sample)	W0500030	"	-30.43	-1.52	54	0.39
0203S13	Bulk sample	W0500031	S 77°39.293' E 162 °52.307'	-	-	-	-
S13a	Hand specimen (sub sample)	W0500032	"	-31.46	-0.53	48	0.70

Summary of chemical features of the carbonates collected from Sollas Bench.

Label	Sample Type	University Collection No.	Grid Reference	δ^{18}Ovpdb	δ^{13}Cvpdb	% $CaCO_3$	Ca/Ar	Halite Present	Gypsum Present
0203S14	Bulk sample	W0500033	S 77°43.326' E 162 °30.738'	-	-	-	-	-	yes
S14a	Hand specimen (sub sample)	W0500034	"	-35.51	4.37	84	1.00	no	yes
S14b	Hand specimen (sub sample)	W0500035	"	-36.76	6.61	83	1.00	no	-
0203S15	Bulk sample	W0500036	S 77°43.090' E 162 °31.900'	-	-	-	-	-	yes
S15a	Hand specimen (sub sample)	W0500037	"	-35.75	6.51	84	0.99	yes	-
0203S16	Bulk sample	W0500038	S 77°42.925' E 162 °32.006'	-	-	-	-	-	yes
S16a	Hand specimen (sub sample)	W0500039	'	-35.89	6.42	86	0.99	no	-
0203S17	Bulk sample	W0500040	S 77°42.925' E 162 °32.087'	-	-	-	-	-	yes
S17a	Hand specimen (sub sample)	W0500041	"	-37.18	8.32	80	0.99	no	-
0203S18	Bulk sample	W0500042	S 77°42.625' E 162 °32.452'	-	-	-	-	-	no
S18a	Hand specimen (sub sample)	W0500043	"	-34.21	7.16	89	1.00	yes	-
0203S19	Bulk sample	W0500044	S 77°42.831' E 162 °37.970'	-	-	-	-	-	yes
S19a	Hand specimen (sub sample)	W0500045	"	-37.15	7.29	89	1.00	no	-
0203S20	Bulk sample	W0500046	S 77°43.060' E 162 °31.475'	-	-	-	-	-	yes
S20a	Hand specimen (sub sample)	W0500047	"	-37.33	8.31	80	1.00	yes	-
0203S21	Bulk sample	W0500048	S 77°43.391' E 162 °30.625'	-	-	-	-	-	yes
S21a	Hand specimen (sub sample)	W0500049	"	-35.28	7.40	81	0.99	yes	-
0203S22	Bulk sample	W0500050	S 77°42.243' E 162 °34.845'	-	-	-	-	-	no
S22a	Hand specimen (sub sample)	W0500051	"	-33.88	8.19	73	0.97	yes	-
S22b	Hand specimen (sub sample)	W0500052	"	-34.32	7.50	88	1.00	no	-
0203S23	Bulk sample	W0500053	S 77°42.077' E 162 °37.002'	-	-	-	-	-	no
S23a	Hand specimen (sub sample)	W0500054	"	-37.15	4.92	91	1.00	no	-

Summary of chemical features of the carbonates collected from Pearse Valley.

Label	Sample Type	University Collection No.	Grid Reference	δ^{18}Ovpdb	δ^{13}Cvpdb	% $CaCO_3$	Ca/Ar
0203S24	Bulk sample	W0500055	S 77°42.232' E 161 °30.437'	-	-	-	-
S24a	Hand specimen (sub sample)	W0500056	"	-37.73	2.70	75	0.98
0203S25	Bulk sample	W0500057	S 77°42.465' E 161 °29.206'	-	-	-	-
S25a	Hand specimen (sub sample)	W0500058	"	-38.26	2.52	80	1.00
0203S26	Bulk sample	W0500059	Collected between GPS A S 77°43.462' E 161 °34.776' GPS B S 77°43.411' E 161 °34.324'	-	-	-	-
S26a	Hand specimen (sub sample)	W0500060	"	-33.69	0.64	91	0.02
0203S27	Bulk sample	W0500061	S 77°43.401' E 161 °34.202'	-	-	-	-
S27a	Hand specimen (sub sample)	W0500062	"	-36.34	7.10	96	0.96
S27b	Hand specimen (sub sample)	W0500063	'	-33.50	3.17	87	0.88
S27c	Hand specimen (sub sample)	W0500064	'	-35.42	7.35	96	0.91
0203S28	Bulk sample	W0500065	S 77°44.365' E 161 °33.078'	-	-	-	-
S28a	Hand specimen (sub sample)	W0500066	"	-35.81	7.16	87	0.95
0203S30	Bulk sample	W0500067	S 77°43.201' E 161 °31.885'	-	-	-	-
S30a	Hand specimen (sub sample)	W0500068	"	-38.19	2.59	76	-
0203S31	Bulk sample	W0500069	S 77°43.189' E 161 °29.669'	-	-	-	-
S31a	Hand specimen (sub sample)	W0500070	"	-38.00	2.87	90	0.96
0203S32	Bulk sample	W0500071	S 77°43.221' E 161 °29.306'	-	-	-	-
S32a	Hand specimen (sub sample)	W0500072	"	-33.58	3.78	93	0.00